

NORTHWESTERN UNIVERSITY

Chemically-Modified Peptide Nucleic Acids: A Versatile Approach to Complex Molecular
Scaffolding and Control of Nucleic Acid Secondary Architecture

A DISSERTATION

SUBMITTED TO THE GRADUATE SCHOOL IN PARTIAL FULFILLMENT OF THE
REQUIREMENTS

for the degree

DOCTOR OF PHILOSOPHY

Field of Chemistry

By

Ethan Andrew Englund

EVANSTON, ILLINOIS

December, 2007

Abstract

Chemically-Modified Peptide Nucleic Acids: A Versatile Approach to Complex Molecular Scaffolding and Control of Nucleic Acid Secondary Architecture

Ethan Andrew Englund

This dissertation covers the synthesis and study of peptide nucleic acids (PNAs), specifically, derivatives of PNA containing amine-bearing sidechains or cyclopentane portions. PNAs are non-natural nucleic acids that have far reaching potential in therapeutics and nucleic acid detection. Despite immense potential and widespread application, improving on the design and applications of PNA are areas of heavy research. This dissertation describes the successful synthesis of several PNA derivatives that show very promising binding properties while giving us unprecedented control of oligomer characteristics, both as scaffolds for complex molecular display and control of secondary structure.

The first chapter contains the necessary background into nucleic acids and their applications. The development of non-natural nucleic acids, specifically PNA, is described. The chapter also examines the precedent and logic used in the design of the PNA derivatives and experimental approach.

The second chapter pertains to the development of a chiral PNA derivative based on amine-containing “sidechains”. The utility of this modification is that further functionality can be appended to each sidechain residue. As these sidechains are amenable to conjugation through amide bond-forming reactions during oligomer synthesis, very few starting PNA monomers need to be synthesized to achieve a wide variety of derivatized PNA residues. Our subsequent studies on the stability of this sidechain PNA demonstrated that the molecular recognition properties (affinity, selectivity) were enhanced for both DNA and RNA. Furthermore, we showed initial

evidence that this modification strategy can be useful when designing light-up molecular probes, molecules that fluoresce only when bound to a target nucleic acid.

The third chapter explores a cyclic derivative of PNA in the context of non-Watson-Crick hydrogen bonding motifs. Despite the interest in non-standard PNA secondary structure, very few studies have focused on the effects that cyclic PNA or tethering can produce in non-duplex secondary structure. We discovered significant control over binding affinity and stoichiometry is possible through several entropy-reducing methods.

In the fourth and final chapter, I briefly summarize the dissertation and discuss future avenues of research in this area.

Acknowledgements

For the past five years, as I have meticulously slogged through the magical experience that is graduate school, I have been indisputably fortunate to have ample help every step of the way. I have heard the horror stories of graduate school experiences gone awry: lab mates you dislike, arduous research seemingly guaranteed to fail, and an advisor that you (and everybody else, for that matter) cannot stand and who teaches you nothing. How unfortunate I am not to be able to add to *that* lore! Far from a road to perdition, there has not been a moment in the last five years when I have regretted the decision to continue with my education, seeking a career in chemistry research. That is one accomplishment I cannot take any credit for and owe a debt of gratitude to countless people. The people in the chemistry and graduate school offices, my fellow graduate students and professors, undergraduates who had to endure me as a teaching assistant: all have played varying but important rolls in this achievement. Making all the appropriate acknowledgements is a task more ominous than writing the rest of this thesis has been and trying to thank everybody who is deserving of mention is tilting at windmills.

First and foremost, I would be hard pressed to think of anybody who deserves more thanks than my advisor. Dan, it was your exuberant enthusiasm for your research that persuaded me to come to Northwestern in the first place, and your skills as a teacher and mentor have not disappointed. The way I approach research would be an exercise in futility without the insight and perspective you have instilled in all our graduate students. A special thanks is also due to the other distinguished gentlemen on my thesis committee. Karl, whether it was in your infamous class, the Appella/Scheidt combined group meetings or just hanging out, there was never a time I did not learn something about chemistry around you. I was genuinely disappointed to hear that you could not make it for my final defense. (And, considering the

boom you were probably planning to lower on me, that really is saying something.) SonBinh, I have always enjoyed talking chemistry with you and hold your mechanisms class (and the long days grading your undergraduate exams) in the highest regards. You are an excellent teacher and I have greatly missed our conversations while I have been in Maryland. I graciously thank Regan Thomson for standing in on my thesis committee on such short notice. From our brief meeting and all that I have heard subsequent, I am sorry our time at Northwestern did not coincide. Although most of the professors at Northwestern I interacted with were very helpful, I must single out Fred Lewis for his wise counsel. I learned about more about physical organic chemistry in my two quarters as your teaching assistant than I ever came close to otherwise.

The graduate school experience would have been nothing short of disaster were it not for coworkers and lab mates, current and former, that make showing up for work everyday interesting and enjoyable. Jon, it has been nothing short of illuminating going through the vast bulk of graduate school with you. And as the cofounder of the Englund-Pokorski Center for Angstrom Technology, you will be entitled to much of the vast wealth it is guaranteed to generate one day. Mark, whether it was helping with my chemistry or drinking, you were always willing go that extra yard (especially with the latter). Out-wrestling you at Jon's place might be the highlight of my graduate career. Jackie, you have always injected some much-needed normalcy into our lab. I hope you stick with chemistry even after you marry your professional athlete. Mike, your obvious virtues are surpassed only by your unmistakable wit. Because of you, I smile every time I walk by a Hooters. Graham, it has been a pleasure having you as a lab mate. I look forward to the day your fine English accent is replaced by one more typical of the south side of Chicago. I also need to acknowledge the many folks in the Scheidt lab. Bill,

you're a filthy good chemist and great guy. I would probably like you even if you were not a Vikings fan. Custar, Brooks, Schwin, Troy: we should golf more often.

Out in Maryland, I have had the opportunity to meet many new people. Qun, you have been a friendly (and immensely talented) addition to the Appella lab. Ning, working with you never ceases to amaze (and entertain) me. If this new guy, what's his face, is half as cool as you, we should get along fine. Tanya, our erstwhile zeroth-year graduate student, even though you constantly called me fat and said I should be on a diet, I wish you the best in Colorado. We will all work for you one day. It has been great times getting to know and work with Craig and his lab: Amanda, Chris and Jack. Ken, it is always a pleasure to converse with you about science or anything. Sometimes, I am glad I am a better singer than I am a chemist. I must also thank all my chemistry professors back at Augustana College. They were instrumental in not only proving the virtues and rewards of scientific research but also for rigorously preparing me for the challenges that were ahead. Hopefully, this thesis is evidence that your many efforts were not wasted. Last, but obviously not least, I need to thank my family, especially my parents to whom I dedicate this dissertation. Without your constant guidance and caring, this would certainly not have been possible. I swear: I will not make you call me Dr. Englund for too long.

DEDICATION

Dedicated to my mom and dad.

*Without you both there,
With your effort and care,
I would not be the same man today.
I have been well raised,
Great parenting, unfazed,
And thanks for your great DNA.*

TABLE OF CONTENTS

ABSTRACT	2
ACKNOWLEDGEMENTS	4
DEDICATION	7
TABLE OF CONTENTS	8
LIST OF FIGURES	14
LIST OF SCHEMES	18
LIST OF TABLES	19
ABBREVIATIONS	20

Chapter I. Introduction: Non-Natural Nucleic Acids: Background and

Design.....21

I.1	Introduction: Nucleic Acid Design and Application.....	22
	I.1.1 Nucleic Acids for Medicinal Purposes.....	25
	I.1.2 Nucleic Acids for Diagnostic Purposes.....	27
I.2	Natural Nucleic Acid Analogues.....	27
	I.2.1 Alternatives to Phosphate Linkages.....	28
	I.2.2 Structural Changes to the Sugar Molecule.....	29
I.3	Peptide Nucleic Acids.....	30
	I.3.1 Aminoethylglycine (<i>aeg</i>) PNA.....	30
	I.3.2 Formation of Non-Duplex Secondary Structure with PNA.....	31

	9
I.4 PNA Derivatives and Additional Modification.....	32
I.4.1 PNA Modification: Oligomer Conjugations.....	33
I.4.2 PNA Derivatives.....	34
I.4.2a PNA Derivatives: Sidechain PNA.....	35
I.4.2b PNA Derivatives: Cyclic PNA and (<i>S,S</i>)- <i>trans</i> -cyclopentane PNA (<i>tcyp</i> PNA).....	38
I.4.3 PNA Sidechain Conjugation.....	39
I.5 Design and Potential Applications.....	40
I.5.1 Versatile PNA Monomers for Multifunctional Display.....	40
I.5.2 Exploring the Effect of PNA Preformation on Non-Duplex Secondary Structure.....	44
References: Chapter 1.....	185

Chapter II. Synthesis and Studies of Versatile γ -Substituted Sidechain

PNA.....	47
II.1 Introduction: Initial Experimental Design and Synthetic Targets.....	48
II.2 Synthesis of γ -PNA Possessing Amine-Containing Sidechains.....	48
II.2.1 (L)-2,3-diaminopropionic acid(Cbz) γ -substituted PNA Monomer (^L Dap γ - PNA).....	49
II.2.2 Lysine(Cbz) γ -Substituted PNA Monomers (^L K γ -PNA).....	54
II.2.3 (L)-Lysine(Fmoc) γ -Substituted PNA Monomers (^L K γ -PNA).....	56
II.3 Oligomer/Solid-Phase Synthesis.....	58

	10
II.3.1 PNA Oligomer Synthesis Incorporating γ -PNA(Cbz).....	58
II.3.2 Modification of L K γ -PNA Sidechains while on Solid Support.....	59
II.3.3 Automation of Solid Phase PNA Oligomer Synthesis.....	60
II.4 Thermal Melting Analysis of Substituted γ -PNA with DNA.....	61
II.4.1 The Effect of Unconjugated L K γ -PNA on PNA/DNA Duplex Stability.....	61
II.4.2 The Effect of Stereochemistry on K γ -PNA Duplexes.....	63
II.4.3 Effect of Chain Length for Amine-Containing γ -PNA Oligomers.....	65
II.4.4 Effect of Amide Conjugation on the Stability of L K γ -PNA Oligomers.....	66
II.4.5 L K γ -PNA Mismatch Selectivity.....	71
II.5 Thermal Melting Analysis of L K γ -PNA with RNA.....	73
II.6 Circular Dichroism Studies of L K γ -PNA.....	74
II.7 L K γ -PNA as Scaffolds for Fluorescent Molecules.....	75
II.7.1 L K γ -PNA Light-Up Probes Using Fluorene.....	76
II.7.2 L K γ -PNA Light-Up Probes Using Thiazole Orange.....	78
II.8 Summary and Discussion.....	80
II.9 Experiment Procedures and Data.....	82
II.9.1 γ -PNA Monomer Synthesis.....	82
II.9.1a General Methods.....	82
II.9.1b L Dap γ (Cbz)-PNA Monomer Synthesis.....	83
II.9.1c L K γ (Cbz)-PNA Monomer Synthesis.....	92
II.9.1d L K γ (Fmoc)-PNA Monomer Synthesis.....	97
II.9.2 PNA Oligomer Synthesis and Characterization.....	101

	11
II.9.2a General Solid-Phase Synthesis Procedure.....	101
II.9.2b PNA Purification and Characterization.....	105
II.9.3 PNA UV-Melting and Circular Dichroism Studies.....	107
II.9.4 PNA Fluorescent Studies.....	107
II.9.5 Selected Spectra.....	108
II.9.5a Small-Molecule NMR Spectra.....	108
II.9.5b PNA Oligomer Mass Spectrometry Data.....	123
References: Chapter II.....	194

Chapter III. Control of PNA Non-Duplex Secondary Structure Through

Preorganization.....	139
III.1 Introduction: Initial Experimental Design.....	140
III.2 <i>tcypPNA</i> Influence on the Formation and Stability of Bis-PNA Triplexes.....	140
III.2.1 Bis-PNA Constructed from <i>aegPNA</i> : Design, Synthesis and Application.....	140
III.2.2 Bis-PNA Constructed from <i>tcypPNA</i> Synthesis.....	142
III.2.2a Synthesis of <i>tcypPNA</i> Monomers.....	142
III.2.2b Synthesis of <i>tcypPNA</i> Oligomers.....	143
III.2.3 Melting Studies of Bis-PNA-Containing <i>tcypPNA</i>	144
III.3 G_4 PNA Constructed from (<i>S,S</i>)- <i>tcypPNA</i>	146
III.3.1 (<i>S,S</i>)- <i>tcypPNA</i> Effect on the G_4 Quadruplex: Melting Studies.....	146
III.3.1a (<i>S,S</i>)- <i>tcypPNA</i> G_4 Quadruplex Stability: PNA Homodimers.....	147
III.3.1b (<i>S,S</i>)- <i>tcypPNA</i> G_4 Quadruplex Stability: PNA/DNA	
Heterotetramers.....	148

	12
III.3.2 (<i>S,S</i>)- <i>tcyp</i> PNA Effect on the G ₄ Quadruplex: Circular Dichroism.....	151
III.3.2a (<i>S,S</i>)- <i>tcyp</i> PNA G ₄ Circular Dichroism: Heterotetramers.....	151
III.3.2b (<i>S,S</i>)- <i>tcyp</i> PNA G ₄ Circular Dichroism: Homodimers.....	152
III.3.2c (<i>S,S</i>)- <i>tcyp</i> PNA G ₄ Circular Dichroism: Stoichiometry.....	154
III.4 G ₄ PNA Constructed from a Tethered Lysine Core.....	155
III.4.1 Synthesis of Tethered Guanine <i>aeg</i> PNA.....	155
III.4.2 Melting Studies of Tethered Guanine <i>aeg</i> PNA.....	156
III.4.3 Circular Dichroism Studies of Tethered Guanine <i>aeg</i> PNA.....	157
III.5 Summary and Conclusions.....	160
III.6 Experimental Data and Procedures.....	160
III.6.1 Synthesis of <i>tcyp</i> PNA N7 Guanine(^t Bu) Monomer from Benzyl Ester Backbone.....	160
III.6.2 Solid-Phase Synthesis <i>tcyp</i> PNA and Tethered Oligomers.....	162
III.6.2a Solid-Phase Synthesis of <i>tcyp</i> PNA Oligomers.....	163
III.6.2b Solid-Phase Synthesis Tethered Oligomers.....	163
III.6.3 Characterization of <i>tcyp</i> PNA and Tethered Oligomers.....	164
III.6.4 Melting Experiments of <i>tcyp</i> PNA and Tethered Oligomers.....	164
III.6.5 Circular Dichroism Experimental.....	165
III.6.6 Additional Selected Spectra.....	166
III.6.6a Additional Melting Experiments.....	166
III.6.6b Mass Spectrometry Data.....	171
References: Chapter III.....	198

	13
Chapter IV. Conclusions and Future Studies	177
IV.1 Conclusion.....	178
IV.2 Future Projects and Avenues of Research.....	178
IV.2.1 Overview: Basic Studies.....	178
IV.2.2 Useful ^L K _γ -PNA Monomer Targets.....	179
IV.2.2a Extended Fmoc-Protected Bases: Adenine, Cytosine.....	179
IV.2.2b Guanine Monomers.....	180
IV.2.2c Fmoc-Mediated Oligomer Synthesis.....	181
IV.2.3 ^L K _γ -PNA Compatibility with (<i>S,S</i>) <i>tcyp</i> PNA.....	182
IV.2.4 ^L K _γ -PNA As Protein-Binding Molecules.....	183
References: Chapter IV.....	201
Curriculum Vitae	203

LIST OF FIGURES

Chapter I. Introduction: Nonnatural Nucleic Acids: Background and Design

Figure I-1.	Watson-Crick Hydrogen Bonding Mode in DNA Duplex Formation.....	22
Figure I-2.	The Central Dogma of Molecular Biology.....	23
Figure I-3.	Triplex-Forming Oligonucleotides.....	24
Figure I-4.	Guanine Quadruplex Formation.....	25
Figure I-5.	Telomere Quadruplex Formation.....	26
Figure I-6.	Targeting Natural Nucleic Acids for Medicinal Purposes.....	26
Figure I-7.	Nucleic Acid Analogues with Non-Phosphodiester Backbones.....	28
Figure I-8.	Nucleic Acid Analogues with Altered Sugar Structures.....	29
Figure I-9.	Peptide Nucleic Acids: Comparison to DNA.....	30
Figure I-10.	Arrangement for Hoogsteen Hydrogen Bonding by Pseudo-Isocytosine (J).....	31
Figure I-11.	PNA:DNA Quadruplex Formation.....	32
Figure I-12.	PNA Conjugation Strategies.....	33
Figure I-13.	Functionalized PNA Derivatives.....	34
Figure I-14.	Detrimental PNA Derivatives.....	35
Figure I-15.	Side-Chain Peptide Nucleic Acids.....	36
Figure I-16.	α -Sidechain PNA.....	37
Figure I-17.	β,γ -Carbocyclic PNA.....	38
Figure I-18.	Amine-Containing γ -Side Chain PNA.....	41
Figure I-19.	Examination of the γ -Position in the PNA:DNA Duplex.....	41

	15
Figure I-20. Newman Projection About the β - γ Carbon Bond.....	43
Figure I-21. Bis-PNA Triple Helix Formation.....	44
Figure I-22. N7-Guanine Hoogsteen Bonding as a Protonated Cytosine Mimic.....	45
Figure I-23. Model for Three Covalently Linked PNA Guanine Oligomers.....	46

Chapter II. Synthesis and Studies of Versatile γ -Substituted Sidechain PNA

Figure II-1. Initial γ -PNA monomer Targets.....	48
Figure II-2. Orthogonally Protected 2,3 diaminopropionic acid (Dap).....	49
Figure II-3. Route to Dap using the Hofmann Rearrangement.....	49
Figure II-4. ^L K γ -PNA Monomer Enantiomers Synthesized.....	56
Figure II-5. Nielsen Sequence of <i>aeg</i> PNA.....	62
Figure II-6. ^L K γ -PNA with Unconjugated Primary Amines: Various Bases.....	62
Figure II-7. ^L K γ -PNA with Unconjugated Primary Amines: Different Stereochemistry.....	63
Figure II-8. Newman Projection About the β - γ Carbon Bond.....	64
Figure II-9. ^L γ -PNA with Unconjugated Primary Amines: Different Sidechain Length.....	65
Figure II-10. Possible Rearrangement of ^L Dap γ -PNA Causing Duplex Destabilization.....	66
Figure II-11. Conjugates from ^L K γ -PNA Examined in PNA oligomers.....	66
Figure II-12. Molecular Model of Adjacent/Conjugated ^L K γ -PNA.....	70
Figure II-13. Circular Dichroism Spectrum of PNA II-5.....	74
Figure II-14. Sidechain PNA Used in Preorganization Studies.....	75
Figure II-15. Nucleic Acid Molecular Beacons.....	76
Figure II-16. Fluorene γ -PNA “Light-Up” Probe Design.....	77
Figure II-17. Fluorene γ -PNA Probe Fluorescent Emission.....	78

	16
Figure II-18. Typical Thiazole Orange-PNA Molecular Probe.....	79
Figure II-19. Thiazole Orange γ -PNA Probe Fluorescent Emission.....	79
Figure II-20. Recent Advances in γ -PNA Research.....	81
Chapter III. Control of PNA Non-Duplex Secondary Structure Through Preorganization	
Figure III-1. Plasmid DNA Functionalized with Conjugated Bis-PNA Anchors.....	140
Figure III-2. <i>aeg</i> PNA N7-Guanine(ⁱ Bu) and Incorporation into an Bis-PNA.....	141
Figure III-3. PNA III-1/Oregon Green Conjugate Used in Cell Studies.....	142
Figure III-4. Acyl-Transfer Reactions Common in PNA Under Basic Conditions.....	143
Figure III-5. Non-Standard PNA Residues Incorporated in Bis and Quadruplex PNA.....	144
Figure III-6. Melting Curves of PNA III-1 and PNA III-4.....	145
Figure III-7. Quadruplex formation of G ₄ DNA.....	146
Figure III-8. PNA III-7/G ₄ DNA Tetraplex Hysteresis.....	150
Figure III-9. CD Spectrum of G ₄ DNA Homodimer.....	151
Figure III-10. CD Spectra of PNA III-7 and PNA III-8 with G ₄ DNA.....	152
Figure III-11. CD Spectra of PNA III-7 and PNA III-8 Annealed Without DNA.....	153
Figure III-12. CD Spectrum of PNA III-7 Annealed With and Without NaCl.....	154
Figure III-13. Job Plots of PNA III-7 and PNA III-8 with G ₄ DNA.....	155
Figure III-14. Short Guanine PNAs Tethered to a Lysine Core.....	155
Figure III-15. Annealing Profiles of PNA III-9 at 15 and 50 μ M.....	157
Figure III-16. CD Spectrum of PNA III-9 with Guanine-Rich ssDNA.....	158
Figure III-17. Job Plot of PNA III-9 with Guanine-Rich ssDNA.....	158
Figure III-18. Possible Modes of PNA III-9 Binding DNA.....	159

	17
Figure III-19. CD Spectra of PNA III-9 with G ₄ DNA.....	159

Chapter IV. Conclusions and Future Studies

Figure IV-1. Proposed ^L K γ -PNA Monomers for Fmoc Solid-Phase Synthesis.....	181
Figure IV-2. The Combination of ^L K γ -PNA and <i>tcyp</i> PNA: Solubility.....	182
Figure IV-3. The Combination of ^L K γ -PNA and <i>tcyp</i> PNA: Molecular Beacons.....	183

LIST OF SCHEMES

Chapter II. Synthesis and Studies of Versatile γ -Substituted Sidechain PNA

Scheme II-1. Failed Synthesis of Dap, Intramolecular Isocyanide Trapping.....	50
Scheme II-2. Synthesis of Protected Dap Starting from Aspartic Acid.....	51
Scheme II-3. Confirming the Optical Purity of Dap.....	53
Scheme II-4. The Synthesis of ^L Dap γ -PNA Monomer.....	54
Scheme II-5. Synthesis of ^L K γ -PNA Backbone.....	55
Scheme II-6. Final Steps of ^L K γ -PNA(Cbz) Monomers: Thymine, Adenine, and Cytosine.....	56
Scheme II-7. Synthesis of ^L K γ -PNA(Fmoc) Thymine Monomer.....	57
Scheme II-8. Synthesis of ^L K γ -PNA(Fmoc) Cytosine(Cbz) Monomer.....	58
Scheme II-9. General PNA Oligomer Synthesis via Solid Support.....	59
Scheme II-10. PNA Oligomer Functionalization using ^L K γ -PNA(Fmoc) Residues.....	60

Chapter III. Control of PNA Non-Duplex Secondary Structure Through Preorganization

Scheme III-1. Coupling of ^t Bu-Protected N7-Guanine Acetic Acid on <i>tcyp</i> PNA Backbone.....	143
Scheme III-2. Solid Phase Synthesis of Tethered PNA Trimer.....	156

Chapter IV. Conclusions and Future Studies

Scheme IV-1. Proposed Synthesis of Adenine and Cytosine ^L K γ -PNA(Fmoc) Monomers.....	180
-----------------------------------------------------------------------------------------------------------------	-----

LIST OF TABLES

Chapter II. Synthesis and Studies of Versatile γ -Substituted Sidechain PNA

Table II-1.	T_m Analysis of $^L\text{K}\gamma$ -PNA with Free Amines to Complementary DNA.....	63
Table II-2.	Effect of $^L\text{K}\gamma$ -PNA Stereochemistry on PNA:DNA T_m	64
Table II-3.	T_m Analysis of $^L\text{K}\gamma$ -PNA versus $^L\text{Dap}\gamma$ -PNA.....	65
Table II-4.	T_m Analysis of Substituted $^L\text{K}\gamma$ -PNA with Complementary DNA.....	67
Table II-5.	T_m Analysis of Thiazole Orange-Substituted Polypyrimidine PNA.....	68
Table II-6.	T_m Analysis of Adjacent, Substituted $^L\text{K}\gamma$ -PNA.....	69
Table II-7.	$^L\text{K}\gamma$ -PNA Mismatch Specificity.....	71
Table II-8.	Adjacent Substituted $^L\text{K}\gamma$ -PNA Residues Mismatch Specificity.....	72
Table II-9.	T_m Analysis of $^L\text{K}\gamma$ -PNA with Complementary RNA.....	73
Table II-10.	PNA Oligomer Mass Spectroscopy Data.....	106

Chapter III. Control of PNA Non-Duplex Secondary Structure Through Preorganization

Table III-1.	T_m Analysis of Bis-PNA ₂ :DNA Triplexes.....	145
Table III-2.	T_m Analysis of G ₄ PNA: PNA Quadruplexes.....	148
Table III-3.	T_m Analysis of G ₄ PNA/G ₄ DNA: Hybrid Quadruplexes.....	149
Table III-4.	Comparison of Melting Characteristics between Homodimers and Heterotetramers.....	150
Table III-5.	PNA Oligomer Mass Spectroscopy Data.....	164

ABBREVIATIONS

(A^{Cbz}-CH₂-CO₂H), 6-N-(benzyloxycarbonyl)adenin-9-ylacetic acid; (Ac₂O), acetic anhydride; (Boc₂O), di-*tert*-butyl dicarbonate; (C^{Cbz}-CH₂-CO₂H), 4-N-(benzyloxycarbonyl)cytosine-1-ylacetic acid; (DCM), dichloromethane; (DIEA), *N,N*-diisopropylethylamine; (DMF), *N,N*-dimethylformamide; (DMAP), *N,N*-dimethyl-4-aminopyridine; (EtOAc), ethyl acetate; (EDC), *N*-Ethyl-*N'*-(3-dimethylaminopropyl)carbodiimide; ((Fmoc)mini-PEG), Fmoc 8-amino 3,6 dioctanoic acid; (HATU), O-(7-Azabenzotriazol-1-yl)-*N,N,N',N'*- tetramethyluronium hexafluorophosphate (HBTU), O-(Benzotriazol-1-yl)-*N,N,N',N'*- tetramethyluronium hexafluorophosphate; (HOBt), 1-Hydroxybenzotriazole hydrate; (MBHA), Methyl benzhydryl amine; (MDCHA), *N*-Methyldicyclohexylamine; (NMP), 1-Methyl-2-pyrrolidinone; (RBF), round-bottom flask; (rt), room temperature; (TFA), trifluoroacetic acid; (TFMSA), Trifluoromethanesulfonic acid; (THF), tetrahydrofuran

Chapter I.

Introduction: Nonnatural Nucleic Acids: Background and Design

I.1 Introduction: Non-Natural Nucleic Acid Design and Application

The duplication, rearrangement, and mutation of DNA have shaped all life on earth for over 3 billion years. When Watson and Crick elucidated the structure of duplex DNA¹ and discerned the genetic implications,² new and exciting possibilities for manipulating biology became evident. Through nucleobase hydrogen bonding in purine/pyrimidine pairs (adenine with thymine, guanine with cytosine), single-stranded DNA (ssDNA) is recognizable to a unique DNA complement (Figure I-1). This self-recognition allows DNA replication, transcription into RNA (same nucleobase recognition), and RNA translation into proteins (Figure I-2).³ Although there are a few exceptions to this flow of information in nature, all cellular life on earth follows the so-called “Central Dogma” of molecular biology and the genetic code inherent in the nucleic acids has proven to be universal.

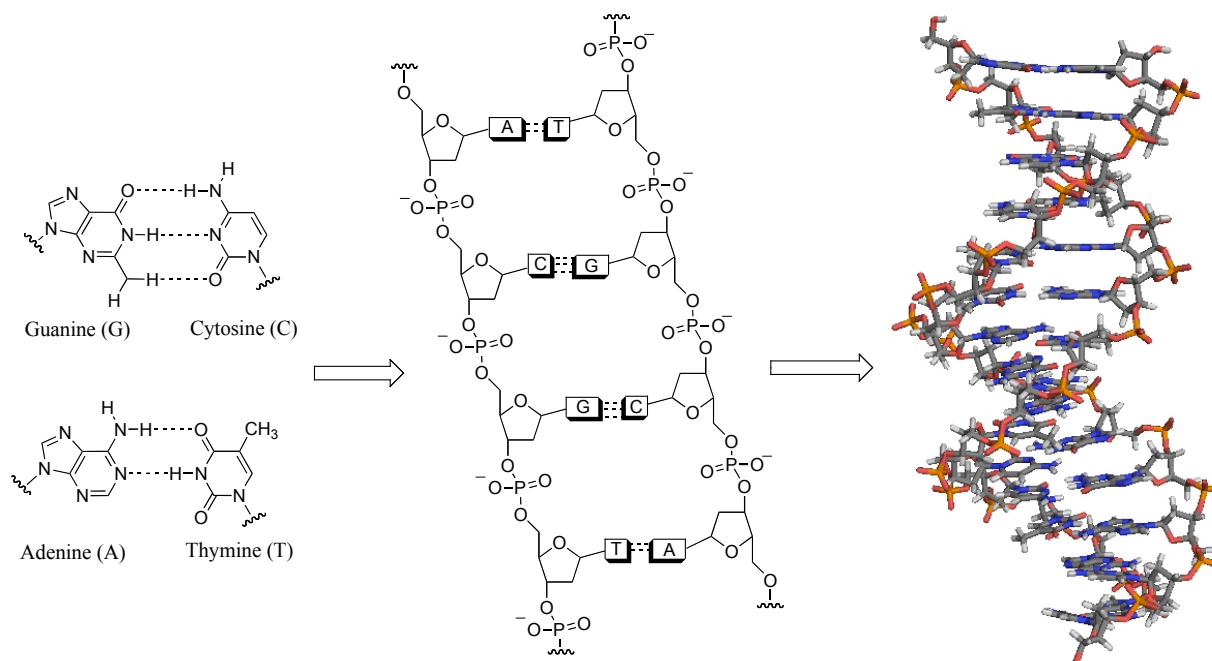


Figure I-1: Watson-Crick Hydrogen Bonding Mode in DNA Duplex Formation. This B-form DNA double helix figure was generated from the PDB 1k8j submitted by Volk and coworkers.⁴

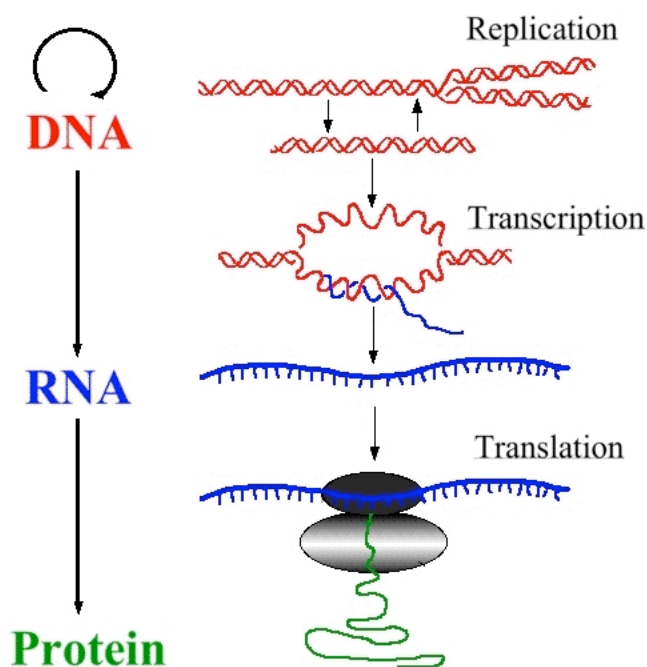
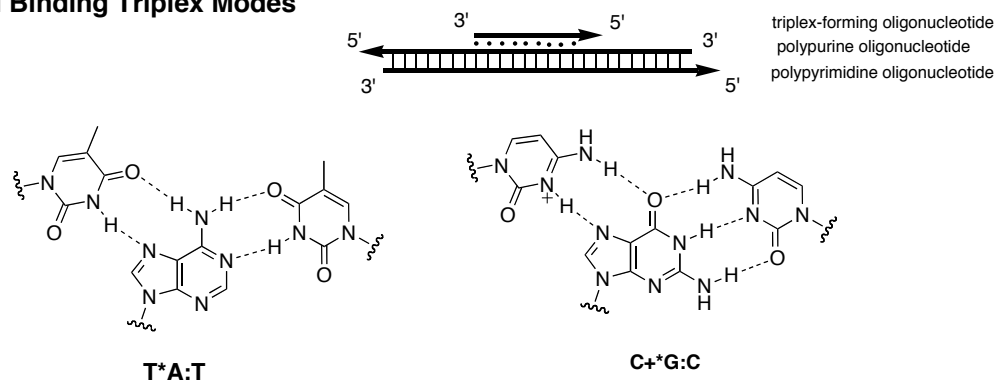


Figure I-2: The Central Dogma of Molecular Biology. Figure adapted from <http://www.accessexcellence.org/RC/VL/GG/central.html>.⁵

In addition to the stable DNA double helix, DNA can assemble into other secondary structures depending on the sequence and mode of hydrogen bonding. A triplex-forming oligonucleotide binds to the major groove of polypurine/polypyrimidine duplexes via hydrogen bonds to the Hoogsteen face of the purines (Figure I-3).⁶ The formation of triplex DNA in vivo is linked to higher rates of mutagenesis and repair mechanisms,⁷ and the application of triplex forming oligonucleotides could be useful in gene therapy.⁸ In triplexes, the presence of a third oligonucleotide results in a more stable complex compared to a duplex.

Guanine has the ability to form tetrads via hydrogen bonding to its Hoogsteen face exclusively (Figure I-4).⁹ Forming in tracts of nucleic acids with intermittent guanine residues, tetrads form in the presence of stabilizing metal ions, most commonly sodium or potassium. Guanine quadruplexes form with four separate nucleic acid strands as well as intramolecular

Anti-Parallel Binding Triplex Modes



Parallel Binding Triplex Modes

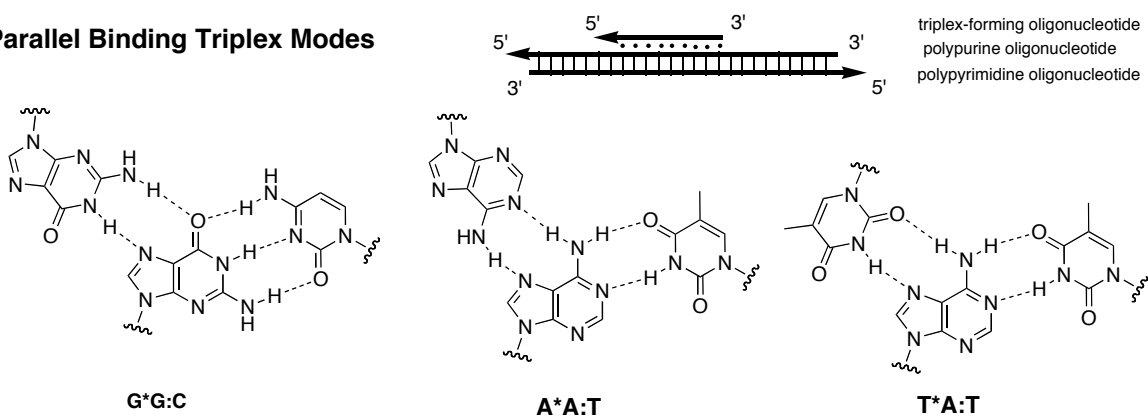


Figure I-3: Triplex-Forming Oligonucleotides.

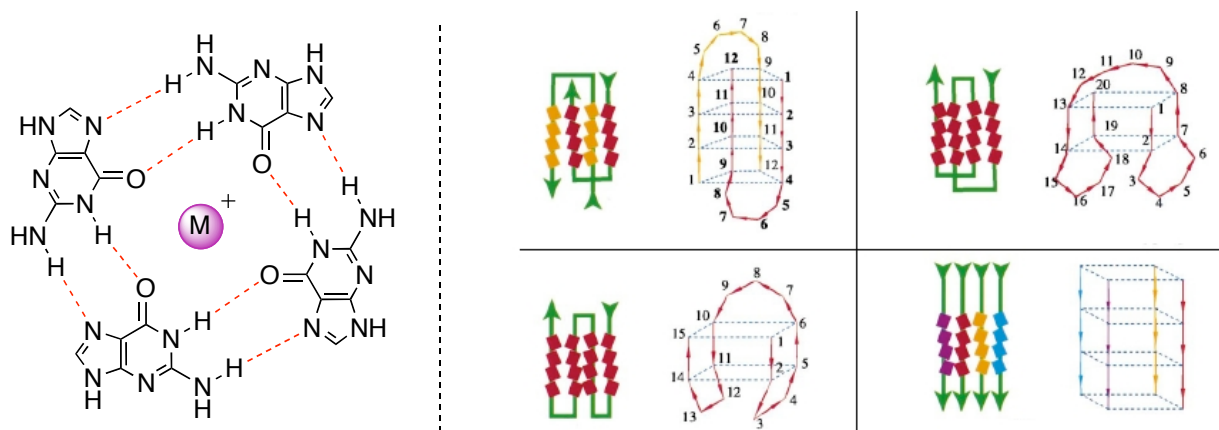


Figure I-4: Guanine Quadruplex Formation.

structures and the formation of guanine-rich tetrads appears to have important roles in cellular regulation.¹⁰ This is especially true of telomeres, the guanine rich single-stranded overhangs on the 3' terminus of chromosomes (Figure I-5).¹¹

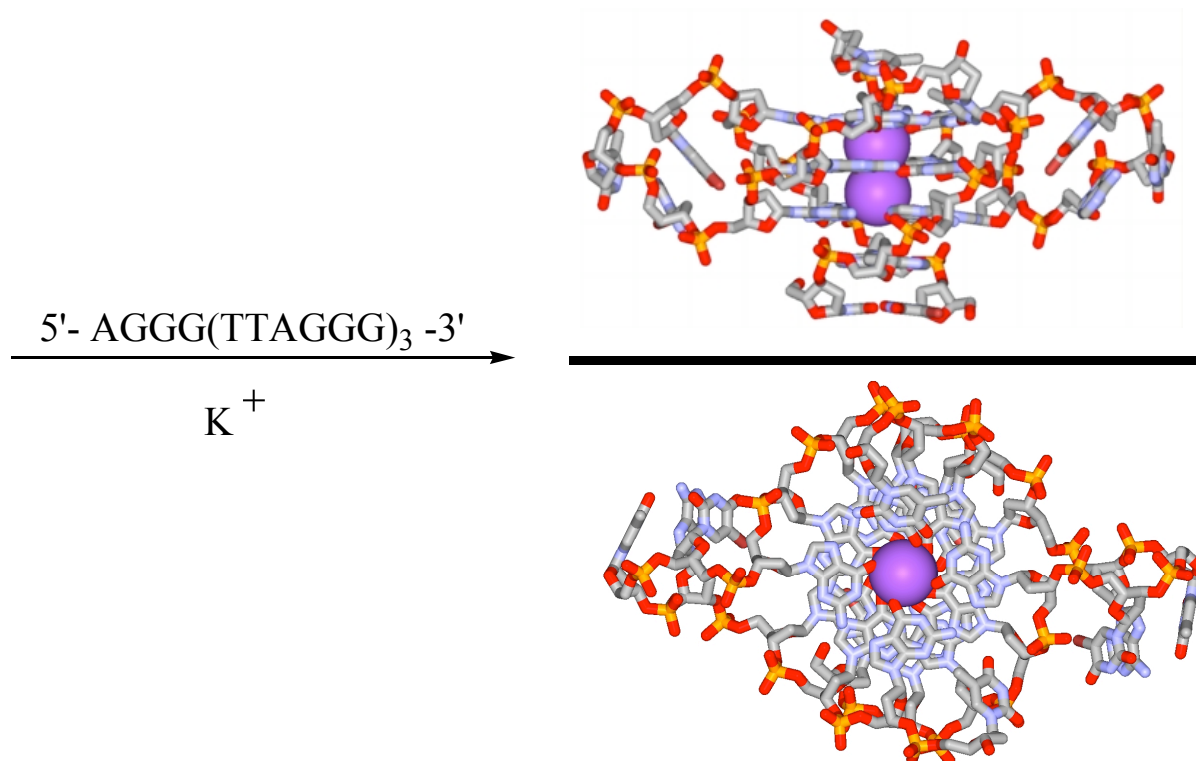


Figure I-5: Formation of Telomere Quadruplex.

Because of their high fidelity, self-association, and obvious biochemical significance, researchers have sought to take advantage of the many unique attributes that nucleic acids possess, both as biological targets as well as a molecular tool.¹²

I.1.1 Nucleic Acids for Medicinal Purposes

Many diseases are linked to the over-expression of specific proteins. Although disabling protein function using small molecules has proven extremely useful in combating illness, many potential protein targets are poor substrates for small molecule binding. Synthesizing ligands to

selectively target a particular protein without binding to other biological targets is challenging for drug design. Furthermore, it is difficult to target protein-protein interactions with small molecules.¹³ Natural nucleic acids are attractive drug targets due to the ubiquitous role they play in protein production. If a ligand binds with an affinity high enough to disrupt DNA transcription (anti-gene)¹⁴ or RNA translation (anti-sense),¹⁵ the “downstream” synthesis of any protein can be inhibited (Figure I-6).

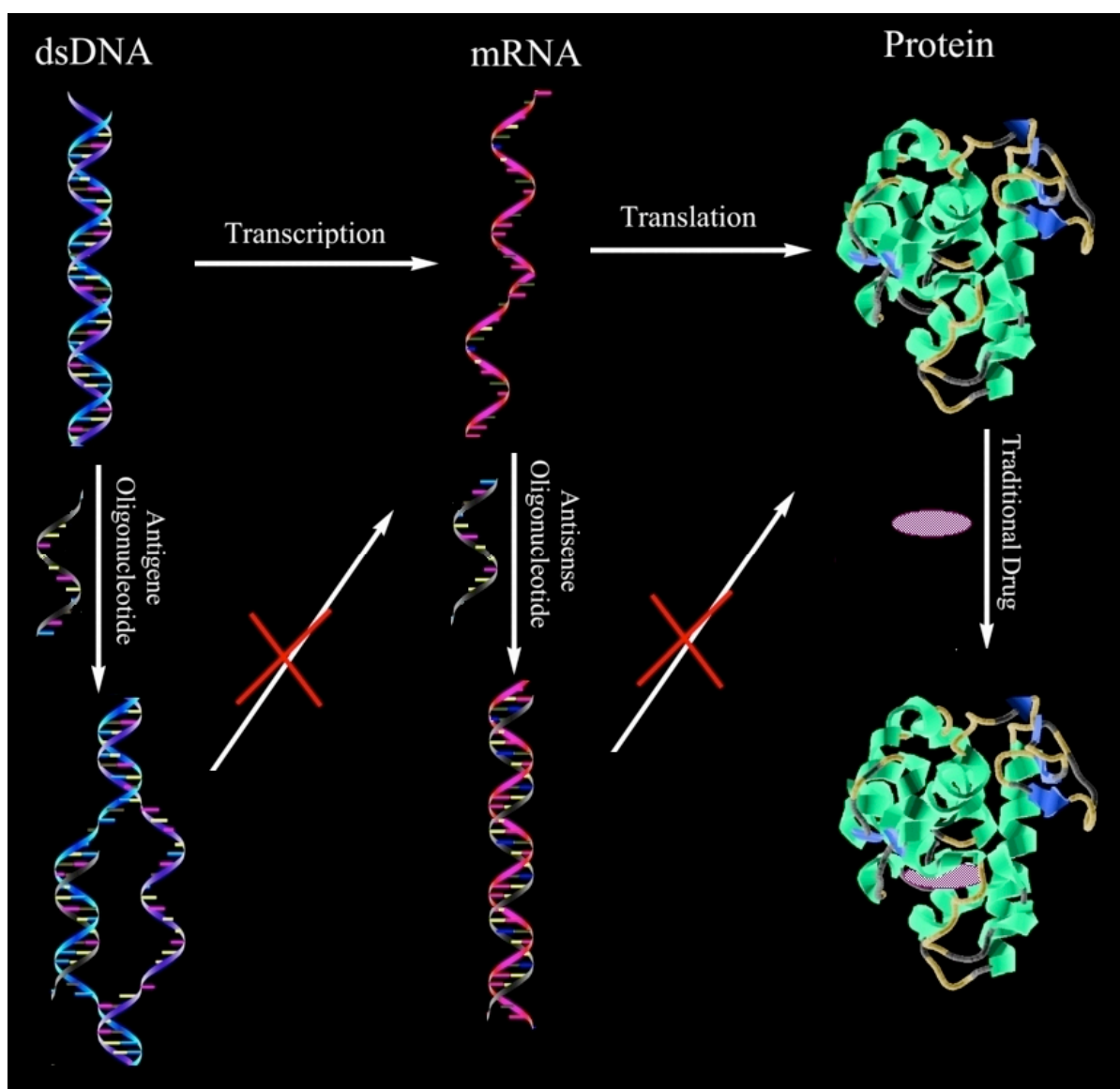


Figure I-6: Targeting Natural Nucleic Acids for Medicinal Purposes.

Peptides and synthetic molecules have been shown to bind to specific portions of natural nucleic acids with high affinity and selectivity.¹⁶ Employing nucleic acids themselves as drugs by taking advantage of the recognition properties of natural nucleotides is a highly attractive tactic because any nucleic acid (and therefore, any protein) can be targeted independent of the sequence. For example, Stephenson and Zamecnik first showed that ssDNA exhibited anti-sense characteristics targeting the complementary Rous sarcoma viral RNA.¹⁷

I.1.2 Nucleic Acids for Diagnostic Purposes

Whether detecting genetic mutations or dangerous pathogens, detecting the presence of specific natural nucleic acids is an important means of diagnosing various diseases, possibly before the manifestation of symptoms.^{18,19} Therefore, the ability to selectively identify natural nucleic acids in a sequence specific manner is important. The difference between wild-type genes and mutant genes differ by as little as one nucleotide base; hence, high selectivity to specific nucleic acid sequences is essential in detection. Methods employing nucleic acid-based detection, sensitive to single nucleobase polymorphisms include fluorescent strategies such as molecular beacons,²⁰ nano-particle-based scanometric assays²¹ and electrochemical techniques.²²

I.2 Natural Nucleic Acid Analogues

Despite the use of nucleic acids as molecular tools for diagnostic or medicinal purposes, natural nucleic acids are poorly suited towards many potential applications. Natural nucleic acids are nuclease-sensitive and rapidly degrade *in vivo*. Also, unlike most small molecule drugs, natural nucleic acids are large and highly charged, making cellular uptake difficult *in vivo*. A large amount of research has focused on synthesizing non-natural nucleic acids to overcome these limitations without disrupting the affinity and selectivity. The most common means of

accomplishing this goal is by carefully altering the architecture of the ribose-phosphate backbone of natural nucleic acids.

I.2.1 Alternatives to Phosphate Linkages

Because the phosphodiester bond is vulnerable to enzymatic cleavage, efforts to improve the pharmacological characteristics of nucleic acids have involved altering or eliminating the phosphate group. These alterations can range from single atom substitution within or around the phosphate group, to the complete replacement of the phosphate in favor of a different molecular linker. This strategy is used to eliminate the charge, changing the backbone from anionic to cationic, and imparting resistance to nucleases (Figure I-7).²³⁻²⁶

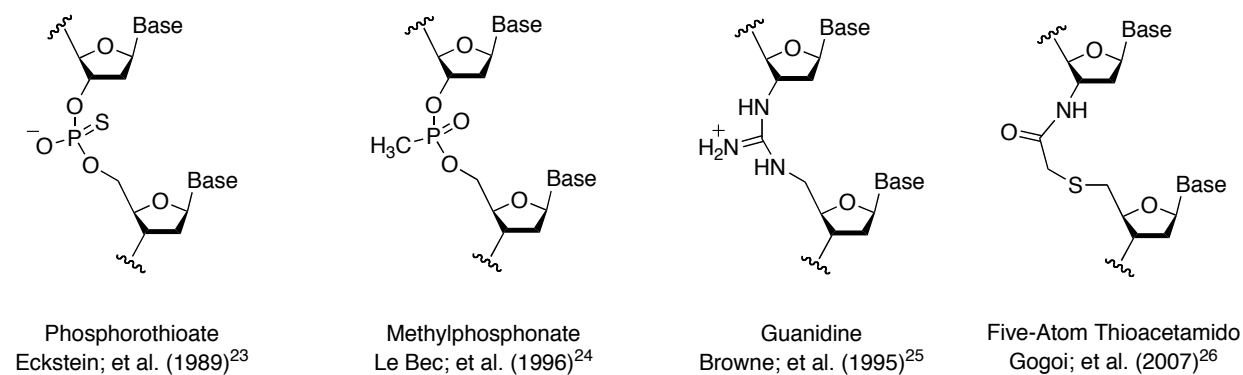


Figure I-7: Nucleic Acid Analogues with Non-Phosphodiester Backbones.

The most commonly used derivative of this type is the phosphorothiolate linkage.²⁷ Although this type of modification reduces the rate of hydrolysis by a variety of nucleases and can activate RNase H, the nuclease stability is still far from ideal. Regardless, phosphorothioates have proven to be a useful “first-generation” synthetic nucleic acid for anti-sense applications. Furthermore, whereas synthetic routes to make oligomers of natural nucleic acids have been successfully optimized, many of the novel linkages between nucleic acids remain challenging to synthesize; many have to be constructed as dimers before incorporation into oligomers.

I.2.2 Structural Changes to the Sugar Molecule

Strategies that alter the ribose portion of a nucleotide are effective at altering the physical properties of oligonucleotides while maintaining or improving the binding characteristics to DNA/RNA sequences. There are currently many strategies for appending functionality to the ribose portion of DNA/RNA or incorporating a completely different sugar (Figure I-8). This type of modification often has the effect of locking the sugar ring into a favorable conformation for binding.

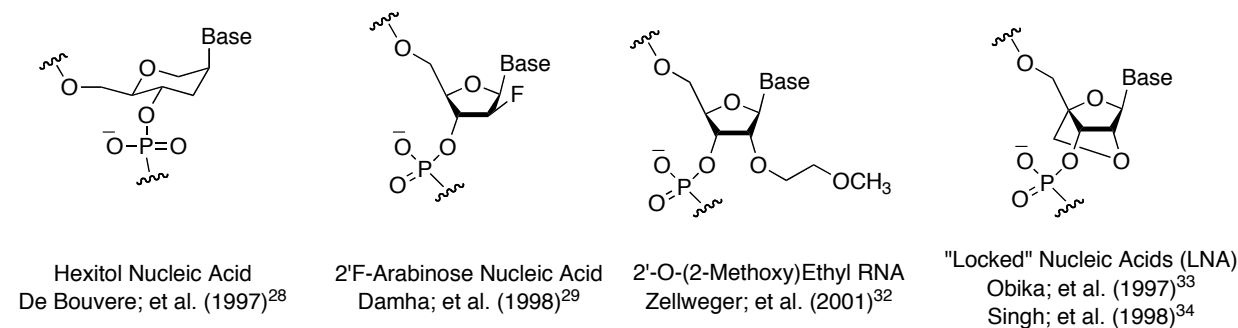


Figure I-8: Nucleic Acid Analogues with Altered Sugar Structures.

Hexitol nucleic acids (HNA) make use of the increased rigidity of a six-membered ring to maintain a 3'-endo conformation.²⁸ Using a 2'-fluorinated arabinose (*D*) in place of the ribose portion results in a ribonuclease resistant substrate that binds RNA with higher affinity than ssDNA²⁹ by maintaining a rigid O4'-endo pucker.³⁰ Derivatives appending functionality to the 2' position of ribose are also effective at increasing binding affinities to natural nucleic acids while imparting a certain amount of enzymatic resistance. The 2'-O-methoxyethylribose modification, when incorporated into DNA oligomers, displays promising resistance to enzymatic degradation³¹ and significant anti-sense activity.³² Locked nucleic acids (LNA) are also promising RNA analogues. 2'-O-4'-(*C*)-methylene-beta-(*D*)-ribofuranosyl nucleotides (LNA monomers), are conformationally locked bicyclic molecules that force the ribose to remain

fixed in a C3'-endo sugar pucker.³³ Because of this, oligomers containing LNA have an extremely strong affinity for natural nucleic acids³⁴ and have demonstrated significant anti-sense activity as well.³⁵ Recent studies, however, suggest that sequence independent hepatotoxicity may hinder the long-term medicinal use of LNA.³⁶

I.3 Peptide Nucleic Acids

I.3.1 Aminoethylglycine (*aeg*) PNA

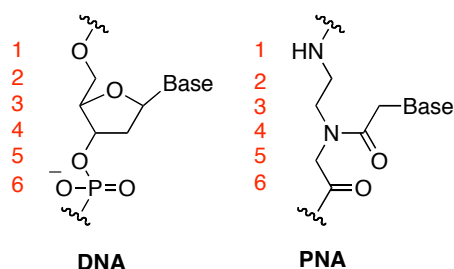


Figure I-9: Peptide Nucleic Acids: Comparison to DNA.

Peptide nucleic acids (PNAs), developed by Nielsen and coworkers, were the first successful example of oligomers in which the entire sugar-phosphate backbone of DNA/RNA was replaced with an acyclic peptide-based backbone (Figure I-9).³⁷ Modeled by means of a computer as an atom-by-atom replacement of DNA for use as a triplex-forming oligonucleotide, the nucleobases are preserved and attached to an aminoethylglycine (*aeg*) backbone via an amide bond. Oligomers constructed from *aeg*PNA exhibit high thermal stability to complementary nucleic acids, and also demonstrate higher selectivity, as mismatched base pairs cause a much larger decrease in complex stability compared to natural nucleic acids.³⁸ In contrast to DNA or RNA, *aeg*PNA oligomers are uncharged, and therefore binding to complementary nucleic acids is not salt dependant,³⁹ and hybridization can even occur in the presence of polar organic solvents.⁴⁰ PNA oligomers are also stable to nuclease degradation that hinders the use of natural nucleic acids for in vivo applications.⁴¹ Researchers are actively investigating the use of

*aeg*PNA for anti-gene therapy,⁴² anti-sense activity,⁴³ and both solution-phase⁴⁴ and surface-based nucleic acid-detection systems.⁴⁵

I.3.2 Formation of Non-Duplex Secondary Structure with PNA

PNA was first shown to form very stable PNA₂:DNA triplexes with polythymine PNA oligomers and the complementary polyadenine DNA.⁴⁶ Besides the stability afforded by the additional Hoogsteen hydrogen bonding motif (although weak relative to Watson-Crick bonding), PNA₂:DNA triplexes may be additionally stable because of the secondary structure formed. PNA duplexes (commonly referred to as P-form type duplexes) are wider (about 27 Å diameter) than B-form duplexes observed in dsDNA.⁴⁷ However, in order for DNA to undergo triplex formation, a much broader, wider helix is formed, resembling the PNA:PNA helix.⁴⁸ This implies that the natural conformation of triplex DNA is much better suited to the conformational tendencies of *aeg*PNA oligomers. The stability of PNA₂:DNA triplexes can be strengthened further if cytosine residues are replaced with a protonated cytosine mimic, such as pseudo-isocytosine (J), in the parallel Hoogsteen strand (Figure I-10).⁴⁹

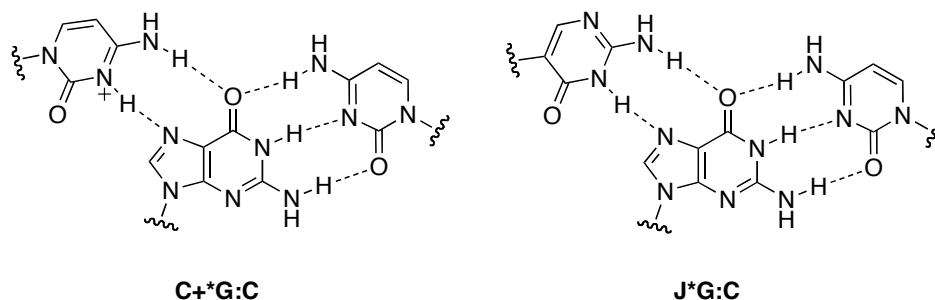


Figure I-10: Arrangement for Hoogsteen Hydrogen Bonding by Pseudo-Isocytosine (J).

As with DNA, PNA forms guanine tetraplexes in the presence of metal ions, which stabilize the structure through carbonyl coordination. Krishnan-Gosh and coworkers first demonstrated evidence of this property using PNA tetramers containing three successive

guanine residues.⁵⁰ A longer PNA oligomer (G₄ PNA) was later shown to form dimers⁵¹ as well as stable 2:2 quadruplex structures with the G₄ DNA (Figure I-11).⁵²

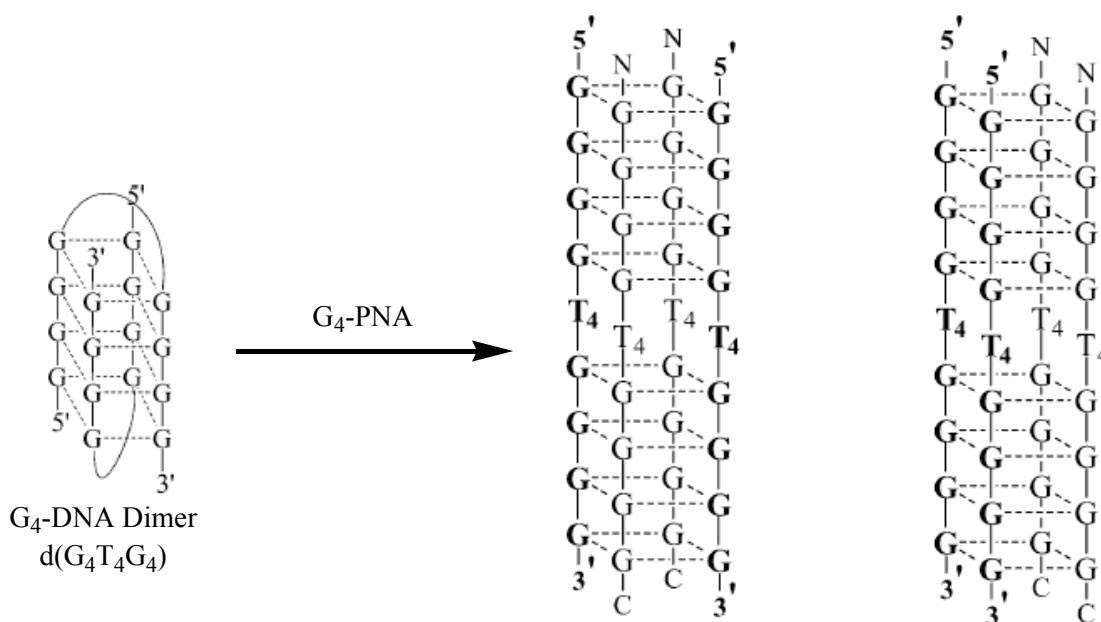


Figure I-11: PNA:DNA Quadruplex Formation.⁵²

I.4 PNA Derivatives and Additional Modification

Despite extensive research and many successful applications of *aeg*PNA, there are many drawbacks associated with *aeg*PNA. PNA oligomers, especially those with extensive numbers of guanine and thymine, have low solubility under biologically relevant conditions. Also, lack of solubility limits the length of PNA oligomers. PNA oligomers are not cell-permeable,⁵³ and bioavailability is poor because PNA administered *in vivo* is promptly sequestered and excreted through the kidneys.⁵⁴ Furthermore, binding to biological targets is complicated by the presence of stable nucleic acid secondary⁵⁵ and tertiary structures that prevent PNA invasion.⁵⁶ Because

of these limitations, many strategies have been developed to optimize PNA binding characteristics or alter PNA oligomer physical properties.

I.4.1 PNA Modification: Oligomer Conjugations

Conjugation of various moieties to nucleic acids can overcome inherent medicinal limitations and increase the number of potential applications.⁵⁷ Similarly, conjugation has been employed to change the physical characteristics of PNA oligomers.⁵⁸ This is usually accomplished by appending moieties directly to the termini, or to the nucleobases within the oligomer (Figure I-12).

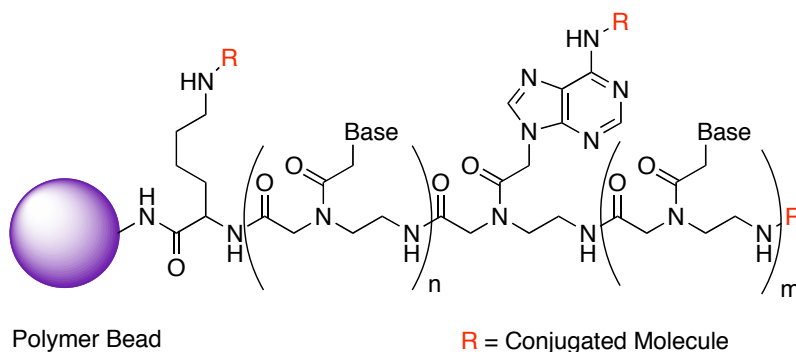


Figure I-12: PNA Conjugation Strategies.

Conjugates are often used to improve cellular uptake of PNA oligomers using a variety of strategies. This can be accomplished by appending sugar derivatives,⁵⁹ positively charged or cell-penetrating peptides,⁶⁰ or large hydrophobic molecules.^{61,62} Coupling planar, aromatic molecules to the termini of PNA can improve the kinetics of binding and promote DNA duplex strand invasion via intercalation.⁶³ Furthermore, fluorophores can be attached to PNA oligomers for stemless molecular beacons,⁶⁴ polymerase chain reaction (PCR) clamps,⁶⁵ and other light-up probes.⁶⁶ By adding functional moieties, the utility and number of potential applications are expanded for PNA.

I.4.2 PNA Derivatives

Although *aeg*PNA oligomers have many desirable characteristics, much research has focused on synthesizing and studying PNA derivatives to optimize or augment its existing properties. Common goals include increased binding affinity, greater mismatch discrimination, differentiation between DNA/RNA, parallel vs. anti-parallel binding affinity, selectivity for binding to natural nucleic acid oligomers (i.e., PNA that does not bind to its complementary PNA oligomer), and greater aqueous solubility (Figure I-13).⁶⁷⁻⁷² Many attempts to alter the basic *aeg*PNA monomer destabilize secondary structures, however (Figure I-14).⁷³⁻⁷⁶ Changing the length of the pseudo-peptide backbone or the length of the nucleobase linker also yields

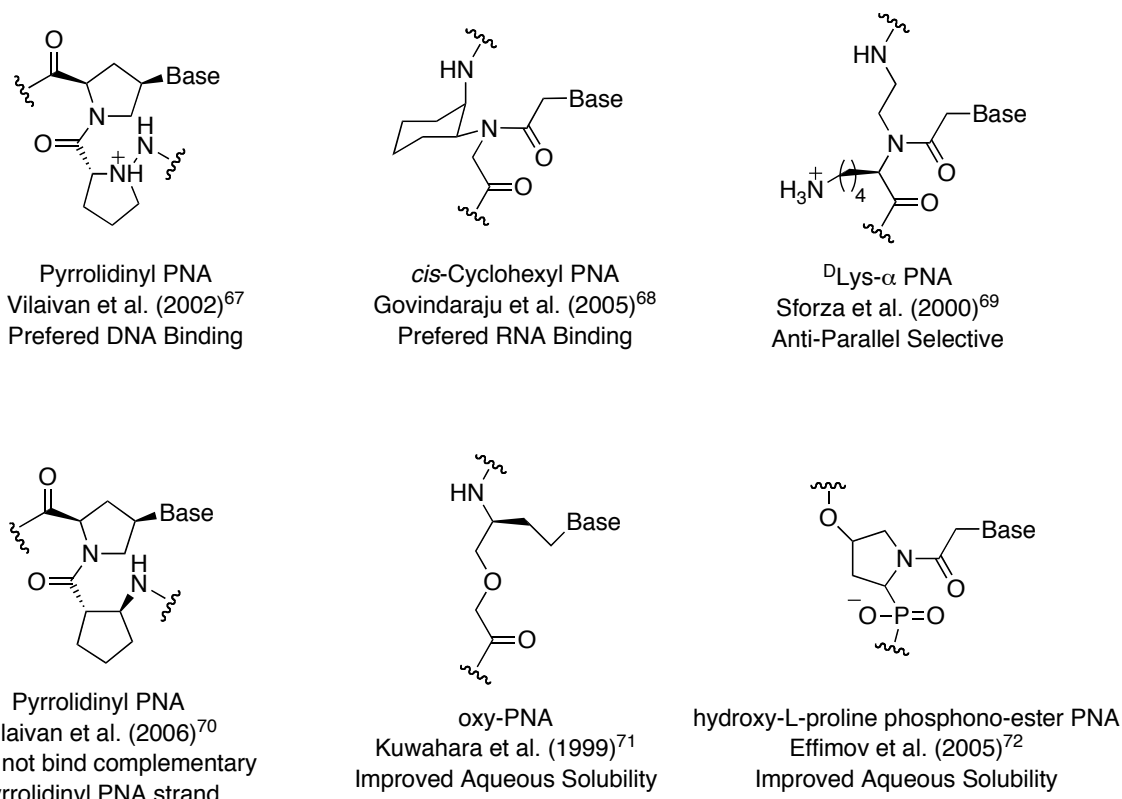


Figure I-13: Functionalized PNA Derivatives.

oligomers with reduced binding affinity.⁷⁷ As was the case with DNA and RNA derivatives, the most promising PNA derivatives invented thus far are those that pay special attention to the spacing, conformational considerations and binding properties of *aeg*PNA.

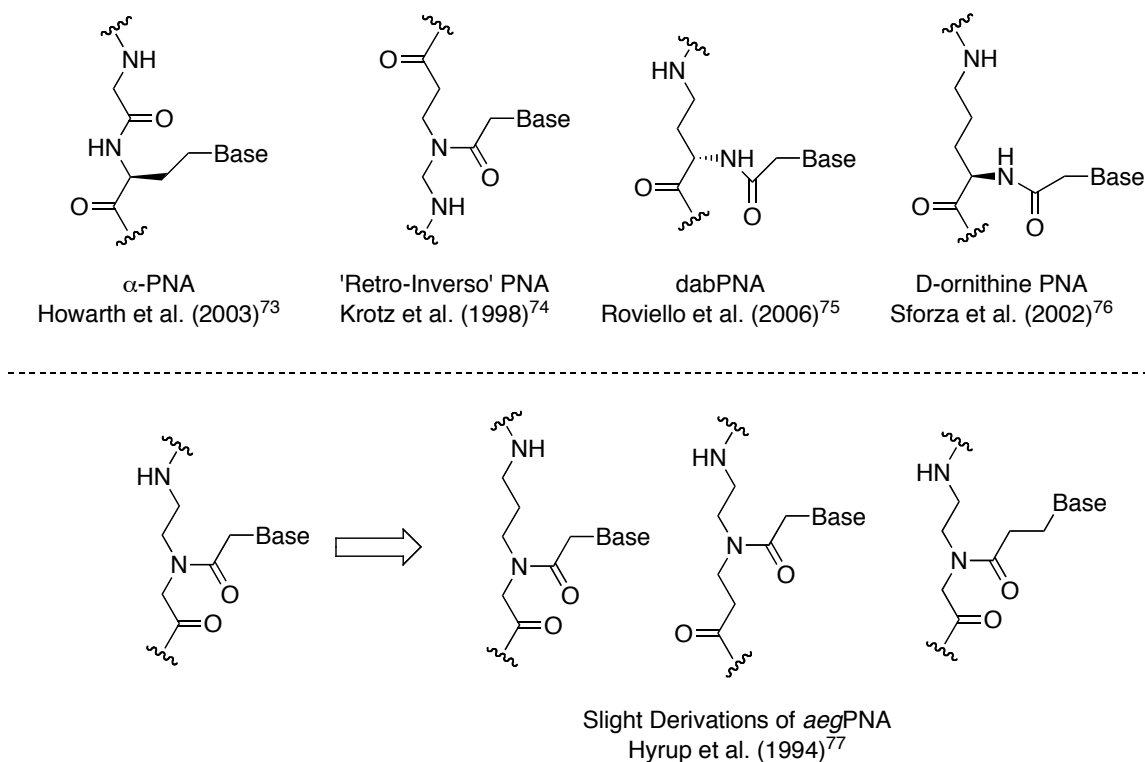


Figure I-14: Detrimental PNA Derivatives. Slight changes in backbone structure can decrease or abolish nucleic acid binding affinity.

I.4.2a PNA Derivatives: Sidechain PNA

Expanding the characteristics and utility of PNA by using the existing aminoethylglycine backbone as the core template to attach further functionality has yielded promising initial results (Figure I-15). Sidechain-bearing PNA monomers have been successfully synthesized, incorporated into *aeg*PNA oligomers and analyzed. The first example of a PNA monomer containing a rudimentary sidechain was synthesized with alanine in place of the glycine portion of *aeg*PNA (aminoethylalanine backbone).⁷⁸ The incorporation of an additional methyl group at

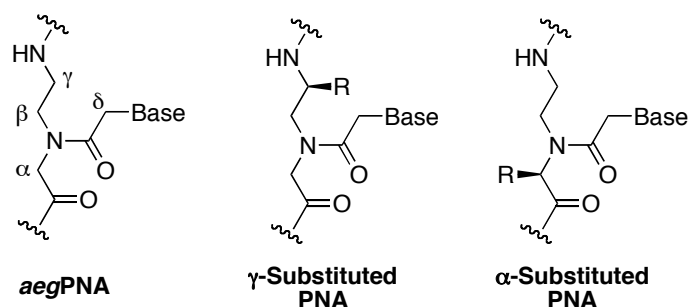


Figure I-15: Side-Chain Peptide Nucleic Acids.

the α -position of PNA had two important effects: the binding affinity only slightly decreased and PNA oligomers incorporating alanine were no longer devoid of stereogenic centers, showing that stereochemistry influences binding characteristics, such as non-racemic PNA duplexes. After examination of numerous examples, it was found that α -substituted PNA derived from D-amino acids (*R* stereochemistry) bind with higher affinity than their L-amino acid enantiomers.⁷⁹ Oligomers containing α side chains were attractive for multiple reasons. Synthetically, α -substituted PNA monomers were readily accessible by substituting other amino acids in the place of glycine. Furthermore, even when side chains substantially decrease the complementary melting temperature, the mismatch discrimination increases, regardless of stereochemistry.⁸⁰ This is probably due to the added rigidity (bulky groups hindering free bond rotation) resisting the realignment that a nucleobase mismatch would require. The effect is even amplified when mismatches are present in a series of α -substitutions.⁶⁹ This has led to multiple interesting uses from α -carbon substituted PNA, especially cationic side chains that do not detract from binding affinity when used non-adjacently. This strategy has led to PNA oligomers with greater solubility,⁸⁰ cellular uptake,^{81,82} and desirable pharmacodistribution⁸³ while either maintaining duplex stability or slightly reducing binding affinity to levels still acceptable (Figure I-16).

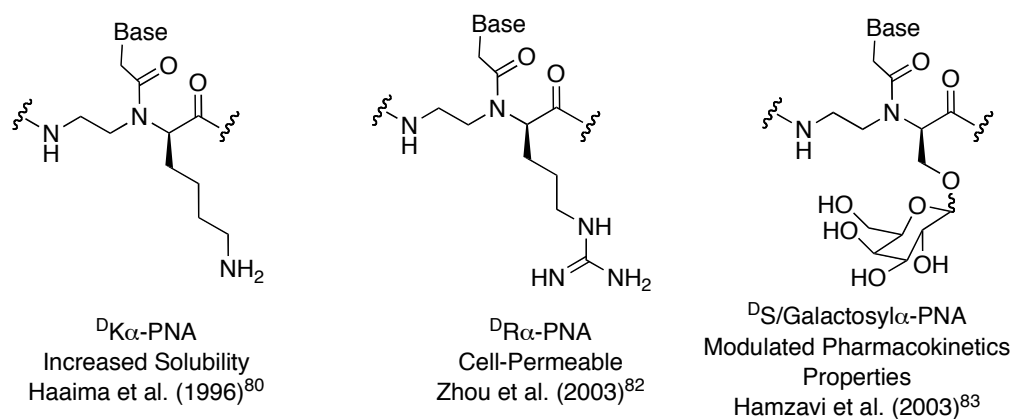


Figure I-16: α -Sidechain PNA.

Despite the initial success and implementation of α -side chain-containing PNAs, several important limitations became apparent. As the size of the substituent at the α -position increased, it invariably interfered with duplex formation, decreasing the melting temperature. Also, α -substituted, D-Lysine PNA ($^D\text{K}\alpha\text{-PNA}$) monomers diminish the binding affinity to fully complementary DNA and RNA when used in an adjacent series, even when destabilization does not occur when used separately or alone.

Regardless of the initial utility and potential impact of α -substituted PNA, other strategies for substitution along the PNA backbone have been less focused until recently. A synthetic strategy for both the Fmoc-protected and Boc-protected PNA monomers with methyl groups substituted at the γ -position (L-Alanine γ -PNA or $^L\text{A}\gamma\text{-PNA}$) were proposed and carried out.^{84,85} Oligomers incorporating the $^L\text{A}\gamma\text{-PNA}$ were synthesized on solid support using Fmoc chemistry; however, the binding studies were never reported. Densely functionalized monomers possessing multiple side chains have been synthesized through both Mitsunobu⁸⁶ and Ugi four-component coupling reactions,⁸⁷ but these monomers have yet to be incorporated into PNA oligomers or examined in a biophysical context. In our lab, PNA monomers containing methyl esters substituted at the α - and β -positions were synthesized from 2,3 diaminopropionic acid.

Unfortunately, when incorporated into poly-thymine PNA oligomers via Boc solid-phase synthesis, no binding to the complementary DNA was observed.⁸⁸

I.4.2b PNA Derivatives: Cyclic PNA and (*S,S*)-*trans*-cyclopentane PNA (*tcyp*PNA)

Preorganization by the restriction of bond rotation is an effective means for improving the recognition properties of nucleic acid derivatives.⁸⁹ In this regard, cyclic PNA is an important type of modified PNA in which the standard *aeg*PNA residue has one or multiple rings.⁹⁰ By eliminating potential bond rotations in the normally flexible *aeg*PNA oligomers, the entropic penalty for assuming the correct binding formation is reduced.

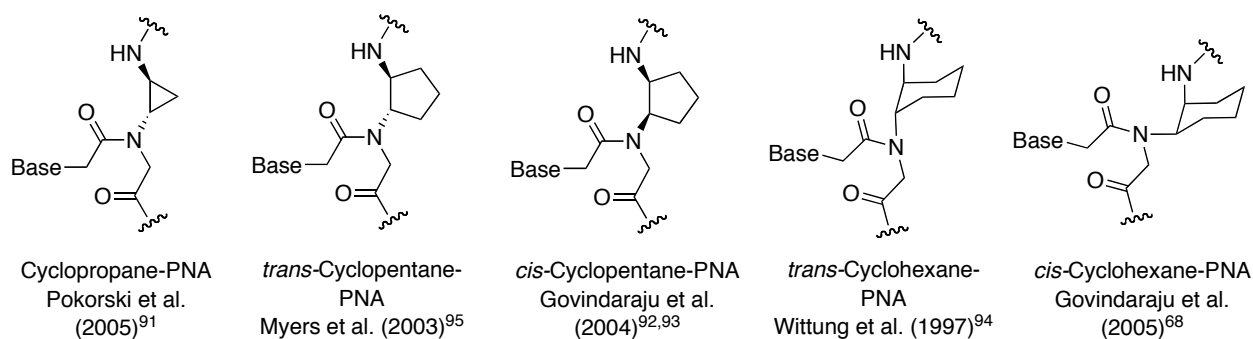


Figure I-17: β,γ -Carbocyclic PNA.

Although there are many strategies employing PNAs with cyclic constraints currently being explored, a particularly promising subclass of cyclic PNA incorporates carbocycles at the β and γ carbons of *aeg*PNA (Figure I-17). This strategy has distinct advantages. First, the chemistry to attach the nucleobase to the PNA backbone remains the same. When nucleobases are directly attached to the ring of cyclic PNA, they enforce different ring conformations leading to distinct differences in binding characteristics for different bases. Second, the ethylene portion of *aeg*PNA is usually regarded as the more flexible part of each PNA residue. The reduction of bond rotation is an effective method to change the flexibility and preorganize PNA oligomers for

binding. Indeed, mixed *aeg*PNA/cyclic PNA chimeras based on this design have led to PNA oligomers with diverse and beneficial binding characteristics.^{91-95,68}

One particular cyclic PNA of this subclass has potential in both medicinal and diagnostic applications. The (*S,S*)-*trans*-cyclopentane PNA monomer (*tcyp*PNA) was first developed by our group.⁹⁵ This residue increases the binding affinity and selectivity of PNA oligomers in a regular, predictable fashion. The effects of *tcyp*PNA are also independent of residue nucleobase, sequence, and position.⁹⁶ There is also no difference between separated and adjacent *tcyp*PNA residues on overall oligomer stability. These derivatives have already found use in both scanometric⁹⁷ and colorimetric⁹⁸ sandwich-complex DNA detection assays.

I.4.3 PNA Sidechain Conjugation

Being able to alter each PNA residue within a PNA oligomer has instant applications, but the functional groups coming from the basic PNA backbone can have a profound effect on the binding characteristics of PNA oligomers. Because side chains containing cationic groups (ammonium) are best tolerated at the α -position, and large or uncharged moieties detract from the binding affinity, little effort has gone into using side chain PNA as a versatile point to attach substituents. When Nielsen and coworkers recently utilized D-Lysine α -substituted PNA (D K α -PNA) as the point for glycosylation, the binding affinity decreased up to 6 °C per residue in a ten residue long oligomer.⁸³ Furthermore, the sugar molecules had to be attached to the sidechain in solution, before oligomer synthesis. Ideally, an orthogonally protected side chain, which could be selectively deprotected on solid support before further modification, would be more convenient than modification of PNA residues in solution. Since our initial studies and publication on the subject,⁹⁹ Sietz and coworkers have used the D K α -PNA sidechain as the site to attach fluorophores during Fmoc-mediated solid phase synthesis by deprotecting Alloc-protected

sidechain-amine.¹⁰⁰ The fluorophore acid can then be coupled to the primary amine through a standard amide bond-forming reaction. Despite the realization that having multiple points to attach useful functionality would be beneficial for many applications, ^DK α -PNA has not seen widespread use as a means for multifunctional display because of the increasingly reduced binding affinity. The γ -position has not been explored as a point to attach further functionality.

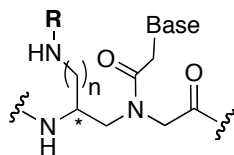
I.5 Design and Potential Applications

Despite the continuing utility of *aeg*PNA and the numerous PNA derivatives that have been developed in the last decade, there remain many avenues for research and applications. The potential for more versatile PNA monomers and better control over complex secondary structure is of interest to many nucleic acid researchers. It is with this in mind that we began our own investigation into these systems.

I.5.1 Versatile PNA Monomers for Multifunctional Display

Changing the physical characteristics of PNA oligomers by the introduction of non-*aeg*PNA residues is effective but inefficient. Designing PNA residues that possess hydrophilic, hydrophobic, or fluorescent properties normally requires the synthesis of distinct PNA monomers. Conjugation to a PNA oligomer is more versatile in this regard. Although PNA conjugations have increased the utility of PNA by altering the physical characteristics, this technique is hampered by having to append functionality to the termini or to the nucleobases. Conjugation to the termini limits the number of moieties that can be appended, while nucleobase conjugation involves difficult chemistry and the possibility of disrupting base pairing. A strategy allowing the functionalization of any individual residue without disrupting the overall oligomer binding would add to the versatility of PNA. If this modification tactic were possible during solid phase PNA oligomer synthesis, a relatively small number of PNA monomers would need to

be synthesized to produce almost any desired trait. Therefore, we began an investigation into the design, synthesis, and binding characteristics of γ -carbon side chains containing orthogonally protected primary amines (Figure I-18).



R = Conjugated Molecule

Figure I-18: Amine-Containing γ -Side Chain PNA.

When we began our project to investigate the γ -position of *aeg*PNA, no binding studies of PNA oligomers containing such residues had ever been documented. Accordingly, we analyzed what was already known about PNA duplex formation. Based on the NMR-determined structures of PNA:DNA duplexes,¹⁰¹ and prior PNA modifications, we hypothesized that carbon side chains from the γ -carbon would be tolerated with few steric interactions. Our modeling of the short PNA:DNA duplex showed that sidechains or substituents at the γ -position could take

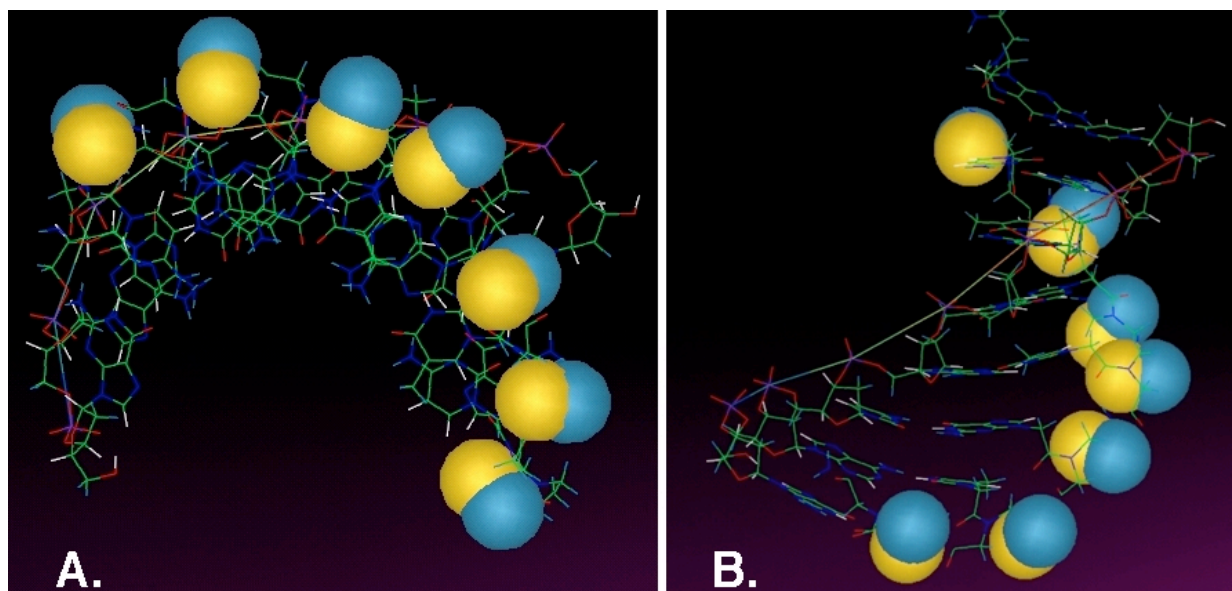


Figure I-19: Examination of the γ -Position in the PNA:DNA Duplex. The blue spheres denote the area around the *S* stereochemistry; the yellow spheres denote the *R* stereochemistry.

two distinct structural profiles based on the stereochemistry (Figure I-19). Sidechains with *S* stereochemistry (derived from L-amino acids) lined the periphery of the duplex minor groove and projected out from the π -stacked nucleobases. We surmised that, depending on the length of the linking sidechain, the appended moiety should not have any size limitation. Sidechains emanating from the γ -position with the opposite stereochemistry would project into the duplex, possibly interfering with base pairing.

Even using the NMR-determined structure of PNA:DNA and PNA:RNA duplexes and the crystal structures of PNA₂/DNA triplexes or PNA/PNA duplexes, it is difficult to predict the effect that stereochemistry will have on oligomer binding properties *a priori*. Since *aeg*PNA is achiral, PNA oligomers are not energetically predisposed to forming either right-handed or left-handed helices (as opposed to the exclusively right-handed helices of natural nucleic acids). Having a chiral amino acid appended to the C-terminus of a PNA oligomer can effectively bias *aeg*PNA duplexes to predominantly form either right-handed or left-handed helices, but this effect is dampened when amino acids are appended to the N-terminus, suggesting a difference in the influence of preorganization when substituents are at different points in the PNA architecture.¹⁰² Circular dichroism studies of unbound α -substituted PNA oligomers show only a very weak signal.¹⁰³ This is usually indicative of oligomers with only minor base stacking or helical excess, which are the hallmarks of preorganized oligonucleotides. Therefore, in addition to modeling for steric effects, special attention must be paid to the stereochemical effect substituents at the γ -carbon have on preorganization. NMR spectroscopy experiments of γ -substituted monomer esters showed early evidence that the substitution of different groups had a distinct effect on the bond rotation of the secondary amide.¹⁰⁴ Examining the Newman projection around the β - γ carbon-carbon bond suggests a stable structure because an *S*-

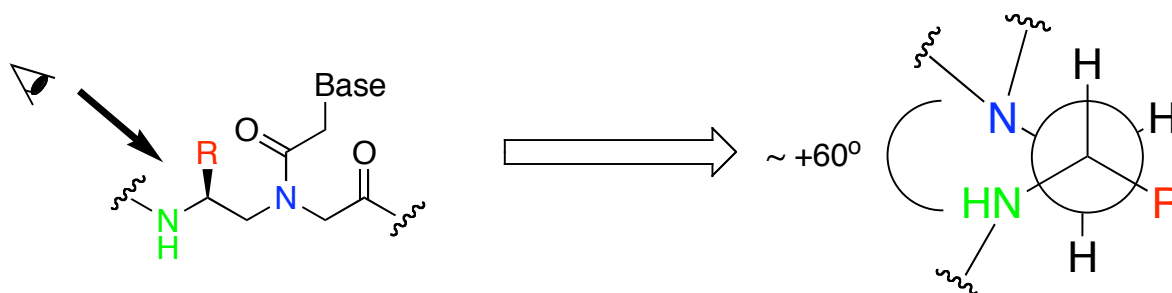


Figure I-20: Newman Projection About the β - γ Carbon Bond.

substituted chain present at the γ -carbon is anti to the tertiary amide (Figure I-20). As opposed to the *R* stereochemistry (sidechain gauche to tertiary amide), the *S* stereochemistry should be favored based on the known PNA:RNA structure.¹⁰⁵ Based on this monomer model, PNA:DNA duplexes might not see this effect of preorganization due to hindered bond rotation. In contrast to cyclic PNA that show preferential binding towards either DNA or RNA,⁶⁷ however, the γ -substituted PNA is not completely “locked” into a small range of bond angles.

We chose to use an orthogonally protected primary amine on the sidechain as our chemical handle for several reasons. First, since PNA oligomer synthesis, like standard peptide synthesis, involves the deprotection and amide bond-forming reactions of primary amines, this method is well suited to this type of modification. Oligomer synthesis would also remain amenable to automation. Second, this strategy also insures a wide variety of derivations due to the plethora of appropriate, commercially available acids (including fluorophores and peptide chains). Finally, if the primary amine is simply deprotected during the cleavage of the oligomer from the solid support without coupling, the primary amine will serve as a hydrophilic moiety, positively charged at physiological pH.

I.5.2 Exploring the Effect of PNA Preformation on Non-Duplex Secondary Structure

Most PNA derivatives are examined in relation to their ability to form Watson-Crick hydrogen bonding motifs, despite the fact that *aeg*PNA oligomers also have the ability to form other types of secondary structure such as triplexes and guanine tetrads. Since the secondary and tertiary structure of natural nucleic acids are important in biology and PNA based applications, the effect that PNA alterations has on the stability, structure and stoichiometry of cyclic PNA/DNA complexes needs to be properly understood.

Initial binding studies of *tcyp*PNA indicated that poly-thymine PNA oligomers formed triple helices in 2:1 stoichiometry with poly-adenine DNA.⁹⁵ Although *tcyp*PNA was later shown to have very similar effects in mixed base sequences, it is difficult to discern the contribution this cyclic preformation has on the Hoogsteen binding residues during triplex formation. To investigate this contribution, we proposed a series of tethered (or Bis-PNAs) in which a duplex-forming PNA is linked covalently to a triplex-forming PNA (Figure I-21).

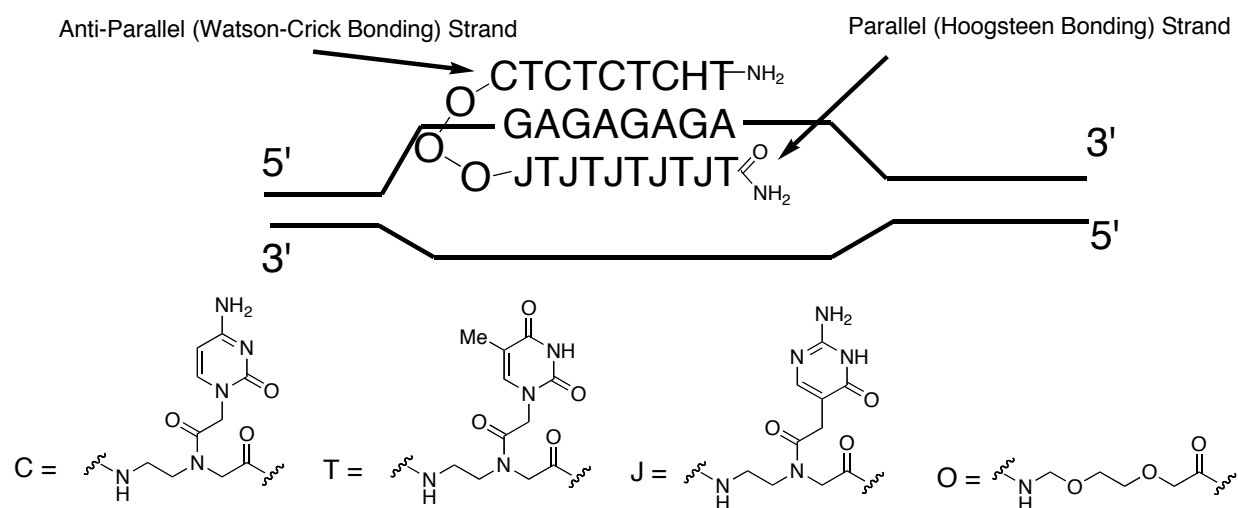


Figure I-21: Bis-PNA Triple Helix Formation.

We proposed the use of N7-guanine (Figure I-22) as a protonated cytosine mimic for these studies as opposed to more commonly used pseudo-isocytosine (J) for several reasons. As opposed to the pseudo-isocytosine residue, N7-guanine cannot form Watson-Crick base pairs, insuring that our parallel strand is a triplex-forming oligomer. The N7-guanine residue was also synthetically accessible as a byproduct of the isobutyryl protected N9-guanine acetic acid synthesis developed by Dr. Mark Witschi in our laboratory.¹⁰⁶

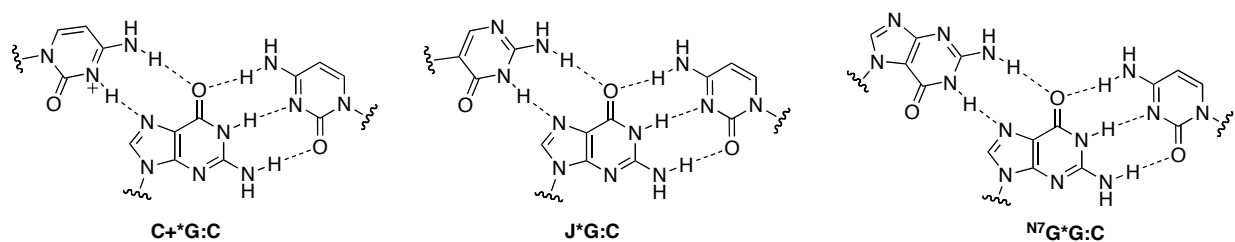


Figure I-22: N7-Guanine Hoogsteen Bonding as a Protonated Cytosine Mimic.

Minimizing the entropic contribution of PNA could be beneficial to applications targeting polyguanine or quadruplex-forming DNA. First, to determine the effects that *tcyp*PNA residues had on the formation of guanine tetrads, we proposed incorporating *tcyp*PNA monomers into G₄ PNA oligomers and looking for evidence of homo-quadruplexes and hetero-complexes with the G₄ DNA. Through a series of binding experiments and circular dichroism studies, the properties of *tcyp*PNA-containing oligomers in quadruplexes could be better understood. Second, we are beginning to examine the possibility of forming highly stable PNA quadruplexes by covalently attaching guanine rich oligomers (Figure I-23). Our modeling showed that through the use of orthogonally protected lysine as a core structure and short linkers, we could realistically form parallel quadruplex structures with the C-termini of the PNA covalently attached. This tethering

strategy can increase nucleic acid-recognition properties through the reduction of entropy,⁸⁹ and may also allow us to alter the binding stoichiometry of PNA:DNA quadruplex structures.

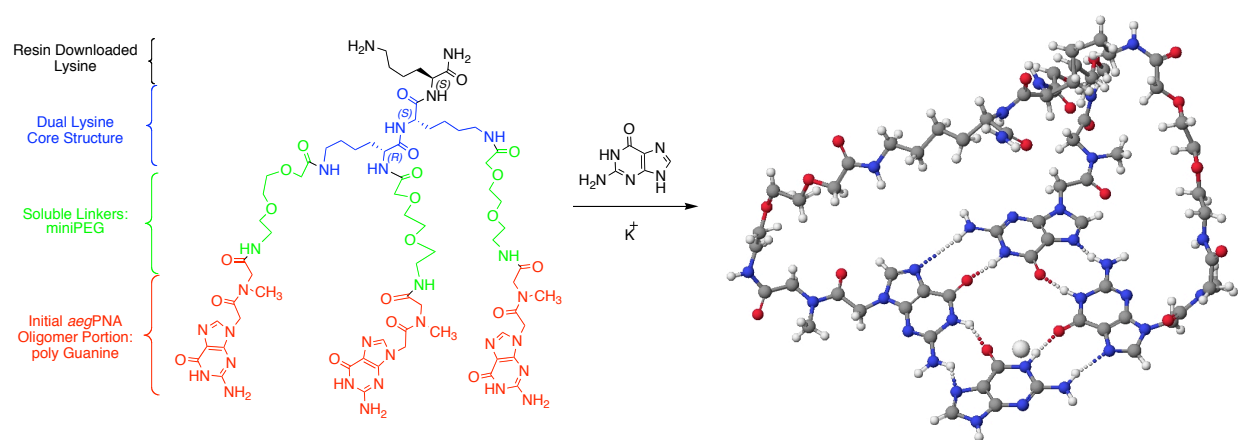


Figure I-23: Model for Three Covalently Linked PNA Guanine Oligomers.

Chapter II

Synthesis and Studies of Versatile γ -Substituted Sidechain PNA

Portions of this work appear in the following manuscripts:

Englund, E. A.; Gopi, H. N.; Appella, D. H., "An efficient synthesis of a probe for protein function: 2,3-diaminopropionic acid with orthogonal protecting groups." *Org. Lett.* **2004**, *6*, 213-215.

Englund, E. A.; Appella, D. H., "Synthesis of γ -substituted peptide nucleic acids: a new place to attach fluorophores without affecting DNA binding." *Org. Lett.* **2005**, *7*, 3465-3467.

Englund, E. A.; Appella, D. H., " γ -Substituted peptide nucleic acids constructed from L-lysine are a versatile scaffold for multifunctional display." *Angew. Chem. Int. Ed.* **2007**, *46*, 1414-1418.

II.1 Introduction: Initial Experimental Design and Synthetic Targets

We postulated that using the γ -position of *aeg*PNA as a handle to modify and couple additional functionality had the potential to enhance the utility of PNA. When we began this project, however, it was unknown how substitution at the γ -position of PNA would affect the high binding affinity and selectivity of PNA oligomers. To address this dearth of information, we envisioned synthesizing several initial target PNA monomers to probe the effects that sidechain length, charge, and stereochemistry at the γ -position had on the binding affinity to natural nucleic acids (Figure II-1). It was also important to examine the versatility of this sidechain modification and determine which moieties could be supported without detrimental binding characteristics. With a firm grasp of γ -PNA binding characteristics, we could then examine simple applications, such as DNA detection using fluorescent “light-up” probes.

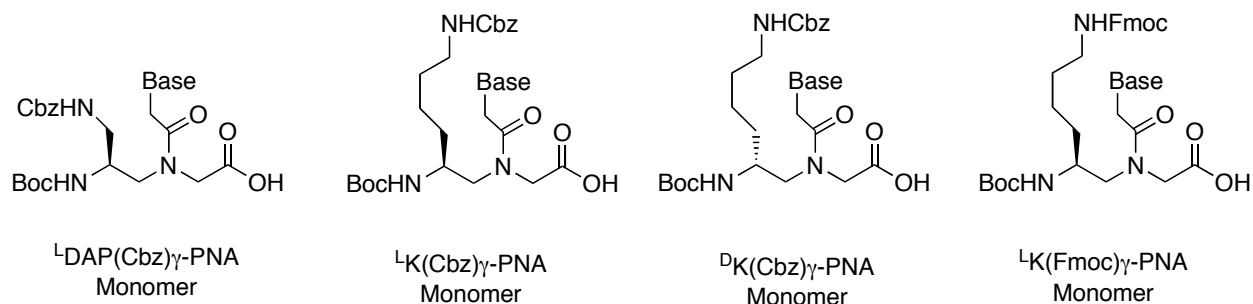
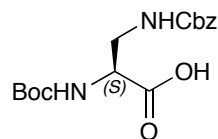


Figure II-1: Initial γ -PNA monomer Targets.

II.2 Synthesis of γ -PNA Possessing Amine-Containing Side Chains

The γ -substituted monomers were designed for *tert*-butoxycarbonyl (Boc) mediated oligomer synthesis on solid support.¹ Although conditions for Boc-deprotection and cleavage from the resin require strongly acidic conditions, Boc solid phase synthesis is usually considered cleaner and higher yielding than the fluorenyl-methoxycarbonyl (Fmoc) mediated peptide synthesis.

II.2.1 (L)-2,3-diaminopropionic acid(Cbz) γ -substituted PNA Monomer (L Dap γ -PNA)



(S) - BocDap(Cbz)-OH

Figure II-2: Orthogonally Protected 2,3 diaminopropionic acid (Dap).

To examine how the sidechain length would effect duplex formation, the first γ -substituted PNA monomer with a primary amine-containing side chain was synthesized from orthogonally-protected (*S*)-diaminopropionic acid (Dap) (Figure II-2). Although commercially available as a single enantiomer with all functional groups orthogonally-protected, Dap is expensive (~\$115/g or ~\$50/mmol).² The most common synthesis of Dap involves a Hofmann rearrangement of protected asparagine using a trivalent iodine reagent, most often bis-[trifluoroacetoxy]-iodo benzene (Figure II-3).³ When this reagent is used, the trifluoroacetic acid formed in solution is believed to catalyze the hydrolysis of the isocyanate intermediate to an amine, which reduces urea formation that could occur from reaction of the amine with remaining isocyanate.⁴

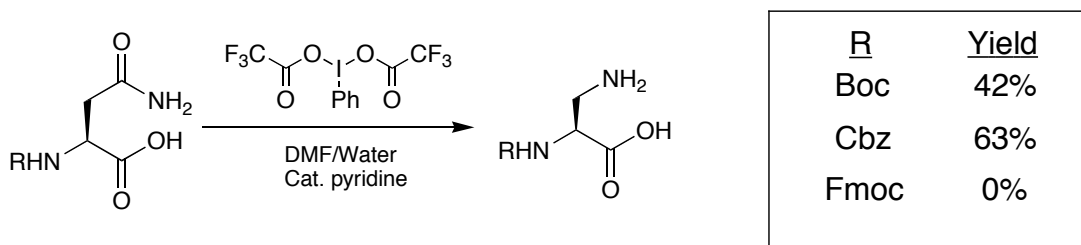
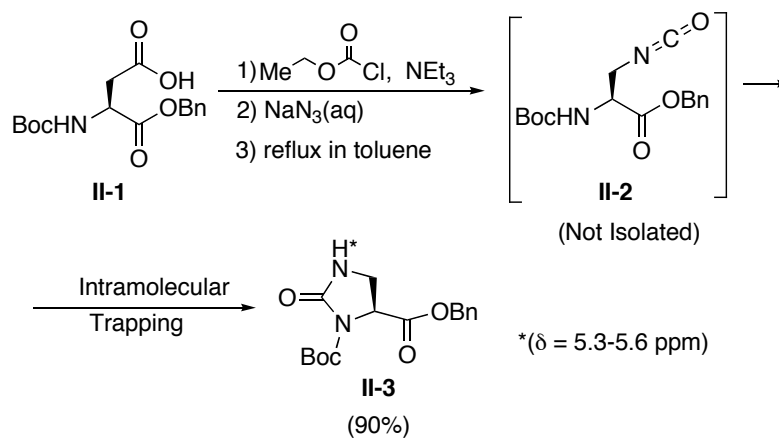


Figure II-3: Route to Dap using the Hofmann Rearrangement.⁵

The acid generated during this transformation can also remove the Boc protecting group. As shown in Figure II-3, Boc-protected asparagine produced significantly lower yields than Cbz-protected asparagine when subjected to the same conditions for the Hofmann rearrangement.⁵

Fmoc-protected asparagine has poor solubility under the same reaction conditions, which accounts for the failure of the Hofmann rearrangement when using this form of protected asparagine. If Cbz protection is used, which is optimal, then an α -amine protecting group must be converted to a Boc or Fmoc group to be compatible with solid phase peptide synthesis.⁶ The main problems we encountered were the constant need to exchange protecting groups, the high cost of bis-[trifluoroacetoxy]-iodo benzene (\sim \$0.95/mmol),⁷ and the requirement to use an excess (at least two equivalents) of this reagent. Therefore, we sought to develop a more direct and less costly route to Dap.

Scheme II-1: Failed Synthesis of Dap: Intramolecular Isocyanate Trapping.

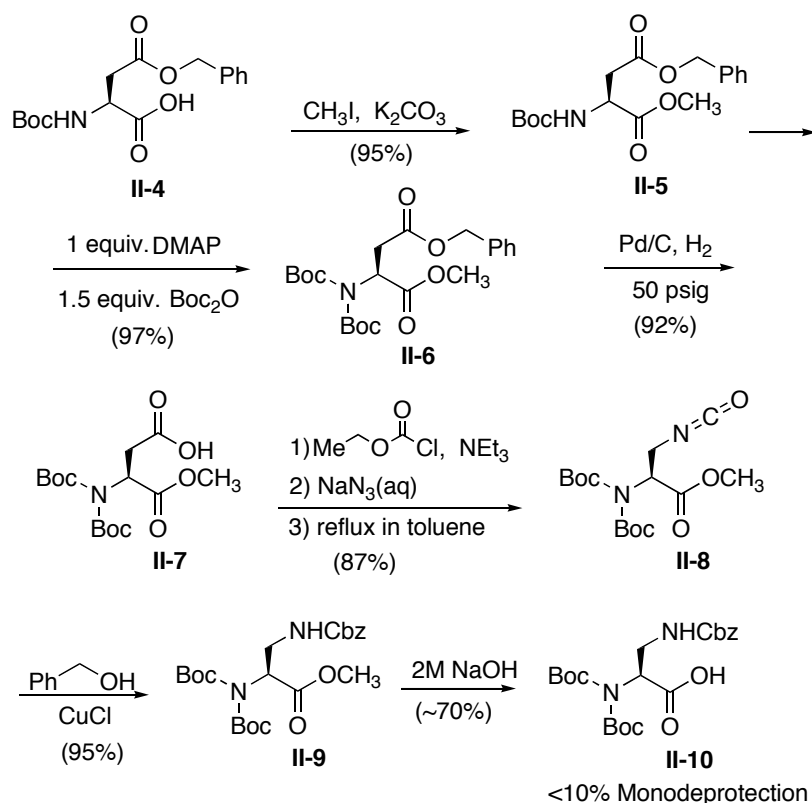


We felt that a Curtius rearrangement of an aspartic acid derivative would afford an isocyanate that could be trapped with benzyl alcohol to directly afford a derivative of Dap with orthogonal protecting groups suitable for solid phase peptide synthesis (Scheme II-1). Starting from Boc-Asp-OBn (**II-1**), a Curtius rearrangement proceeded to give a product with ^1H NMR signals consistent with the expected isocyanate intermediate **II-2**. To our surprise, multiple efforts to trap the supposed isocyanate failed. Additional ^{13}C NMR spectroscopy, IR, and mass spectrometry data confirmed that cyclic urea **II-3** was present instead. In the ^1H NMR spectrum of **II-3**, the urea proton (H^*) appeared in the same region (5.3-5.6 ppm in CDCl_3) as most

carbamate protons, which was initially deceptive. Also, there was no discernable change in the couplings or chemical shifts of the α or β protons to indicate urea versus isocyanate formation. Removal of the Boc group from **II-3** provided the free urea, which was fully characterized. A number of studies have shown that carbamate-protected amines can trap isocyanates through intramolecular cyclization.^{8,9} In our case, the cyclization to form a 5-membered cyclic urea was especially efficient. We were unable to intercept the isocyanate with other nucleophiles.

We were able to prevent the intramolecular trapping of the isocyanate after the Curtius rearrangement by doubly protecting the reactive nitrogen (Scheme II-2).¹⁰ A similar strategy was employed by Deng and coworkers for the synthesis of Dap.¹¹ Starting from protected aspartic acid **II-4**, which is commercially available, the carboxylic acid was first converted to methyl ester **II-5**, followed by introduction of a second Boc group to give **II-6**.⁸ The benzyl

Scheme II-2: Synthesis of Protected Dap Starting from Aspartic Acid.

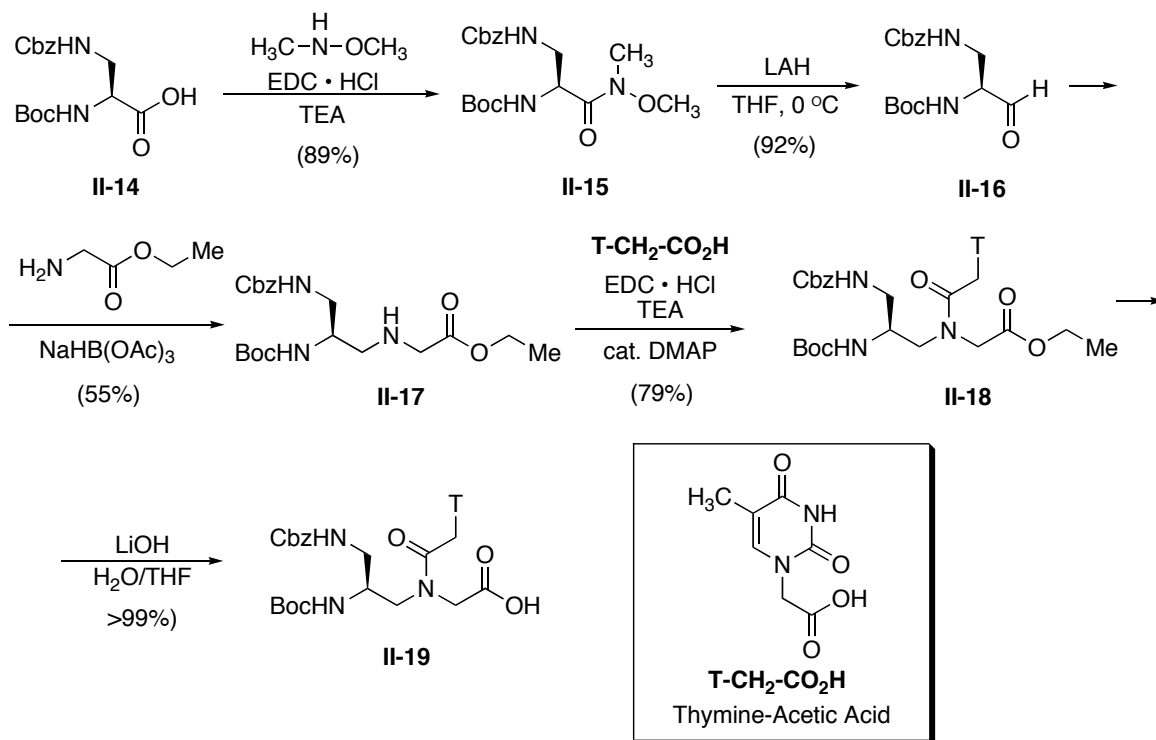


ester was then removed by hydrogenolysis under pressure (50 psig). Next, the Curtius rearrangement was performed by first converting the acid **II-7** to a mixed anhydride, followed by conversion to the corresponding acyl azide, and then heated in toluene at reflux for 2 hours. These conditions cleanly formed isocyanate **II-8**, which has been characterized by ^1H NMR, ^{13}C NMR, and IR spectroscopy. Once isolated, the isocyanate was trapped with benzyl alcohol, using CuCl as a Lewis acid, to form the Cbz-protected amine **II-9**.¹² Hydrolysis of the methyl ester then gave protected Dap **II-10**.

A minor side product formed during this synthetic route results from loss of one Boc group of the diprotected nitrogen. Partial monodeprotection most likely occurs during acidic work up after the ester hydrolysis. This by-product is easily identified in the ^1H NMR spectrum of **II-10**, and is present in quantities of less than 10% relative to the main product (estimated by ^1H NMR spectroscopy). We have used **II-10** directly in solid phase peptide synthesis without complications in the deprotection or coupling steps associated with peptide synthesis. The partially deprotected by-product is not detrimental to the conditions of solid phase peptide synthesis.

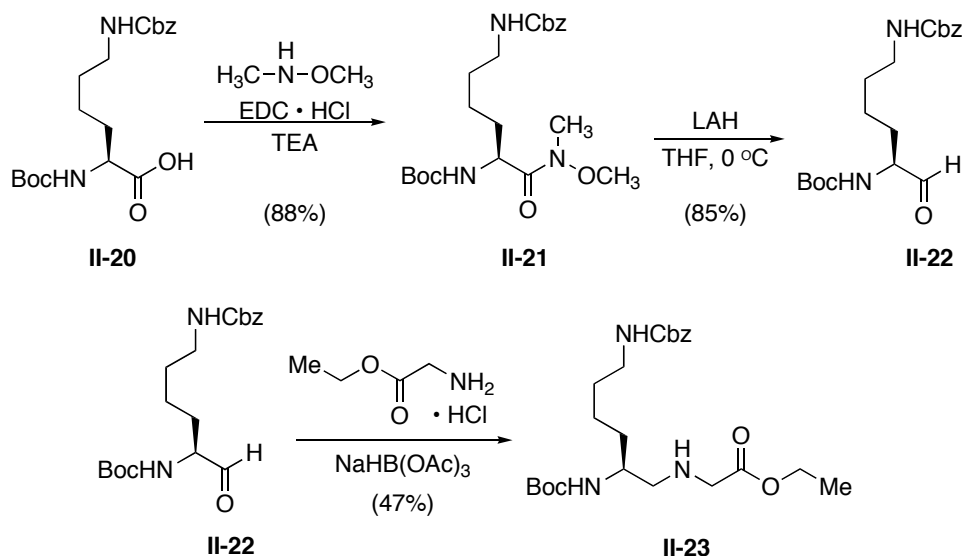
To confirm the enantiomeric purity of Dap Methyl Ester **II-9**, we prepared **II-13** and compared the optical rotation to the identical compound prepared from commercial Dap. Conversion of **II-9** to **II-13** is shown in Scheme II-3. Boc-Dap(Fmoc)-OH (from Advanced Chemtech) was methylated to give **II-13**. The optical rotations of both compounds were within experimental error of each other, confirming that racemization does not occur in our synthesis of Dap. Although the bis-Boc protected DAP could be manipulated in a similar fashion to mono-Boc protected DAP, the Boc groups were removed with TFA, and the free amine was reprotected with a single Boc to afford Dap derivative **II-14** in high yield.

Scheme II-4: The Synthesis of ^LDapγ-PNA Monomer.

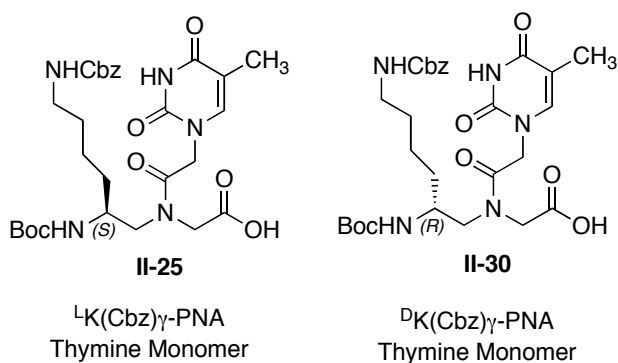
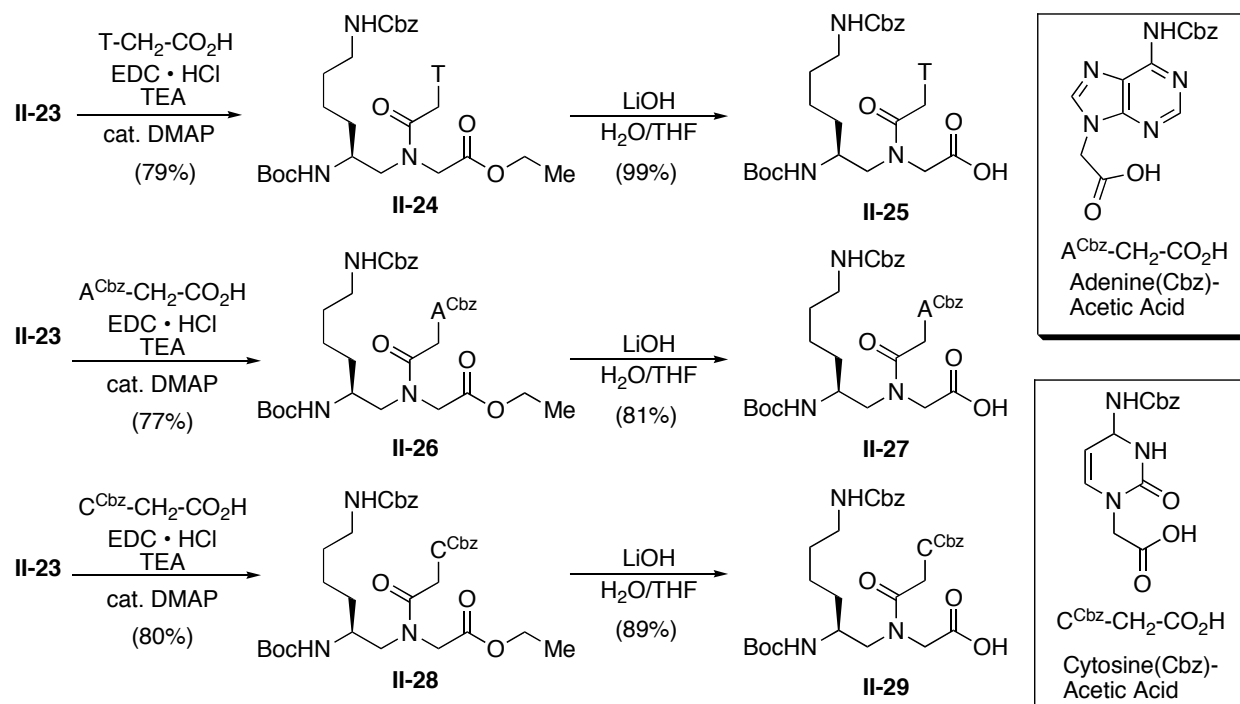


II.2.2 Lysine(Cbz) γ-Substituted PNA Monomers (^LKγ-PNA)

PNA monomers containing γ-Cbz-protected “lysine” sidechains were synthesized from commercially available orthogonally protected lysine (BocLys(Cbz)-OH). The BocLys(Cbz)-OH was coupled to N,O-dimethylhydroxylamine using EDC in high yield (Scheme II-5). The resulting Weinreb amide (**II-21**) was reduced with LAH to afford the Boc/Cbz lysinal (**II-22**).

Scheme II-5: Synthesis of ^LK γ -PNA Backbone.

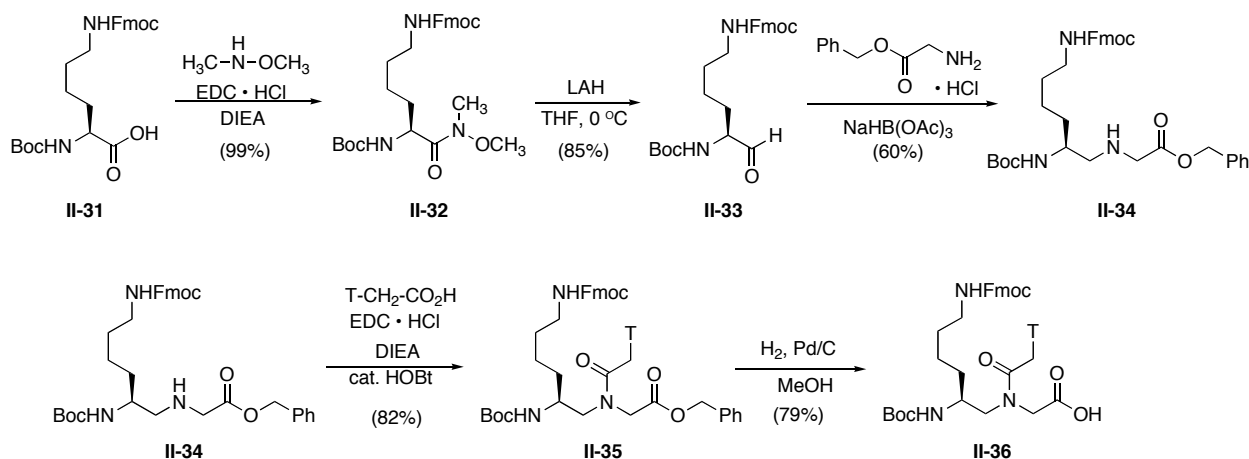
Although Boc protected amino aldehydes have been known to racemize during column chromatography,^{14,15} no additional purification was needed in this reaction and **II-22** was always carried on without additional manipulation after work up. The aldehyde was condensed with ethyl glycinate and reduced using sodium triacetoxyborohydride to yield the γ -substituted PNA backbone (**II-23**). After purification by column chromatography, several different nucleobase acetic acids were coupled to the secondary amine (Scheme II-6). Thymine acetic acid is commercially available, while cytosine and adenine acetic acids (where the exocyclic amines are Cbz-protected) were produced through previously reported methods.¹⁶ Each monomeric ethyl ester was then hydrolyzed with LiOH in aqueous/THF affording thymine, adenine and cytosine ^LK γ -PNA(Cbz) monomers (**II-25**, **II-27**, **II-29**). The thymine monomer was synthesized from both L and D enantiomers of the commercially available BocLys(Cbz)-OH (Figure II-4).

Scheme II-6: Final Steps of $^L\text{K}\gamma\text{-PNA}(\text{Cbz})$ Monomers: Thymine, Adenine, and Cytosine.**Figure II-4:** $^L\text{K}\gamma\text{-PNA}$ Monomer Enantiomers Synthesized.**II.2.3 (L)-Lysine(Fmoc) γ -Substituted PNA Monomers ($^L\text{K}\gamma\text{-PNA}$)**

PNA monomers containing γ -Fmoc-protected “lysine” sidechains were synthesized from commercially available BocLys(Fmoc)-OH (**II-31**). The Boc/Fmoc protected lysinal (**II-33**) was synthesized in a manner similar to the Cbz-protected monomers by reduction of the corresponding Wienreb amide (**II-32**). The conditions of this transformation were altered

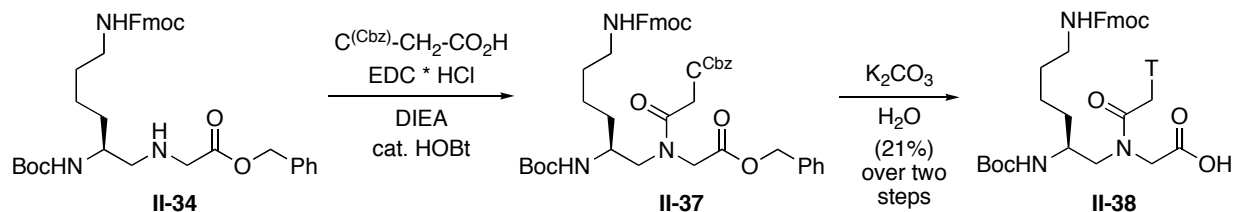
slightly to accommodate the base labile Fmoc group (Scheme II-7). The γ -PNA backbone **II-34** was produced by means of reductive amination with benzyl glycinate. After coupling to thymine acetic acid to yield monomer ester **II-35**, hydrogenolysis via H_2 and Pd/C afforded the $^L K\gamma$ -PNA(Fmoc) thymine monomer in high yield **II-36**.

Scheme II-7: Synthesis of $^L K\gamma$ -PNA(Fmoc) Thymine Monomer



Cytosine(Cbz) acetic acid was also coupled to the $^L K\gamma$ -PNA(Fmoc) backbone to afford $^L K\gamma$ -PNA(Fmoc) cytosine(Cbz) monomer ester (**II-37**), but was not subjected to reducing conditions because of the Cbz group on the exocyclic nitrogen of cytosine (Scheme II-8). Hydrolysis of benzyl esters can be achieved under mildly alkaline conditions (aqueous K_2CO_3),¹⁷ while Fmoc groups are cleaved in the presence of base, deprotect very slowly under aqueous conditions.¹⁸ Although the yield was not optimal because of the lengthy reaction time needed for hydrolysis and due to partial deprotection of the side chain Fmoc, $^L K\gamma$ -PNA(Fmoc) Cytosine(Cbz) monomer (**II-38**) was produced.

Scheme II-8: Synthesis and Hydrolysis of ^LK γ -PNA(Fmoc) Cytosine(Cbz) Benzyl Ester.



II.3 Oligomer/Solid Phase Synthesis

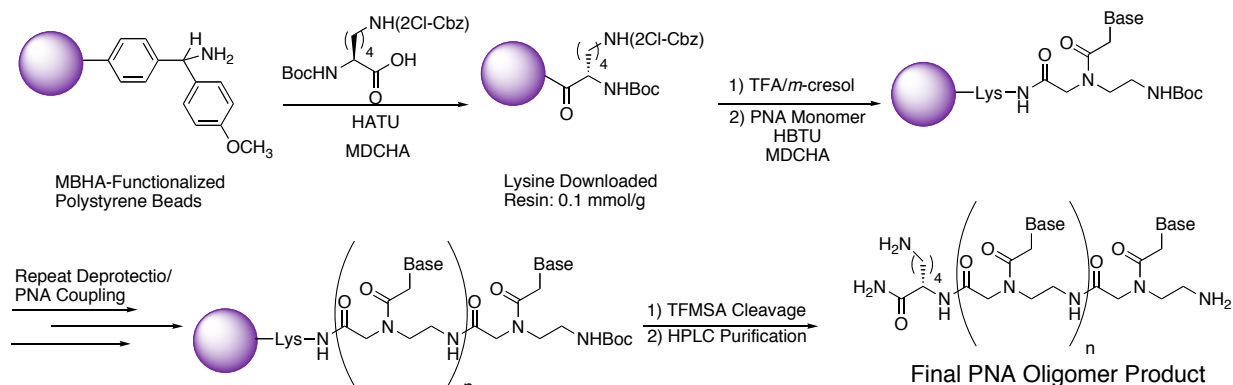
Once γ -PNA monomers were synthesized, they were incorporated into short *aeg*PNA oligomers at various positions. The procedure described has been adapted from Koch and coworkers.¹⁹

II.3.1 PNA Oligomer Synthesis Incorporating γ -PNA(Cbz)

Methylbenzylhydroxyamine (MBHA) functionalized polystyrene beads were downloaded to 0.1 mmol/g with L-BocLys(2Cl-Cbz)-OH (Scheme II-9). Lysine has been traditionally appended to the carboxy terminus (C terminus) of PNA oligomers for several reasons. Having the lysine on the solid support improves the yield and purity of the PNA oligomers by reducing non-covalent interactions with the solid support. Furthermore, the additional primary amine greatly improves the notoriously poor solubility of PNA oligomers and the additional positive charge reduces aggregation.¹ Having an amino acid on the C terminus also predisposes PNA to form anti-parallel duplexes with DNA or RNA.²⁰ Once downloaded, the Boc group is removed with trifluoroacetic acid to give the primary amine. The PNA monomers can then be coupled using HBTU to form the primary amine bond. This cycle is repeated until the oligomer is of appropriate length. The completed oligomer can then be cleaved from the resin under strongly acidic conditions, such as treatment with trifluoromethane sulfonic acid. The Cbz groups on protected nucleobases and the γ -sidechain amines are also labile under such conditions.²¹ The

oligomers are then precipitated from ether, purified by HPLC, and characterized by mass spectrometry.

Scheme II-9: General PNA Oligomer Synthesis on Solid Support.



II.3.2 Modification of γ -PNA Sidechains while on Solid Support

Incorporating γ -PNA(Fmoc) monomers into PNA oligomers was accomplished as described for the γ -PNA(Cbz) monomers. After the γ -PNA(Fmoc) monomer was coupled, the Fmoc on the side chain amine can be removed using a 20% piperidine in DMF (Scheme II-10). The exposed amine can then be coupled using amide bond-forming reactions to any number of acid-containing substrates. If the coupled moiety also contains an Fmoc protected amine (such as an Fmoc-protected amino acid), the piperidine/coupling cycle can continue on the side chain to construct more complex functionality or peptide conjugates. After modification of the side chain, Boc deprotecting/PNA-coupling can be resumed.

requires. Dr. Zhang of our laboratory and I developed conditions to synthesize PNA oligomers incorporating either Cbz-protected or Fmoc-protected $^L\text{K}\gamma$ -PNA on an automated peptide synthesizer. Increased coupling times and extra Boc deprotection accompanied the incorporation of $^L\text{K}\gamma$ -PNA monomers. The purity and yield of PNA oligomers constructed than automated synthesis were much higher than the manual method.

II.4 Thermal Melting Analysis of Substituted γ -PNA with DNA

Any useful contribution to the ever-expanding library of PNA derivatives should not detract from the impressive binding affinity and selectivity that *aeg*PNA displays towards natural nucleic acids. Considering the paucity of melting studies carried out on γ -substituted PNA oligomers, a thorough analysis of the binding properties of our synthesized γ -PNA oligomers was vital to establishing possible utility of such a modification. To our knowledge, before we began our studies there were no known examples of any PNA oligomer containing γ -substituted residues. The melting temperatures (T_m) were determined via variable temperature ultraviolet (UV) absorbance.²³ When nucleic acids undergo duplex formation, the intensity of UV light absorbed by the nucleobases decreases (hypochromic effect) yielding a sigmoidal curve. Assuming the transition is due to only two states, bound and unbound, the midpoint of the transition can be assumed to be the point where there is a 1:1 ratio of bound to unbound oligomers. Therefore, the temperature of this transition provides a rough estimate of the duplex stability.²⁴

II.4.1 The Effect of Unconjugated $^L\text{K}\gamma$ -PNA on PNA/DNA Duplex Stability

The short, mixed base PNA sequence H-GTAGATCACT-Lys-NH₂ (PNA II-1), commonly referred to as the “Nielsen Sequence”, was used for our initial studies because of the modest number of G:C pairs (4 pairs, 40%), balanced pyrimidine/purine ratio (1:1) and extensive

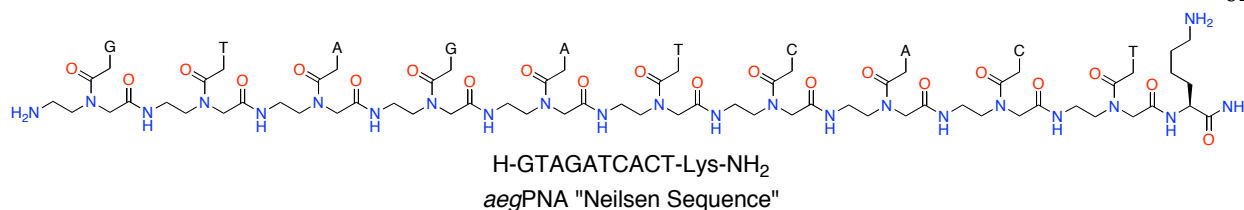


Figure II-5: Nielsen Sequence of *aeg*PNA. Shown N terminus to C terminus.

literature precedent for comparison (Figure II-5).²⁰ The “Nielsen Sequence” binds to the complementary DNA sequence (5'-AGTGATCTAC- 3') in phosphate buffered saline (PBS) solution at a T_m of 48.7 °C (150 mM NaCl).

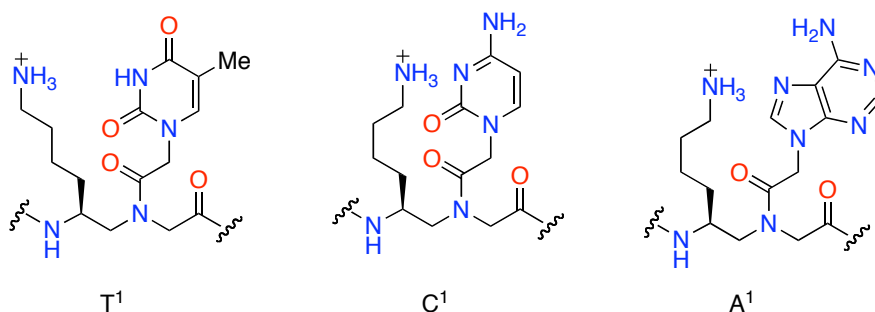


Figure II-6: ^LK γ -PNA with Unconjugated Primary Amines: Various Bases.

The *aeg*PNA/^LK γ -PNA chimeras (Figure II-6) synthesized from the ^LK γ -PNA(Cbz) monomers were tested under identical conditions. When the internal *aeg*PNA thymine residue was replaced with the ^LK γ -PNA monomer, as in **PNA II-2**, a melting temperature of 51.4 °C was observed (Table II-1). This increase in melting temperature proved general to the central cytosine (**PNA II-3**) and adenine (**PNA II-4**) residues of the “Nielsen Sequence”, differing only slightly from the T_m of **PNA II-2**. Furthermore, when multiple ^LK γ -PNA monomers were present in the oligomer, a greater increase in binding stability was observed, indicating that the modified residues have an additive stabilizing effect.

Table II-1: T_m Analysis of $^L\text{K}\gamma$ -PNA with Free Amines to Complementary DNA.

PNA	Sequence	T_m ($^{\circ}\text{C}$) DNA ^a	ΔT_m ($^{\circ}\text{C}$) ^b
II-1	H-GTAGATCACT-Lys-NH ₂	49.7	---
II-2	H-GTAGAT $\underline{\text{T}}$ CACT-Lys-NH ₂	51.4	1.7
II-3	H-GTAGAT $\underline{\text{C}}$ ACT-Lys-NH ₂	51.8	2.1
II-4	H-GTAGA $\underline{\text{A}}$ TCACT-Lys-NH ₂	53.1	3.4
II-5	H-G $\underline{\text{T}}$ A $\underline{\text{T}}$ GAT $\underline{\text{T}}$ CACT $\underline{\text{T}}$ -Lys-NH ₂	54.5	4.8

^a Thermal denaturation studies were undertaken with complementary DNA (3'-CAT CTA GTG A-5'). Data were collected from cooling runs from 90 $^{\circ}\text{C}$ to 15 $^{\circ}\text{C}$ at a rate of 1 $^{\circ}\text{C}/\text{min}$. ^b ΔT_m represents the difference in melting temperature between the chimera sequence and *aeg*PNA, II-1.

II.4.2 The Effect of Stereochemistry on $\text{K}\gamma$ -PNA Duplexes

Although initial modeling and examination of the γ -position of PNA highly suggested that (*S*) stereochemistry (derived from L-lysine) would be tolerated better than (*R*), an oligomer containing $^D\text{K}\gamma$ -PNA at the internal thymine position was bound to the complementary DNA (Figure II-7). Melting experiments revealed a large decrease in the binding affinity compared to both $^L\text{K}\gamma$ -PNA and fully *aeg*PNA oligomers (Table II-2). This result was expected for several reasons. First, based on the bond angles the PNA adopts when bound to DNA, (*S*) stereochemistry at the γ -position would set the sidechain in the anti-position to secondary amine

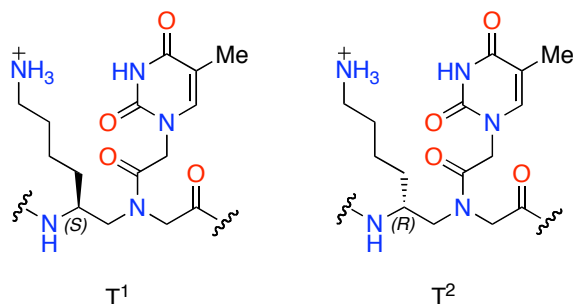
**Figure II-7:** $^L\text{K}\gamma$ -PNA with Unconjugated Primary Amines: Different Stereochemistry.

Table II-2: Effect of ^LK γ -PNA Stereochemistry on PNA:DNA T_m .

PNA	Sequence	T_m (°C) DNA ^a	ΔT_m (°C) ^b
II-1	H-GTAGATCACT-Lys-NH ₂	49.7	---
II-2	H-GTAGAT $\underline{1}$ CACT-Lys-NH ₂	51.4	1.7
II-6	H-GTAGAT $\underline{2}$ CACT-Lys-NH ₂	36.4	-13.3

^a Thermal denaturation studies were undertaken with complementary DNA (3'-CAT CTA GTG A-5'). Data were collected from cooling runs from 90 °C to 15 °C at a rate of 1 °C/min. ^b ΔT_m represents the difference in melting temperature between the chimera sequence and *aeg*PNA, II-1.

nitrogen (Figure II-8). (*R*) stereochemistry at the γ -position would set the sidechain in the slightly less favorable gauche position. We theorized that this “preformation”, or setting of the bond angles, could account for the modest increase in binding affinity to DNA. Modeling suggests that even if the gauche formation is only slightly less energetically favorable than the anti formation, the (*R*) stereochemistry directs sidechains towards the nucleobases. If sidechain projection disrupts base pairing, such an effect could account for the large decrease in binding affinity.

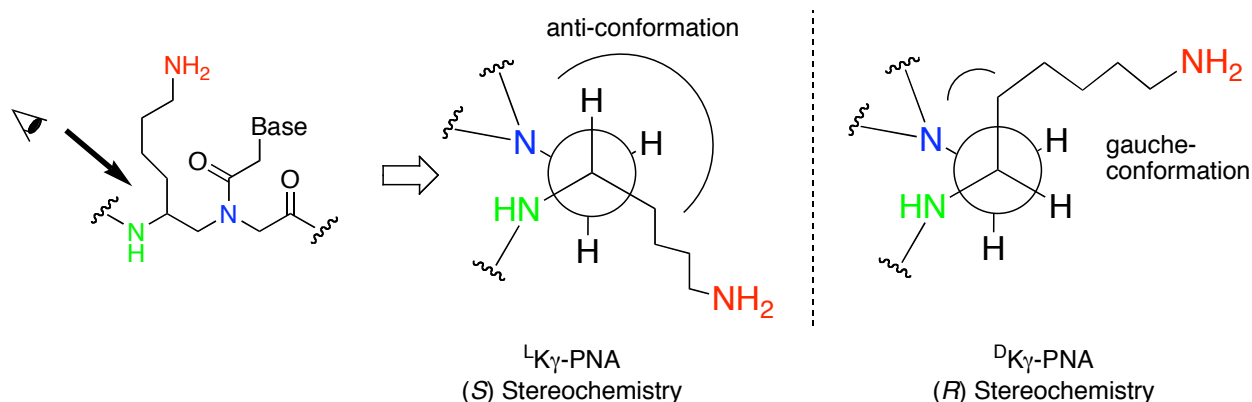


Figure II-8: Newman Projection About the β - γ Carbon Bond. This conformation is based on *aeg*PNA bound in a right-handed helix.

II.4.3 Effect of Chain Length for Amine-Containing γ -PNA Oligomers

The influence of sidechain length on binding characteristics was examined by inserting the L DAP γ -PNA residue into the central thymine residue of the “Nielsen Sequence” (Figure II-9).

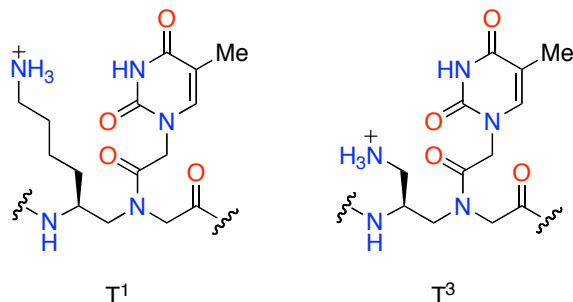


Figure II-9: L γ -PNA with Unconjugated Primary Amines: Different Sidechain Length.

Table II-3: T_m Analysis of L K γ -PNA versus L DAP γ -PNA.

PNA	Sequence	T_m ($^{\circ}$ C) DNA ^a	ΔT_m ($^{\circ}$ C) ^b
II-1	H-GTAGATCACT-Lys-NH ₂	49.7	---
II-2	H-GTAGAT $\underline{1}$ CACT-Lys-NH ₂	51.4	1.7
II-7	H-GTAGAT $\underline{3}$ CACT-Lys-NH ₂	44.0	-5.7

^a Thermal denaturation studies were undertaken with complementary DNA (3'-CAT CTA GTG A-5'). Data were collected from cooling runs from 90 $^{\circ}$ C to 15 $^{\circ}$ C at a rate of 1 $^{\circ}$ C/min. ^b ΔT_m represents the difference in melting temperature between the chimera sequence and *aeg*PNA, II-1.

In contrast to the L K γ -PNA residue, the L DAP γ -PNA substitution detracts from, the binding affinity compared to *aeg*PNA (Table II-3). Several factors may account for this effect. The proximity of a protonated amine could interfere with the pseudo-peptide PNA backbone through hydrogen bonding. However, a kinetically favorable chemical rearrangement cannot be ruled out, and would certainly disrupt the aforementioned *aeg*PNA spacing requirements (Figure II-10).

result helps to confirm that the increase in binding affinity of unconjugated ^LK γ -PNA is not due to charge-charge interaction with the anionic DNA phosphates. The synthesis of PNA-peptide conjugates are important for many biologically relevant applications.²⁵ **PNA II-8** showed that the lysine side chain of ^LK γ -PNA could maintain a substantial amount of steric bulk in the form of a short peptide chain (alanine-alanine-glycine) without affecting DNA binding. Since one of the desired applications of ^LK γ -PNA is fluorescent probes or molecular beacons, several fluorescent molecules were coupled to the γ side chain. Neither the linker-appended fluorene acetic acid nor a derivative of the fluorophore “thiazole orange” attached to undecanoic acid, showed any detrimental binding consequences in the “Nielsen Sequence”. Fluorene-substitution was tested on both the internal thymine and cytosine position, with very similar results in binding affinity.

Table II-4: T_m Analysis of Substituted ^LK γ -PNA with Complementary DNA.

PNA	Sequence	T_m (°C) DNA ^a	ΔT_m (°C) ^b
II-1	H-GTAGATCACT-Lys-NH ₂	49.7	---
II-8	H-GTAGAT ⁴ CACT-Lys-NH ₂	51.2	1.5
II-9	H-GTAGAT ⁵ CACT-Lys-NH ₂	51.7	2.0
II-10	H-GTAGAT ⁶ CACT-Lys-NH ₂	50.5	0.8
II-11	H-GTAGAT ⁶ CACT-Lys-NH ₂	50.3	0.6
II-12	H-GTAGAT ⁷ CACT-Lys-NH ₂	65.4	15.7

^a Thermal denaturation studies were undertaken with complementary DNA (3'-CAT CTA GTG A-5'). Data were collected from cooling runs from 90 °C to 15 °C at a rate of 1 °C/min. ^b ΔT_m represents the difference in melting temperature between the chimera sequence and *aeg*PNA, II-1.

To examine the effect that multiple fluorophores would have on the binding affinity of PNA oligomers, a homo-pyrimidine oligomer (H-CCTCTTCCTC-Lys-NH₂, **PNA II-12**) was synthesized. The low binding affinity is characteristic of homo-pyrimidine PNA (Table II-5).²⁶ Successive thiazole orange derivatives appended from the γ -side chain (with two 8-amino 3,6-dioxooctanoic acid linkers) increased the melting temperature compared to the *aeg*PNA oligomer.

Table II-5: T_m Analysis of Thiazole Orange-Substituted Polypyrimidine PNA.

PNA	Sequence	T_m (°C) DNA ^a	ΔT_m (°C) ^b
II-13	H-CCTCTTCCTC-Lys-NH ₂	34.5	---
II-14	H-CCTCT ⁸ TCCTC-Lys-NH ₂	44.6	10.1
II-15	H-CCTCT ⁸ TCCT ⁸ C-Lys-NH ₂	46.4	11.9

^a Thermal denaturation studies were undertaken with complementary DNA (3'-GGA GAA GGA G-5'). Data were collected from cooling runs from 80 °C to 5 °C at a rate of 1 °C/min. ^b ΔT_m represents the difference in melting temperature between the chimera sequence and *aeg*PNA, II-13.

A mixed base sequence with three internal, adjacent thymine residues was designed and synthesized with the intention of probing the effect of multiple, bulky groups appended to the ^LK γ -PNA side chain in succession (Table II-6). When ^LK γ -PNA(Fmoc) was substituted at the three internal thymine residues of PNA and each coupled to hydrocinnamic acid, the resulting oligomer (**PNA II-16**) showed a melting temperature of 49.3 °C, an increase of 4.9 °C compared to the *aeg*PNA oligomer (**PNA II-15**). These melting temperatures demonstrate that successive residues present no impediment to the PNA binding conformation, indicated by the increased overall binding affinity and the per residue T_m increase (~ 1.6 °C) consistent with earlier modifications.

Table II-6: T_m Analysis of Adjacent Substituted ^LK γ -PNA.

PNA	Sequence	T_m (°C) DNA ^a	ΔT_m (°C) ^b
II-16	H-GACTTTACGA-Lys-NH ₂	42.4	---
II-17	H-GACT ⁹ T ⁹ T ⁹ ACGA-Lys-NH ₂	49.3	4.9

^a Thermal denaturation studies were undertaken with complementary DNA (3'-CTG AAA TGC T-5'). Data were collected from cooling runs from 90 °C to 15 °C at a rate of 1 °C/min. ^b ΔT_m represents the difference in melting temperature between the chimera sequence and *aeg*PNA, II-16.

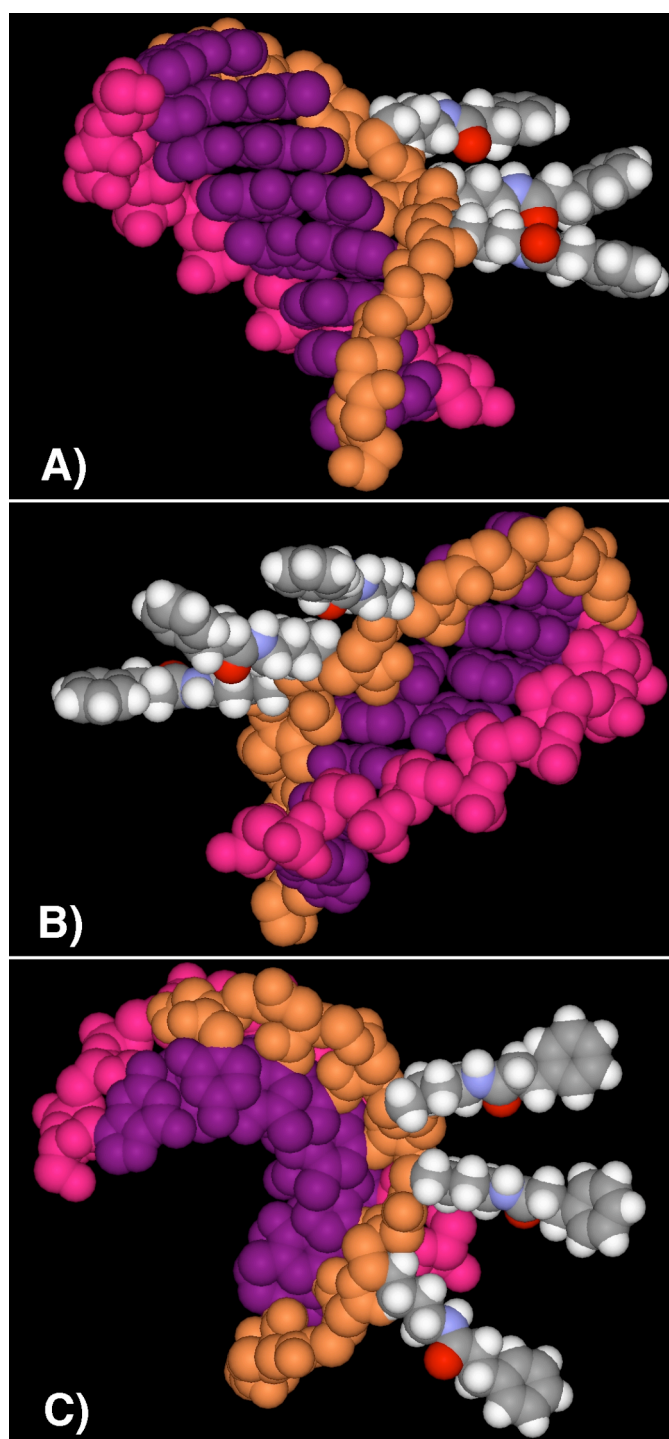


Figure II-12: Molecular Model of Adjacent/Conjugated $^L\text{K}\gamma$ -PNA. Nucleobases are colored purple. DNA sugar-phosphate backbone is colored fuchsia. The PNA backbone is colored gold. The hydrocinnamic acid-coupled $^L\text{K}\gamma$ -sidechains are primarily grey. A) Major Groove of DNA: $^L\text{K}\gamma$ -PNA Duplex. B) Minor Groove of DNA: $^L\text{K}\gamma$ -PNA Duplex. C) Top View of DNA: $^L\text{K}\gamma$ -PNA Duplex.

II.4.5 ^LK γ -PNA Mismatch Selectivity

While binding affinity is important, any PNA modification that causes the loss of sequence specificity or binds to nucleic acids indiscriminately would be less useful for many current applications. Therefore, we undertook a concerted effort to examine the binding affinity with complementary DNA containing one nucleobase mismatch across from the PNA modification. **PNA II-2**, with one unconjugated ^LK γ -PNA residue at the center thymine position, was annealed to the three mismatch DNA strands showing reduced binding (Table II-7).

Table II-7: ^LK γ -PNA Mismatch Specificity.

PNA	Target DNA Sequence ^a	T_m (°C) DNA ^b	ΔT_m (°C) ^c	$\Delta\Delta T_m$ (°C) ^d
II-1	3'-CAT CTA GTG A-5'	48.7	---	---
II-1	3'-CAT CG <u>T</u> GTG A-5'	36.0	-12.9	---
II-1	3'-CAT CTC <u>C</u> GTG A-5'	32.0	-16.9	---
II-1	3'-CAT CT <u>G</u> GTG A-5'	34.0	-14.9	---
II-2	3'-CAT CTA GTG A-5'	51.4	---	---
II-2	3'-CAT CG <u>T</u> GTG A-5'	36.1	-15.3	2.4
II-2 ^e	3'-CAT CTC <u>C</u> GTG A-5'	---	---	---
II-2	3'-CAT CT <u>G</u> GTG A-5'	35.3	-16.1	1.2
II-10	3'-CAT CTA GTG A-5'	50.3	---	---
II-10	3'-CAT CG <u>T</u> GTG A-5'	30.0	-20.5	7.6
II-10	3'-CAT CTC <u>C</u> GTG A-5'	34.9	-15.6	-1.3
II-10	3'-CAT CT <u>G</u> GTG A-5'	29.9	-20.6	5.7

^a Anti-parallel complementary DNA. Residues that are in bold and underlined denote the location of a single mismatch. ^b Data were collected from cooling runs from 90 °C to 15 °C at a rate of 1 °C/min. ^c ΔT_m represents the difference in melting temperature between the fully complementary DNA and the singly mismatched. ^d $\Delta\Delta T_m$ represents the difference in mismatch selectivity (T_m Fullymatched- T_m Mismatch) between the chimera sequences and *aeg*PNA, II-1. ^e No melting curves were observed after multiple attempts.

The net loss in stability from fully complementary DNA to mismatched DNA was slightly higher than the difference associated with *aeg*PNA oligomers. The consistency or slight improvement of the mismatch selectivity is further evidence against a purely charge-charge interaction between the protonated primary amine on *PNA II-2* and the polyanionic backbone of DNA. Similar results were observed for *PNA II-9* with the miniPEG/fluorene conjugated side chain. In both cases, the mismatch discrimination of the modified PNA oligomers was similar to, or better than, the discrimination of their *aeg*PNA counterparts; the only anomaly is the TC mismatch DNA binding to *PNA II-9* with slightly reduced selectivity compared to *aeg*PNA.

The same trend was apparent when *PNA II-16* was annealed to mismatches across from the central γ -PNA residue (Table II-8). Rigidification of the PNA backbone, either through

Table II-8: Adjacent Substituted L K γ -PNA Residues Mismatch Specificity.

PNA	Target DNA Sequence ^a	T_m (°C) DNA ^b	ΔT_m (°C) ^c	$\Delta\Delta T_m$ (°C) ^d
II-16	3'-CTG AAA TGC T-5'	42.4	---	---
II-16	3'-CTG A <u>T</u> A TGC T-5'	25.6	-16.8	---
II-16	3'-CTG A <u>C</u> A TGC T-5'	34.0	-8.4	---
II-16	3'-CTG A <u>G</u> A TGC T-5'	30.0	-12.4	---
II-17	3'-CTG AAA TGC T-5'	49.3	---	---
II-17	3'-CTG A <u>T</u> A TGC T-5'	30.8	-18.5	1.7
II-17	3'-CTG A <u>C</u> A TGC T-5'	38.8	-10.5	2.1
II-17	3'-CTG A <u>G</u> A TGC T-5'	33.6	-15.7	3.3

^a Anti-parallel complementary DNA. Residues that are in bold and underlined denote the location of a single mismatch. ^b Data were collected from cooling runs from 90 °C to 15 °C at a rate of 1 °C/min. ^c ΔT_m represents the difference in melting temperature between the fully complementary DNA and the singly mismatched. ^d $\Delta\Delta T_m$ represents the difference in mismatch selectivity (T_m Fullymatched- T_m Mismatch) between the chimera sequences and *aeg*PNA, II-16.

cyclic constraints²⁷ or side chains hindering bond rotation,²⁸ have shown similar increases in mismatch toleration and differentiation. This, however, is in contrast to ^DK α -PNA which greatly increases the selectivity of PNA oligomers when adjacent residues are employed, but at the expense of some binding affinity.²⁹

II.5 Thermal Melting Analysis of ^LK γ -PNA with RNA

To characterize binding to RNA, several of the ^LK γ -PNA oligomers were bound to the complementary RNA (Table II-9). *aeg*PNA typically binds to RNA with a slightly higher affinity than single-stranded DNA. This is also the case with the ^LK γ -PNA modifications. Also noteworthy is the observation that the ^DK γ -PNA residue in **PNA II-6** destabilized the RNA/PNA duplex (-12.7 °C). The destabilization effect that **PNA II-6** has on the RNA/PNA duplex (-13.3 °C) is similar in DNA/PNA duplex formation, and suggests that the factors influencing the stability of DNA and RNA complexes are the same in the case of γ -PNA.

Table II-9: T_m Analysis of ^LK γ -PNA with Complementary RNA.

PNA	Sequence	T_m (°C) RNA ^a	ΔT_m (°C) ^b
II-1	H-GTAGATCACT-Lys-NH ₂	54.8	---
II-2	H-GTAGAT ¹ CACT-Lys-NH ₂	57.3	2.5
II-6	H-GTAGAT ² CACT-Lys-NH ₂	42.1	-12.7
II-16	H-GACTTTACGA-Lys-NH ₂	52.6	---
II-17	H-GACT ⁹ T ⁹ T ⁹ ACGA-Lys-NH ₂	56.6	4.0

^a Thermal denaturation studies were undertaken with complementary RNA; PNAs II-1, II-2, and II-6 were annealed to RNA 3'-CATCTAGTGA-5'), PNAs II-16 and I-17 to RNA (3'-CTG AAA TGC T-5'). Data were collected from cooling runs from 90 °C to 15 °C at a rate of 1 °C/min. ^b ΔT_m represents the difference in melting temperature between the chimera sequence and *aeg*PNA, II-1 or II-16.

II.6 Circular Dichroism Studies of $^L\text{K}\gamma$ -PNA

Circular Dichroism (CD) can be used to detect the presence of helical base stacking, an indirect indication of preorganization in single-stranded nucleic acids. Either because of a lack of bases stacking or excess helical sense, *aeg*PNA does not produce an exciton coupling pattern.³⁰ Sforza and coworkers demonstrated that several modifications at the α -carbon, including uncoupled L and D lysine side chains, induce a CD signal when bound to complementary PNA, but unhybridized α -PNA gave only a faint CD signal.³¹ When *PNA II-5* was examined in buffered solution without its complementary strand, a definite CD spectrum was observed (Figure II-13).

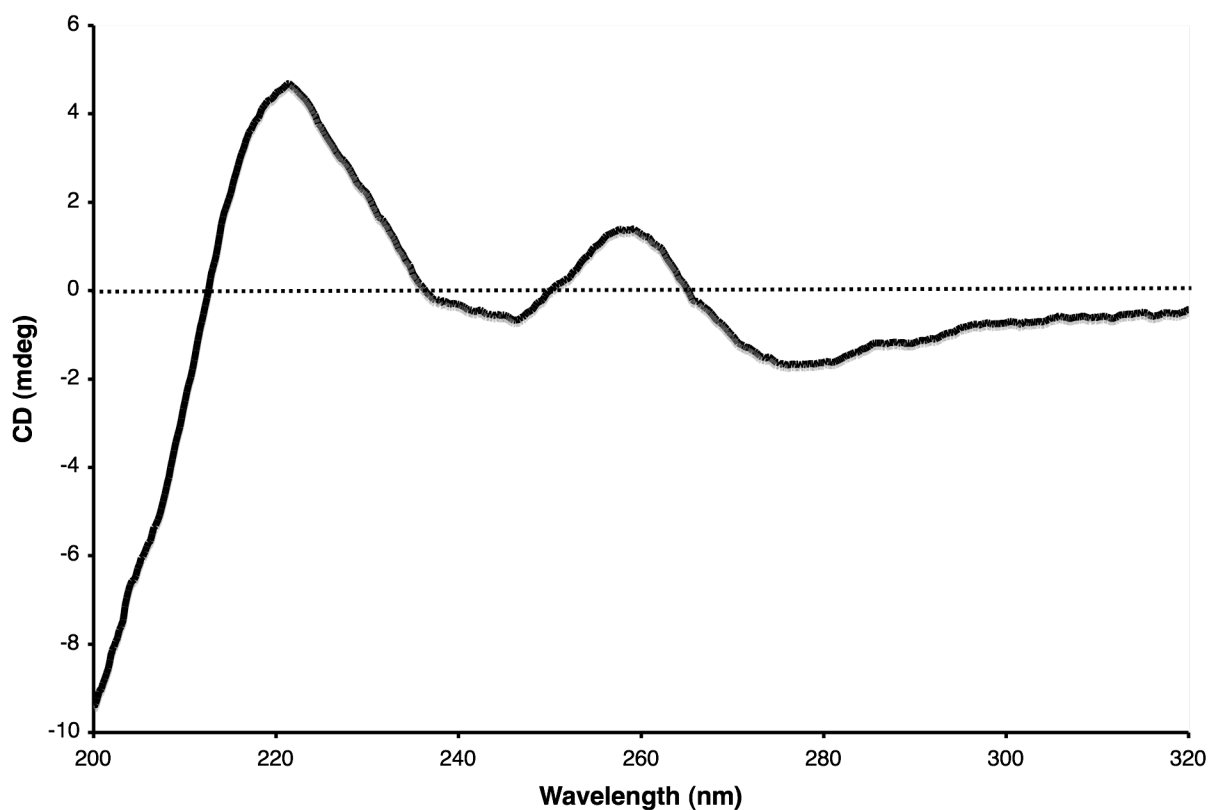


Figure II-13: Circular Dichroism Spectrum of *PNA II-5*.

The maxima around 225 nm and 265 nm, along with troughs around 250 nm and 280 nm were in excellent agreement with CD studies on the preorganization of $^L\text{S}\gamma$ -PNA oligomers conducted by Dragulescu-Andrasi and coworkers.³² Although the CD intensity of PNA II-5 was lower than expected compared to the $\text{S}\gamma$ -PNA, compared to the $\text{K}\alpha$ -PNA oligomers, it was both more distinct and higher in intensity (Figure II-14). This is further evidence for the proclivity of $^L\text{K}\gamma$ -PNA to self-organize versus the analogous $^D\text{K}\alpha$ -PNA.

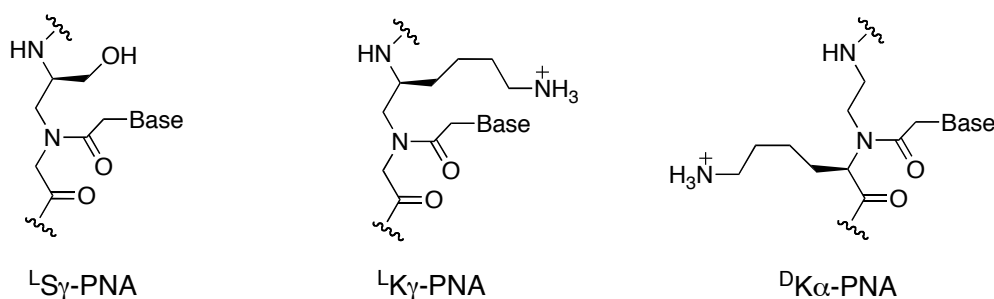


Figure II-14: Sidechain PNA Used in Preorganization Studies

II.7 $^L\text{K}\gamma$ -PNA as Scaffolds for Fluorescent Molecules

With the increasing interest in detection assays using fluorescent conjugates to PNA, we sought to examine the potential of $^L\text{K}\gamma$ -PNA as hybridization “light-up” probes. This type of fluorescent probe utilizes nucleic acid-fluorophore conjugates that demonstrate very little fluorescence emission when unbound or in the presence of non-complementary nucleic acids. Upon binding to a complementary nucleic acid, the fluorophore emits light with induced excitation, indicating the presence of the complement. Molecular beacons employ this method of nucleic acid detection, by diminishing the fluorescent intensity of the appended molecule by bringing it into proximity of a quencher, either by built in loop structures³³ or, in the case of PNAs, general hydrophobic interactions (Figure II-15).³⁴

Although the $^L\text{K}\gamma$ -PNA derivatives we have developed could lend themselves well to this type of detection strategy (discussed in Chapter IV), we began our initial studies into these types of applications by examining systems where the addition of a fluorescence-quenching molecule was not necessary.

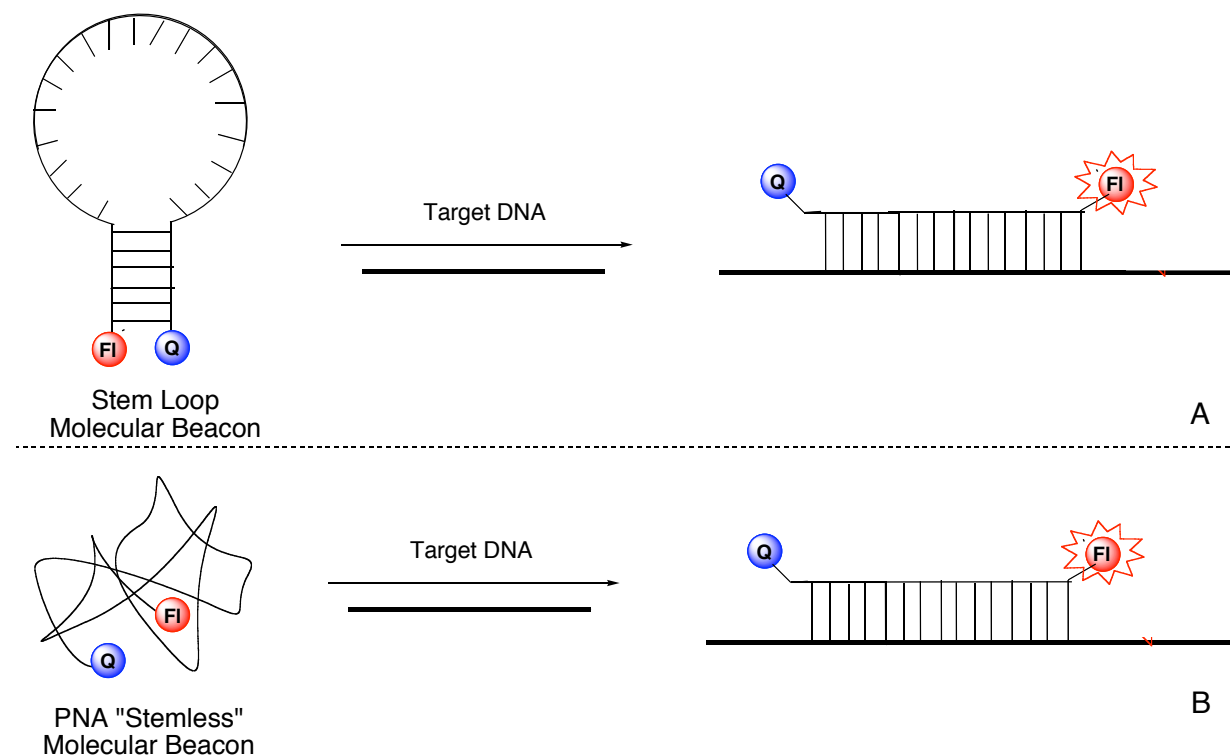


Figure II-15: Nucleic Acid Molecular Beacons. Molecular beacons usually require a stem-loop structure to ensure efficient quenching of the fluorophore (A). Because of hydrophobic interactions, PNA MBs can be constructed without this loop (B).

II.7.1 $^L\text{K}\gamma$ -PNA Light-Up Probes Using Fluorene

Fluorene is a fluorophore with a high quantum yield, and many affordable derivatives are commercially available.³⁵ The fluorescence produced by fluorene is very efficiently quenched by thymine.³⁶ In a recent study, Hwang and coworkers utilized this property to design a DNA light-up probe in which a fluorene derivative was cross coupled directly to thymine.³⁷ We postulated that because PNA folds on itself in aqueous solution, an appended fluorene should be

brought into proximity with the nucleobases, thus greatly diminishing the fluorescent intensity of the probe while unbound.³⁸ Upon duplex formation with the complementary oligonucleotide, thymine residues would be stacked within the double helix, essentially shielding the nucleobases from the appended fluorene (Figure II-16).

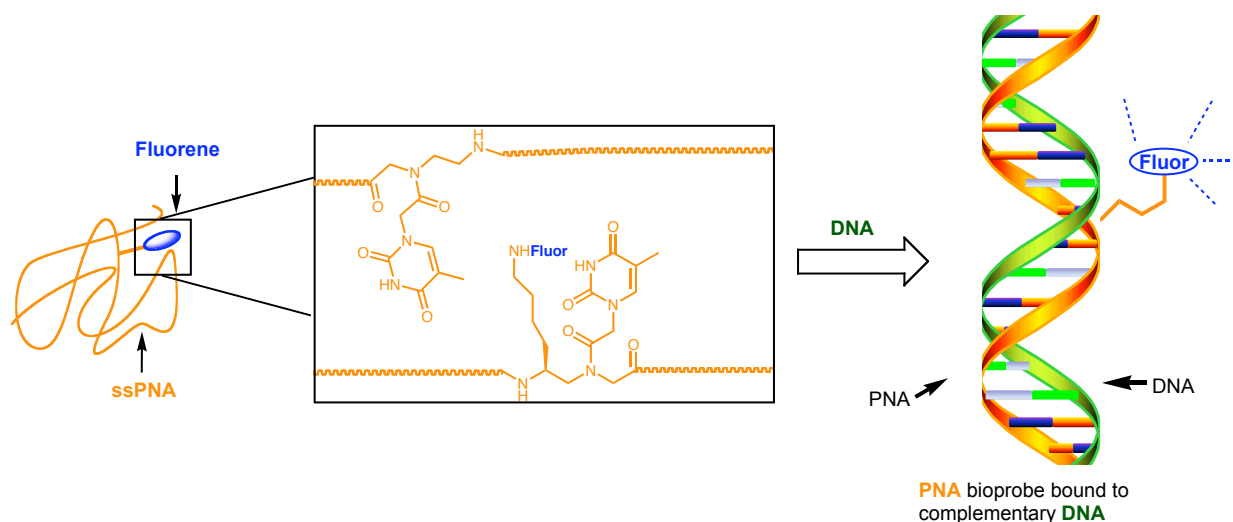


Figure II-16: Fluorene γ -PNA “Light-Up” Probe Design. In the absence of DNA, the fluorene is in proximity to multiple thymine residues, which quench the fluorescence. Upon duplex formation, the thymine is inaccessible, resulting in a fluorescent signal from the fluorene.

When excited with light at 340 nm, *PNA II-9* was faintly fluorescent ($\lambda_{\text{max}} = 425$) in the absence of DNA (Figure II-17). Annealing of *PNA II-10* to the complementary DNA produced a 4-fold fluorescence intensity increase compared to the unbound PNA. When *PNA II-10* was annealed to DNA with a single mismatch across from the $^L\text{K}\gamma$ -PNA residue, the fluorescence intensity did not change from the base line or showed a slight increase (TT mismatch). *PNA II-11* showed a similar increase in fluorescent intensity (~4-fold) when annealed to the complementary DNA. Furthermore, the fluorene remained efficiently quenched when unbound despite not being attached to a thymine-containing PNA residue.

Although the fluorescence was very efficiently quenched when the PNA oligomers were unbound, especially considering the high fluorescent yield of fluorene, the modest increase in fluorescent intensity suggests that the fluorene still interacts with the thymine residues. This could be due to intercalation of the fluorene residue into the duplex or aggregation effects.

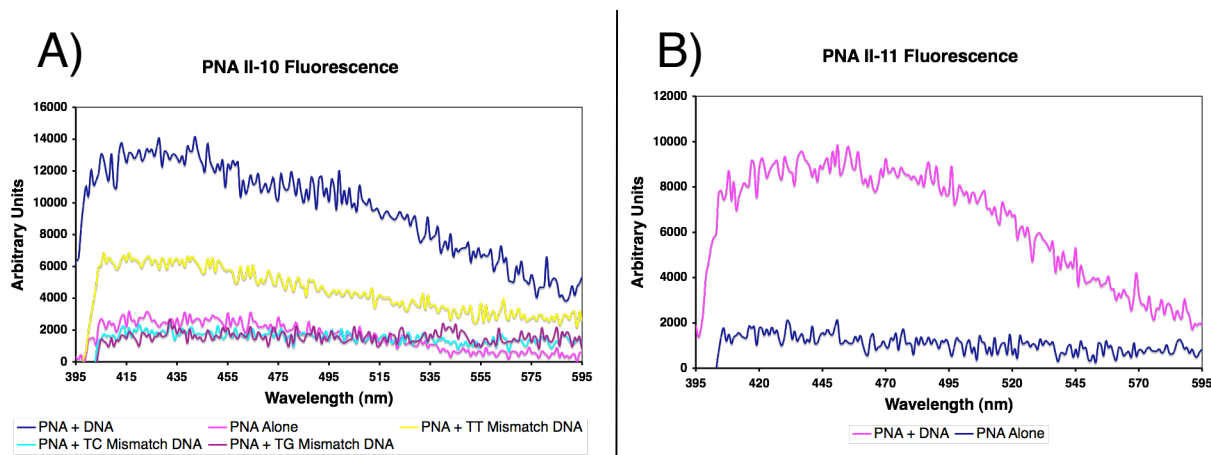


Figure II-17: Fluorene γ -PNA Probe Fluorescent Emission.

II.7.2 ^LK γ -PNA Light-Up Probes Using Thiazole Orange

Thiazole orange (TO)³⁹ is a cyanine dye that is often used in PNA-based “light-up” probes. The fluorescence of TO is quenched by excited state intramolecular twisting.⁴⁰ In aqueous solution, TO is allowed to freely rotate, and emits very little fluorescence.⁴¹ TO readily interacts with paired nucleobases, either through intercalation or stacking, thus reducing internal bond rotation and emitting a large fluorescent signal (Figure II-18). When an oligomer containing the T⁸ residue (*PNA II-14*) was unbound, there was very low background fluorescence (Figure II-19). When annealed to the complementary DNA (3'- GGA GAA GGA G-5'), *PNA II-14* gave a large increase in fluorescent intensity (about two orders of magnitude). This increase was consistent with the increase when thiazole orange was coupled to the N-terminus of the same oligomer (~42 times greater fluorescent intensity at 530 nm).⁴² Due

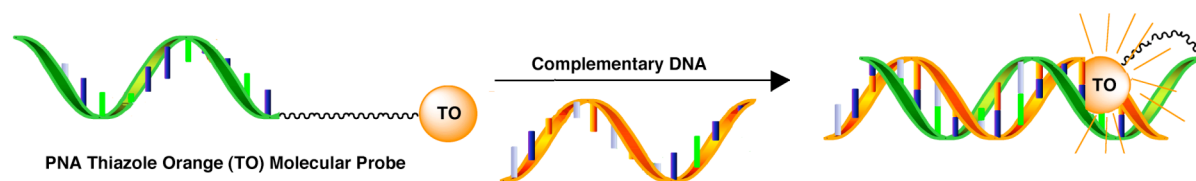


Figure II-18: Typical Thiazole Orange-PNA Molecular Probe. Unbound to DNA, the thiazole orange (TO) gives off very little fluorescence.

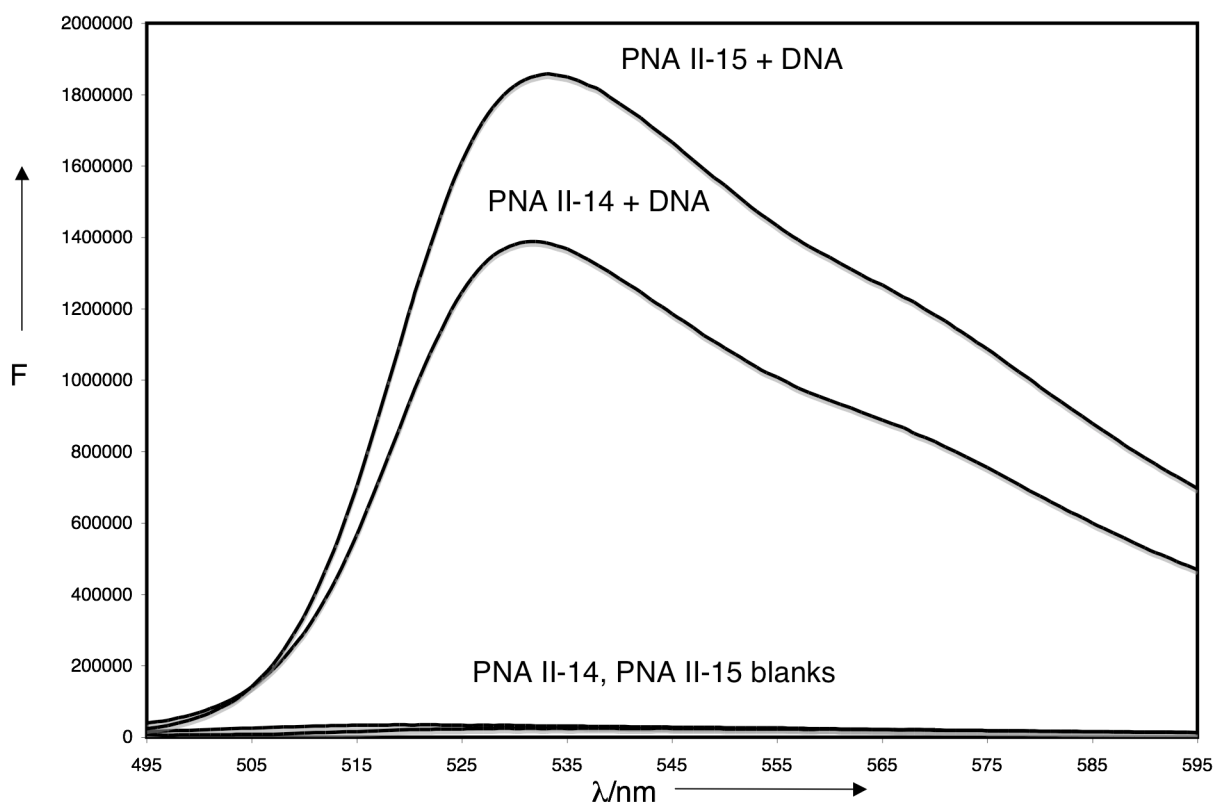


Figure II-19: Thiazole Orange γ -PNA Probe Fluorescent Emission.

to the central position of the $^L\text{K}\gamma$ -PNA residue and the length of the linkers, base stacking on the end of the duplex is prevented. Therefore, thiazole orange bond rotation must be restricted due to intercalation⁴⁴ or a nonintercalative hybridization. Because *aeg*PNA lacks positions where further functionality can be easily appended, most *aeg*PNA oligomers only have one functional group attached per oligomer, usually to the N-terminus. By using the $^L\text{K}\gamma$ -PNA, multiple fluorophores can be incorporated into a single molecular probe, increasing sensitivity of the

probe without negatively affecting the T_m of the PNA-DNA duplex. When the oligomer containing two T⁸ residues (*PNA II-15*) was combined with the complementary DNA, a similar increase in fluorescent intensity was observed. While the effect of having two thiazole orange molecules attached to *PNA II-15* did not double the fluorescent intensity, there was a 30% larger fluorescent intensity compared to the oligomer with one thiazole orange fluorophore attached.

II.8 Summary and Discussion

We have successfully synthesized multiple γ -substituted PNA monomers and incorporated them into PNA oligomers. Our subsequent studies have demonstrated that ^LK γ -PNA can bind to complementary DNA and RNA with higher affinity and selectivity than *aeg*PNA. Furthermore, the binding affinity is independent of charge or substituent size providing a useful point for functionalization. We have also investigated initial uses of this functionalization property by applying the ^LK γ -PNA in fluorescent light-up probes.

These traits we have outlined compare very favorably to the ^DK α -PNA, which has also shown favorable binding characteristics when the side chains contain positive electronic charges. Furthermore, as demonstrated with PNA II-16, ^LK γ -PNA side chains could be introduced adjacently without detriment to DNA or RNA binding. This is in contrast to the “chiral box” example of three adjacent ^DK α -PNA residues in the Nielsen sequence, which reduces the binding affinity towards the complementary DNA and RNA.²⁹ The most exciting difference between ^LK γ -PNA and ^DK α -PNA is the ability to support bulky conjugates, regardless of size or charge. This ability alone should prove extremely useful in cases that have already made beneficial use of α -sidechain conjugation.⁴⁴ In combination with the ability to alter and append sidechain functionality on the solid phase with ^LK γ -PNA(Fmoc) monomers, there is no limit to the variety

and sophistication that PNA oligomers can possess. The $^L\text{K}\gamma$ -PNA modification should prove extremely useful in augmenting the physical characteristics of PNA oligomers and providing an unexplored scaffold for the display of many different substituents.

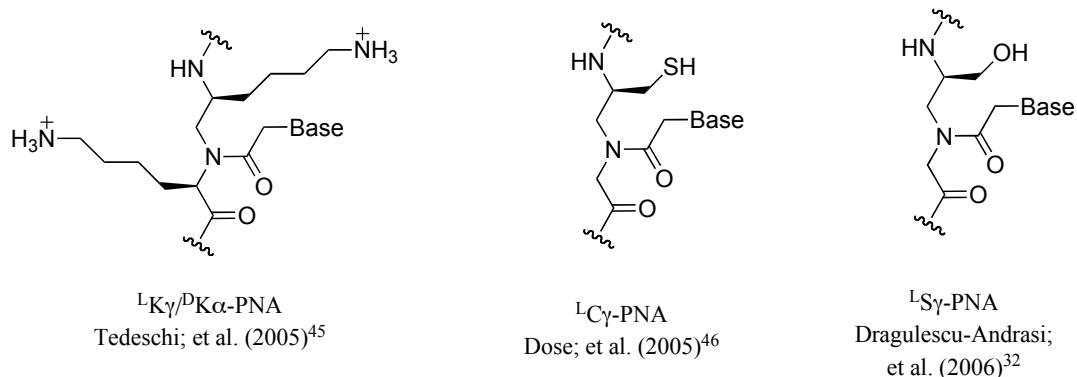


Figure II-20: Recent Advances in γ -PNA Research.

Since our initial studies and publications, several other groups have explored the γ -position on PNA and added important detail and perspective to our results while exploring unique γ -PNA (Figure II-20). Sforza and coworkers also studied at $\text{K}\gamma$ -PNA confirming our stereochemistry results.⁴⁵ Furthermore, the $\text{K}\gamma$ -modification was used in combination with the $\text{K}\alpha$ -side chain producing additive binding effects. Dragulescu-Andrasi and coworkers developed a serine side chain PNA ($^L\text{S}\gamma$ -PNA) that showed self-organization via CD, and provided insight into efficient ways to better understand our $^L\text{K}\gamma$ -PNA in terms of preformation and organization.³² Finally, Sietz and coworkers developed a cysteine γ -PNA ($^L\text{C}\gamma$ -PNA) that can be used as a means of constructing elongated PNA through native chemical ligation.⁴⁶ This modification was also used as a link to fluorophores through a disulfide bridge, with detrimental binding effects. It can be objectively stated that the interest in γ -substituted PNA is in its initial stages but is gaining adherents. It is also reasonable to believe that as more is understood about

the underlying system and derivatives continue to be synthesized and optimized, γ -substituted PNA should find itself in more practical applications in the near future.

II.9 Experiment Procedures and Data

II.9.1 γ -PNA Monomer Synthesis

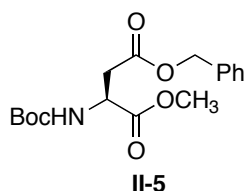
II.9.1a General Methods

Proton nuclear magnetic resonances ($^1\text{H NMR}$) and ^{13}C nuclear magnetic resonances ($^{13}\text{C NMR}$) were recorded in deuterated solvents on an iNOVA (500 MHz) or a Mercury (400 MHz) spectrometer. Chemical shifts are reported in parts per million (ppm, δ) relative to tetramethylsilane (δ 0.00). $^1\text{H NMR}$ splitting patterns are designated as singlet (s), doublet (d), triplet (t), doublet of doublets (dd). Splitting patterns that could not be interpreted or easily visualized are designated as multiplet (m). Coupling constants are reported in Hertz (Hz). Electrospray mass spectra (ESI-MS) were obtained using a Micromass Quattro II Triple Quadrupole HPLC/MS/MS Mass Spectrometer. High-resolution mass spectra (HRMS) were obtained on a Micromass Q-ToF Ultima at the University of Illinois at Urbana-Champaign Mass Spectrometry Center. Optical rotation was determined on an Optical Activity AA-100 Automatic Digital Polarimeter at wavelength 589 nm. All samples were analyzed in MeOH at 24 °C, with 5 cm long path length.

Analytical thin-layer chromatography (TLC) was carried out on Sorbent Technologies TLC plates precoated with silica gel (250 μm layer thickness). Flash column chromatography was performed on EM Science silica gel 60 (230-400 mesh) or using a Biotage Flash12+ apparatus on Biotage Si 25+M columns. Solvent mixtures used for TLC and flash column chromatography are reported in v/v ratios. Acetonitrile and DMF were passed through activated alumina.⁴⁷ Unless otherwise noted, all other commercially available reagents and solvents were purchased from

Aldrich and used without further purification. CuCl grade was 98+%. Benzyl alcohol was 99.8% anhydrous grade. Boc-Asp(OBn)-OH, Boc-Dap(Fmoc)-OH, Boc-Lys(Cbz)-OH, D-Boc-Lys(Cbz)-OH, and Boc-Lys(Fmoc)-OH were purchased from Advanced ChemTech. C^{Cbz}-CH₂-CO₂H and A^{Cbz}-CH₂-CO₂H were synthesized by PolyOrg Inc. via methods previously described.¹⁶ The Thiazole Orange derivative was synthesized as previously described.⁴² Unless otherwise indicated, all reactions were performed under an inert atmosphere of N₂. Glassware was dried in an oven at 180 °C for 2 hours prior to use. Fmoc 8-amino-3,6-dioctanoic acid was purchased from Peptides International, Inc.

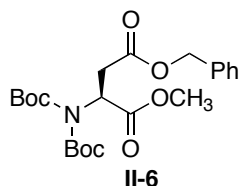
II.9.1b ¹Dapy(Cbz)-PNA Monomer Synthesis



Boc-Asp(OBn)-OMe (II-5). Boc-Asp(OBn)-OH (4.8 g, 14.9 mmol) was dissolved in dry DMF (35 mL) in a 100 mL RBF. Finely ground K₂CO₃ (3.0 g, 22 mmol) was added to the solution to form a suspension. The

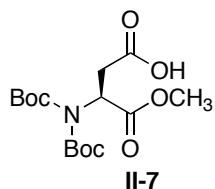
mixture was cooled to 0 °C in an ice bath over five minutes. Methyl iodide (2.0 mL, 30 mmol) was then added to the RBF over 30 seconds. The resulting mixture was stirred at 0 °C for 3 hours. A yellow color developed within 20-30 minutes. The ice bath was removed, and H₂O (50 mL) was added, producing a grayish white precipitate. The mixture was extracted with EtOAc (3 x 50 mL). The organic layers were combined and washed with saturated NaHCO₃ (1 x 50 mL) and saturated NaCl (4 x 50 mL). The organic layer (which was yellow) was dried over Na₂SO₄, and passed through a plug of silica, eluting with ethyl acetate. Evaporation under reduced pressure afforded 2.52 g of a white powder (98 %). ¹H NMR (CDCl₃, 500 MHz): δ 7.34 (m, 5H, phenyl-CH), 5.48 (d, *J* = 7.9 Hz, 1 H, NH), 5.13 (dd, *J*₁ = 12.3 Hz, *J*₂ = 17.2 Hz, 2H, CH₂), 4.59 (t, *J* = 3.8 Hz, 1 H, NH-CH), 3.70 (s, 3 H, CH₃), 3.05 (dd, *J*₁ = 4.0 Hz, *J*₂ = 16.8 Hz, 1 H, HC-H), 2.86 (dd, *J*₁ = 4.5 Hz, *J*₂ = 13.8 Hz, 1 H, HC-H), 1.44 (s, 9 H, tert-butly-CH₃); ¹³C

NMR (CDCl₃, 126 MHz): δ 171.73, 171.00, 135.62, 128.83, 128.65, 128.54, 80.36, 67.02, 52.89, 50.18, 37.11, 28.51.



Boc₂-Asp(OBn)-OMe (II-6). Di-*tert*-butyl dicarbonate (10.63 g, 49 mmol) and DMAP (3.97 g, 32.5 mmol) were placed into a dry 100 mL RBF. Product **II-5** (10.96 g, 32.5 mmol) was added and the solids were dissolved

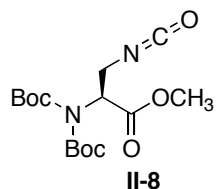
in dry acetonitrile (30 mL). The resulting solution was stirred for 24 hours, during which time the reaction color went from light to dark yellow. Water (50 mL) was added, and the solution became cloudy white. The resulting mixture was extracted with EtOAc (3 x 50 mL). The combined organic layers were washed with 1 M HCl (1 x 50 mL) and saturated NaCl (4 x 50 mL). The combined organic layers were dried over Na₂SO₄ and evaporated under reduced pressure to afford 13.71 g of a viscous red oil (96 %). ¹H NMR (CDCl₃, 500 MHz): δ 7.34 (m, 5H, phenyl-CH), 5.48 (dd, $J_1 = 6.9$ Hz, $J_2 = 6.8$ Hz, 1 H, N-CH), 5.13 (dd, $J_1 = 12.3$ Hz, $J_2 = 18.1$ Hz, 2H, CH₂), 3.70 (s, 3 H, CH₃), 3.30 (dd, $J_1 = 7.3$ Hz, $J_2 = 16.7$ Hz, 1 H, HC-H), 2.77 (dd, $J_1 = 6.4$ Hz, $J_2 = 16.5$ Hz, 1 H, HC-H), 1.48 (s, 18 H, tert-butyl-CH₃); ¹³C NMR (CDCl₃, 126 MHz): δ 170.75, 170.49, 151.80, 135.96, 128.76, 128.47, 83.79, 66.86, 55.10, 52.73, 36.11, 28.17.



Boc₂-Asp-OMe(II-7). Product **II-6** (12.81 g, 29.3 mmol) was dissolved in MeOH (70 mL), and the solution was placed into a dry Parr reaction vessel. Palladium on activated carbon (2.5g, 10% by weight) was added to the

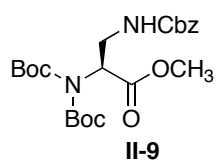
solution. The solution was shaken on a Parr apparatus for 2 hours under an H₂ atmosphere of 50 psig. The Pd/C was filtered off through Celite 545, eluting with MeOH. The MeOH was evaporated under reduced pressure to give 9.02 g of a white powder (89 %). ¹H NMR (CDCl₃, 500 MHz): δ 5.42 (dd, $J_1 = 6.6$ Hz, $J_2 = 6.8$ Hz, 1 H, N-CH), 3.74 (s, 3 H, CH₃), 3.30 (dd, $J_1 =$

7.0 Hz, $J_2 = 17.0$ Hz, 1 H, HC-H), 2.81 (dd, $J_1 = 6.4$ Hz, $J_2 = 17.0$ Hz, 1 H, HC-H), 1.49 (s, 18 H, *tert*-butyl-CH₃). ¹³C NMR (CDCl₃, 126 MHz): δ 176.96, 170.39, 151.76, 83.89, 54.81, 52.81, 35.85, 28.14.



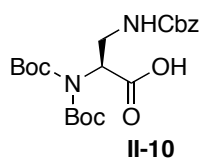
Isocyanate II-8. Product *II-7* (3.00 g, 8.6 mmol) was dissolved in dry THF (6 mL) in a 50 mL RBF, cooled to -10 °C via an ice bath of saturated NaCl solution, and stirred for 10 minutes. Ethylchloroformate (1.24 mL, 13 mmol)

was added via syringe to the solution. Triethylamine (4 mL, 28.7 mmol) was added over 30 seconds and stirred for 30 minutes. A solution of NaN₃ (2.8 g, 43 mmol) in H₂O (15 mL) was added to the solution. The solution was allowed to stir for 1.5 hours as the temperature was maintained at -10 °C. The solution was then extracted with EtOAc (4 x 50 mL). The combined organic layers were washed with H₂O (1 x 50 mL) and saturated NaCl solution (3 x 50 mL), and then dried over Na₂SO₄ and evaporated under reduced pressure to give clear oil. NOTE! This solution was not evaporated to dryness. In some cases, acyl azides can explode when concentrated to dryness.⁴⁸ After concentration, toluene (100 mL) was added, and the resulting solution was refluxed for 2 hours. The toluene was then removed under reduced pressure to afford 2.52 g of a light red oil (85 %). ¹H NMR (CDCl₃, 500 MHz): δ 5.13 (dd, $J_1 = 5.5$ Hz, $J_2 = 9.1$ Hz, 1 H, N-CH), 3.94 (dd, $J_1 = 4.9$ Hz, $J_2 = 13.4$ Hz, 1 H, HC-H), 3.83 (dd, $J_1 = 9.2$ Hz, $J_2 = 13.4$ Hz, 1 H, HC-H), 3.75 (s, 3 H, CH₃), 1.52 (s, 18 H, *tert*-butyl-CH₃). ¹³C NMR (CDCl₃, 126 MHz): δ 169.06, 152.09, 128.46, 84.23, 58.23, 52.74, 43.00, 28.16. IR: 2266 cm⁻¹ (N=C=O), 1749 cm⁻¹ (C=O), 1701 cm⁻¹ (C=O).



Boc₂-Dap(Cbz)-OMe (II-9). In a dry 50 mL RBF, CuCl (2.60 g, 26.3 mmol) and benzyl alcohol (2.72 mL, 26.3 mmol) were suspended in DMF (15 mL) to

afford a yellowish green mixture. A solution of **II-8** (8.82 g, 25.6 mmol) in dry DMF (7 mL) was added. The resulting suspension turned brownish red, and was stirred for 1 hour. Water (100 mL) was added to the reaction, and the resulting mixture was extracted with EtOAc (4 x 100 mL). The combined organic layers were then washed with 1 M HCl (100 mL) and saturated NaCl (4 x 100 mL), dried over Na₂SO₄ and evaporated under reduced pressure to afford a brownish red oil. The oil was redissolved in EtOAc (100 mL), and eluted through a silica plug to afford 11.01 g of a light yellow oil (95 %). ¹H NMR (CDCl₃, 500 MHz): δ 7.34 (m, 5H, phenyl-CH), 5.25 (t, 1 H, HN-CH₂), 5.11 (m, 2H, CH₂), 5.05 (t, 1 H, N-CH), 3.85 (m, 1 H, HC-H), 3.75 (s, 3 H, CH₃), 3.69 (m, 1 H, HC-H), 1.50 (s, 18 H, *tert*-butyl-CH₃); ¹³C NMR (CDCl₃, 126 MHz): δ 170.30, 151.96, 128.79, 128.35, 127.21, 83.91, 67.00, 57.87, 52.51, 41.35, 28.15.

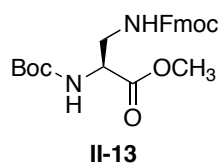


Boc₂-Dap(Cbz)-OH (II-10). A solution of **II-9** (533 mg, 1.18 mmol in 10 mL of MeOH) was added to a 100 mL RBF. To the stirring solution, 2 M NaOH (5 mL) was added slowly. The color changed from a light yellow to gold.

Precipitate briefly formed when all the NaOH solution had been added. After three minutes, the precipitate had dissipated. The reaction was left for two hours. The solution was concentrated by evaporation under reduced pressure, diluted with water (20 mL) and washed with ethyl ether (3 x 10 mL). The organic layer was washed with 2 M NaOH (2 x 25 mL). The combined aqueous layers were made acidic using 1 M HCl (pH ~3), which resulted in formation of a cloudy white solution. The aqueous mixture was extracted with ethyl acetate (3 x 50 mL). The combined organic layers (yellow) were washed with 1 M HCl (2 x 20 mL), and saturated NaCl (2 x 25 mL). The organic layer was dried over Na₂SO₄ and evaporated under reduced pressure to give a sticky yellow solid. Addition of hexanes (~50 mL), followed by vigorous stirring, resulted in precipitation of a slightly yellow solid (350 mg, 68 %). ¹H NMR (CDCl₃, 500 MHz):

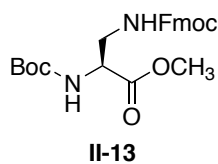
δ 7.36 (m, 5H, phenyl-CH), 5.41 (m, 1 H, N-CH), 5.25 (s, 1 H, HN-CH₂), 5.11 (m, 2H, CH₂), 3.85 (m, 1 H, HC-H), 3.68 (m, 1 H, HC-H), 1.50 (s, 18 H, *tert*-butyl-CH₃).

Note! Due to some monodeprotection, there are small amounts of Boc-Dap(Cbz)-OH that are present along with **II-10**. There are clearly additional peaks present in the ¹H NMR when Boc-Dap(Cbz)-OH is present (i.e. additional Boc and methyl ester peaks). The amount of Boc-Dap(Cbz)-OH is most easily identified and quantified by examination of the α protons in the ¹H NMR spectrum. For Boc-Dap(Cbz)-OH, this proton appears at δ 4.4 ppm, and for Boc-Dap(Cbz)-OH the same proton appears at δ 5.4 ppm. Comparing the integrations of these two peaks gives the relative amounts of the two products. Using this method, there is never more than 10% of Boc-Dap(Cbz)-OH.



Boc-Dap(Fmoc)-OMe (II-13). Boc-Dap(Fmoc)-OH (0.098 g, 0.24 mmol, Advanced Chemtech) was combined with finely ground K₂CO₃ (0.075 g, 0.54 mmol) in dry DMF (1.0 mL). The resulting mixture was cooled to 0 °C in an

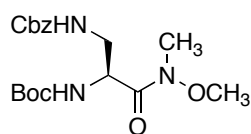
ice bath. Methyl iodide (0.040 mL, 0.5 mmol) was added slowly via syringe, and the resulting solution was stirred for 3 hours. Water (10 mL) was added, and a cloudy white mixture was obtained. The mixture was extracted with EtOAc (1 x 25 mL), and the organic layer was washed with saturated NaHCO₃ solution (1 x 25 mL) and saturated NaCl solution (2 x 25 mL). Next, the organic layer was dried over Na₂SO₄ and evaporated under reduced pressure to afford 105 mg of a fine white powder (>99 %). ¹H NMR (CDCl₃, 400 MHz): δ 7.76 (d, $J = 7.49$ Hz, 2H, Ar), 7.58 (d, $J = 7.49$ Hz, 2H, Ar), 7.36 (m, 4H, Ar), 5.44 (s, 1H, Boc-NH), 5.19 (s, 1 H, Fmoc-NH), 4.39 (m, 3 H, α CH, Fmoc-CH-CH₂O), 4.21 (t, $J = 6.40$ Hz, 1H, Fmoc-CH-CH₂O), 3.76 (s, 3 H, CO₂CH₃) 3.61 (m, 2 H, β CH₂), 1.45 (s, 9 H, *tert*-butyl-CH₃) [α]_D²⁴ = -10⁰ (c 1.0, MeOH).



Boc-Dap(Fmoc)-OMe (II-13). A sample of *II-9* (1.10 g, 2.4 mmol) was dissolved in neat TFA (15 mL) in a 250 mL RBF. The reaction was allowed to stir for 3 hours. TFA was then evaporated under a stream of nitrogen to

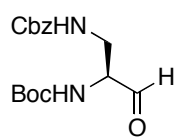
afford a thick, red oil. A crude ^1H NMR confirmed that the *tert*-butyl carbamate had been removed. A solution of saturated NaHCO_3 (20 mL) was added in order to quench any remaining TFA. Additional NaHCO_3 was added until the pH was $\sim 8-9$. Dioxane (20 mL) was added to the aqueous solution, followed by Boc_2O (0.795 g, 3.6 mmol in 10 mL of dioxane). The resulting solution was allowed to stir for 5 hours. The solution was then extracted with EtOAc (3 x 50 mL), the organic layers were washed with saturated NaHCO_3 solution (1 x 100 mL) and saturated NaCl solution (1 x 100 mL) and dried over Na_2SO_4 . Evaporation under reduced pressure produced 0.720 g of yellow oil (85% crude). ^1H NMR confirmed the presence of single *tert*-butyl carbamate protecting group. The yellow oil was dissolved in MeOH (20 mL), then Pd/C (130 mg, 10% by weight) was added to the solution. The solution was put under an H_2 atmosphere (X psig) and agitated vigorously on a Parr apparatus for 3 hours. The solution was filtered through Celite 545, eluting with MeOH. Evaporation under reduced pressure afforded a yellow/green oil. A crude ^1H NMR showed complete loss of benzyl carbamate protecting group. The oil was dissolved in dry THF (10 mL). Triethylamine (0.250 mL, 1.75 mmol) was added to the solution, followed by Fmoc-OSu (0.590 g, 1.75 mmol). The resulting solution was stirred for 5 hours. The solution was then evaporated to dryness under reduced pressure to afford a grayish oil. The grayish oil was dissolved in EtOAc (50 mL), and the organic layer was washed with saturated NaHCO_3 (1 x 50 mL), 1 M HCl (1 x 50 mL) and saturated NaCl solution (2 x 50 mL). The organic layer was dried over Na_2SO_4 , and evaporated under reduced pressure to afford a white precipitate. This crude product was partially soluble in DCM. The white solid that did not

dissolve in DCM was filtered off through Celite 545, eluting with DCM. The crude **II-13** that was obtained after filtration was further purified by flash column chromatography on silica gel eluting first with DCM ($R_F \sim 0$) followed by DCM/MeOH (95:5, $R_F = 0.35$). Purified **II-13** was obtained as a fine white powder (0.510 g, 65 %). The ^1H NMR was consistent with Boc-Dap(Fmoc)-OMe given above. $[\alpha]_D^{24} = -14^\circ$ (c 1.0, MeOH).

**II-15**

Boc-Dap(Cbz)-N(Me)OMe (II-15). Boc-Dap(Cbz)-OH **II-15** (1.87 g, 5.5

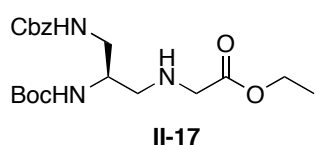
mmol) was dissolved in dry DCM (25 mL) in a 100 mL RBF. N-Methyl, O-methyl hydroxylamine hydrochloride salt (0.70 g, 7.2 mmol) and DMAP (66 mg, 0.55 mmol) were added to the solution. The reaction mixture was then cooled to 0 °C via ice bath and TEA (1.28 mL, 9.2 mmol) was added slowly to the stirring solution. EDC (1.59 g, 8.3 mmol) was added to the solution and the ice bath was removed. The reaction mixture was allowed to stir at rt. for 12 hours. The solution was then transferred to a separatory funnel and washed with 1 M HCl (2 x 10 mL), saturated NaHCO_3 solution (2 x 10 mL) and saturated NaCl solution (2 x 15 mL). The organic layer was dried over Na_2SO_4 and concentrated under reduced pressure on a rotary evaporator to afford 1.87 g (89 % yield) of the desired product as a sticky, white solid. ^1H NMR (CDCl_3 , 500 MHz): δ 7.34 (m, 5H), 5.50 (s, 1H), 5.16 (s, 1H), 5.09 (s, 1H), 4.78 (s, 1H), 3.77 (s, 3H), 3.54 (s, 3H), 3.19 (m, 2H), 1.43 (s, 9H).

**II-16**

Boc-Lys(Cbz)-CHO (II-16). Boc-Dap(Cbz)-N(Me)OMe **II-15** (0.56 g, 1.5

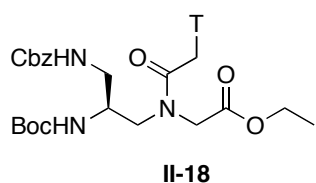
mmol) was dissolved in dry THF (15 mL) in a 50 mL RBF and cooled to 0 °C via ice bath. LAH (97 mg, 2.6 mmol) was added gradually over 45 seconds to the stirring solution. The reaction was monitored via TLC. After 45 minutes, the reaction mixture was quenched with saturated NaHSO_4 solution (8 mL) and allowed to stir for 10 minutes. The solution was then transferred to a separatory funnel and washed with EtOAc (2 x 40 mL). The

combined organic layers were washed with 1 M HCl (2 x 10 mL), saturated NaHCO₃ solution (2 x 10 mL), and saturated NaCl solution (3 x 10 mL). The organic layer was dried over Na₂SO₄ and concentrated under reduced pressure on a rotary evaporator to afford 0.44 g (92 % yield) of Boc-Dap(Cbz)-CHO as a clear, grey oil. ¹H NMR (CDCl₃, 500 MHz): δ 9.52 (s, 1H), 7.34 (m, 5H), 5.59 (s, 1H), 5.16 (s, 1H), 5.08 (s, 2H), 4.25 (m, 1H), 3.69 (m, 2H), 1.45 (s, 9H).



BocLys(Cbz)-PNA Backbone (II-17). Boc-Dap(Cbz)-CHO **II-16** (44

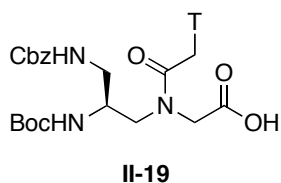
mg, 1.38 mmol) and ethyl glycinate hydrochloride salt (212 mg, 1.52 mmol) were dissolved in dry DCM (10 mL) in a 50 mL RBF. TEA (210 μL) was added drop-wise to the stirring solution and allowed to stir for 10 minutes. Sodium triacetoxyborohydride (409 mg, 1.93 mmol) was then added. The cloudy reaction mixture was allowed to stir for 1 hour and 40 minutes. The reaction was then quenched with saturated NaHCO₃ (15 mL) and saturated Na₂CO₃ (5 mL) and stirred for 10 minutes. The mixture was washed with DCM (2 x 30 mL) and the combined organic layers were dried over Na₂SO₄. Concentration under reduced pressure on a rotary evaporator afforded a yellow oil/solid. The oil was purified via column chromatography (EtOAc/Hexanes 2:1, rf = 0.2) to afford 310 mg (55 % yield) of the desired product as a clear, pale yellow solid. ¹H NMR (CDCl₃, 500 MHz): δ 7.35 (m, 5H), 5.47 (s, 1H), 5.22 (s, 1H), 5.10 (s, 2H), 4.18 (q, 2H), 3.67 (s, 1H), 3.39 (m, 2H), 3.20 (m, 2H), 2.70 (m, 2H), 1.72 (s, 1H), 1.43 (s, 9H) 1.27 (t, 3H). γ -



Boc(Dap)Lys-PNA Thymine Monomer Ethyl Ester (II-18). PNA

Backbone **II-17** (410 mg, 0.73 mmol), thymine acetic acid (175 mg, 0.95 mmol), and DMAP (8 mg, 0.07 mmol) were dissolved in dry DMF (20 mL). EDC hydrochloride salt (211 mg, 1.1 mmol) was added to the stirring solution (clear, yellow). After 36 hours, the reaction mixture was added to H₂O (40 mL) forming a white

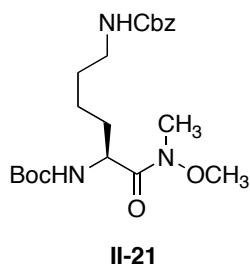
precipitate. The solution was then extracted with EtOAc (3 x 40 mL). The combined organic layers were washed with 1 M HCl (2 x 40), saturated NaHCO₃ (2 x 40 mL), water (2 x 40 mL) and saturated NaCl (3 x 40 mL). The organic layer was dried over Na₂SO₄ and concentrated under reduced pressure on a rotary evaporator to afford 330 mg (79% yield) of γ -Dap(Cbz)-PNA thymine monomer ethyl ester (**II-18**) as a flocculent, white solid. ¹H NMR (DMSO, 500 MHz) Major Rotamer: δ 11.30 (s, 1H), δ 7.34 (m, 5 H), 7.22 (m, 2H), δ 6.86 (d, 1H), δ 5.03 (m, 2H), δ 4.67 (m, 2H), δ 4.39 (m, 2H), δ 4.07 (q, 2H), δ 3.96 (s, 1H), δ 3.31 (m, 2H), δ 3.09 (m, 2H), δ 1.75 (s, 3H), δ 1.36 (s, 9H), δ 1.18 (t, 3H). LRMS (ESI-MS *m/z*): mass calcd for C₂₇H₃₇N₅O₉ [M + Na]⁺, 598.26, found 598.3.



BocDap(Cbz)-PNA Thymine Monomer Acid (II-19). PNA monomer

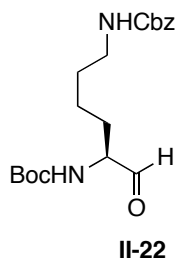
ethyl ester **II-18** (300 mg, 0.52 mmol) was dissolved in THF (8 mL) and cooled to 0 °C via ice bath. LiOH monohydrate (275 mg, 6.5 mmol) was dissolved in 6.5 mL of H₂O and the solution was added slowly dropwise to the stirring reaction mixture. The ice bath was then removed and the reaction was stirred under N₂ for 5 hours. The solution was diluted with H₂O (10 mL) and washed with diethyl ether (2 x 10 mL). The pH of the aqueous layer was carefully lowered to ~1-2 with 3 M HCl forming a white precipitate. The solution was washed with EtOAc (4 x 20 mL) and the organic layers were dried over Na₂SO₄. The solution was concentrated under reduced pressure on a rotary evaporator to afford 290 mg (>99% yield) of γ -Dap(Cbz)-PNA thymine monomer acid as a flocculent, white solid. ¹H NMR (DMSO, 500 MHz) Major Rotamer: δ 11.31 (s, 1H), δ 7.34 (m, 5H), 7.23 (m, 2H), δ 6.86 (s, 1H), δ 5.03 (m, 2H), δ 4.80-4.55 (m, 2H), δ 3.90-3.4 (m, 5H), δ 3.10 (m, 2H), δ 1.76 (s, 3H), δ 1.36 (s, 9H). LRMS (ESI-MS *m/z*): mass calcd for C₂₅H₃₃N₅O₉ [M - H], 546.23, found 546.1.

II.9.1c ^LK γ (Cbz)-PNA Monomer Synthesis



Boc-Lys(Cbz)-N(Me)OMe (II-21). Boc-Lys(Cbz)-OH (2.04 g, 5.36 mmol) was dissolved in dry DCM (40 mL) in a 100 mL RBF. N-Methyl, O-methyl hydroxylamine hydrochloride salt (0.68 g, 6.97 mmol) and DMAP (66 mg, 0.54 mmol) were added to the solution. The reaction

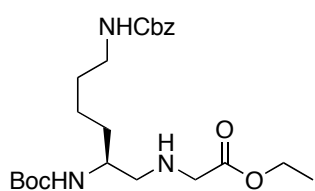
mixture was then cooled to 0 °C via ice bath and TEA (1.27 mL, 9.11 mmol) was added slowly to the stirring solution. EDC (1.54 g, 8.04 mmol) was added to the solution and the ice bath was removed. The reaction mixture was allowed to stir at rt. for 12 hours. The solution was then transferred to a separatory funnel and washed with 1 M HCl (2 x 20 mL), saturated NaHCO₃ solution (2 x 20 mL) and saturated NaCl solution (2 x 20 mL). The organic layer was dried over Na₂SO₄ and concentrated under reduced pressure on a rotary evaporator to afford 2.23 g (88 % yield) of the desired product as a clear, viscous oil. ¹H NMR (CDCl₃, 500 MHz): δ 7.33 (m, 5H), 5.24 (s, 1H), 5.08 (s, 2H), 4.97 (s, 1H), 4.66 (s, 1H), 3.75 (s, 3H), 3.19 (s, 3H), 3.19 (m, 2H), 1.54 (m, 6H), 1.42 (s, 9H); ¹³C NMR (CDCl₃, 126 MHz): δ 156.65, 155.90, 136.89, 128.69, 128.32, 128.24, 79.80, 66.75, 61.81, 50.23, 40.97, 32.79, 32.29, 29.44, 28.56, 22.65. LRMS (ESI-MS *m/z*): mass calcd for C₂₁H₃₃N₃O₆ [M + H]⁺, 424.24, found 424.2.



Boc-Lys(Cbz)-CHO (II-22). Boc-Lys(Cbz)-N(Me)OMe **II-21** (2.33 g, 5.5 mmol) was dissolved in dry THF (60 mL) in a 100 mL RBF and cooled to 0 °C via ice bath. LAH (365 mg, 9.60 mmol) was added gradually over 45 seconds to the stirring solution. The reaction was monitored via TLC. After 45 minutes, the

reaction mixture was quenched with saturated NaHSO₄ solution (20 mL) and allowed to stir for 10 minutes. The solution was then transferred to a separatory funnel and washed with EtOAc (3 x 55 mL). The combined organic layers were washed with 1 M HCl (2 x 50 mL), saturated

NaHCO₃ solution (2 x 50 mL), water (2 x 50 mL) and saturated NaCl solution (2 x 50 mL). The organic layer was dried over Na₂SO₄ and concentrated under reduced pressure on a rotary evaporator to afford 1.70 g (85 % yield) of Boc-Lys(Cbz)-CHO as a white powder. ¹H NMR (CDCl₃, 500 MHz): δ 9.46 (s, 1H), 7.35 (m, 5H), 5.22 (s, 1H), 5.01 (s, 2H), 4.90 (s, 1H), 4.19 (m, 1H), 3.20 (m, 2H), 1.54 (m, 6H), 1.44 (s, 9H).

**II-23**

BocLys(Cbz)-PNA Backbone (II-23). Boc-Lys(Cbz)-CHO **II-22**

(540 mg, 1.48 mmol) and ethyl glycinate hydrochloride salt (228 mg,

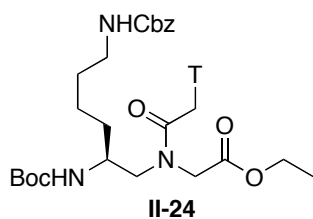
1.63 mmol) were dissolved in dry DCM (10 mL) in a 50 mL RBF.

TEA (230 μL) was added drop-wise to the stirring solution and

allowed to stir for 10 minutes. Sodium triacetoxyborohydride (439 mg, 2.07 mmol) was then added. The cloudy reaction mixture was allowed to stir for 1 hour and 45 minutes. The reaction was then quenched with saturated NaHCO₃ (15 mL) and saturated Na₂CO₃ (5 mL) and stirred for 10 minutes. The mixture was washed with DCM (2 x 30 mL) and the combined organic layers were dried over Na₂SO₄. Concentration under reduced pressure on a rotary evaporator afforded a yellow oil. The oil was purified via column chromatography (EtOAc/Hexanes 2:1, rf = 0.2) to afford 310 mg (47 % yield) of the desired product as a clear, pale yellow oil. ¹H NMR (CDCl₃, 500 MHz): δ 7.35 (m, 5H), 5.01 (s, 2H), 4.92 (s, 1H), 4.77 (s, 1H), 4.18 (q, 2H), 3.67 (s, 1H), 3.39 (dd, 2H), 3.20 (m, 2H), 2.64 (m, 2H), 1.54 (m, 6H), 1.43 (s, 9H) 1.27 (t, 3H); ¹³C NMR (CDCl₃, 126 MHz): δ 172.75, 156.72, 156.19, 136.88, 128.72, 128.35, 128.28, 79.41, 66.78, 61.02, 53.14, 51.13, 50.31, 40.96, 33.01, 29.78, 28.63, 23.136, 14.44. LRMS (ESI-MS *m/z*): mass calcd for C₂₃H₃₇N₃O₆ [M + H]⁺, 452.27, found 452.3.

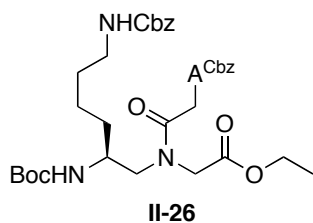
General Procedure II-A: Coupling Bases to ^LK_γ-PNA Backbone (Synthesis of II-24, II-26, II-28 – Scheme II-6). PNA Backbone **II-23** (310 mg, 0.69 mmol), Nucleobase Acetic Acid

(0.89 mmol, 1.3 equiv), and DMAP (8 mg, 0.07 mmol) were dissolved in dry DMF (20 mL). EDC hydrochloride salt (192 mg, 1.00 mmol) was added to the stirring solution. After 36 hours, the reaction mixture was added to H₂O (90 mL) forming a white precipitate. The solution was then extracted with EtOAc (3 x 40 mL). The combined organic layers were washed with 1 M HCl (2 x 40), saturated NaHCO₃ (2 x 40 mL), water (2 x 40 mL) and saturated NaCl (2 x 40 mL). The organic layer was dried over Na₂SO₄ and concentrated under reduced pressure on a rotary evaporator to afford base-coupled monomer esters as flocculent solids.



γ -Lys(Cbz)-PNA Thymine Monomer Ethyl Ester (*II-24*).

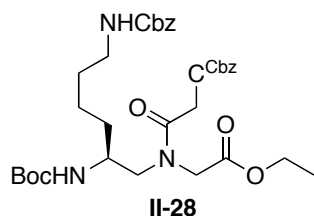
Following general procedure A, PNA Backbone *II-23* (310 mg, 0.69 mmol) was coupled to T-CH₂-CO₂H (170 mg, 0.89 mmol) to afford 335 mg (79% yield) of γ -Lys(Cbz)-PNA thymine monomer ethyl ester (*II-24*) as a flocculent, white solid. ¹H NMR (DMSO, 500 MHz) Major Rotamer: δ 11.30 (s, 1H), δ 7.34 (m, 5 H), 7.21 (m, 2H), δ 6.80 (s, 1H), δ 4.99 (s, 2H), δ 4.67 (dd, 2H), δ 4.3-3.9 (m, 4H), δ 3.64 (br, 1H), δ 3.31 (m, 2H), δ 2.97 (m, 2H), δ 1.75 (s, 3H), δ 1.40 (m, 6H), δ 1.35 (s, 9H), δ 1.17 (t, 3H)



γ -Lys(Cbz)-PNA Adenine(Cbz) Monomer Ethyl Ester (*II-26*).

Following general procedure II-A, PNA Backbone *II-23* (724 mg, 1.60 mmol) was coupled to A^{Cbz}-CH₂-CO₂H (682 mg, 2.08 mmol), to afford 933 mg (76.7% yield) of γ -Lys(Cbz)-PNA adenine(Cbz) monomer ethyl ester (*II-26*) as a flocculent, white solid. ¹H NMR (DMSO, 300 MHz) Major Rotamer: δ 10.70 (s, 1H), δ 8.59 (s, 1H), δ 8.24 (s, 1H), δ 7.37 (m, 11H), δ 6.90 (d, 1H), δ 5.36 (dd, 2H), δ 5.22 (s, 2H), δ 5.00 (s, 2H), δ 4.26-3.94 (m, 4H), δ 3.72 (br, 1H), δ 3.43 (m, 2H), δ

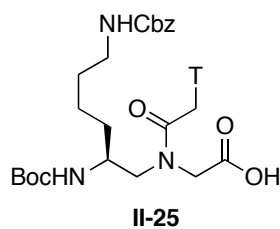
2.98 (m, 2H), δ 1.42 (m, 6H), δ 1.36 (s, 9H), δ 1.15 (t, 3H). LRMS (ESI-MS m/z): mass calcd for $C_{38}H_{48}N_8O_9$ $[M + H]^+$, 761.35, found 761.4.



γ -Lys(Cbz)-PNA Cytosine(Cbz) Monomer Ethyl Ester (II-28**).**

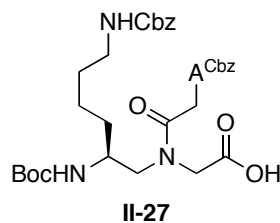
Following general procedure II-A, PNA Backbone **II-23** (724 mg, 1.60 mmol) was coupled to C^{Cbz} -CH₂-CO₂H (512 mg, 2.08 mmol), to afford 937 mg (80 % yield) of γ -Lys(Cbz)-PNA cytosine(Cbz) monomer ethyl ester (**II-28**) as a flocculent, bright yellow solid. ¹H NMR (DMSO, 300 MHz) Major Rotamer: δ 10.79 (s, 1H), δ 7.81 (d, 1H), δ 7.37 (m, 10H), δ 7.23 (m, 1H), δ 7.01 (d, 1H), δ 6.80 (d, 1H), δ 5.19 (s, 2H), δ 5.00 (s, 2H), δ 4.84 (dd, 2H), δ 4.07 (m, 4H), δ 3.65 (br, 1H), δ 3.33 (m, 2H), δ 2.97 (m, 2H), δ 1.45-1.30 (m, 6H), δ 1.36 (s, 9H), δ 1.17 (t, 3H). LRMS (ESI-MS m/z): mass calcd for $C_{37}H_{48}N_6O_{10}$ $[M + H]^+$, 737.34, found 737.3.

General Procedure II-B: Saponification of ¹L γ -PNA Monomer Ethyl Esters (Synthesis of **II-25, **II-27**, **II-29** - Scheme II-6).** A Monomer Ethyl Ester (**II-24**, **II-26**, or **II-28**; 0.53 mmol) was dissolved in THF (8 mL) and cooled to 0 °C via ice bath. LiOH monohydrate (275 mg, 6.5 mmol) was dissolved in H₂O and the solution was added dropwise to the stirring reaction mixture. The ice bath was then removed and the reaction was stirred under N₂ for 5 hours. The solution was diluted with H₂O (10 mL) and washed with diethyl ether (2 x 10 mL). The pH of the aqueous layer was lowered to ~2 with 3 M HCl forming a white precipitate. The solution was washed with EtOAc (4 x 20 mL) and the organic layers were dried over Na₂SO₄. The solution was concentrated under reduced pressure on a rotary evaporator to afford a flocculent solid.



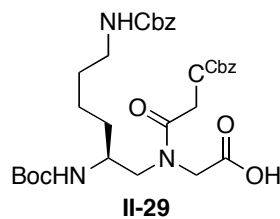
γ -Lys(Cbz)-PNA Thymine Monomer Acid (II-25). Following general procedure II-B, PNA thymine monomer ethyl ester **II-24** (325 mg 0.53 mmol) was saponified to afford 270 mg (99% yield) of γ -Lys(Cbz)-PNA thymine monomer acid as a flocculent, white solid. ^1H NMR (DMSO,

500 MHz) Major Rotamer: δ 11.31 (s, 1H), δ 7.34 (m, 5H), 7.22 (m, 2H), δ 6.81 (s, 1H), δ 4.99 (s, 2H), δ 4.66 (dd, 2H), δ 3.75 (m, 3H), δ 3.37 (m, 2H), δ 2.98 (m, 2H), δ 1.75 (s, 3H), δ 1.40 (m, 6H), δ 1.36 (s, 9H). LRMS (ESI-MS m/z): mass calcd for $\text{C}_{28}\text{H}_{39}\text{N}_5\text{O}_9$ $[\text{M} + \text{H}]^+$, 590.27, found 588.3.



γ -Lys(Cbz)-PNA Adenine(Cbz) Monomer Acid (II-27). Following general procedure II-B, PNA adenine(Cbz) monomer ethyl ester **II-26** (323 mg 0.42 mmol) was saponified to afford 252 mg (81% yield) of γ -Lys(Cbz)-PNA adenine(Cbz) Monomer Acid as a flakey, yellow solid.

^1H NMR (DMSO, 300 MHz) Major Rotamer: δ 10.64 (br s, 1H), δ 8.58 (d, 1H), δ 8.26 (d, 1H), δ 7.37 (m, 10H) δ 7.21 (m, 1H), δ 6.91 (d, 1H), δ 5.33 (dd, 2H), δ 5.22 (s, 2H), δ 4.99 (s, 2H), δ 4.10-3.95 (m, 2H), δ 3.75 (br m, 1H), δ 3.45 (m, 2H), δ 2.97 (m, 2H), δ 1.42-1.20 (m, 6H), δ 1.37 (s, 9H). LRMS (ESI-MS m/z): mass calcd for $\text{C}_{36}\text{H}_{44}\text{N}_8\text{O}_9$ $[\text{M} + \text{H}]^+$, 733.32, found 733.3.

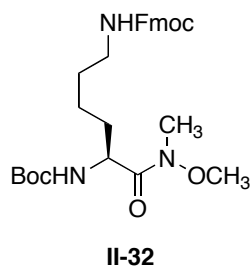


γ -Lys(Cbz)-PNA Cytosine(Cbz) Monomer Acid (II-29). Following general procedure II-B, PNA cytosine(Cbz) monomer ethyl ester **II-28** (334 mg 0.45 mmol) was saponified to afford 280 mg (89% yield) of γ -Lys(Cbz)-PNA cytosine(Cbz) monomer acid as a flocculent, yellow solid.

^1H NMR (DMSO, 300 MHz) Major Rotamer: δ 7.82 (t, 1H), δ 7.37 (m, 10H), δ 7.23 (m, 1H), δ 7.02 (t, 1H), δ 6.81 (d, 1H), δ 5.19 (s, 2H), δ 4.99 (s, 2H), δ 4.83 (dd, 2H), δ 4.11 (m, 2H),

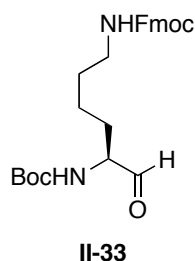
δ 3.67 (br, 1H), δ 3.31 (m, 2H), δ 2.96 (m, 2H), δ 1.45-1.30 (m, 6H), δ 1.35 (s, 9H). LRMS (ESI-MS m/z): mass calcd for $C_{35}H_{44}N_6O_{10}$ $[M + H]^+$, 709.31, found 709.3.

II.9.1d ^LK γ (Fmoc)-PNA Monomer Synthesis



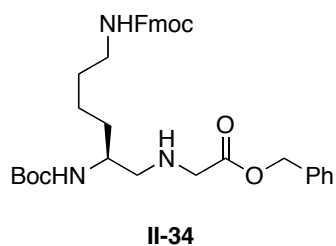
Boc-Lys(Fmoc)-N(Me)OMe (II-32). Boc-Lys(Fmoc)-OH (**II-31**) (5.33 g, 11.4 mmol) was dissolved in dry DCM (66 mL) in a 100 mL RBF. EDC (2.72 g, 14.2 mmol) and HOBt (1.92 g, 14.2 mmol) were added to the solution. The reaction mixture was then cooled to 0 °C with an ice bath and DIEA (2.5 mL, 14.3 mmol) was added slowly to the stirring solution. The

solution was allowed to stir for five minutes. N,O-Dimethylhydroxylamine hydrochloride salt (1.38 g, 14.2 mmol) was added to the solution along with more DIEA (2.5 mL, 14.3 mmol) and the ice bath was removed. The reaction mixture was allowed to stir for 12 hours. The solution was then transferred to a separatory funnel and washed with 1 M HCl (2 x 30 mL), saturated $NaHCO_3$ solution (2 x 30 mL) and saturated NaCl solution (2 x 30 mL). The organic layer was dried over Na_2SO_4 and evaporated under reduced pressure to afford 5.74 g (99 % yield) of the desired product as a colorless, viscous oil. 1H NMR ($CDCl_3$, 500 MHz): δ 7.77 (d, 2 H, Fmoc-CH), 7.60 (d, 2 H, Fmoc-CH), 7.40 (t, 2 H, Fmoc-CH), 7.32 (t, 2 H, Fmoc-CH), 5.22 (d, 1 H, NH), 4.88 (s, 1 H, NH), 4.68 (s, 1 H, HN-CH(CH₂)-CO), 4.39 (d, 2 H, O-CH₂-CH(CH₂)₂), 4.21 (t, 1 H, O-CH₂-CH(CH₂)₂), 3.77 (s, 3 H, CH₃), 3.20 (s, 3 H, N-CH₃), 3.20 (m, 2 H, NH-CH₂-CH₂), 1.73-1.33 (m, 6 H, CH-CH₂-CH₂-CH₂-CH₂), 1.43 (s, 9 H, tert-butly-CH₃); ^{13}C NMR ($CDCl_3$, 126 MHz): δ 173.3, 156.7, 155.9, 144.2, 141.5, 127.9, 127.3, 125.3, 120.2, 79.8, 66.7, 61.8, 50.3, 47.5, 41.0, 32.8, 32.3, 29.5, 28.6, 22.7



Boc-Lys(Fmoc)-CHO (II-33). Boc-Lys(Fmoc)-N(Me)OMe (**II-32**) (2.33 g, 5.5 mmol) was dissolved in a minimal amount of CH₂Cl₂ to form a gray film. The viscous film was then dissolved in dry THF (60 mL) in a 100 mL RBF and cooled to 0 °C with an ice bath. Lithium aluminum hydride (365 mg, 9.60

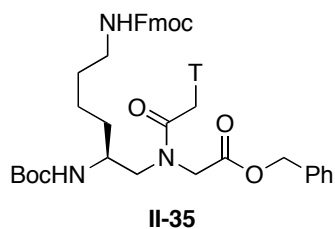
mmol) was added gradually over 45 seconds to the stirring solution. The reaction was monitored via TLC. After 45 minutes, the reaction mixture was quenched with saturated NaHSO₄ solution (20 mL) and allowed to stir for 10 minutes. The solution was then transferred to a separatory funnel and washed with EtOAc (3 x 55 mL). The combined organic layers were washed with 1 M HCl (2 x 50 mL), saturated NaHCO₃ solution (2 x 50 mL), water (2 x 50 mL) and saturated NaCl solution (2 x 50 mL). The organic layer was dried over Na₂SO₄ and evaporated under reduced pressure to afford 1.70 g (85 % yield) of Boc-Lys(Fmoc)-CHO as white solid. ¹H NMR (CDCl₃, 500 MHz): δ 9.58 (s, 1 H, CH-COH), δ 7.76 (d, 2 H, Fmoc-CHH), 7.59 (d, 2 H, Fmoc-CHH), 7.40 (t, 2 H, Fmoc-CHH), 7.31 (t, 2 H, Fmoc-CHH), 5.20 (s, 1 H, NHH), 4.89 (s, 1 H, NHH), 4.41 (d, 2 H, O-CH2-CH(CH)2), 4.21 (m, 1 H, O-CH2-CH(CH)2), 4.21 (m, 1 H, HN-CH2(CH₂)-CO), 3.19 (d, 2 H, NH-CH2-CH₂), 1.73-1.33 (m, 6 H, CH-CH2-CH₂-CH₂-CH₂), 1.44 (s, 9 H, tert-butyl-CH₃)



γ-BocLys(Fmoc)-PNA Backbone (II-34). Boc-Lys(Fmoc)-CHO (**II-33**) (2.45 g, 5.4 mmol) and benzyl glycinate hydrochloride salt (2.01 mg, 5.96 mmol) were dissolved in dry DCM (30 mL) in a 100 mL RBF. DIEA (1.04 mL) was added slowly to the stirring solution,

which was then allowed to stir for 10 minutes. Triacetoxyborohydride (1.60 g, 7.56 mmol) was then added. The cloudy reaction mixture was allowed to stir for 1 hour and 45 minutes. The reaction was then quenched with saturated Na₂CO₃ (15 mL) and stirred for 10 minutes. The

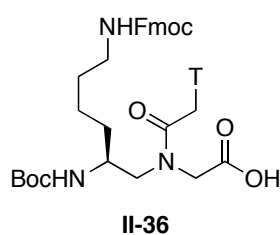
mixture was washed with DCM (2 x 30 mL) and the combined organic layers were dried over Na₂SO₄. Evaporation afforded a clear, colorless oil. The oil was purified via column chromatography (EtOAc, rf = 0.5) to afford 1.96 g (60 % yield) of the desired product as a clear, colorless oil. ¹H NMR (CDCl₃, 500 MHz): δ 7.74 (d, 2 H, Fmoc-CH) 7.58 (d, 2 H, Fmoc-CH) 7.33 (m, 9H, phenyl, Fmoc-CH), 5.13 (s, 2 H, CH₂), 5.11 (s, 1 H, NH), 4.82 (d, 1 H, NH), 4.38 (m, 2 H, O-CH₂-CH), 4.19 (t, 1 H, CH₂-CH-(CH₂)₂), 3.62 (s, 1 H, NH-CH-(CH₂)₂), 3.41(dd, 2 H, NH-CH₂-CO), 3.16 (d, 2 H, NHFmoc-CH₂-CH₂), 2.61 (m, 2 H, NH-CH₂-CH(NHBoc)-CH₂), 1.39 (m, 6 H, CH-CH₂-CH₂-CH₂-CH₂) , 1.43 (s, 9 H, tert-butly-CH₃); ¹³C NMR (CDCl₃, 126 MHz): δ 172.64, 156.79, 156.24, 144.28, 141.53, 135.80, 128.86, 128.66, 128.60, 127.90, 127.29, 125.33, 120.20, 79.40, 66.79, 66.72, 53.15, 51.12, 50.37, 47.52, 40.96, 33.03, 29.80, 28.67, 23.18.



γ-Lys(Fmoc) PNA Thymine Monomer Ester (II-35). PNA

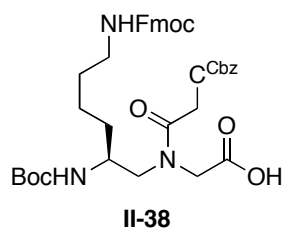
Backbone **II-34** (570 mg, 0.94 mmol), thymine acetic acid (226 mg, 1.23 mmol) and HOBT (7 mg, 0.05 mmol) were dissolved in dry DMF (20 mL). EDC hydrochloride salt (272 mg, 1.42 mg) was added to the stirring solution. After 36 hours, the DMF solution was added to H₂O (40 mL) forming a white precipitate. The solution was then washed with EtOAc (3 x 40 mL). The combined organic layers were washed with 1 M HCl (2 x 40 mL), saturated NaHCO₃ (2 x 40 mL), water (2 x 40 mL), and saturated NaCl (2 x 40 mL). The organic layer was dried over Na₂SO₄ and evaporated under reduced pressure to afford 593 mg (82 % yield) of γ-Lys(Fmoc) PNA Thymine Monomer Ester (**II-35**) as a white solid. ¹H NMR (DMSO, 500 MHz) Major Rotomer Only: δ 11.31 (s, 1 H, Thymine-CH) δ 7.88 (d, 2 H, Fmoc-CH) 7.68 (d, 2 H, Fmoc-CH) 7.36 (m, 9 H, phenyl, Fmoc-CH), 7.20 (s, 1 H, Thymine-NH) 5.12 (s, 2 H, O-CH₂-phenyl), 4.70

(dd, 2 H, OC-CH₂-Thymine), 4.28 (s, 2 H, O-CH₂-CH), 4.20 (s, 1 H, CH₂-CH-(CH)₂), 4.09 (m, 2 H, N-CH₂-CO), 3.66 (s, 1 H, NH-CH-(CH₂)₂), 3.32 (m, 2 H, N-CH₂-CH(NHBoc)-CH₂), 2.97 (m, 2 H, NHFmoc-CH₂-CH₂), 1.74 (s, 3 H, Thymine-CH₃) 1.35 (s, 9 H, tert-butyl-CH₃), 1.35 (m, 6 H, CH-CH₂-CH₂-CH₂-CH₂); ¹³C NMR (DMSO, 126 MHz): δ 169.5, 168.2, 165.0, 156.7, 156.3, 151.6, 144.6, 142.4, 141.4, 136.5, 129.2, 129.1, 128.7, 128.5, 128.3, 127.7, 125.8, 120.8, 108.9, 78.6, 66.5, 65.8, 52.3, 49.3, 48.8, 48.4, 47.4, 31.7, 29.9, 28.8, 23.6, 12.6; HRMS (ESI-MS *m/z*) mass calcd for C₄₂H₄₉N₅O₉ [M + H]⁺, 768.3564, found 768.3586



γ-Lys(Fmoc) PNA Thymine Monomer (II-36). PNA Thymine Monomer Benzyl Ester **II-35** (126 mg, 0.16 mmol), was dissolved in of MeOH (15 mL). Pd/C (30 mg) was added slowly to the solution over 2 minutes. Solution was placed under an atmosphere of H₂ (balloon

pressure) for 12 hours, stirring vigorously. The Pd/C was filtered off with celite and the solvent was evaporated under reduced pressure to afford 86 mg (79 % yield) of γ-Lys(Fmoc) PNA Thymine Monomer Acid (**II-36**) as a flakey, off-white solid. ¹H NMR (DMSO, 500 MHz) Major Rotamer Only: δ 11.29 (s, 1 H, Thymine-CH) δ 7.89 (d, 2 H, Fmoc-CH) 7.68 (d, 2H, Fmoc-CH) 7.33 (m, 5 H, Thymine-NH, Fmoc-CH), 6.81 (d, 1 H, NH), 6.70 (d, 1 H, NH), 4.66 (dd, 2 H, CH₂), 4.28 (s, 2 H, O-CH₂-CH), 4.20 (s, 1 H, CH₂-CH-(CH)₂), 3.96 (m, 2 H, N-CH₂-CO), 3.66 (s, 1 H, NH-CH-(CH₂)₂), 3.32 (m, 2 H, NHFmoc-CH₂-CH₂), 2.96 (m, 2 H, N-CH₂-CH(NHBoc)-CH₂), 1.74 (s, 3 H, Thymine-CH₃) 1.37 (s, 9 H, tert-butly-CH₃), 1.37 (m, 6 H, CH-CH₂-CH₂-CH₂-CH₂); HRMS (ESI-MS *m/z*) mass calcd for C₃₅H₄₃N₅O₉ [M + H]⁺, 678.3094, found 678.3140



γ -Lys(Fmoc) Cytosine(Cbz) PNA Monomer Acid (*II-38*). PNA

Backbone *II-34* (142 mg, 0.23 mmol), cytosine acetic acid (95 mg, 0.31 mmol) and HOBt (2 mg, 0.01 mmol) were dissolved in dry DMF (5 mL). EDC hydrochloride salt (68 mg, 0.36 mmol) was added to stirring solution. After 36 hours, the DMF solution was added to H₂O (10 mL) forming a white precipitate. The solution was then washed with EtOAc (3 x 10 mL). The combined organic layers were washed with 1 M HCl (2 x 10 mL), saturated NaHCO₃ (2 x 10 mL), water (2 x 10 mL), and saturated NaCl (2 x 10 mL). The organic layer was dried over Na₂SO₄ and evaporated under reduced pressure to afford 157 mg of crude γ -Lys(Fmoc) PNA Cytosine Monomer Benzyl Ester (*II-37*) as a white solid. Mass spec and ¹H NMR confirmed presence of product. The crude product was then dissolved in THF (8 mL). A solution of saturated K₂CO₃ (20 mL) was added slowly to the solution over 2 minutes. The ice bath was removed and the solution was allowed to stir for an additional 48 hours. The solution was concentrated, diluted with a solution of saturated K₂CO₃ (10 mL) and washed with Et₂O (1 x 5 mL). The reaction was then made acidic (pH = 1-2) with 3 M HCl forming a white precipitate. The solution was washed with EtOAc (4 x 20 mL). The combined organic layers were dried over Na₂SO₄ and evaporated under reduced pressure. Trituration with hexanes and decanting afforded 42 mg (21 % yield over 2 steps) of γ -Lys(Fmoc) PNA Cytosine(Cbz) Monomer Acid (*II-38*) as a flakey, off-white solid. LRMS (ESI-MS *m/z*) mass calcd for C₄₂H₄₈N₆O₁₀ [M + H]⁺, 797.35, found 797.4

II.9.2 PNA Oligomer Synthesis and Characterization

II.9.2a General Solid Phase Synthesis Procedure

*aeg*PNA monomers were purchased from Applied Biosystems. Kaiser test solutions were purchased from Fluka. HATU and Boc-Lys-(2-Cl-Z)-OH were purchased from Advanced

Chemtech. All other chemicals were purchased from Sigma-Aldrich.

Note on resin washes: All washes used at least enough solution to cover the resin (~1.5 mL for 50 mg resin, and ~5 mL for 1 g resin). Values in parentheses describe the number of times the resin is washed with the indicated solution, and the agitation time for each wash. For example, (4x-30s) indicates four washes, with each having an agitation time of 30 seconds and each followed by draining under vacuum. If no time or number of repetitions is indicated, a single wash and/or a five second agitation period is used.

1. Downloading Resin

Methyl benzhydryl amine (MBHA) resin (1.0 g, 0.3 mmol active sites/gram) is downloaded to 0.1 mmol/g with Boc-Lys-(2-Cl-Z)-OH. The resin is first swelled in DCM for anytime between 1 and 12 hours. The following solutions are prepared: 0.2 M Boc-Lys-(2-Cl-Z)-OH in NMP (A), 0.2 M HATU in NMP (B), and 0.5 M DIEA in NMP (C). These solutions are then combined appropriately to give two additional solutions: 0.45 mL of A + 0.46 mL of C + 1.59 mL NMP (Solution 1), and 0.55 mL of B + 1.95 mL NMP (Solution 2). Solutions 1 and 2 are pre-mixed for one minute and then added to the resin.

The resin is agitated with a mechanical shaker for one hour and then drained under vacuum. The resin is subsequently washed with DMF (4x), DCM (4x), 5% DIEA in DCM (1x-30s), and again with DCM (4x). The remaining active sites are then capped with a 1:2:2 solution of Ac₂O:NMP:pyridine for 1.5 hours. This is followed by washes with DCM (2x-5s) and a qualitative Kaiser1 test to confirm that no primary amines remain. Resin is then washed with DCM (2x) and allowed to dry under vacuum for 30-60 minutes. Downloaded resin is stored in a dessicator until further use.

2. *aeg*PNA Oligomer Synthesis¹⁹

The following is a representative coupling cycle for one PNA monomer. Downloaded resin (50 mg) is swelled in DCM for 1hr. The solvent is drained under vacuum and a solution of 5% *m*-cresol in TFA is added to the resin. The resin is shaken for 4 minutes, and the solution is removed under vacuum. (Note: The TFA deprotection is repeated three times for deprotection of the lysine residue and then twice for every subsequent monomer.) This is followed by subsequent washes with DCM, DMF (1x-5s, 1x-30s, 1x-5s), DCM (2x-5s), and pyridine (2x-5s). A Kaiser test⁴⁹ is performed to confirm deprotection. Upon positive Kaiser test, 150 μ L of a 0.4 M solution of PNA monomer in NMP is pre-mixed with 150 μ L of 0.8 M MDCHA in pyridine and 300 μ L of 0.2 M HBTU in DMF for one minute. This solution is then added to the resin and agitated for 30 minutes. Following coupling, the resin was drained under vacuum and washed with DMF, 5% DIEA/DCM (1x-30s) and DCM (2x-5s). Again, a qualitative Kaiser test is performed and, if negative, the resin is capped with a 1:25:25 mixture of Ac₂O: NMP: pyridine (2x-2min). (Note: If the Kaiser test is positive, the coupling cycle is repeated, beginning with the pyridine washes.) The capping step is followed by washes with DCM, 20% piperidine/DMF and finally DCM (1x-5s, 1x-30s, 1x-5s). This cycle is then repeated iteratively until the oligomer is complete on resin.

3. γ -Lysine PNA Synthesis/ Attachment of Linker and Fluorophore

The following is a representative coupling cycle for γ -lysine/linker/fluorophore PNA monomer. The resin is washed with a solution of 5% *m*-cresol in TFA (3x-4min) and removed under vacuum. This is followed by subsequent washes with DCM, DMF (1x-5s, 1x-30s, 1x-5s), DCM (2x-5s), and pyridine (2x-5s). A Kaiser test is performed to confirm deprotection. Upon positive Kaiser test, 150 μ L of a 0.4 M solution of γ -lysine PNA monomer in NMP is pre-mixed

with 150 μL of DIEA and 300 μL of 0.2 M HBTU in DMF for one minute. This solution is then added to the resin and agitated for 60 minutes. Following coupling, the resin is drained and washed with DMF, 5% DIEA/DCM (1x-30s) and DCM (2x-5s). Again, a qualitative Kaiser test is performed and, if negative, the resin is capped with a 1:25:25 mixture of Ac_2O : NMP: pyridine (2x-2min). (Note: If the Kaiser test is positive, the coupling cycle is repeated, beginning with the pyridine washes.) The capping step is followed by washes with DCM, DMF and finally DCM (1x-5s, 1x-30s, 1x-5s). The resin is then washed with 20% piperidine in DMF (3x-4min) to remove the Fmoc protecting group on the γ -side chain. Upon positive Kaiser test, 150 μL of a 0.4 M solution of (Fmoc)mini-PEG in NMP is pre-mixed with 150 μL of DIEA and 300 μL of 0.2 M HBTU in DMF for one minute. This solution is then added to the resin and agitated for 60 minutes. Following coupling, the resin is drained and washed with DMF, 5% DIEA/DCM (1x-30s) and DCM (2x-5s). Again, a qualitative Kaiser test is performed and, if negative, the resin is capped with a 1:25:25 mixture of Ac_2O : NMP: pyridine (2x-2min). The capping step is followed by washes with DCM, DMF and finally DCM (1x-5s, 1x-30s, 1x-5s). The resin is then washed with 20% piperidine in DMF (3x-4min). Upon positive Kaiser test, 150 μL of a 0.4 M solution of 9-fluoreneacetic acid in NMP is pre-mixed with 150 μL of DIEA and 300 μL of 0.2 M HBTU in DMF for one minute. This solution is then added to the resin and agitated for 60 minutes. Following coupling, the resin is drained and washed with DMF, 5% DIEA/DCM (1x-30s) and DCM (2x-5s). Again, a qualitative Kaiser is performed and, if negative, the resin is capped with a 1:25:25 mixture of Ac_2O : NMP: pyridine (2x-2min). The capping step is followed by washes with DCM, 20% piperidine in DMF and finally DCM (1x-5s, 1x-30s, 1x-5s).

4. Cleavage of PNA from Resin

Cleavage from the resin is accomplished under acidic conditions. First, the resin is washed with TFA (2x-4min) and drained under vacuum. Next, 750 μL of a solution cooled to 0 $^{\circ}\text{C}$ consisting of 75 μL thioanisole, 75 μL m-cresol, 150 μL TFMSA, and 450 μL TFA is added to the resin and agitated for one hour. The resulting solution is collected using positive N_2 pressure to force liquid through the fritted vessel. Another 750 μL portion of cleavage solution is added. After an additional hour of agitation, cleavage solutions are combined in a glass vial and volatiles are removed by passing a stream of dry nitrogen over the product to afford a yellow/brown oil.

5. Crude PNA Isolation

The resulting oil is partitioned between five 2.0 mL microcentrifuge tubes using a micropipeter, to typically yield 100-150 μL of the oil per tube. A 10-fold excess (by volume) of diethyl ether is added to each tube. The solutions are mixed by vortexing until the brown color no longer remains and a cloudy white precipitate forms. The solutions are then placed on dry ice for ten minutes. This is followed by centrifugation (5 min at 7000 rpm) and removal of solvent via decanting or pipeting to yield a white solid as the crude PNA product. The ether precipitation cycle is repeated four times with the following dry ice incubation times; (2x-5min), (2x-2min). Repeating the cycle twice more with no dry ice incubation completes crude PNA isolation. After decanting the final ether wash, residual solvent is removed by passing a stream of N_2 over the crude PNA product.

II.9.2b PNA Purification and Characterization

All peptide nucleic acid (PNA) oligomers were purified on reverse-phase HPLC with UV detection at 260 nm. VYDEK C18 (d=10 mm, l=250 mm, 5 microns) semi-prep columns were

utilized, eluting with 0.05% TFA in water (Solution A) and 0.05% TFA in acetonitrile (Solution B). An elution gradient of 100% A to 100% B over 60 minutes at flow rate 5.05 mL/mi was employed. The gradient was slowed if impurities were extremely close to product peak. PNAs were characterized by mass spectroscopy, using a PerSeptive Biosystems Voyager DE MALDI-TOF system with 2',4',6'-trihydroxyacetophenone monohydrate matrix. MALDI mass spectra were acquired using a N₂ laser (337 nm wavelength, 5 ns pulse), with at least 100 shots per sample. All PNA oligomers gave molecular ions consistent with the final product.

Table II-10: PNA Oligomer Mass Spectroscopy Data

PNA	Sequence	Mass (Calculated) ^a	Mass (Observed)
II-1 ^b	H-GTAGATCACT-Lys-NH ₂	2855.2	2855.6
II-2 ^b	H-GTAGAT ¹ CACT-Lys-NH ₂	2925.3	2924.9
II-3 ^b	H-GTAGAT ¹ C ¹ ACT-Lys-NH ₂	2925.3	2928.6
II-4 ^b	H-GTAGA ¹ TC ¹ ACT-Lys-NH ₂	2925.3	2926.4
II-5 ^b	H-GT ¹ AGAT ¹ CACT ¹ -Lys-NH ₂	3067.4	3064.3
II-6 ^b	H-GTAGAT ² CACT-Lys-NH ₂	2925.3	2925.9
II-7 ^b	H-GTAGAT ³ CACT-Lys-NH ₂	2883.2	2882.5
II-8 ^b	H-GTAGAT ⁴ CACT-Lys-NH ₂	2967.3	2968.2
II-9 ^b	H-GTAGAT ⁵ CACT-Lys-NH ₂	3126.1	3124.3
II-10 ^b	H-GTAGAT ⁶ CACT-Lys-NH ₂	3278.4	3278.7
II-11 ^b	H-GTAGAT ⁶ C ⁶ ACT-Lys-NH ₂	3278.4	3277.5
II-12 ^b	H-GTAGAT ⁷ CACT-Lys-NH ₂	3381.5	3384.9
II-13 ^c	H-CCTCTTCCTC-Lys-NH ₂	2716.1	2717.8
II-14 ^c	H-CCTCT ⁸ TCCTC-Lys-NH ₂	3535.6	3535.8
II-15 ^c	H-CCTCT ⁸ TCCT ⁸ C-Lys-NH ₂	4354.4	4353.5
II-16 ^c	H-GACTTTACGA-Lys-NH ₂	2854.2	2854.8
II-17 ^c	H-GACT ⁹ T ⁹ T ⁹ ACGA-Lys-NH ₂	3463.6	3464.5

^a Calculated as the M+1 Peak. ^b Determined using MALDI-TOF mass spectrometry. ^c Determined using electrospray.

II.9.3 PNA UV-Melting and Circular Dichroism Studies

Oligonucleotides were purchased from Integrated DNA Technologies, Inc. (IDT) and were dissolved in autoclaved deionized water. Concentrations of oligonucleotide and PNA solutions were determined by UV absorption at 260 nm on an Agilent 8453 UV/Vis spectrometer equipped with an Agilent 89090A peltier temperature controller. Extinction coefficients for PNA were calculated using the nearest neighbor method.⁵⁰ Extinction coefficients for oligonucleotides were reported by the supplier (IDT). Solutions of 1:1 oligonucleotide:PNA were prepared in pH=7.0 buffer consisting of 10 mM sodium phosphate, 0.1 mM EDTA, and 150 mM NaCl. Strand concentrations were 5 μ M in each component. The solutions were degassed under vacuum for 1-2 minutes prior to melting analysis. Thermal denaturation profiles (absorbance vs. temperature) of the hybrids were measured at 260 nm with a diode array UV/Vis spectrophotometer equipped with a Peltier temperature controller that is interfaced to a personal computer. For the temperature range 90 °C to 5 °C, UV absorbance was recorded at 260 nm every 1 °C, with an equilibration time of 60 s for each measurement point. A cooling profile was recorded for each complex. All samples were run in duplicate. The melting temperature (T_m) was determined from the maximum of the first derivative of the cooling curves and reported as the average of the two runs.

II.9.4 PNA Fluorescent Studies

Fluorescent studies on PNA II-10 and PNA II-11 were performed on a SPEX Fluoromax fluorimeter using an ozone free xenon lamp. All samples were excited at 340 nm and the emission was monitored from 400-600 nm. Solutions of 1:1 oligonucleotide:PNA were prepared in pH=7.0 buffer consisting of 10 mM sodium phosphate, 0.1 mM EDTA, and 150 mM NaCl. Strand concentrations were 5 μ M in each component. All samples were heated to 90 °C for 5

minutes and cooled to room temperature slowly. All samples were run in duplicate and gave consistent results.

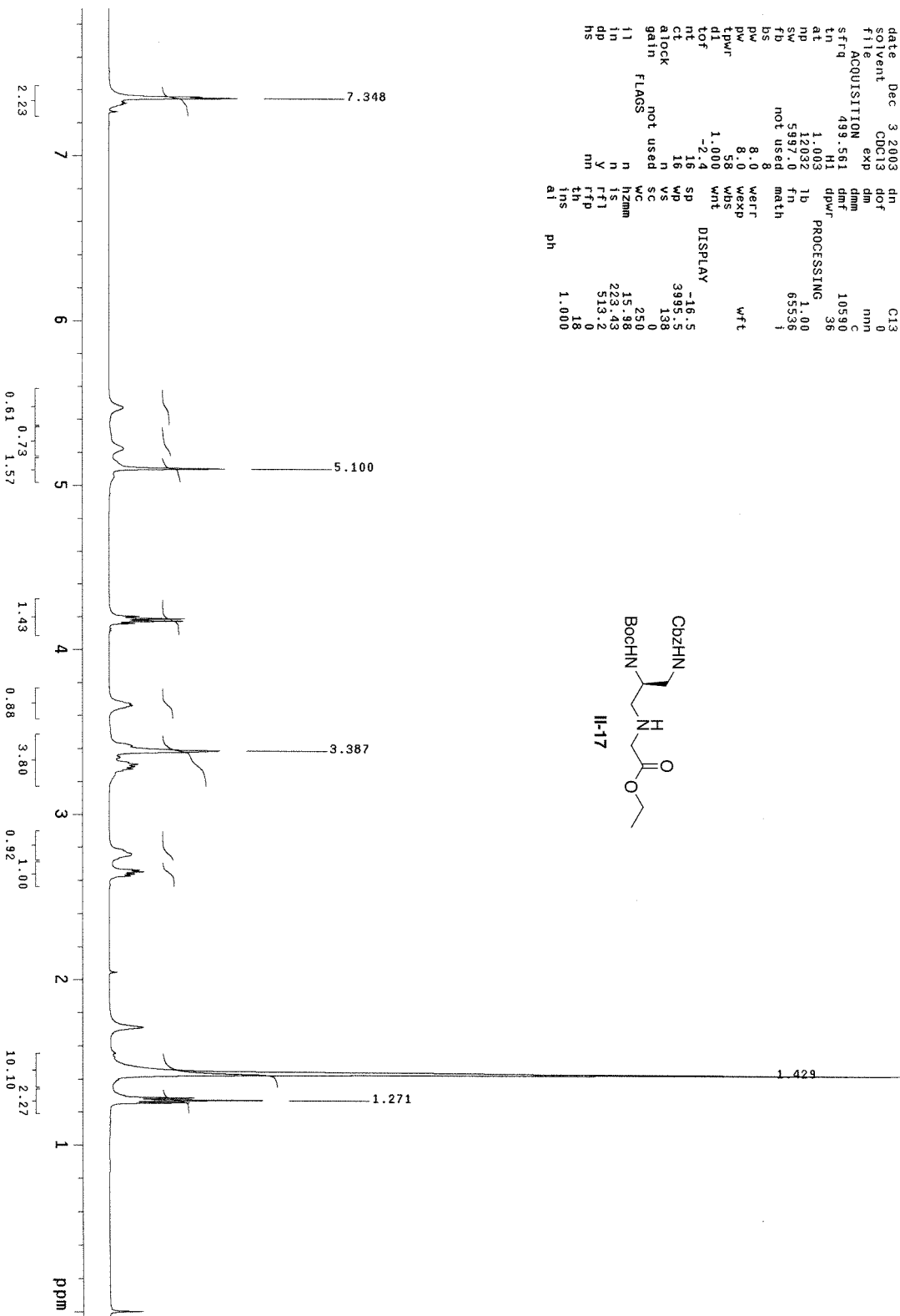
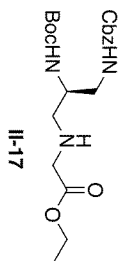
Fluorescent studies on PNA II-12, PNA II-14 and PNA II-15 were carried out on a Jobin Yvon Fluoromax 3, using a duplex concentration of 0.5 μM to 2 μM . Samples were prepared either by annealing oligomers under the same conditions used for the thermal denaturation studies, or without without annealing. Results were the same under both conditions. Samples were excited using a wavelength of 470 nm and fluorescence monitored at 495 nm to 595 nm.

II.9.5 Selected Spectra

II.9.5a Small-Molecule NMR Spectra

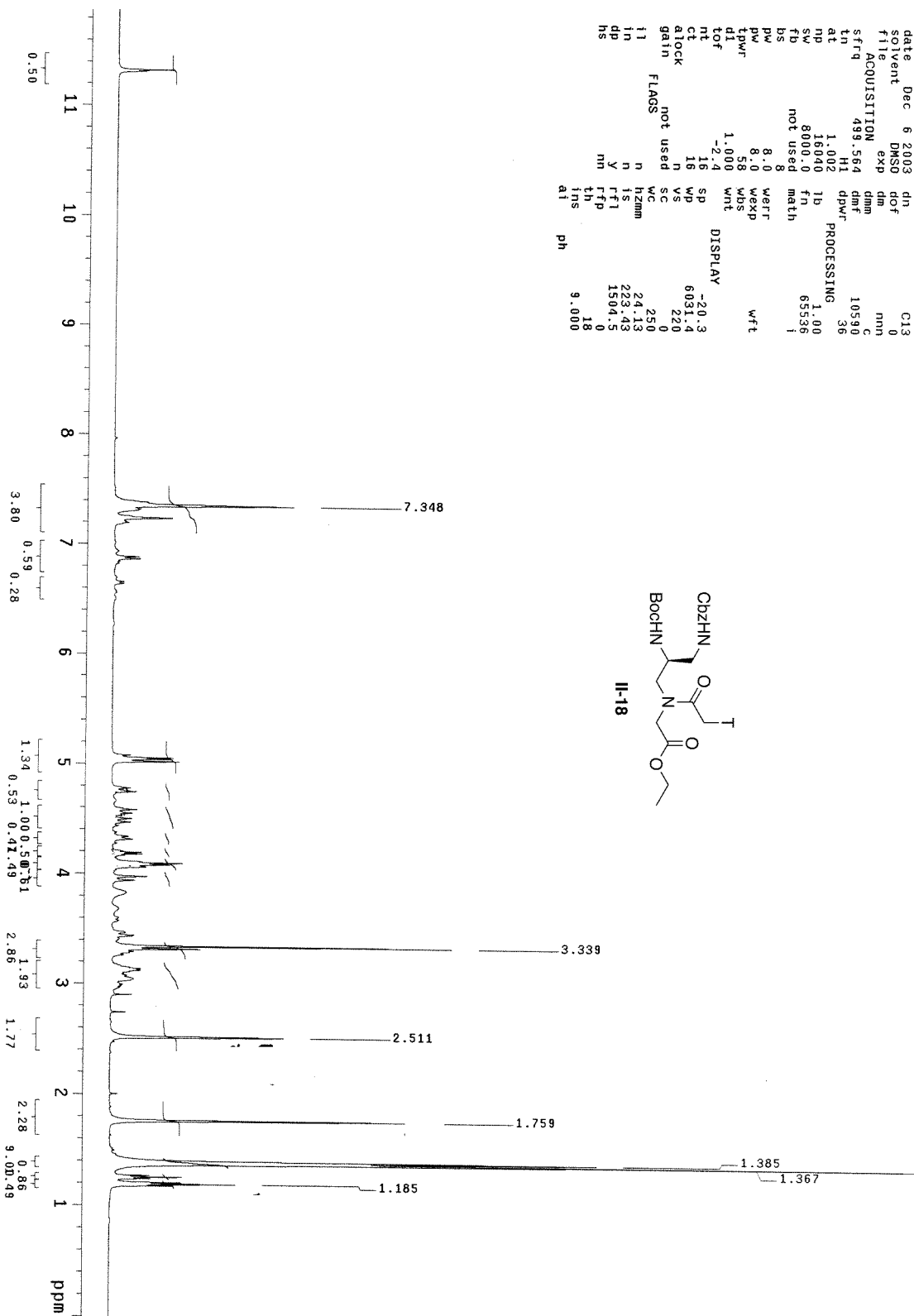
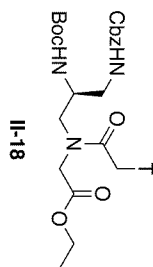
H1 stdpar 25C idpfg_5mm innova500
 exp1 s2pu1

SAMPLE	Dec 3 2003	dn	DEC. & VT	C13
date	Dec 3 2003	dn	DEC. & VT	C13
solvent	ODC13	dof		0
file	exp	dm		mn
ACQUISITION	exp	dmm		mn
strq	499.561	dmf		10590
tn	H1	dpwr		36
at	1.003	lb	PROCESSING	1.00
np	12032	fn		1.00
sw	5397.0	math		65538
fd	not used			1
DS	8	verf		wft
pw	8.0	wekp		
tpwr	58	wps		
di	1.000	wrt		
nt	-2.4	sp	DISPLAY	-16.5
ct	16	wp		3995.5
atlock	n	vs		138
gain	not used	sc		0
FLAGS	not used	WC		250
l1	n	hzm		15.98
l2	n	is		223.43
dp	y	rf1		513.2
hs	mn	rfp		0
		th		18
		ins		1.000
		at		ph



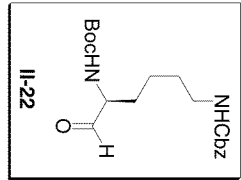
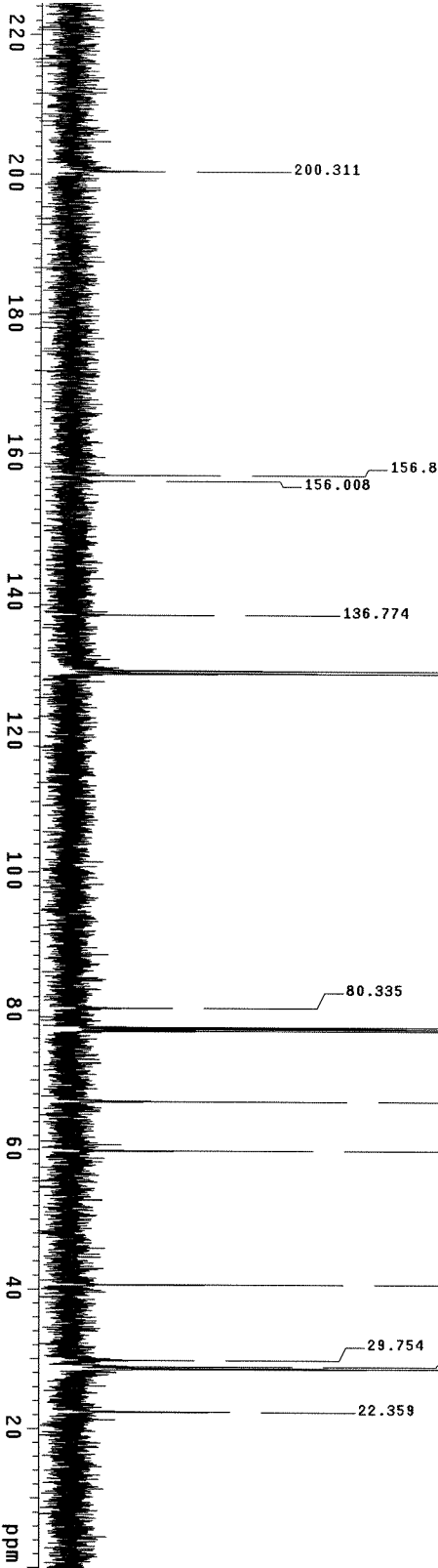
H1 stdpar RT DB_5mm inovas500
exp4 s2pul

date	Dec 6 2003	dn	DEC. & VT	C13
solvent	DMSO	dof		0
file	exp	dm		non
ACQUISITION		dmm		C
sfrq	499.564	dmf		10590
in	H1	dpwr		36
at	1.002	PROCESSING		
np	16040	fb		1.00
sw	8000.0	fn		65536
fb	not used	math		i
bs	8			
pw	8.0	werr		wft
plw	8.0	wexp		
tdwr	58	wbs		
dl	1.000	wht		
tof	-2.4	DISPLAY		
ti	16	sp		-20.3
tr	16	wp		6031.4
alock	n	vs		220
gain	not used	sc		0
FLAGS		hscmm		250
ij	p	is		24.13
in	n	rf1		23.43
dp	y	rfp		1504.0
hs	nh	th		18
		ins		9.000
		ai		ph



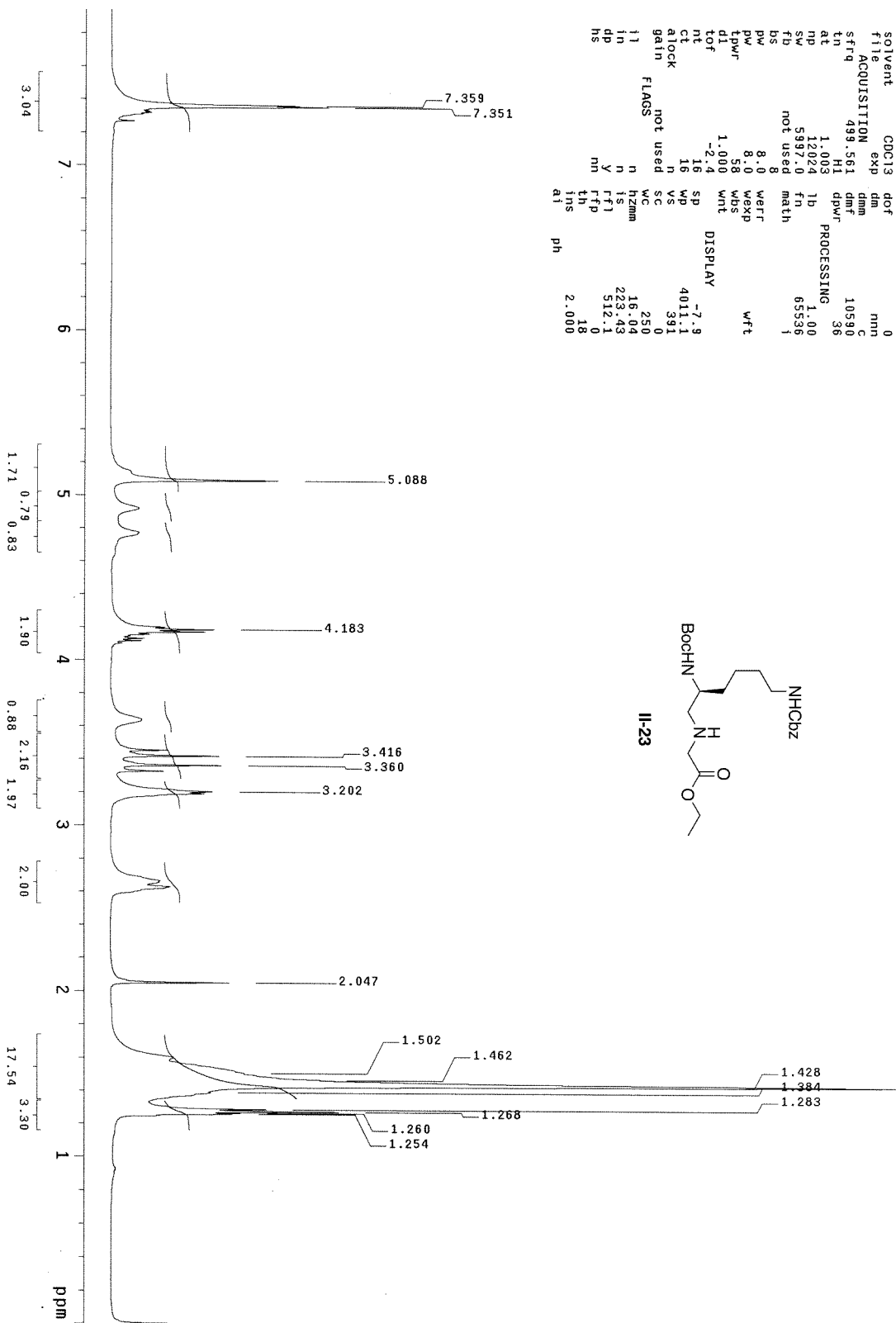
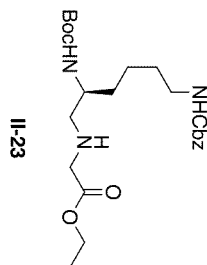
C13_std p-500 bh_5mm RT nonspin
 exp1 s2pu1

date	Aug 11 2004	DEC. & VT	499.758
solvent	CDCl3	dn	H1
ft1	ACQUISITION	exp	36
ft2	ACQUISITION	exp	36
sfreq	125.676	dm	nmr
tn	C13	dm	nmr
at	1.000	dmf	5952
np	100000	dres	1.0
sw	50000.0	dres	1.0
fb	28000	homo	n
bs	64	PROCESSING	1.00
tpwr	48	lb	wfite
pw	12.0	proc	ft
dl	1.000	fn	not used
tof	0	math	f
nt	64	weff	not used
ct	64	wexp	not used
atlock	n	wbs	not used
gain	not used	wrt	not used
fl	n	hs	nm
in	n	dp	Y
in	Y	hs	nm
dp	Y	hs	nm
hs	nm	hs	nm



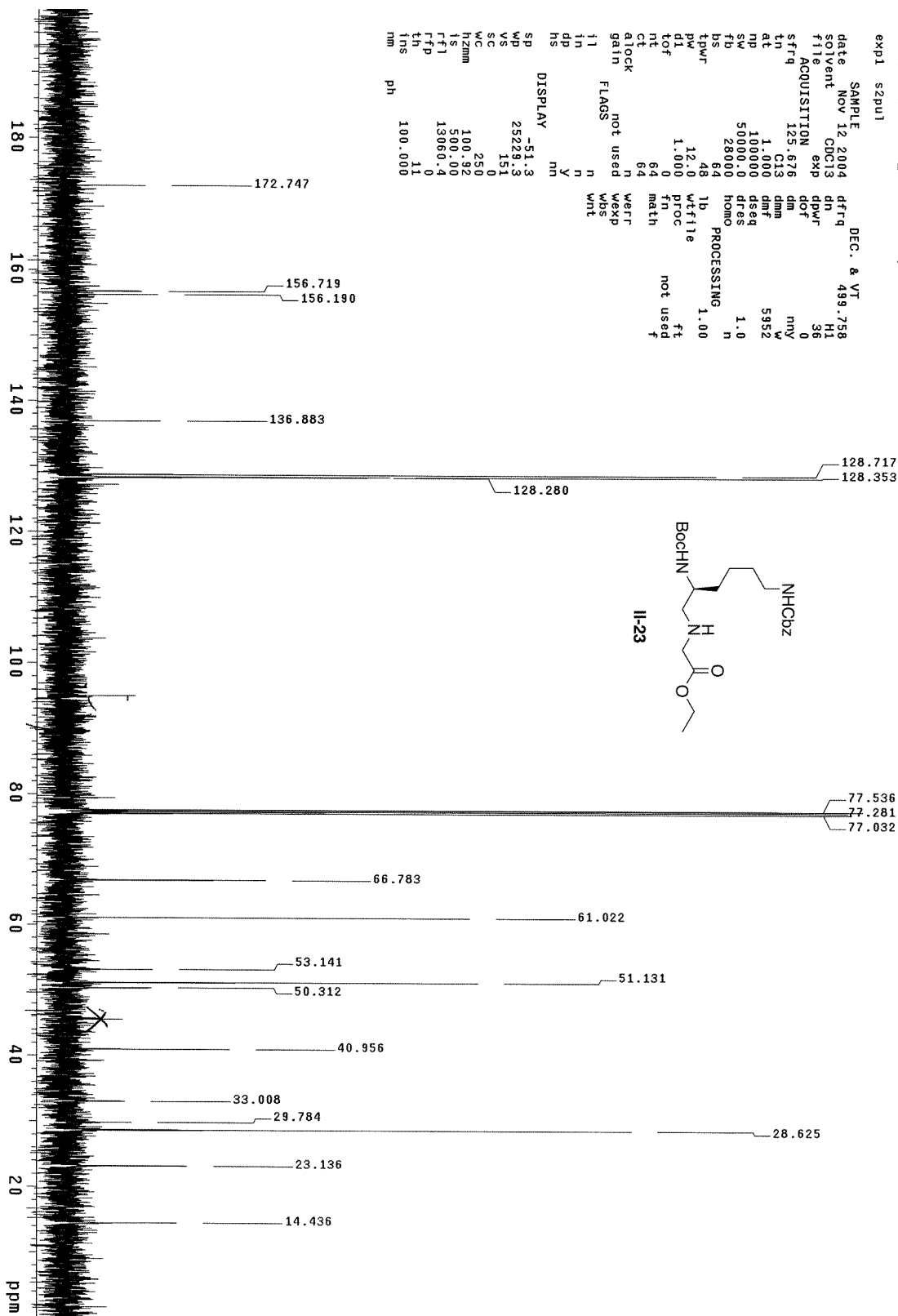
H1 stdpar RT DB_5mm inovas500
exp4 s2pul1

SAMPLE DEC. & VT C13
 date Jan 23 2004 dn
 solvent CDCl3 dof
 file exp dm
 ACQUISITION exp dnm 10596
 sfrq 499.561 dmf 38
 tn H1 dpwr
 at 1.003 lb
 mp 12024 fn 1.00
 SW 5997.0 fn 65536
 fd not used math i
 bs 8
 pw 8.0 warr wft
 tpwr 8.0 wexp
 d1 58 wds
 tof 1.000 wlt
 nt -2.4
 ct 16 sp
 alock n wp 4011.1
 gain not used vs 391
 flags n sc 0
 ll n hzmm 16.04
 ln n is 223.43
 dp y rfp 512.1
 ns mn tps 18
 al ph 2.000



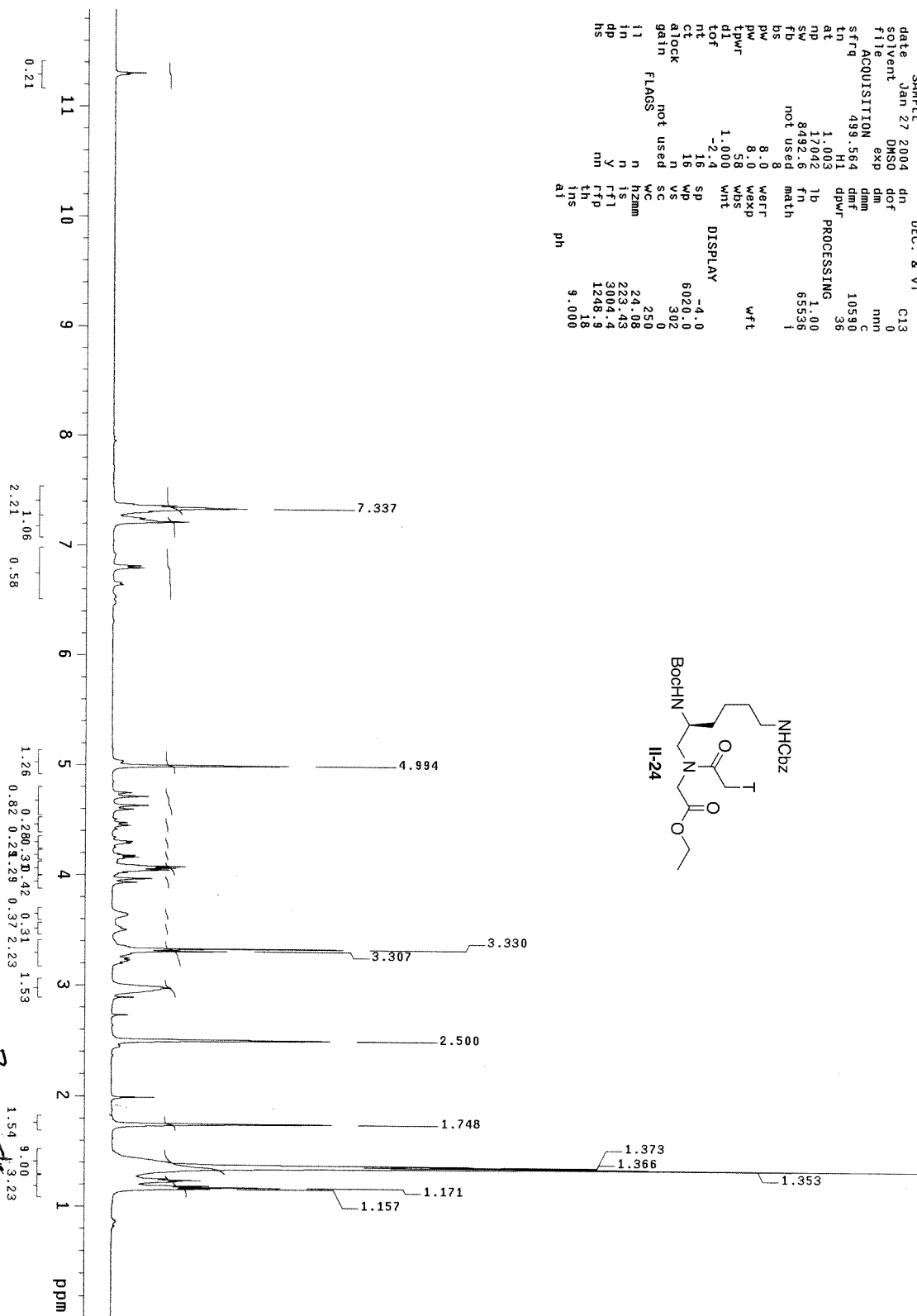
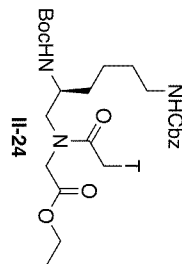
C13_std p-500 bh_5mm RT nonspin
 exp1 s2pu1

SAMPLE DEC. & VT
 date Nov 12 2004 dfreq 499.758
 solvent CDCl3 dn H1
 file CDC13 exp dpwr 36
 ACQUISITION dof 0
 sfrq 125.676 dm my
 tn C13 dmm nny
 at 1.000 dmf w
 np 100000 dseq 5952
 sw 50000.0 dres 1.0
 fb 28000 homo n
 bs 64
 tpwr 48 1b
 pw 12.0 wtfile 1.00
 d1 1.000 proc ft
 tof 0 fn not used f
 nt 64 math
 ct 64
 clock n weff
 gain not used wep
 flags not used wds
 i1 n wht
 in n
 dn y
 hs nm
 DISPLAY -51.3
 sp 25229.3
 vs 151
 sc 0
 wc 250
 hzmm 100.92
 is 500.00
 rf1 13060.4
 rfp 0
 th 11
 tns 100.000
 nm



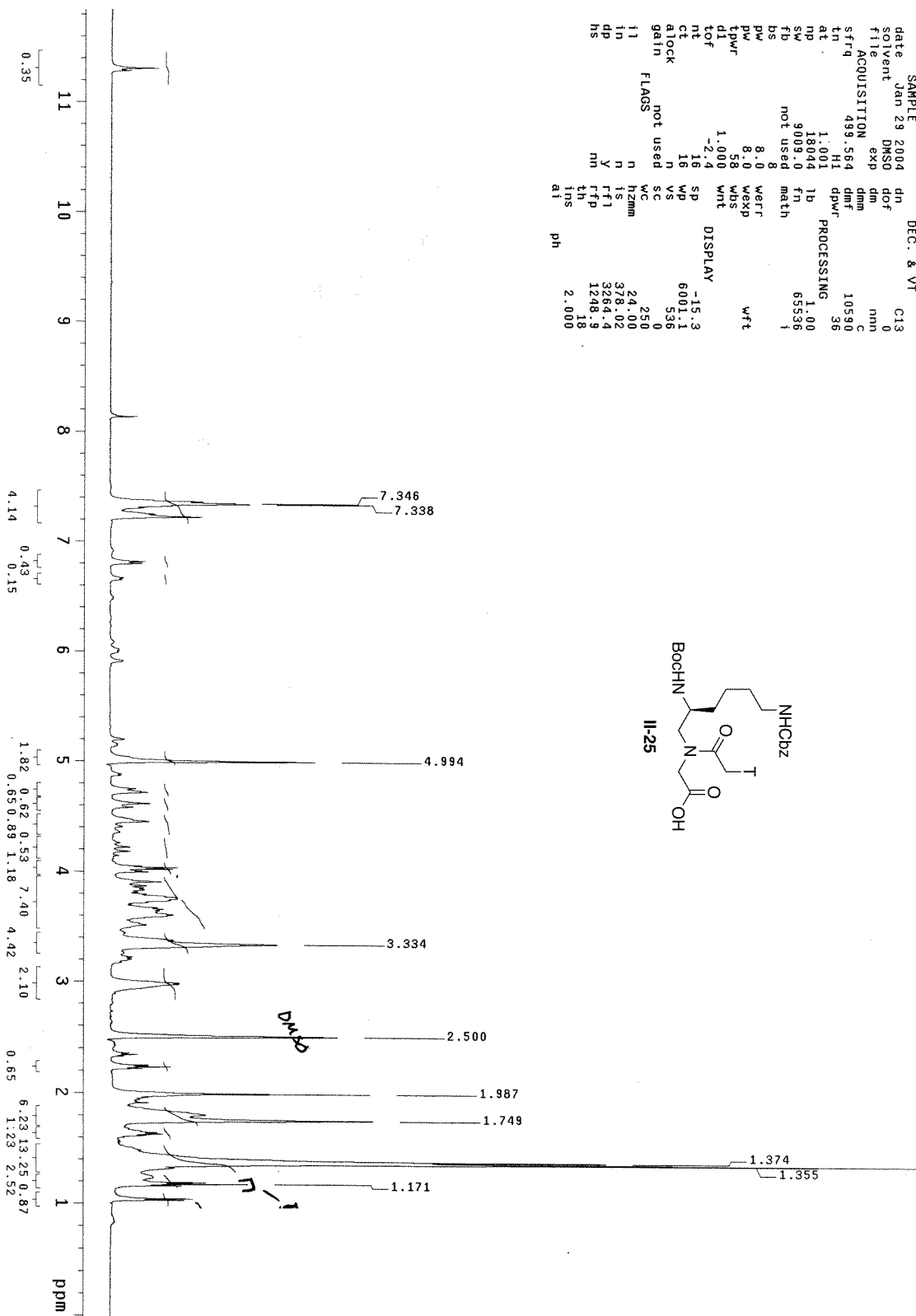
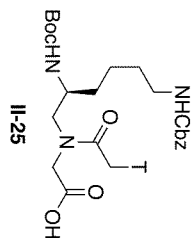
H1 stdpar RI DB_Smm inovas500
 exp1 szpu1

date	Jan 27 2004	DEC. & VT	C13
solvent	DMSO	doF	0
file	exp	dm	mm
ACQUISITION		dm	C
sfrq	499.564	dmf	10590
tn	H1	dpwr	36
at	1.003	PROCESSING	1.00
np	17942	fb	65536
sw	8492.6	fn	i
fb	not used	math	
bs	8		
pw	8.0	werr	wft
tpwr	8.0	wexp	
d1	58	wbs	
tof	1.000	wrt	
nt	-2.4	DISPLAY	-4.0
ct	16	sp	6020.0
atocx	16	wp	302
gain	not used	vs	250
FLAGS	not used	sc	0
fl	n	hzm	24.08
in	n	is	283.43
dp	y	ffl	3004.4
ns	nm	thp	1248.3
		th	18
		tlis	9.000
		at	ph



H1 stdpar RT DB_5mm inovas500
 exp8 szpul

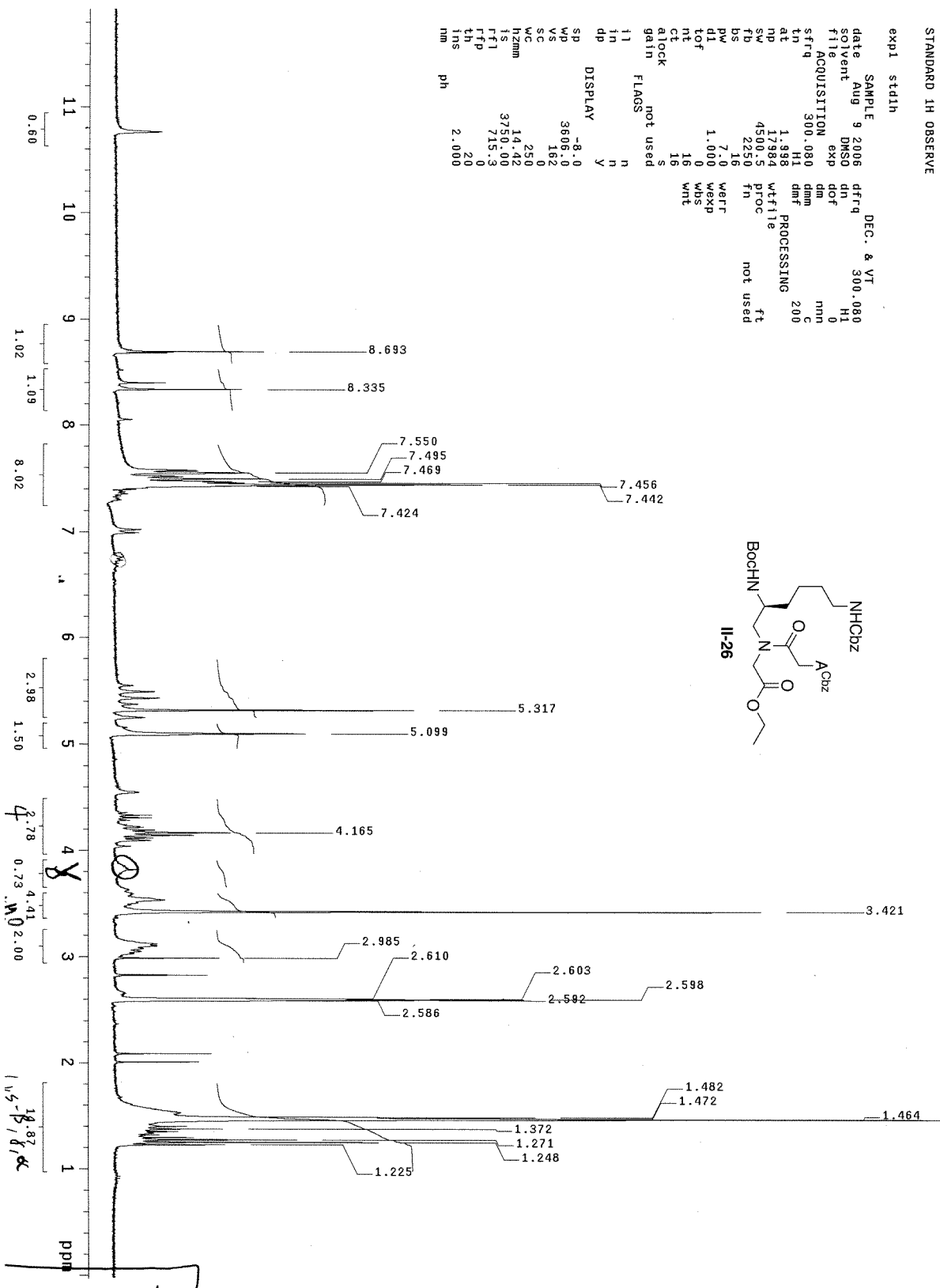
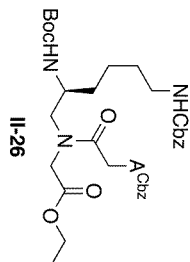
SAMPLE	Jan 29 2004	dn	DEC. & VT	C13
date	Jan 29 2004	dn	DEC. & VT	C13
solvent	DMSO	dof		0
file	exp	dm		mm
ACQUISITION	499.564	dmm		10590
sfrq	499.564	dmf		36
tn	H1	dpwr		36
at	1.001	PROCESsing		1.00
np	18044	lb		65536
sw	9009.0	fn		1
fb	not used	math		
bs	8	werr		wft
pw	8.0	wexp		
tpwr	58	wbs		
dl	1.000	wnt		
tof	-2.4	DISPLAY		-15.3
nt	18	sp		6001.1
ct	16	wp		336
clock	n	sc		250
gatin	not used	h2mm		24.00
fl	FLAGS	is		378.02
in	n	rfl		3264.4
dp	y	th		1248.9
hs	ni	ins		18
		ai		2.000
		ph		



STANDARD 1H OBSERVE

expl std1h

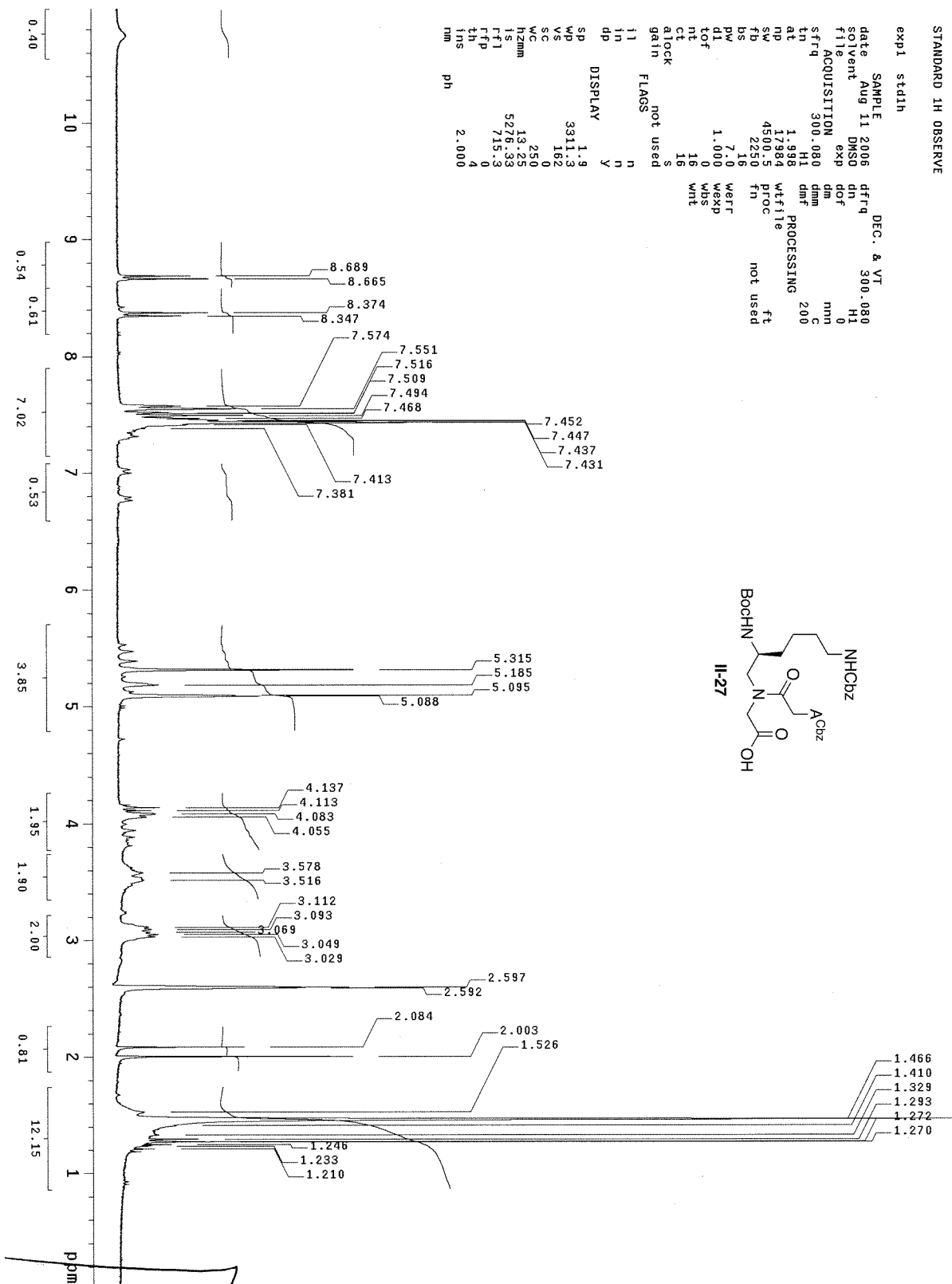
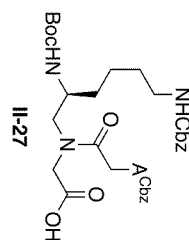
date	Aug 9 2006	dfreq	300.080	DEC. & VT
solvent	DMSO	dn	H1	
file	exp	dm	0	
ACQUISITION	dm	nmn	C	
sfrq	300.080	dm	200	
tn	H1	dmf	PROCESSING	
at	1.998	wf	ft	
np	17984	proc	not used	
sw	4500.5	fn		
td	2250			
bs	16			
pw	7.0	WARR		
pl	1.000	WEXP		
tdf	WDS	WTE		
ct	16			
gain	not used			
flags	not used			
ll	n			
in	n			
dp	y			
DISPLAY				
sp	-8.0			
wp	3606.0			
vs	162			
sc	0			
wc	250			
hzmm	14.42			
ts	3750.00			
ffl	715.3			
ffp	0			
th	20			
ins	2.000			
nm				



STANDARD 1H OBSERVE

expt stddh

SAMPLE DEC. & VT
 date Aug 11 2006 dfrq 300.080
 solvent DMSO dn H1
 file exp dof 0
 ACQUISITION nmh C
 sfrq 300.080 dmf
 tn H1
 at 1.998 wifile
 np 17984 wifile
 sw 4500.5 proc
 fb 2250 fn
 bs 16
 pw 7.0 werr
 DI 1.000 wexp
 TOF 0 wds
 nt 16 wht
 clock not used
 gain S
 il il
 in n
 dp y
 DISPLAY 1.9
 sp 3311.3
 wp 182
 vs 0
 sc 0
 WC 250
 hzmm 13.25
 IS 5276.33
 rfi 715.3
 rfp 0
 th 4
 ins 4
 nm 2.000
 ph

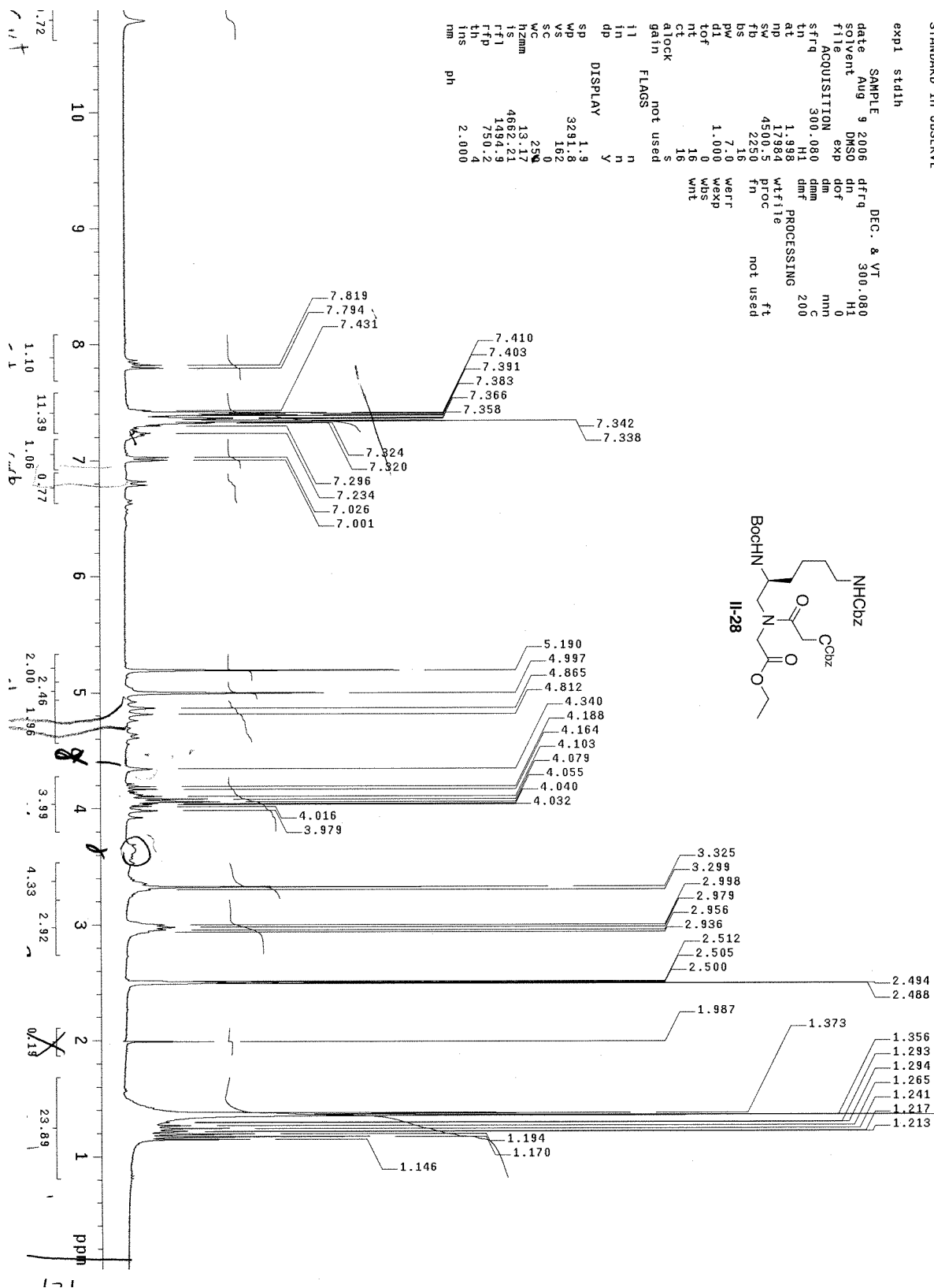
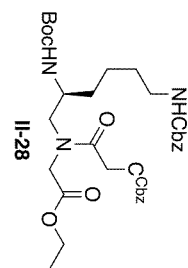


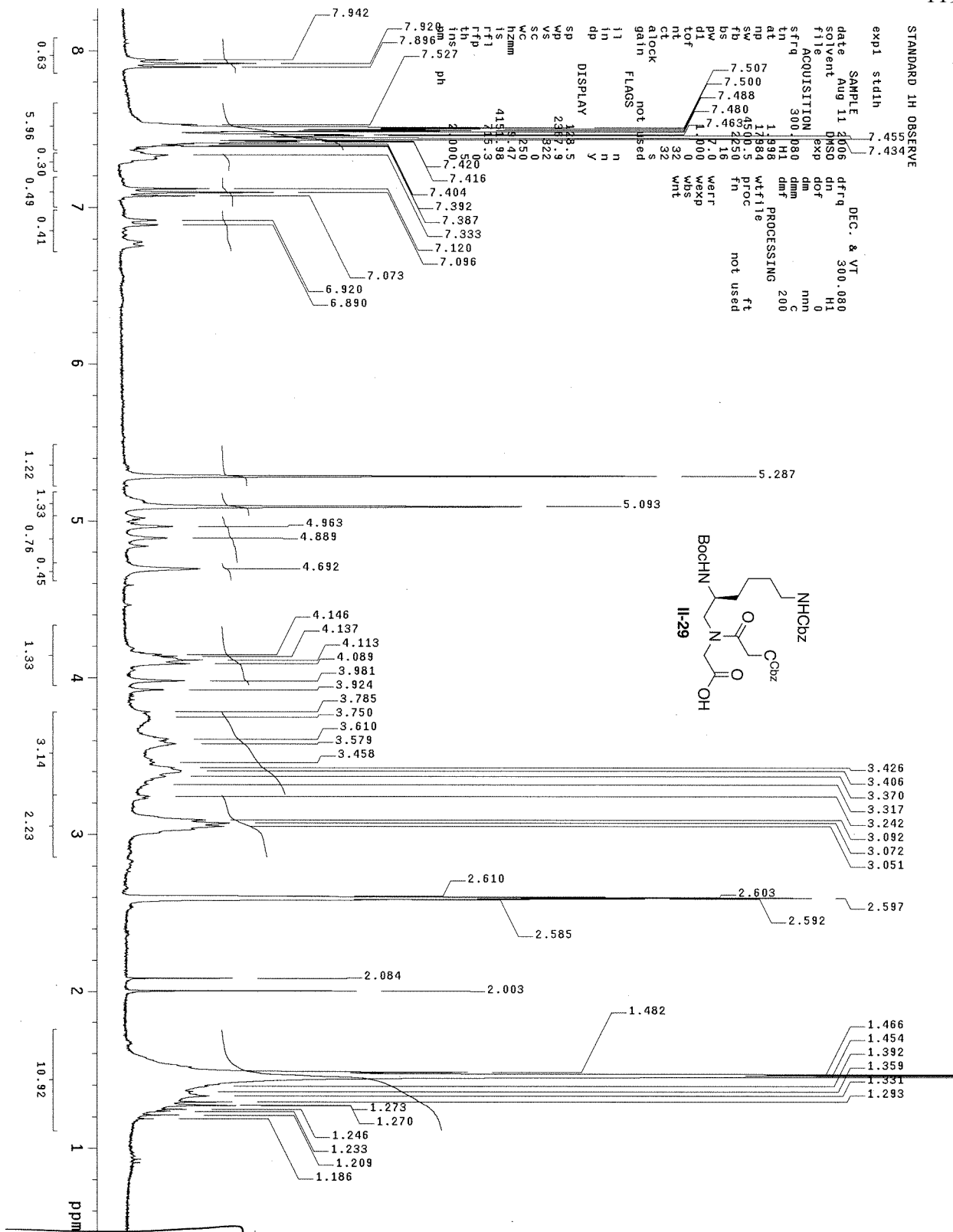
201

STANDARD 1H OBSERVE

```

expt 1          stdlh
SAMPLE 9 2006   DEC. & VT 300.080
date Aug      DMSO      dn  HI
solvent      exp      dof  0
file         dm        mm  C
ACQUISITION 300.080   dm   200
sfrq        HI       C
ln          1.983     dmf
at         1788      wtf file
np         45005     proc
fn         22250     fn
bs         16       not used
pw         7.0      weff
d1         1.000    wexp
nt         0        wbs
ct         16      wnt
atlock    not used
gain      not used
DISPLAY  1.9
SP        3291.8
WP        162
VS        2500
WC        0
Hzmm      13.17
IS        4662.21
FTF       1994.9
TTP       750.2
IN        2.000
MS        2.000
ph
  
```

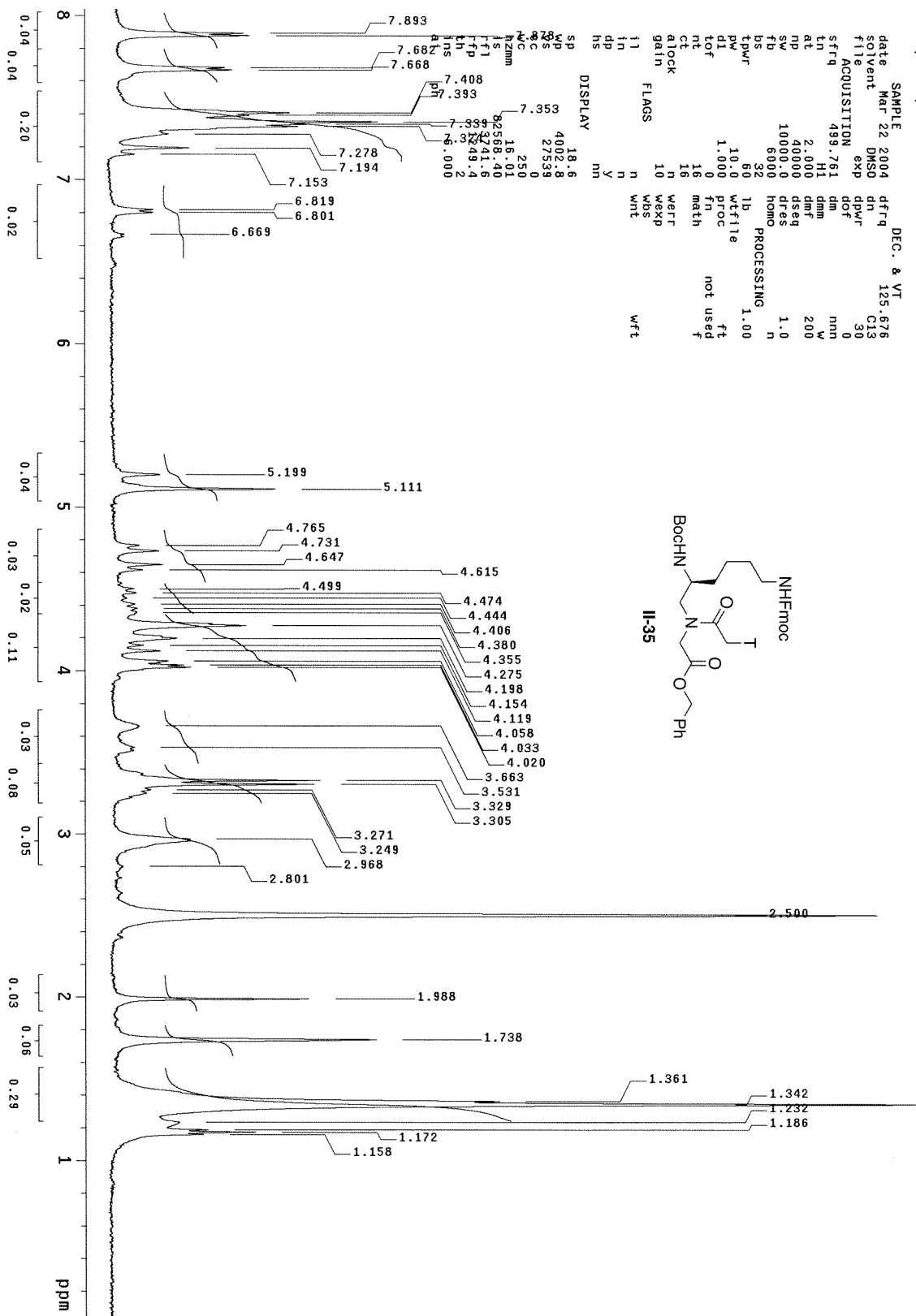


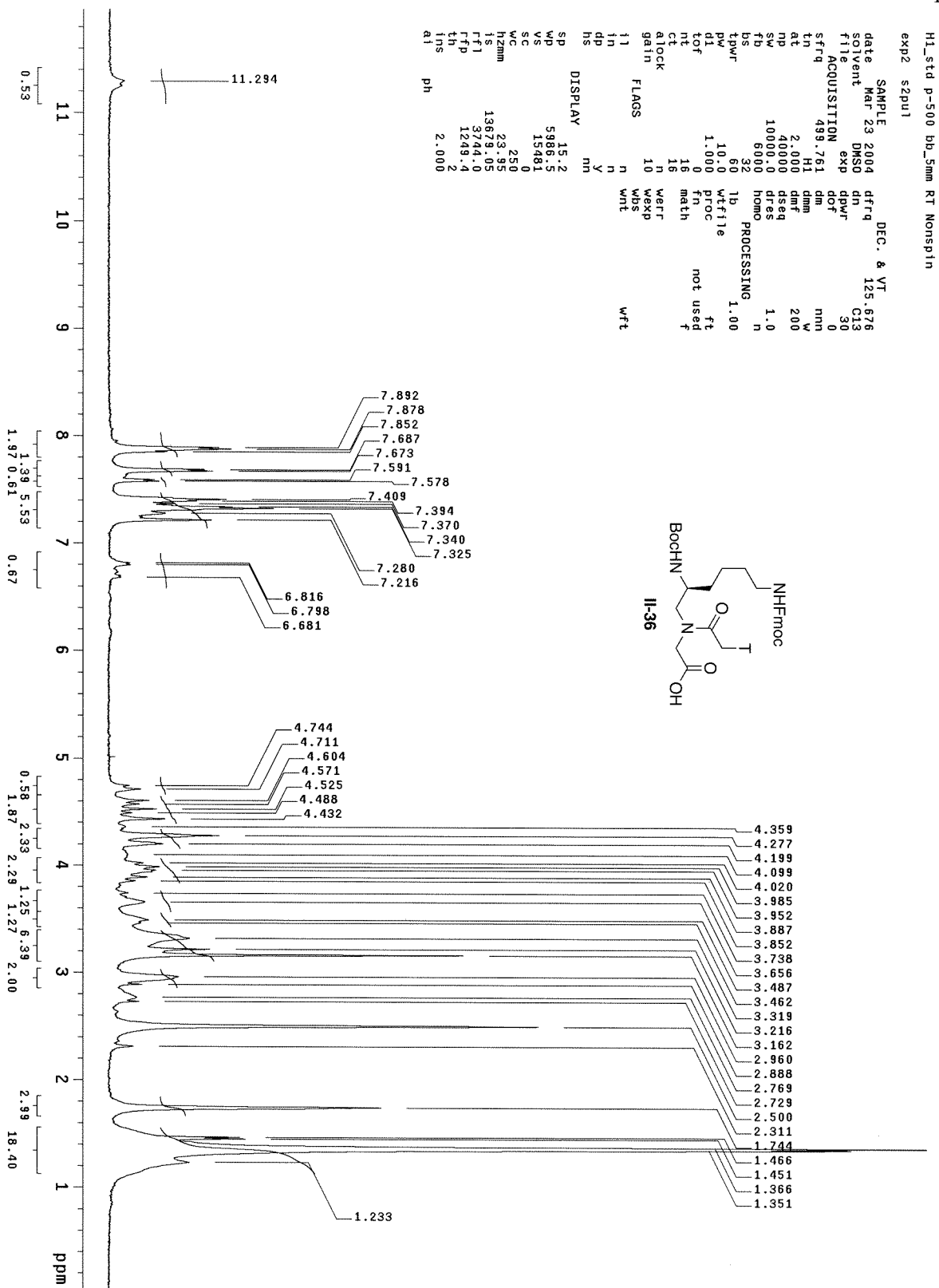


HI_std p-500 bb_5mm RT Nonspin
 exp3 s2pul1

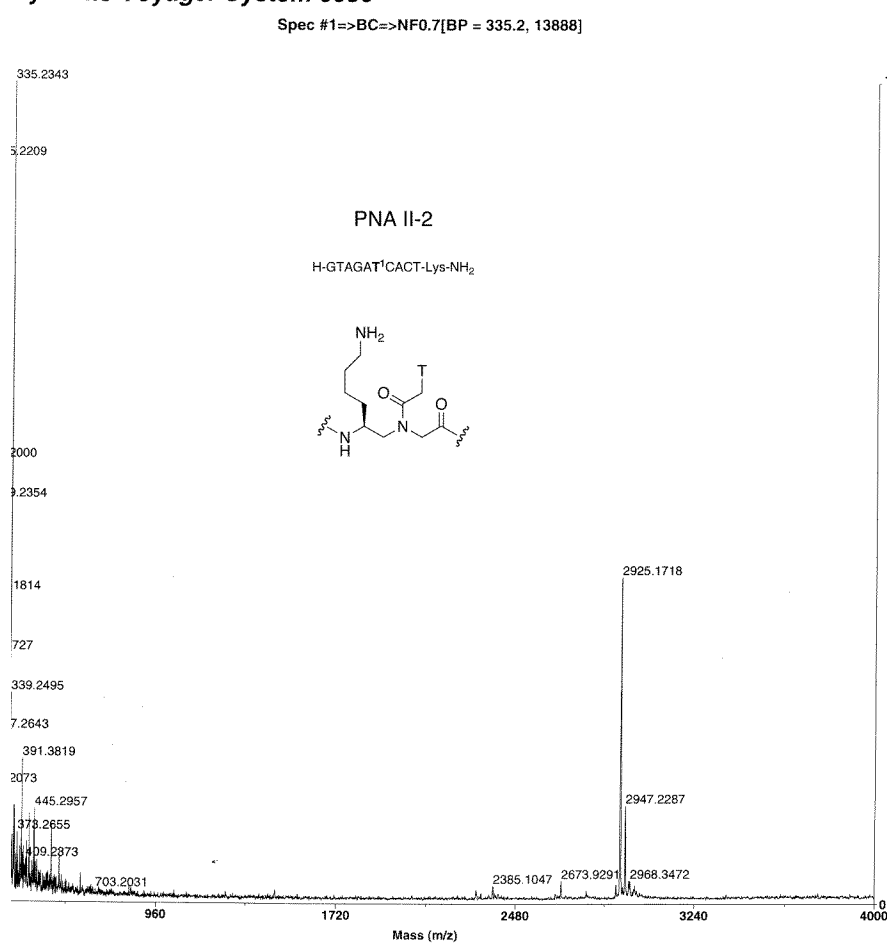
SAMPLE DEC. & VT
 date Mar 22 2004 dfrq 125.676
 solvent DMSO d1 30
 file ACQUISITION exp d1 30
 sfreq 439.761 dm 0
 tn H1 dmm mmm
 at 2.000 dmf w
 np 40000 dseq 200
 sw 10000.0 dres 1.0
 fb 6000 homo n
 bs 32
 tpwr 60
 pw 10.0 wtfile 1.00
 d1 1.000 proc ft
 tof 0 fn not used
 nt 16 math f
 ct 16
 atlock n werr
 gain 10 wexp
 wds Wds
 wnt
 fwt

DISPLAY nm
 sp 18.6
 wd 4002.8
 rs 27539
 ac 250
 hzmm 16.01
 fs 82568.40
 f1 3241.46
 fh 3249.4
 fns 76.000
 ph





II.9.5b PNA Oligomer Mass Spectrometry Data



Mode of operation: Reflector
Extraction mode: Delayed
Polarity: Positive
Acquisition control: Manual

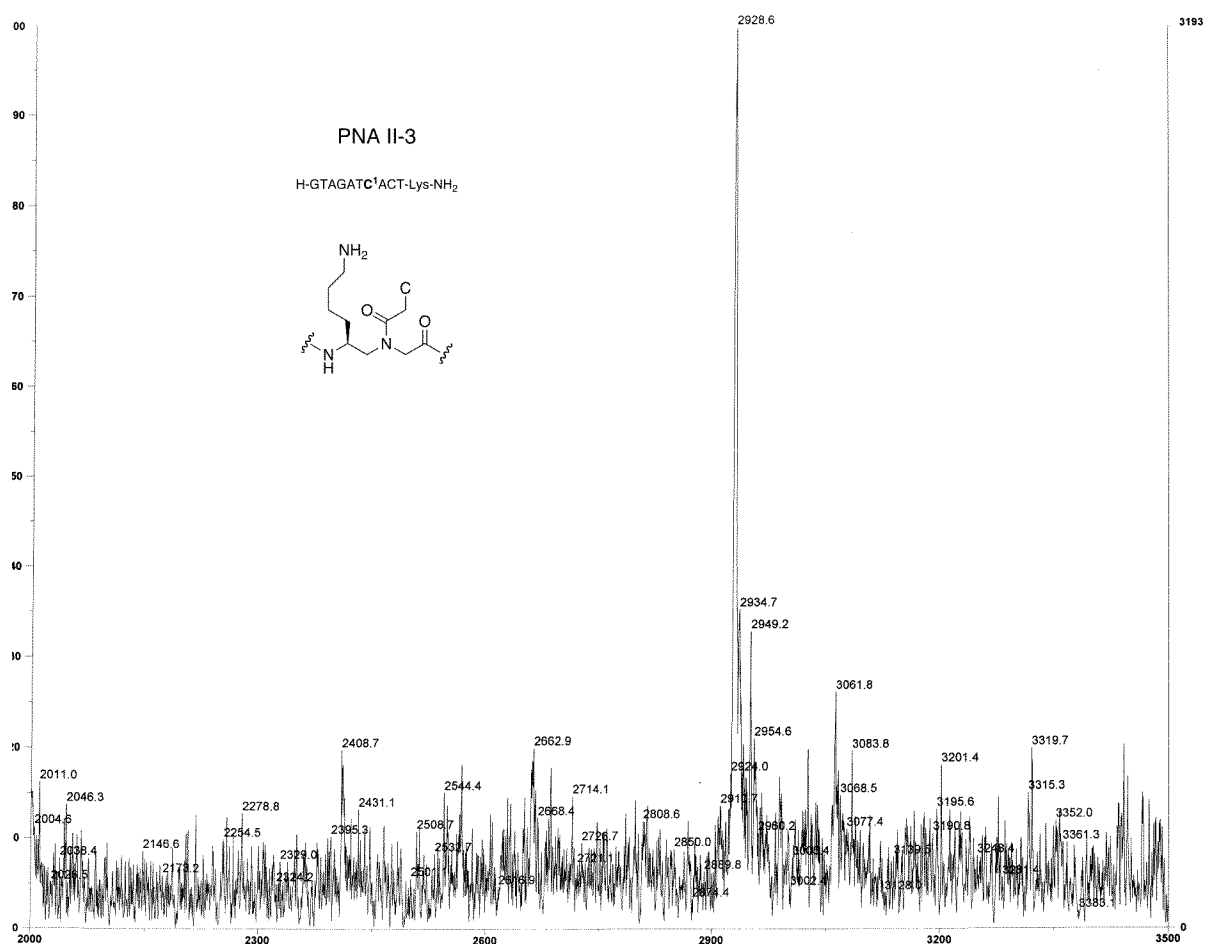
Accelerating voltage: 20000 V
Grid voltage: 70%
Mirror voltage ratio: 1.12
Guide wire 0: 0.03%
Extraction delay time: 140 nsec

Acquisition mass range: 200 -- 4000 Da
Number of laser shots: 200/spectrum
Laser intensity: 3579
Calibration type: Default
Calibration matrix: 2,5-Dihydroxybenzoic acid
Low mass gate: 200 Da
Timed ion selector: Off

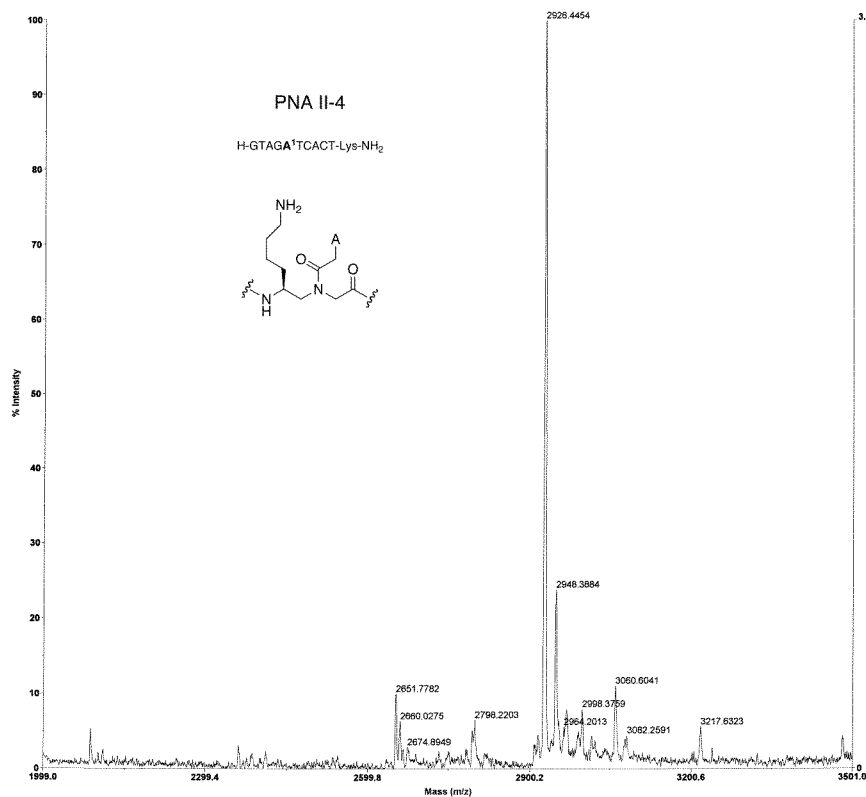
Digitizer start time: 14.2542
Bin size: 2 nsec
Number of data points: 50000
Vertical scale 0: 1000 mV
Vertical offset: 0%
Input bandwidth 0: 0 MHz

Sample well: 93
Plate ID: 100
Serial number: 6050
Instrument name: Voyager-DE PRO
Plate type filename: C:\VOYAGER\100 well plate
Lab name: PerSeptive Biosystems

Absolute x-position: 11441
Absolute y-position: 730.792
Relative x-position: -306.454
Relative y-position: -856.708
Shots in spectrum: 60
Source pressure: 1.22e-006
Mirror pressure: 1.529e-007
TC2 pressure: 0.01475
TIS gate width: 6
TIS flight length: 680



Voyager Spec #1=>BC[BP = 2926.2, 32981]



Mode of operation: Reflector
Extraction mode: Delayed
Polarity: Positive
Acquisition control: Manual

Accelerating voltage: 25000 V
Grid voltage: 70%
Mirror voltage ratio: 1.12
Guide wire 0: 0.03%
Extraction delay time: 140 nsec

Acquisition mass range: 2000 -- 3500 Da
Number of laser shots: 200/spectrum
Laser intensity: 3819
Laser Rep Rate: 20.0 Hz
Calibration type: Default
Calibration matrix: 2,5-Dihydroxybenzoic acid
Low mass gate: 2000 Da
Timed ion selector: Off

Digitizer start time: 40.11
Bin size: 2 nsec
Number of data points: 6459
Vertical scale 0: 50 mV
Vertical offset: 0%
Input bandwidth 0: 25 MHz

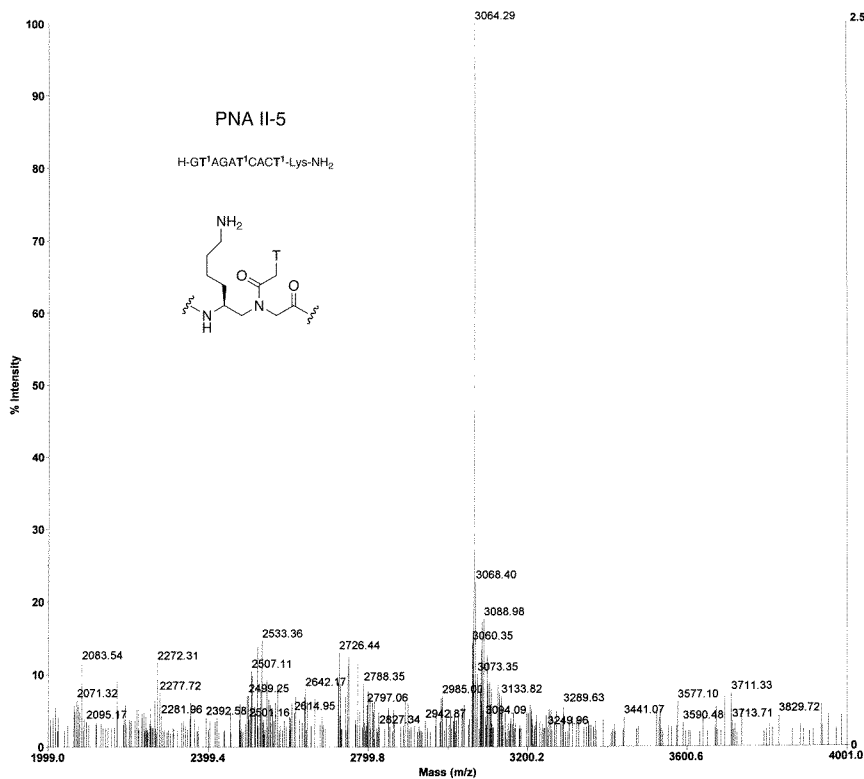
Sample well: 09
Plate ID: 100
Serial number: 6050
Instrument name: Voyager-DE PRO
Plate type filename: C:\VOYAGER\100 well plate.pl
Lab name: PE Biosystems

Absolute x-position: 42156.3
Absolute y-position: 47306.4
Relative x-position: -71.1803
Relative y-position: -1.06089
Shots in spectrum: 200
Source pressure: 1.38e-006
Mirror pressure: 1.892e-007
TC2 pressure: 0.01525
TIS gate width: 30
TIS flight length: 678

Acquired: 11:33:00, October 13, 2004

Printed: 11:35, October 13, 2004

Spec #1=>BC=>DI[BP = 3064.3, 25396]



mode or operation: Linear
Extraction mode: Delayed
Polarity: Positive
Acquisition control: Manual

Accelerating voltage: 25000 V
Grid voltage: 95%
Guide wire O: 0.03%
Extraction delay time: 100 nsec

Acquisition mass range: 2000 -- 4000 Da
Number of laser shots: 200/spectrum
Laser intensity: 3258
Calibration type: Default
Calibration matrix: a-Cyano-4-hydroxycinnamic aci
Low mass gate: 500 Da

Digitizer start time: 27.4144
Bin size: 2 nsec
Number of data points: 50000
Vertical scale: 1000 mV
Vertical offset: 0%
Input bandwidth: 0 MHz

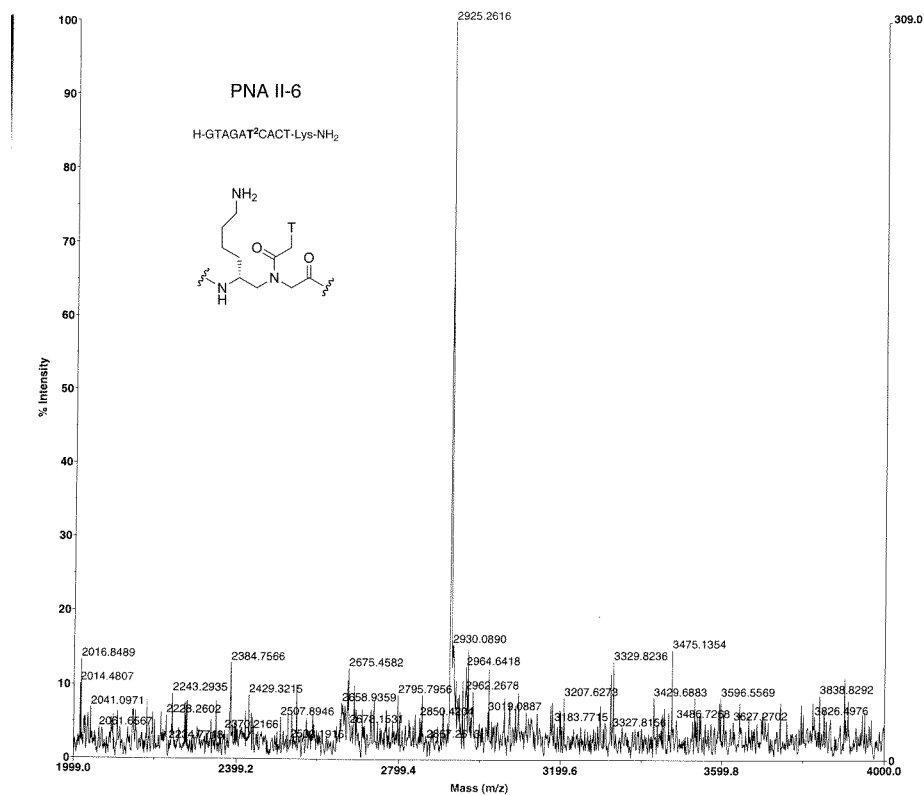
Sample well: 23
Plate ID: 100
Serial number: 6050
Instrument name: Voyager-DE PRO
Plate type filename: C:\VOYAGER\100 well plate.plt
Lab name: PerSeptive Biosystems

Absolute x-position: 12132.7
Absolute y-position: 37190.3
Relative x-position: 385.193
Relative y-position: 42.7689
Shots in spectrum: 175
Source pressure: 8.809e-007
Mirror pressure: 1.332e-007
TC2 pressure: 0.01286
TIS gate width: 6
TIS flight length: 680

Acquired: 17:24, July 01, 2004

Printed: 17:34, July 01, 2004

Spec #1=>BC=>NF0.7[BP = 2925.2, 309]



Acquired: 11:19, March 10, 2004

Mode of operation: Reflector
Extraction mode: Delayed
Polarity: Positive
Acquisition control: Manual

Accelerating voltage: 25000 V
Grid voltage: 70%
Mirror voltage ratio: 1.12
Guide wire 0: 0.03%
Extraction delay time: 140 nsec

Acquisition mass range: 2000 -- 4000 Da
Number of laser shots: 200/spectrum
Laser intensity: 4079
Calibration type: Default
Calibration matrix: 2,5-Dihydroxybenzoic acid
Low mass gate: 200 Da
Timed ion selector: Off

Digitizer start time: 40.1002
Bin size: 2 nsec
Number of data points: 50000
Vertical scale 0: 1000 mV
Vertical offset: 0%
Input bandwidth 0: 0 MHz

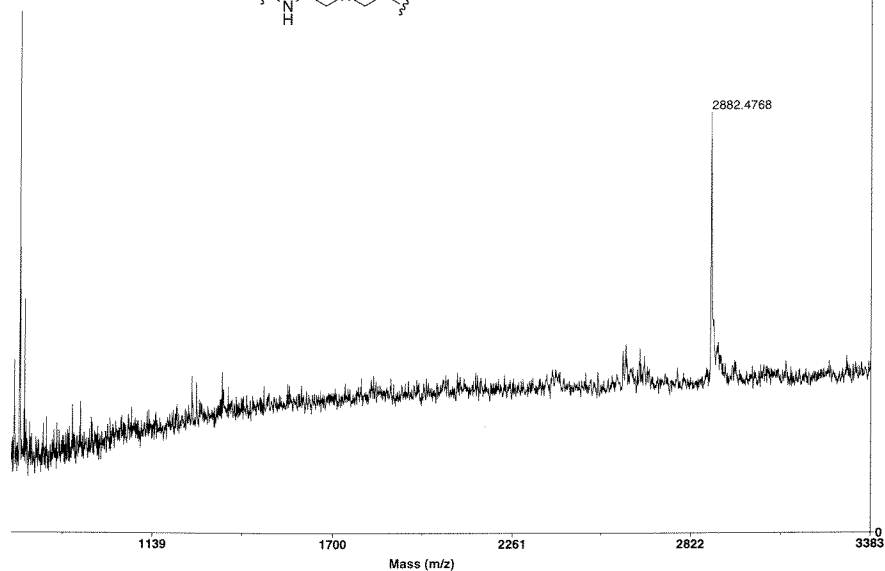
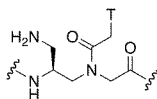
Sample well: 11
Plate ID: 100
Serial number: 6050
Instrument name: Voyager-DE PRO
Plate type filename: C:\VOYAGER\100 well plate.ph
Lab name: PerSeptive Biosystems

Absolute x-position: 752.431
Absolute y-position: 41580
Relative x-position: -835.069
Relative y-position: -647.507
Shots in spectrum: 180
Source pressure: 1.024e-006
Mirror pressure: 1.345e-007
TC2 pressure: 0.01173
TIS gate width: 6
TIS flight length: 680

Printed: 11:20, March 10, 2004

Spec #1=>BC=>BC=>NF0.7[BP = 215.2, 50078]

PNA II-7

H-GTAGAT³CACT-Lys-NH₂

Mode of operation: Reflector
 Extraction mode: Delayed
 Polarity: Positive
 Acquisition control: Manual

Accelerating voltage: 16000 V
 Grid voltage: 70%
 Mirror voltage ratio: 1.12
 Guide wire 0: 0.03%
 Extraction delay time: 140 nsec

Acquisition mass range: 200 -- 3500 Da
 Number of laser shots: 1000/spectrum
 Laser intensity: 3679
 Calibration type: Default
 Calibration matrix: 2,5-Dihydroxybenzoic acid
 Low mass gate: 200 Da
 Timed ion selector: Off

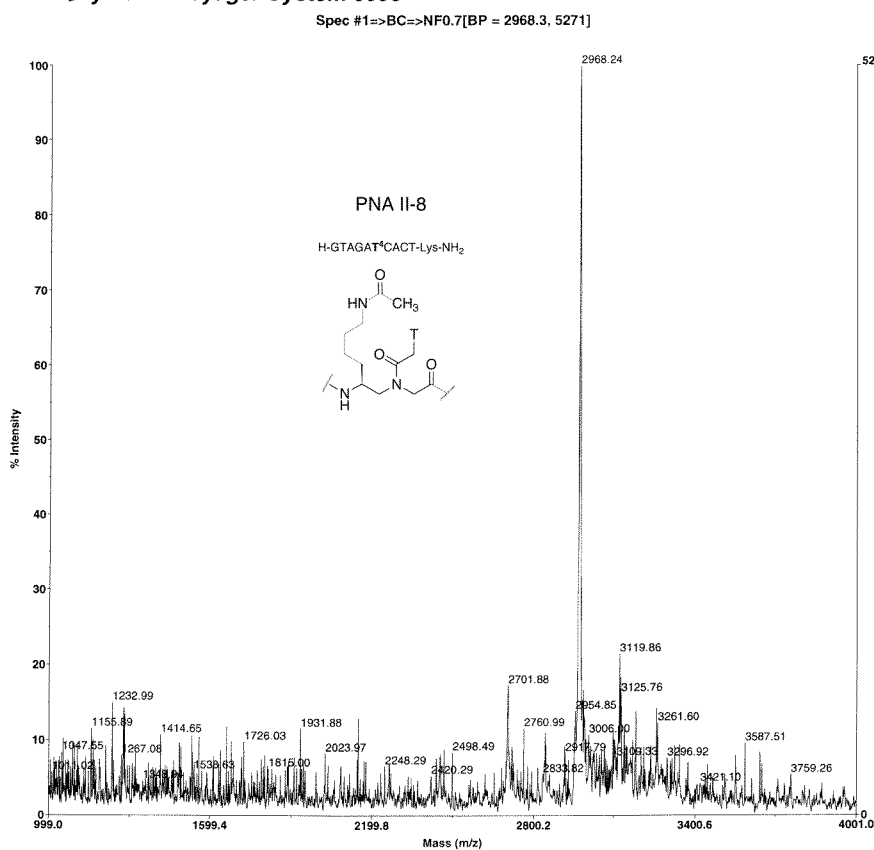
Digitizer start time: 15.9221
 Bin size: 2 nsec
 Number of data points: 50000
 Vertical scale 0: 1000 mV
 Vertical offset: 0%
 Input bandwidth 0: 0 MHz

Sample well: 13
 Plate ID: 100
 Serial number: 6050
 Instrument name: Voyager-DE PRO
 Plate type filename: C:\VOYAGER\100 well plate.
 Lab name: PerSeptive Biosystems

Absolute x-position: 10772.5
 Absolute y-position: 41880.7
 Relative x-position: -974.95
 Relative y-position: -346.789
 Shots in spectrum: 201
 Source pressure: 7.301e-007
 Mirror pressure: 8.663e-008
 TC2 pressure: 0.01136
 TIS gate width: 6
 TIS flight length: 680

3 January 20 2004

Printed: 10:14 January 20 2004



Mode of operation: Linear
Extraction mode: Delayed
Polarity: Positive
Acquisition control: Manual

Accelerating voltage: 20000 V
Grid voltage: 95%
Guide wire 0: 0.03%
Extraction delay time: 100 nsec

Acquisition mass range: 1000 -- 4000 Da
Number of laser shots: 200/spectrum
Laser intensity: 3894
Calibration type: Default
Calibration matrix: 2,5-Dihydroxybenzoic acid
Low mass gate: 500 Da

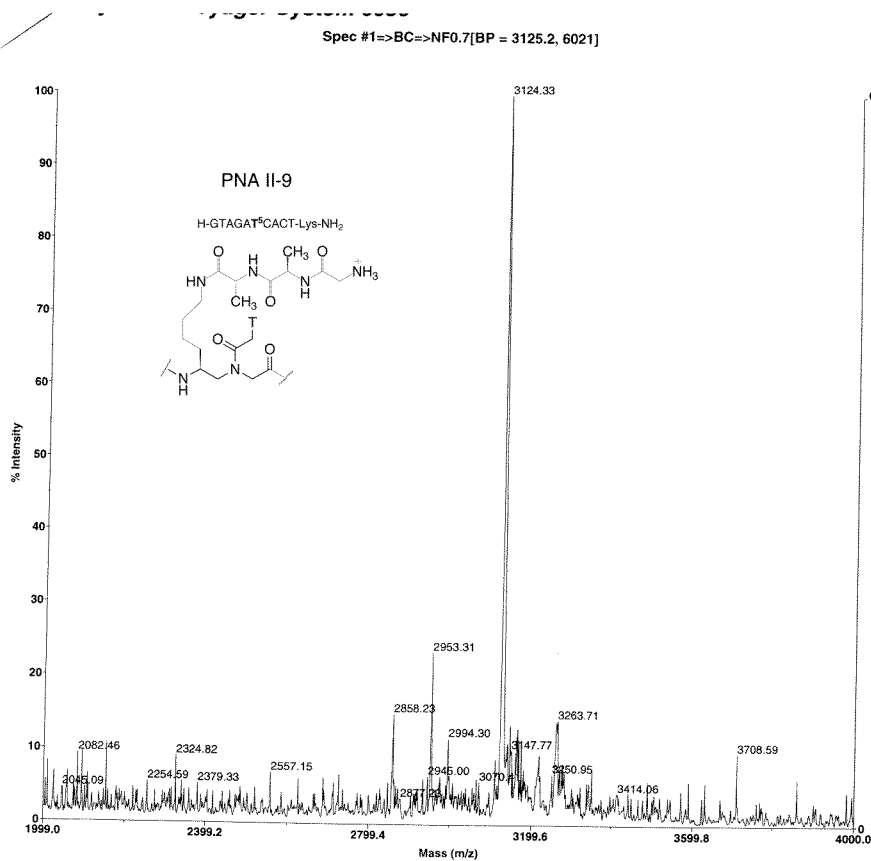
Digitizer start time: 21.6986
Bin size: 2 nsec
Number of data points: 50000
Vertical scale: 1000 mV
Vertical offset: 0%
Input bandwidth: 0 MHz

Sample well: 54
Plate ID: 100
Serial number: 6050
Instrument name: Voyager-DE PRO
Plate type filename: C:\VOYAGER\100 well plate.plt
Lab name: PerSeptive Biosystems

Absolute x-position: 17013.6
Absolute y-position: 21322.1
Relative x-position: 186.125
Relative y-position: -585.402
Shots in spectrum: 126
Source pressure: 1.122e-006
Mirror pressure: 1.685e-007
TC2 pressure: 0.01333
TIS gate width: 6
TIS flight length: 680

Acquired: 16:47, April 02, 2004

Printed: 16:47, April 02, 2004



Mode of operation: Linear
 Extraction mode: Delayed
 Polarity: Positive
 Acquisition control: Manual

Accelerating voltage: 25000 V
 Grid voltage: 95%
 Guide wire 0: 0.03%
 Extraction delay time: 100 nsec

Acquisition mass range: 2000 - 4000 Da
 Number of laser shots: 200/spectrum
 Laser intensity: 4133
 Calibration type: Default
 Calibration matrix: 2,5-Dihydroxybenzoic acid
 Low mass gate: 500 Da

Digitizer start time: 27.4123
 Bin size: 2 nsec
 Number of data points: 50000
 Vertical scale: 1000 mV
 Vertical offset: 0%
 Input bandwidth: 0 MHz

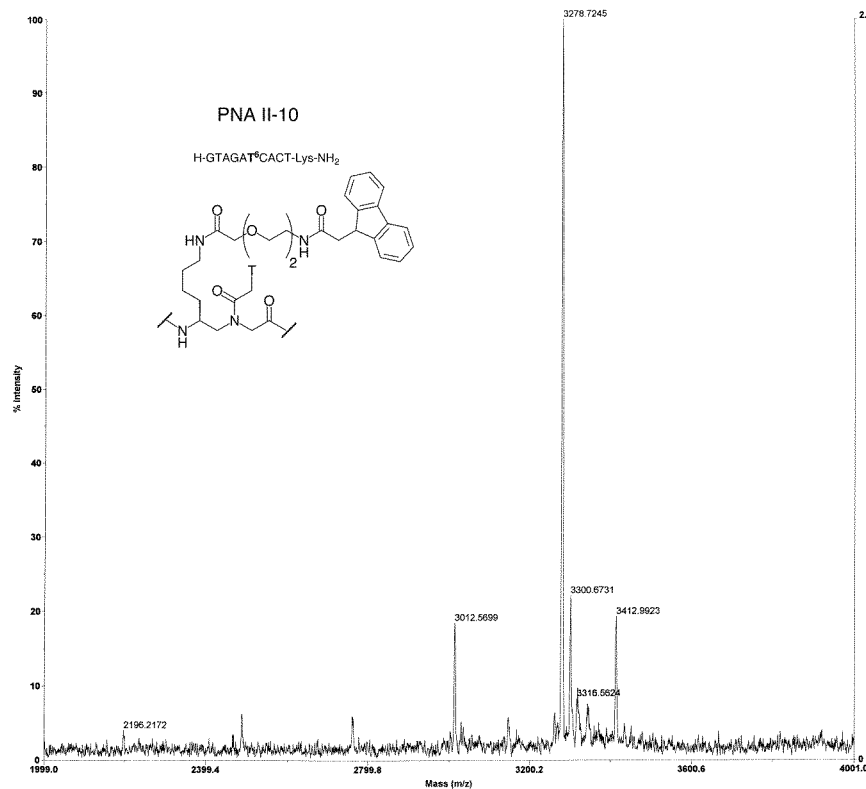
Sample well: 59
 Plate ID: 100
 Serial number: 6050
 Instrument name: Voyager-DE PRO
 Plate type filename: C:\VOYAGER\100 well plate.p
 Lab name: PerSeptive Biosystems

Absolute x-position: 42456
 Absolute y-position: 21893.2
 Relative x-position: 228.543
 Relative y-position: -14.2626
 Shots in spectrum: 163
 Source pressure: 9.701e-007
 Mirror pressure: 1.235e-007
 TC2 pressure: 0.01307
 TIS gate width: 6
 TIS flight length: 680

Acquired: 20:30, April 15, 2004

Printed: 20:30, April 15, 2004

Voyager Spec #1[BP = 3278.6, 21087]



Mode of operation: Reflector
Extraction mode: Delayed
Polarity: Positive
Acquisition control: Manual

Accelerating voltage: 25000 V
Grid voltage: 70%
Mirror voltage ratio: 1.12
Guide wire 0: 0.03%
Extraction delay time: 140 nsec

Acquisition mass range: 2000 -- 4000 Da
Number of laser shots: 200/spectrum
Laser intensity: 3819
Laser Rep Rate: 20.0 Hz
Calibration type: Default
Calibration matrix: 2,5-Dihydroxybenzoic acid
Low mass gate: 200 Da
Timed ion selector: Off

Digitizer start time: 40.11
Bin size: 2 nsec
Number of data points: 8285
Vertical scale 0: 50 mV
Vertical offset: 0%
Input bandwidth 0: 25 MHz

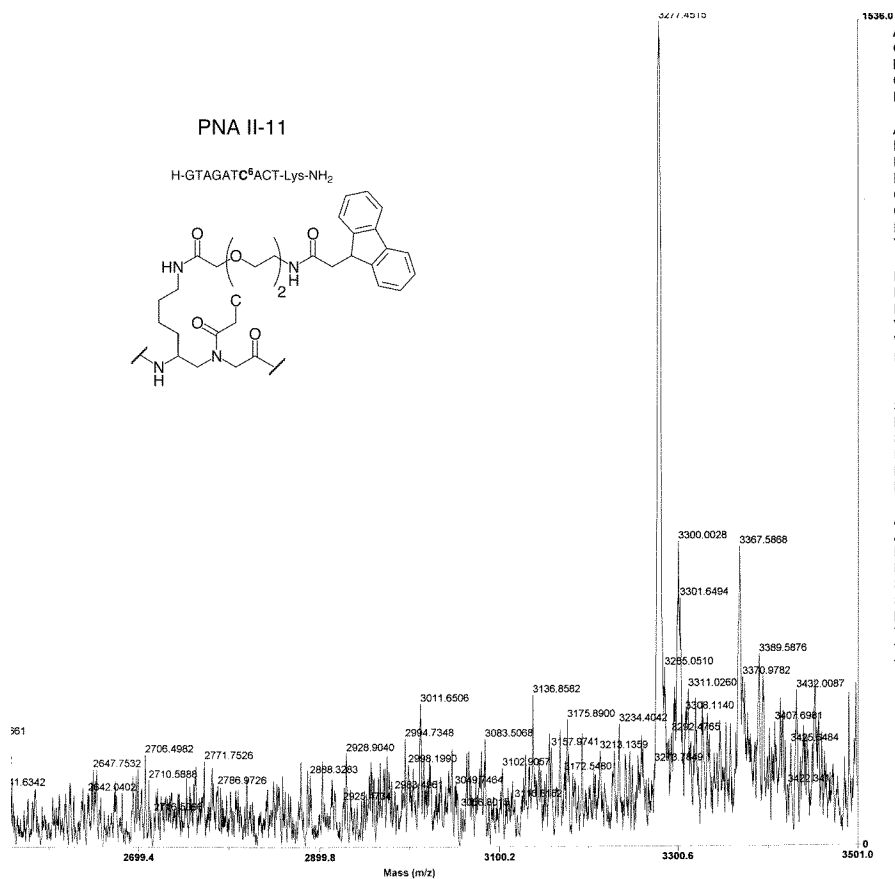
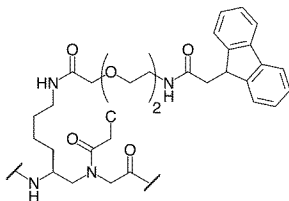
Sample well: 74
Plate ID: 100
Serial number: 6050
Instrument name: Voyager-DE PRO
Plate type filename: C:\VOYAGER\100 well plate.pl
Lab name: PE Biosystems

Absolute x-position: 16267.2
Absolute y-position: 12326.1
Relative x-position: -560.302
Relative y-position: 578.553
Shots in spectrum: 124
Source pressure: 1.167e-006
Mirror pressure: 1.88e-007
TC2 pressure: 0.01604
TIS gate width: 30
TIS flight length: 678

Acquired: 09:50:00, September 21, 2004

Printed: 09:50, September 21, 2004

PNA II-11

H-GTAGATC⁶ACT-Lys-NH₂

Accelerating voltage: 25000 V
 Grid voltage: 70%
 Mirror voltage ratio: 1.12
 Guide wire 0: 0.03%
 Extraction delay time: 140 nsec

Acquisition mass range: 2500 -- 3500 Da
 Number of laser shots: 200/spectrum
 Laser intensity: 3819
 Laser Rep Rate: 20.0 Hz
 Calibration type: Default
 Calibration matrix: 2,5-Dihydroxybenzoic acid
 Low mass gate: 2500 Da
 Timed ion selector: Off

Digitizer start time: 44.832
 Bin size: 2 nsec
 Number of data points: 4098
 Vertical scale 0: 50 mV
 Vertical offset: 0%
 Input bandwidth 0: 25 MHz

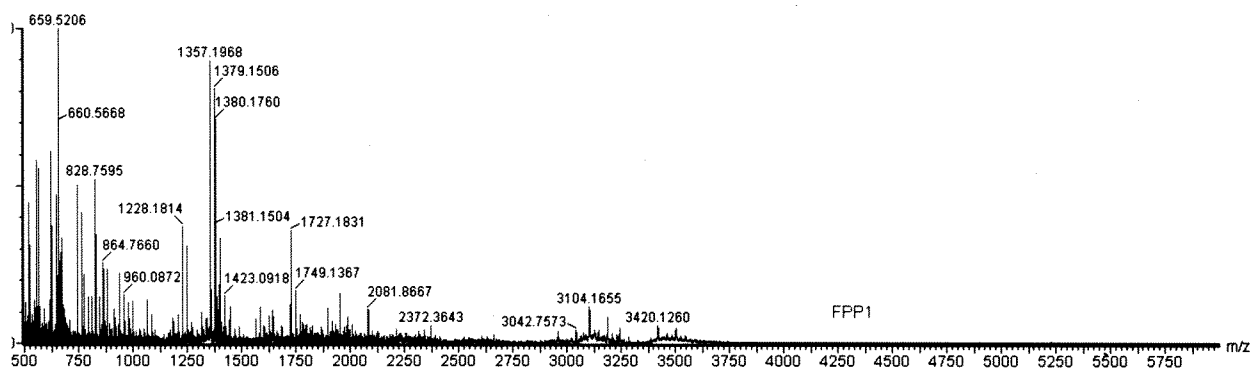
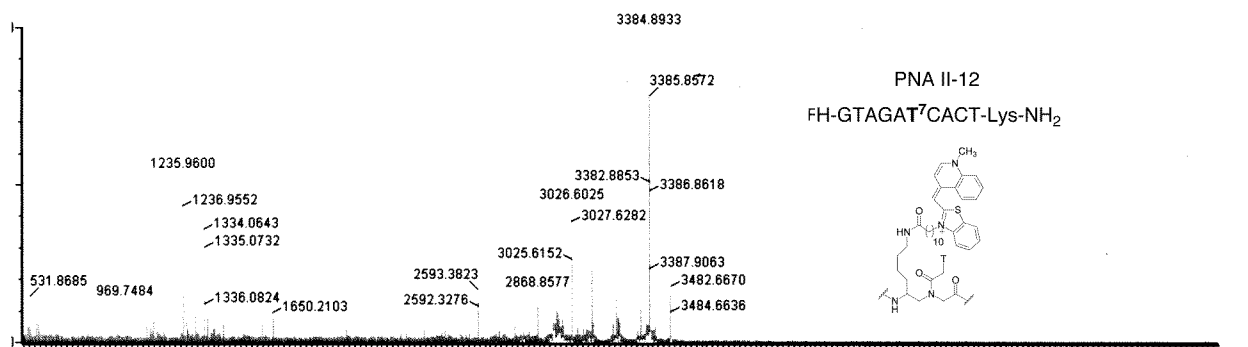
Sample well: 04
 Plate ID: 100
 Serial number: 6050
 Instrument name: Voyager-DE PRO
 Plate type filename: C:\VOYAGER\100 well plate.plt
 Lab name: PE Biosystems

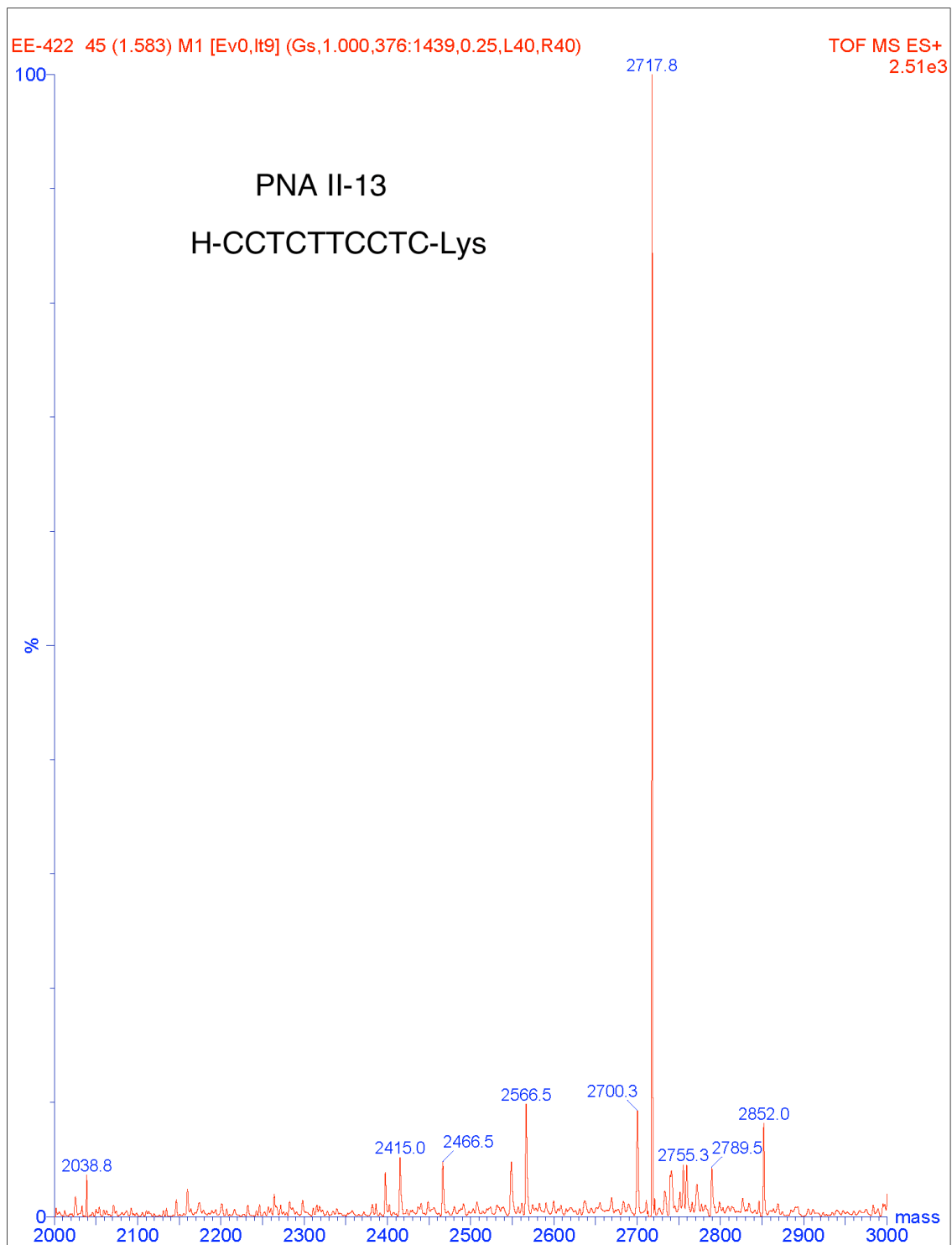
Absolute x-position: 16826.7
 Absolute y-position: 47306.3
 Relative x-position: -0.814063
 Relative y-position: -1.19329
 Shots in spectrum: 200
 Source pressure: 1.148e-006
 Mirror pressure: 1.565e-007
 TCZ pressure: 0.01485
 TIS gate width: 30
 TIS flight length: 678

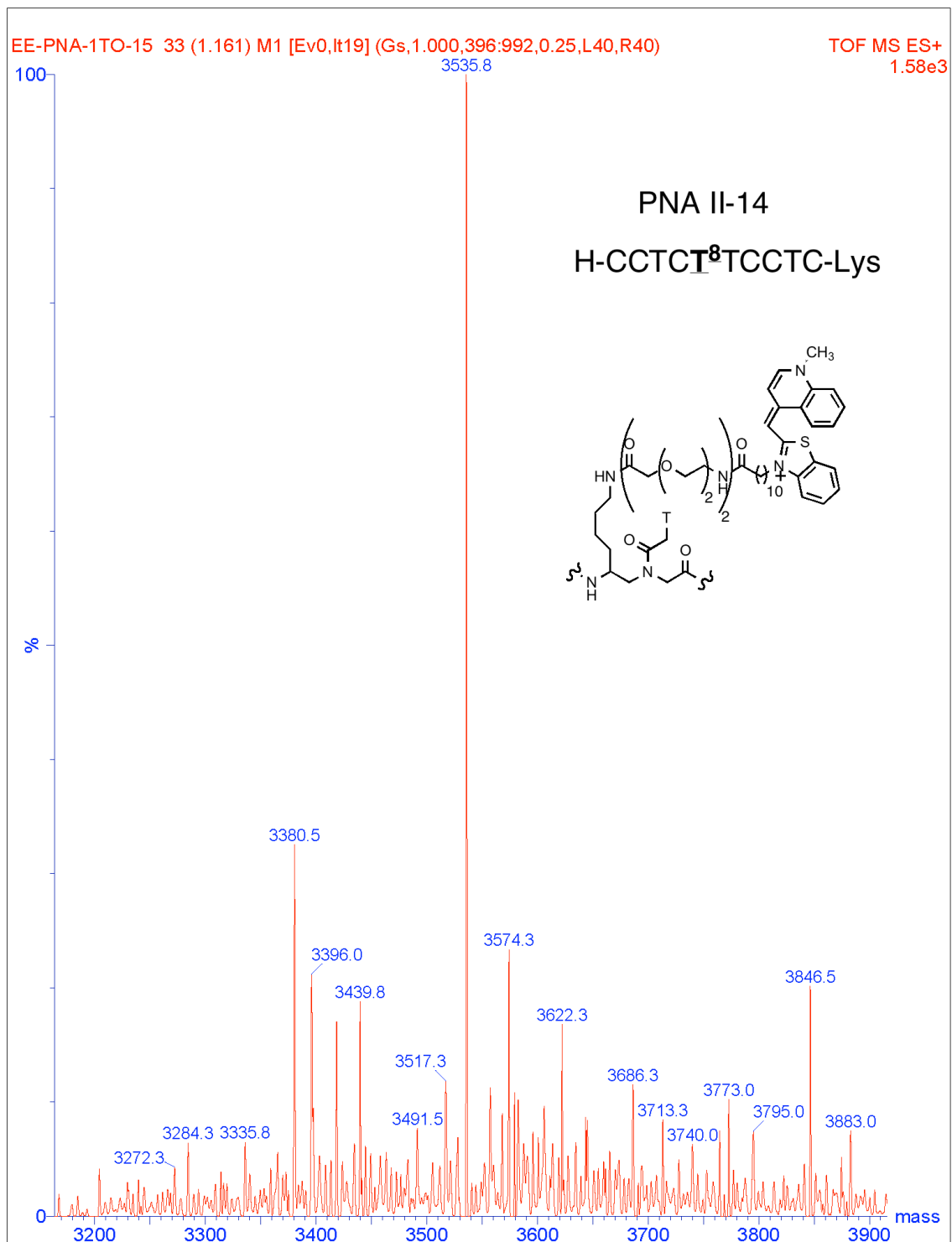
5:00, November 11, 2004

Printed: 22:47, November 11, 2004

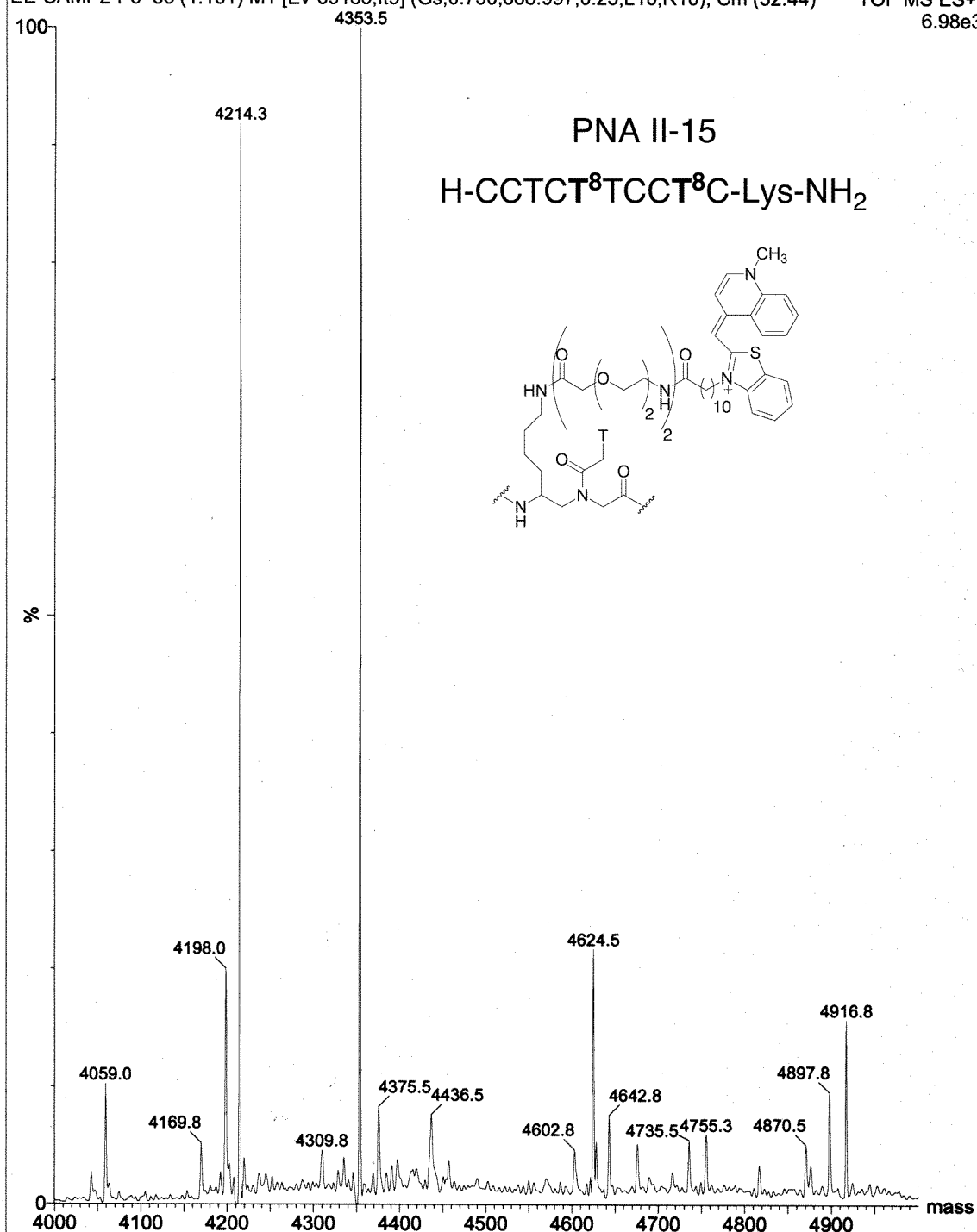
edrive\appella\Ethan\CLysOligomerMPFL_0001.dat

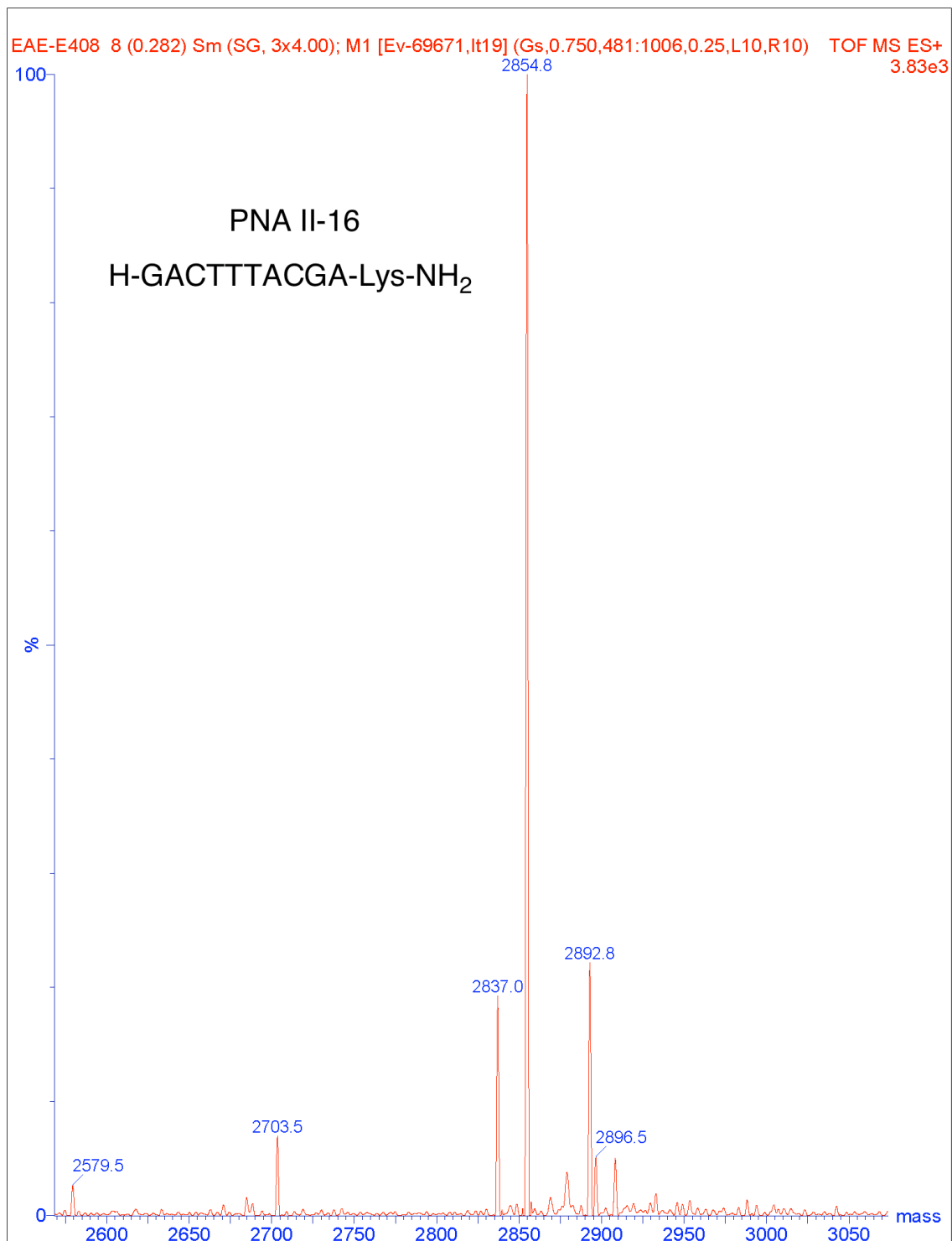
BBA077
ep-2007Laser = 220
Pulse Voltage = 2020
Detector = 2350

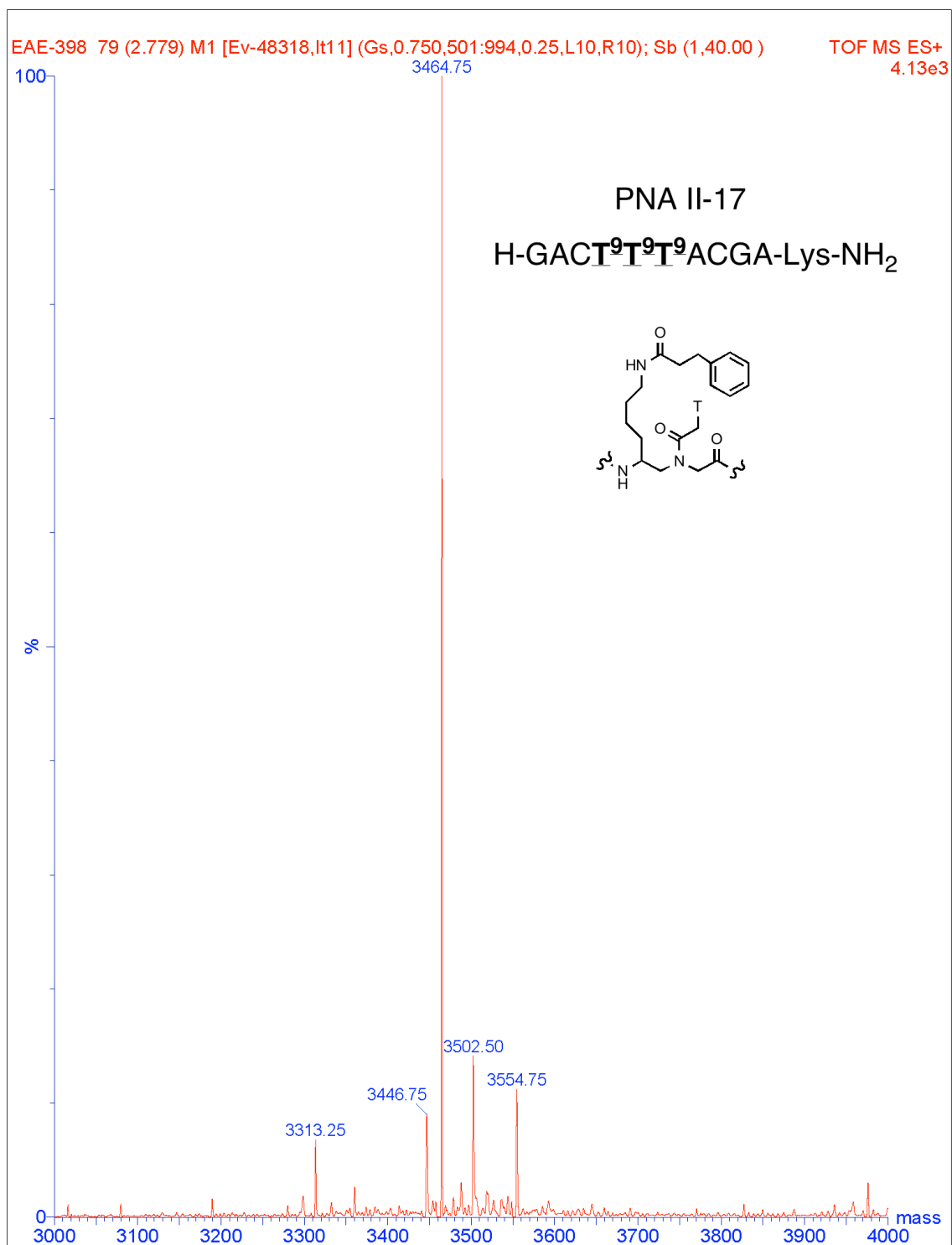




EE-SAMP2-P3 33 (1.161) M1 [Ev-69185.lt9] (Gs,0.750,668:997,0.25,L10,R10); Cm (32:44) TOF MS ES+ 6.98e3







Chapter III

Control of PNA Non-Duplex Secondary Structure Through Preorganization

Portions of this work appear in the following manuscripts:

Englund, E. A.; Xu, Q.; Witschi, M. A.; Appella, D. H., "PNA-DNA duplexes, triplexes, and quadruplexes are stabilized with *trans*-cyclopentane units." *J. Am. Chem. Soc.* **2006**, *128*, 16456-16457.

III.1 Introduction: Initial Experimental Design

With the success of PNA in targeting single stranded nucleic acids through Watson-Crick binding,¹ researchers started applying PNA to other applications based on non-standard modes of hydrogen bonding. In this chapter I describe our group's on going efforts to maximize the potential of these developing PNA applications by focusing on entropy-reducing contributions, such as tethering and rigidification. The research also details the expanded utility of the (*S,S*)-*tcyp*PNA residues, developed in this lab.²

III.2 *tcyp*PNA Influence on the Formation and Stability of Bis-PNA Triplexes

III.2.1 Bis-PNA Constructed from *aeg*PNA: Design, Synthesis and Application

Because of its favorable kinetics of binding³ and its impressive ability to invade and tightly bind duplex DNA,⁴ tethered triplex-forming PNA (bis-PNA) is of interest in the context of anti-gene applications that function by sterically blocking transcription.⁵ Our initial goals were to enhance the properties of Bis-PNA for functionalizing plasmid DNA in a highly selective, non-covalent manner (Figure III-1).

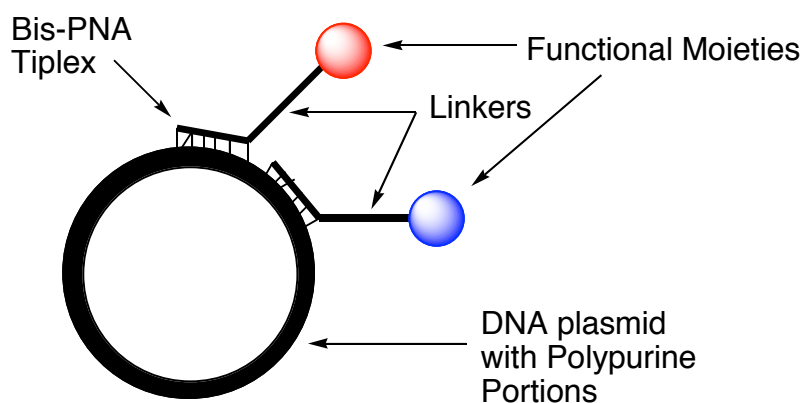


Figure III-1: Plasmid DNA Functionalized with Conjugated Bis-PNA Anchors

Many groups have used Bis-PNA as a means of appending complex functionality to plasmid DNA.⁶ This technique has been used for diagnostic purposes by labeling plasmids containing therapeutic genes. The injection of fluorophore-labeled plasmid DNA into cells is becoming an important means of probing cellular function.⁷ Fluorophore-conjugated bis-PNA has been favored over other means because it is non-invasive, i.e., it binds non-covalently to specific regions of the plasmid and does not alter the plasmid chemical composition.⁸

For our design of *aeg*Bis-PNA oligomers, Dr. Mark Witschi had previously worked out the synthesis for iso-butyl protected, N7-guanine *aeg*PNA monomers (Figure III-2). He further showed that oligomers containing N7-guanine PNA could no longer bind in Watson-Crick fashion. Although not as efficient as cytosine at low pH or pseudo-isocytosine at Hoogsteen hydrogen bonding, N7-guanine has been effectively employed in Bis-PNAs.⁹ I synthesized an *aeg*Bis-PNA by manual solid phase synthesis (as described in Chapter II.9.2a) that had thymine and cytosine in the “anti-parallel” (Watson-Crick) binding portion and thymine and N7-guanine in the “parallel” (Hoogsteen) strand. A Boc-protected form of 8-amino-2,6-dioxooctanoic acid (Boc-miniPEG) was used as a linker to connect the distinct PNA stands (three units) and extend

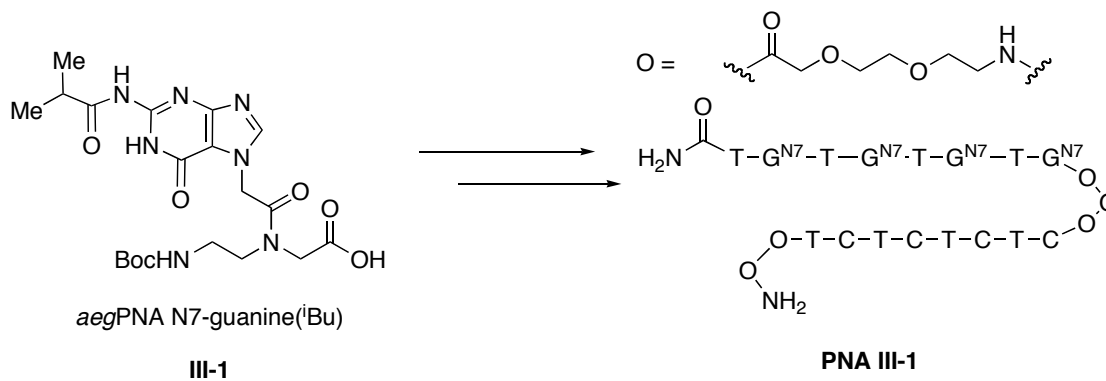


Figure III-2: *aeg*PNA N7-Guanine(^tBu) and Incorporation into an Bis-PNA

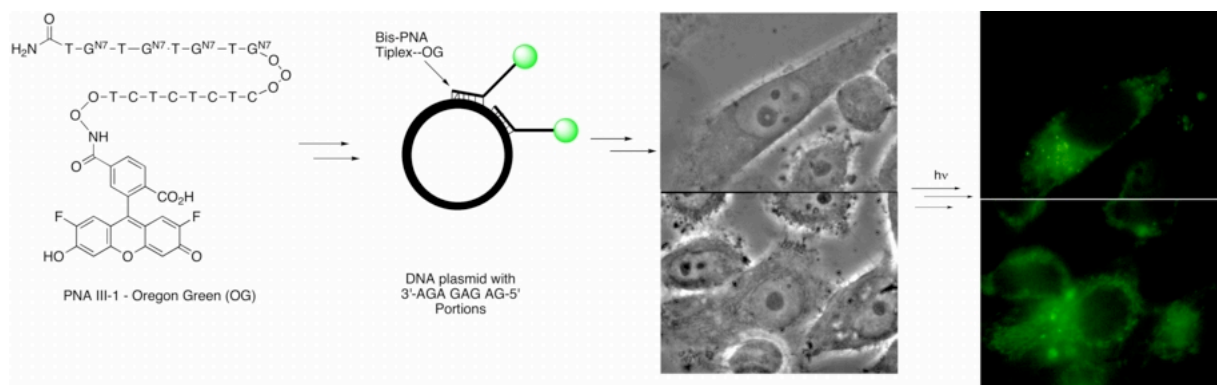


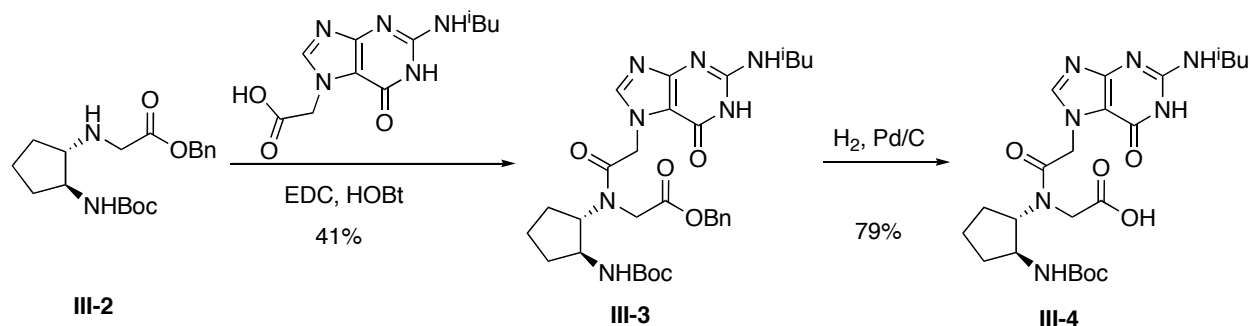
Figure III-3: PNA III-1/Oregon Green Conjugate Used in Cell Studies

from the N-terminus (two units). This Bis-PNA (*PNA III-1*) was then appended to Oregon Green (a commercially available fluorophore).¹⁰ Dr. Sui Huang and coworkers incubated the *PNA III-1* with a specially engineered pBR322 plasmid, and injected the complex into the cytoplasm of HeLa cells. After 20 minutes, the cells were fixed, and phase and fluorescent images were obtained, showing the fluorophore was attached (Figure III-3).

III.2.2 Bis-PNA Constructed from *tcyp*PNA Synthesis

III.2.2a Synthesis of *tcyp*PNA Monomers

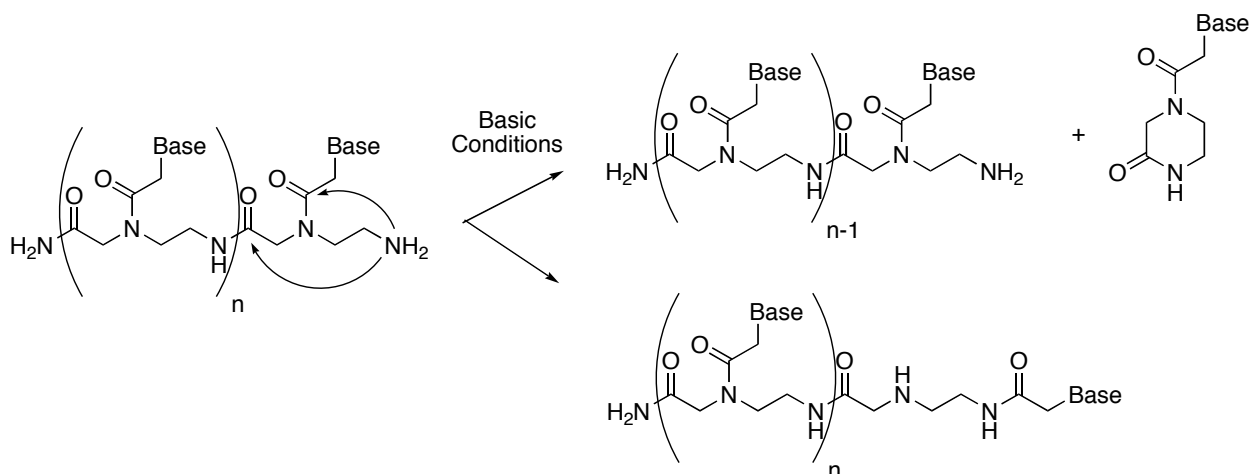
As with the *aeg*PNA monomers, Dr. Witschi worked out the synthesis of *tcyp*PNA guanine and *tcyp*PNA N7-guanine monomers employing the iso-butyl (ⁱBu) moiety as a protecting group on the exocyclic nitrogen of guanine. This protecting group strategy requires an additional deprotection step and also requires the acylation of the N-terminus to avoid elimination-shortened side products. Regardless, this strategy avoids the expensive and time-consuming synthesis of Cbz-protected guanine acetic acid starting from 6-amino-2-chloropurine.¹¹ Due to factors that remain uncertain, the process was not always reproducible and we were forced to make some adjustments to the synthetic route (Scheme III-1).

Scheme III-1: Coupling of ⁱBu-Protected N7-Guanine Acetic Acid on *tcyp*PNA Backbone

The iso-butyryl N7-guanine acetic acid was synthesized by Dr. Qun Xu of our lab from previously reported methods (III.6 Experimental).^{12,13} Dr. Xu also provided the *tcyp*PNA backbone **III-2**, synthesized by the *trans*-cyclopentane diamine chiral resolution recently developed in our lab.¹⁴ The *tcyp*PNA backbone was coupled to the N7 guanine acetic acid using EDC and HOBT in 41% yield. The resulting monomer ester (**III-2**) was hydrogenated under 50 psig in the presence of Pd on carbon to afford *tcyp*PNA N7-guanine(ⁱBu) monomer (**III-3**).

III.2.2b Synthesis of *tcyp*PNA Oligomers

Bis-PNAs were synthesized on solid support using automated PNA synthesis. After the final residue is deprotected with TFA/*m*-cresol, the N-terminus is normally acylated to prevent

**Figure III-4:** Acyl-Transfer Reactions Common in PNA Under Basic Conditions

keto-azapipine elimination or acyl migration during isobutyryl deprotection (Figure III-4).¹⁵ For the aforementioned applications, however, the N-terminus must be free to be conjugated in solution. After cleavage from the resin, the isolated solid was dissolved in methylamine solution and left overnight at room temperature to remove the isobutyryl protecting groups. The PNA oligomers deprotected in this manner, with free N-termini, showed only slightly diminished yields or byproducts as a result of not acylating the N-terminus. Bis-PNAs were successfully synthesized with *aeg*PNA N7-guanine residues, (**III-1**) *tcyp*PNA N7-guanine residues (**III-4**) and *tcyp*PNA thymine residues (**III-5**) (Figure III-5).

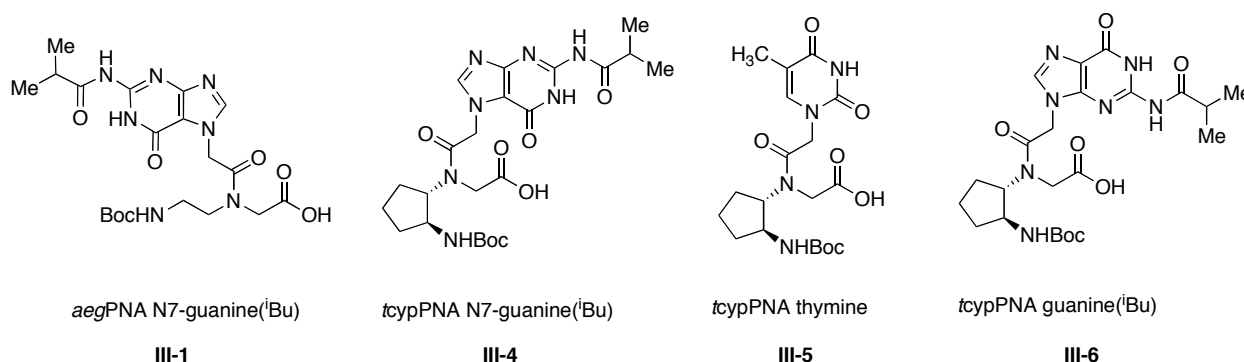


Figure III-5: Non-Standard PNA Residues Incorporated into Bis and Quadruplex PNA.

III.2.3 Melting Studies of Bis-PNA-Containing *tcyp*PNA

To confirm the binding characteristics of *aeg*PNA N7-guanine in the Hoogsteen strand, a Bis-PNA constructed of only cytosine and thymine was synthesized for comparison. The triplex thermal stability of the N7-guanine *PNA III-1* (Table III-1) was similar to the cytosine-thymine derivative (*PNA III-2*) at pH 7, which is consistent with previous studies.^{16,9} As expected, *PNA III-2* was much more susceptible to pH effects than *PNA III-1*. A bis-PNA was constructed that contained *tcyp*PNA thymine residues in both the Watson-Crick and Hoogsteen binding strands (*PNA III-3*). The binding of *PNA III-3* to the complementary DNA demonstrates that the *tcyp*

Table III-1: T_m Analysis of Bis-PNA₂:DNA Triplexes.

PNA	Sequence	T_m (°C) DNA ^a
III-1	H-(egl) ₃ -TCTCTCTC-(egl) ₃ -G ^{N7} TG ^{N7} TG ^{N7} TG ^{N7} T-NH ₂	53.1
III-2	H-(egl) ₃ -TCTCTCTC-(egl) ₃ -CTCTCTCT-NH ₂	54.3
III-3	H-(egl) ₃ -TCTCTCTC-(egl) ₃ -G ^{N7} TG ^{N7} TG^{N7} TG ^{N7} T-NH ₂	58.5
III-4	H-(egl) ₃ -TCTCTCTC-(egl) ₃ - G^{N7}TG^{N7}TG^{N7}TG^{N7} T-NH ₂	57.0

^a cypPNA is denoted by bold/underlined letters; (egl) represent the 8-amino-3,6 dioxaoctonic acid. ^bThermal denaturation studies were undertaken with complementary DNA (3'-GAG AGA GA-5'). Data were collected from heating profiles from 20 °C to 90 °C at a rate of 1 °C/min.

residues continue to increase the binding affinity when in both strands of a triplex. Incorporating four N7-guanine *tcyp*PNA residues into the Hoogsteen-binding (parallel) segment in **PNA III-4** also increased the thermal stability of a BisPNA₂:DNA triplex. Although the increase in stability per *tcyp*PNA residue is modest compared to its duplex counterparts (~ 1.0 °C), this disparity is not surprising because Hoogsteen strand binding affinity is usually lower than Watson-Crick hydrogen bonding at pH 7. As many PNA modifications have been shown to bias parallel versus anti-parallel binding preference, this factor should be investigated in future studies, as it is not

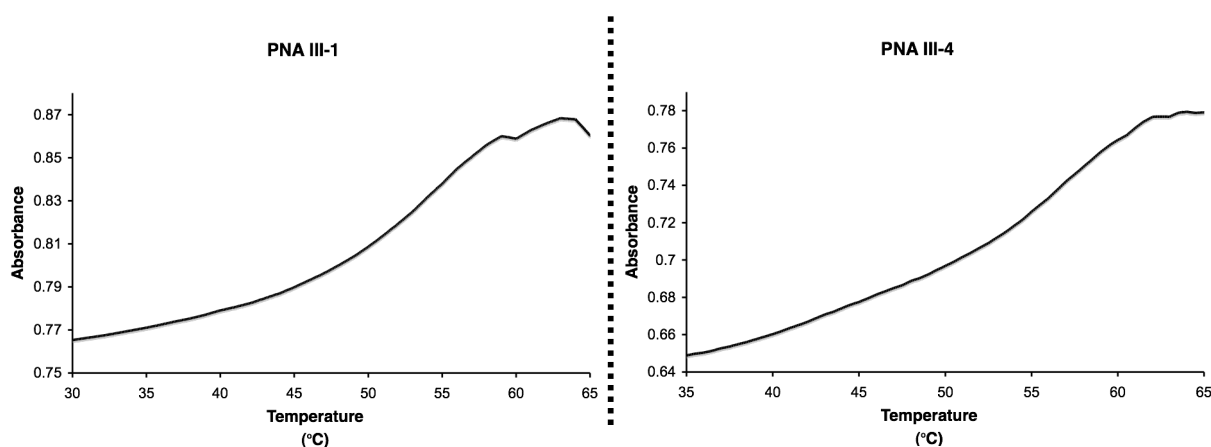


Figure III-6: Melting Curves of PNA III-1 and PNA III-4. Samples annealed with complementary DNA.

well understood in *tcyp*PNA. These results indicate that *tcyp* groups stabilize both W-C and Hoogsteen-binding modes of PNA to DNA in triplex-forming complexes and should be fully compatible with associated applications. The melting curves for these bis-PNA were characteristic of most PNA₂:DNA melting curves (Figure III-6); whether melting or annealing, the binding curves were very broad and showed some evidence of multiple transitions.

III.3 G₄ PNA Constructed from (*S,S*)-*tcyp*PNA

To examine the effect that (*S,S*)-*tcyp*PNA has on the stability of PNA-based guanine tetrads, ¹Bu-protected guanine *tcyp*PNA monomers were incorporated at various positions in a guanine-rich *aeg*PNA oligomer consisting of 12 residues. PNA oligomers containing guanine *tcyp*PNA monomers (**III-6**) were successfully synthesized by both manual and automated peptide synthesis. Oligomers with multiple *tcyp*PNA residues adjacent to each other were also synthesized, an arrangement that has caused synthetic difficulties in the past. In this case, however, the oligomer synthesis, including the ¹Bu deprotection, purification and identification, proceeded without complication.

III.3.1 (*S,S*)-*tcyp*PNA Effect on the G₄ Quadruplex: Melting Studies

Guanine rich oligonucleotides usually have multiple secondary structures accessible because of guanine tetrad formation. Therefore, when targeting guanine rich sequences for quadruplex formation, it is important to consider any stable structures the PNA forms with itself, either inter- or intramolecularly. Therefore, our examination of *tcyp*PNA effects on quadruplex formation focused on a well characterized guanine-rich sequence. The G₄ sequence of DNA (3'-GGG GTT TTG GGG-5') is a naturally occurring telomere sequence that is known to form guanine tetrads in the presence of sodium or potassium ions.¹⁷ The NMR solution structure¹⁸ and

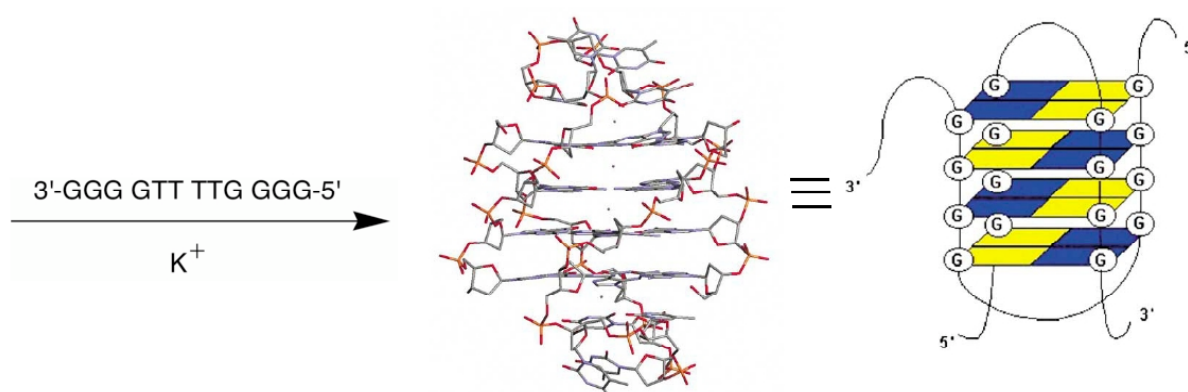


Figure III-7: Quadruplex formation of G₄ DNA.¹⁹

crystallographic data (Figure III-7)¹⁹ show that G₄ DNA forms a dimeric hairpin “basket” conformation. The *aeg*PNA G₄ sequence (H-GGGGTTTTGGGG-NH₂) interacts with itself to form tetrads composed of two PNAs (a homodimer), although the exact configuration is unknown.²⁰ However, in the presence of G₄ DNA, a more stable PNA/DNA 2:2 quadruplex structure (a heterotetramer) is readily formed.²¹

III.3.1a (*S,S*)-*tcyp*PNA G₄ Quadruplex Stability: PNA Homodimers

The melting temperatures (T_m) of quadruplexes can be determined from reverse sigmoidal curves at 295 nm.²² This transition is not present in duplex melting or annealing curves. The G₄ *aeg*PNA (**PNA III-5**, Ac-GGGGTTTTGGGG-NH₂) exhibited a melting temperature of 48.4 °C when in standard phosphate buffered solution (Table III-2). This melting temperature agreed with previous studies despite the acetylated N-terminus.²⁰ When a single **III-4** residue was inserted into the G₄ sequence (**PNA III-6**), the T_m increased by several degrees. This effect was amplified when multiple residues of **III-4** were incorporated into the G₄ sequence, as in PNA III-7.

Table III-2: T_m Analysis of G₄ PNA: PNA Quadruplexes.

PNA	Sequence ^a	T_m (°C) ^b	ΔT_m (°C) ^c
III-5	Ac-GGGG-TTTT-GGGG-Lys-NH ₂	48.4	---
III-6	Ac-GGGG-TTTT-GGGG-Lys-NH ₂	51.9	3.5
III-7	Ac-GGGG-TTTT-GGGG-Lys-NH ₂	61.0	12.6
III-8	Ac-GGGG-TTTT-GGGG-Lys-NH ₂	41.0	-7.4

^a cypPNA is denoted by bold/underlined letters ^b Thermal denaturation studies were collected from cooling runs from 90 °C to 15 °C at a rate of 1 °C/min. ^c This denotes the change in melting temperature due to the inclusion of *tcyp*PNA residues compared to *aeg*PNA.

When four residues of **III-4** were inserted adjacent to each other, the melting curves were less clear than any of the other G₄ sequences. From these annealing curves, however, we could extract a T_m of only 41.0 °C. This shows that the **PNA III-8** dimer is less thermally stable than the *aeg*PNA and other **III-4** containing PNA oligomers. This outcome is in contrast to the behavior of *tcyp*PNA when binding DNA in duplex fashion. When Dr. Pokorski of our lab synthesized mixed sequence PNA oligomers using multiple *tcyp*PNA residues, the proximity of one *tcyp*PNA residue to another did not influence the melting temperature to the complementary anti-parallel DNA.²³ It is unclear what is causing the destabilization of the PNA quadruplex structure formed by **PNA III-8**.

III.3.1b (*S,S*)-*tcyp*PNA G₄ Quadruplex Stability: PNA/DNA Heterotetramers

When annealed in the presence of G₄ DNA and NaCl (150 mM), **PNA III-5** exhibited a T_m near 63 °C, which is in close agreement with the literature (Table III-3).²¹ Further renaturation experiments for **PNA III-6** and **PNA III-7** with G₄ DNA showed the same magnitude of increase in stability for the 2:2 heterotetramers as they had for the homodimers.

Table III-3: T_m Analysis of G₄ PNA/ G₄ DNA: Hybrid Quadruplexes

PNA	Sequence ^a	T_m (°C) ^b	ΔT_m (°C) ^c
III-5	Ac-GGGG-TTTT-GGGG-Lys-NH ₂	62.7	---
III-6	Ac-GGGG-TTTT-GGGG-Lys-NH ₂	67.0	4.3
III-7	Ac- <u>GGGG</u> -TTTT- <u>GGGG</u> -Lys-NH ₂	72.9	10.2
III-8	Ac- <u>GGGG</u> -TTTT-GGGG-Lys-NH ₂	81.6	18.9

^a cypPNA is denoted by bold/underlined letters ^b Thermal denaturation studies were carried out with the G₄ sequence of DNA in a 1:1 ratio with the G₄ PNA sequence. The data were collected from cooling runs from 90 °C to 15 °C at a rate of 1 °C/min. ^c This denotes the change in melting temperature due to the inclusion of *tcyp*PNA residues compared to *aeg*PNA.

Whereas **PNA III-8**, with its four adjacent **III-4** residues, destabilized the PNA homodimers to a large extent, the resulting 2:2 heterotetramer was greatly stabilized. The degree of stabilization was notably larger than what was observed in **PNA III-7**, despite the same number of **III-4** residues. Once again, this is inconsistent with the observations of *tcyp*PNA effects on PNA:DNA duplexes. Besides the unusually high affinity for G₄ DNA, the difference in structure stability presents newfound opportunities. Many factors must be investigated if G-rich PNAs are to be useful in biological systems. When considering the possibility of forming complexes with a G-rich target DNA or RNA, the stability of any PNA-homoquadruplexes must be energetically overcome to ensure effective binding. This is one aspect where using **III-4** residues in succession could address (Table III-4).

Quadruplex formation is often a kinetically slow process, so T_m data collected from annealing experiments can be prone to systematic error if the rate of heating or cooling outpaces thermodynamic equilibrium. Comparing heating and annealing UV profiles of each sample and noting the degree of hysteresis is a useful means of confirming our T_m data, since dissociation is

Table III-4: Comparison of Melting Characteristics between Homodimers and Heterotetramers.

PNA	Sequence ^a	$\Delta\Delta T_m$ (°C) ^b	$\Delta\Delta\Delta T_m$ (°C) ^c
III-5	Ac-GGGG-TTTT-GGGG-Lys-NH ₂	14.3	---
III-6	Ac-GGGG-TTTT-GGGG-Lys-NH ₂	15.1	0.8
III-7	Ac- <u>GGGG</u> -TTTT- <u>GGGG</u> -Lys-NH ₂	11.9	-2.4
III-8	Ac- <u>GGGG</u> -TTTT-GGGG-Lys-NH ₂	40.6	26.3

^a *cyp*PNA is denoted by bold/underlined letters ^b This denotes the difference in the stabilities of PNA:DNA heterotetraplexes and PNA homoduplexes. In all cases, the heterotetraplex was more stable. ^c This denotes the difference between the PNA:DNA preferential formation between PNA containing *tcyo*PNA and *aeg*PNA (PNA III-5).

usually faster than association for complexes containing multiple oligomers.²⁴ Annealing experiments on G₄ PNA in the presence G₄ DNA, followed by denaturing experiments, exhibited very little hysteresis (~ 1 °C) implying relatively fast tetrad formation (Figure III-8).

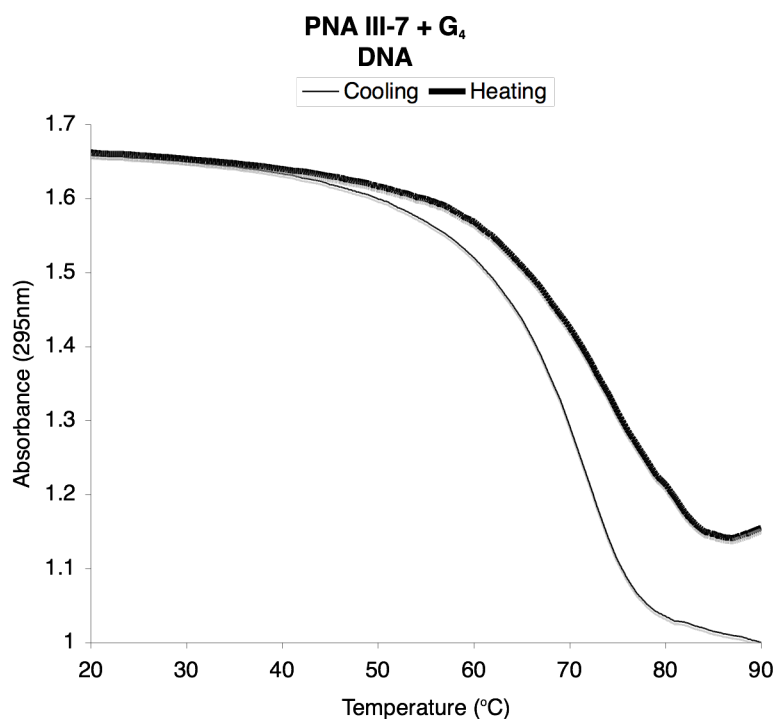


Figure III-8: PNA III-7/G₄ DNA Tetraplex Hysteresis. The average difference between annealing and denaturing profiles differed by less than 1 °C.

III.3.2 (*S,S*)-*tcyp*PNA Effect on the G₄ Quadruplex: Circular Dichroism

Recently, G₄ PNA and G₄ DNA circular dichroism (CD) studies have been used to investigate the structure and binding characteristics of quadruplexes.²⁵ Furthermore, the unique spectra of G₄ PNA:DNA heterotetramer makes it an ideal diagnostic to analyze the effect that *tcyp*PNA has on the structure, stoichiometry and preorganization of G₄ PNA.

III.3.2a (*S,S*)-*tcyp*PNA G₄ Circular Dichroism: Heterotetramers

The distinct CD spectrum of the G₄ *aeg*PNA:DNA 2:2 complex, with local maxima at ~260 nm and ~295 nm and a minima at ~240 nm, agreed with literature values for the PNA:DNA heterotetramer, despite having the N-termini of the PNA oligomer acetylated.²¹ The CD of quadruplex forming DNA varies considerably, and is dependant on the type of secondary structure formed, as demonstrated by the G₄ DNA homodimer (Figure III-9).²⁵

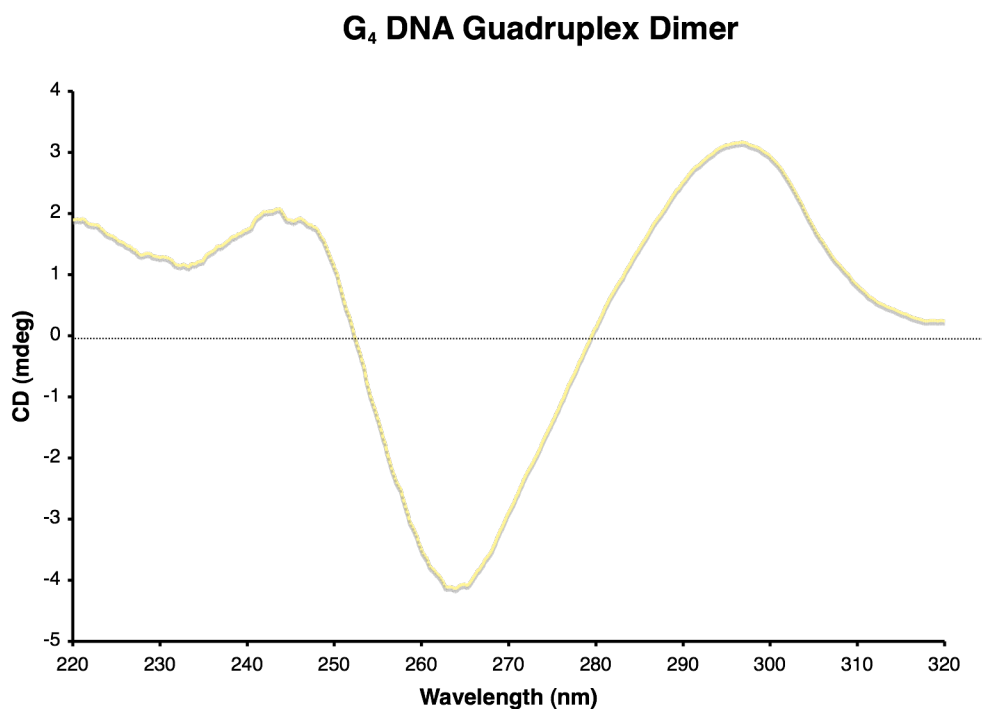


Figure III-9: CD Spectrum of G₄ DNA Homodimer.

Surprisingly, the spectra of *PNA III-7* and *PNA III-8* were both remarkably similar to *PNA III-5*, despite the differences in binding stability between all three (Figure III-10). From this result, one can infer the complex formed from by the sequences including *tcypPNA* are identical (or very similar) to those formed by *aegPNA*. Like the *aegPNA*, the CD spectrum of *PNA III-7* with G₄ showed evidence of tetraplex formation without annealing.

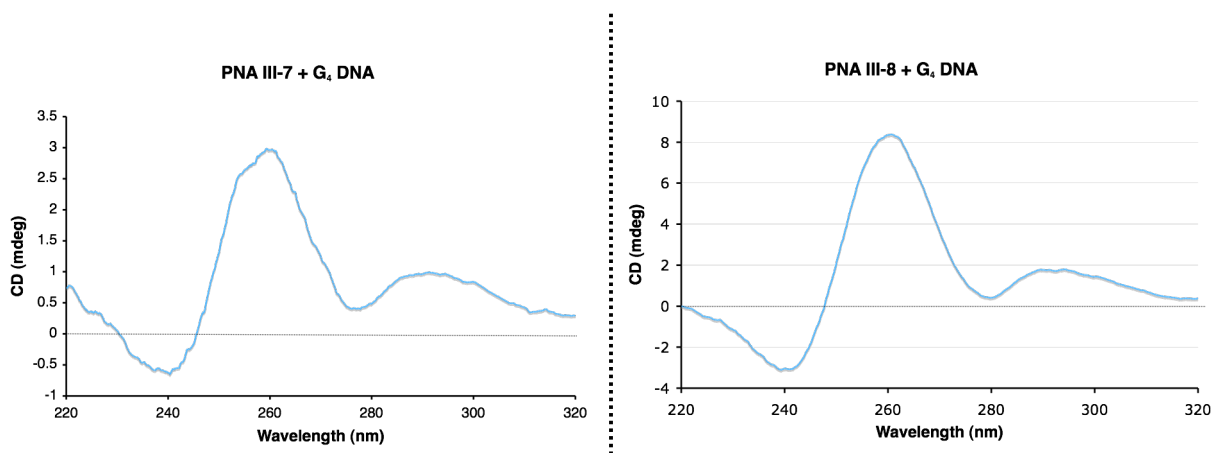


Figure III-10: CD Spectra of *PNA III-7* and *PNA III-8* with G₄ DNA

III.3.2b (*S,S*)-*tcypPNA* G₄ Circular Dichroism: Homodimers

Because *aegPNA* oligomers are devoid of stereogenic centers, quadruplexes formed from *aegPNA* exhibit weak CD signals. This is either because there is no helical formation in the quadruplex structures or a racemic mixture of right and left handed helices. By attaching chiral amino acids to the termini of *aegPNA* oligomers, PNA duplexes can have helical handedness induced.²² Chiral conjugates have not shown any evidence of this effect in G₄ PNA quadruplexes, although guanine-rich PNA tetramers exhibit a CD spectrum similar to an anti-parallel DNA G-quadruplex.²³ It is then noteworthy that both *PNA III-7* and *PNA III-8*, with four *III-4* residues in each, give distinct CD spectra (Figure III-11).

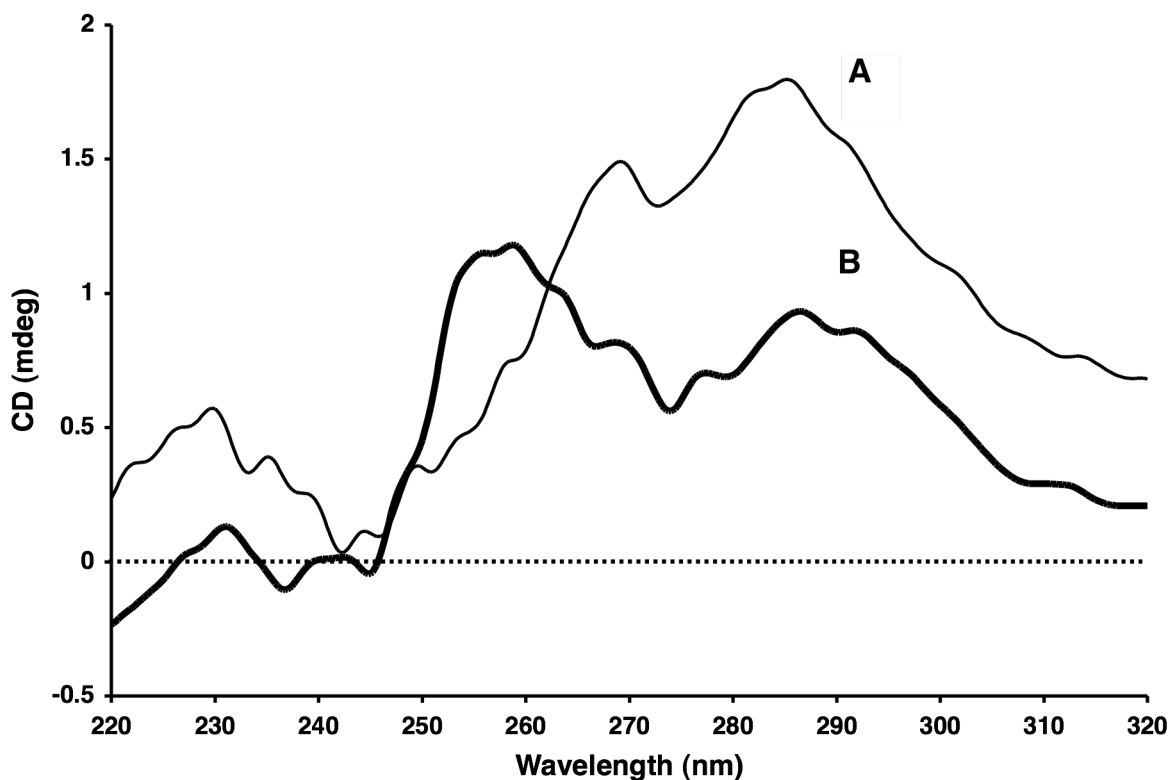


Figure III-11: CD Spectra of *PNA III-7* and *PNA III-8* Annealed Without DNA. A) denotes the spectra of *PNA III-7*. B) denotes the spectra of *PNA III-8*.

Although recent studies show evidence that G₄ PNA preferentially forms dimeric quadruplexes, the CD spectrum of *PNA III-8* has a maximum at 260 nm and a local minimum around 240 nm, which is usually the hallmark of parallel quadruplexes.²⁸ To establish that the CD spectra observed were due to quadruplex formation and not any preformation inherent in *tcypPNA* oligomers, a sample of *PNA III-7* was annealed without the quadruplex-stabilizing presence of NaCl (Figure III-12). The differences in these CD spectra imply that *tcypPNA* not only displays base stacking (preorganization) when uncomplexed, but also gives a distinct quadruplex CD signal when annealed with NaCl.

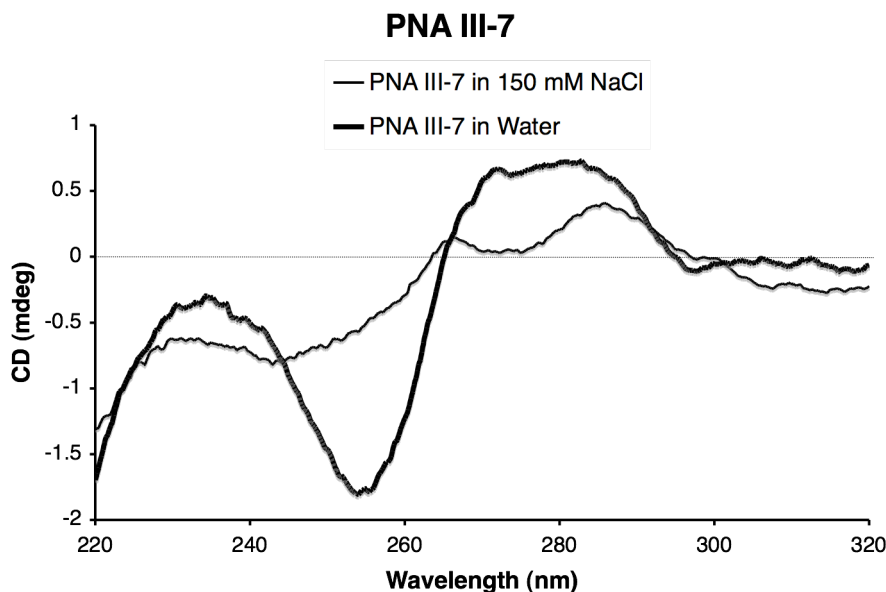


Figure III-12: CD Spectrum of PNA III-7 Annealed With and Without NaCl. PNA III-7 shows signs of helicity without evident quadruplex formation.

III.3.2c (*S,S*)-*tcyp*PNA G₄ Circular Dichroism: Stoichiometry

The stoichiometry and structure of PNA:DNA quadruplexs are important when considering biological applications. An isolated tract of G-rich DNA would need three PNA strands to form a guanine tetrad; this 3:1 ratio of PNA to DNA has not been reported. Dr. Witschi of our laboratory carried out a number of melting experiments where he altered the ratio of PNA:DNA to 3:1 and observed some unexpected phenomena such as annealing profiles without multiple transitions, an anomaly often seen in the UV annealing profiles of guanine quadruplexes. A series of continuous variation experiments (Job's Method) were conducted to establish the likely stoichiometry of *PNA III-7* and *PNA III-8* (Figure III-13). Because of the difference between the CD spectrum of G₄ DNA homodimers and PNA:DNA heterotetramers, the maximum at 260 nm in the PNA:DNA complex was used as the wavelength to determine the binding stoichiometry. Job Plots indicated in both cases that the ideal stoichiometry was 1:1, suggesting the presence of the 2:2 heterodimers evidenced in the *aeg*PNA:DNA complex.

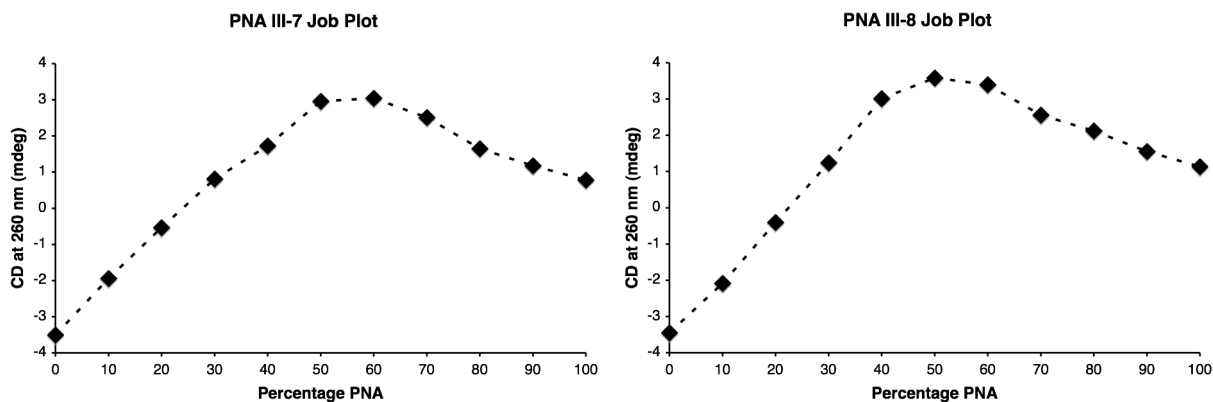


Figure III-13: Job Plots of *PNA III-7* and *PNA III-8* with G_4 DNA.

III.4 G_4 PNA Constructed from a Tethered Lysine Core

Another form of preorganization commonly employed in nucleic acid research is tethering, or covalently linking oligomers together to alter their binding characteristics.²⁹ We employed this strategy specifically to address the problem of achieving a quadruplex-forming PNA to bind to G-rich DNA in a 1:1 or 3:1 stoichiometry. We hypothesized that linking three short guanine PNA oligomers together via the C termini could bias the formation of guanine tetrads with only one G-rich DNA by reducing the binding entropy of the system (Figure III-14).

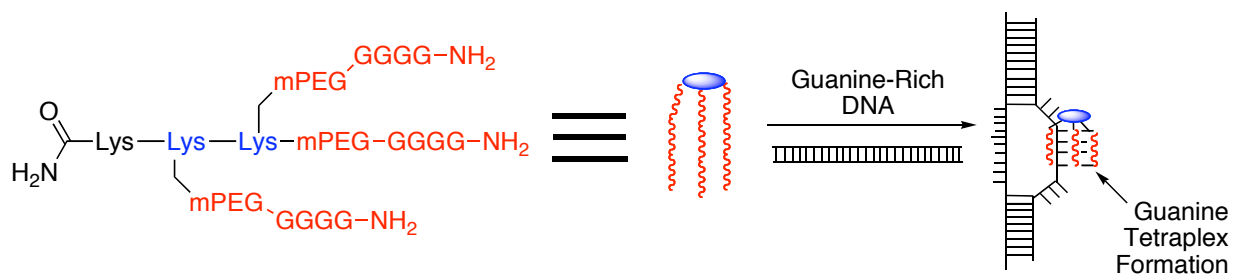


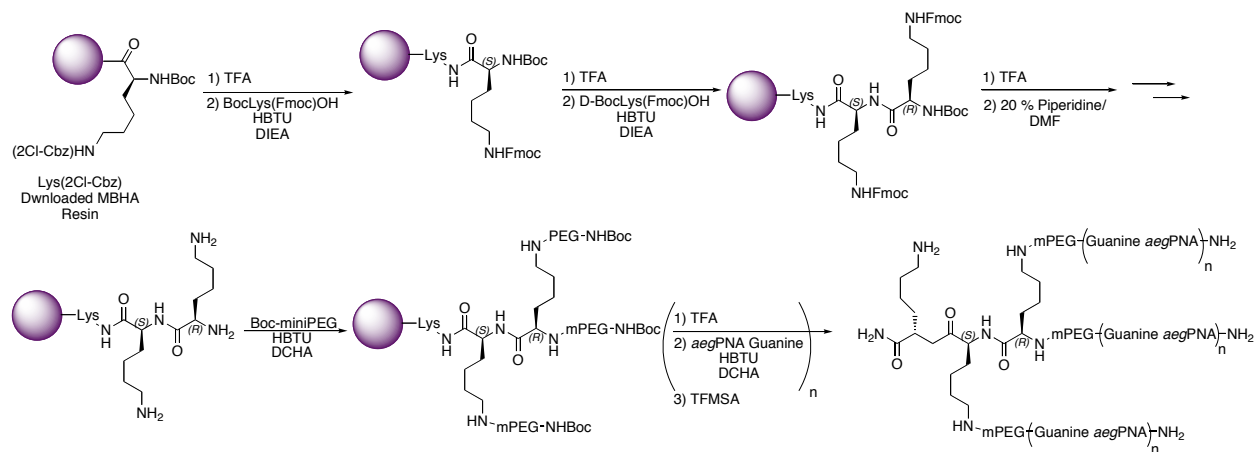
Figure III-14: Short Guanine PNAs Tethered to a Lysine Core.

III.4.1 Synthesis of Tethered Guanine *ae*gPNA

The tethered PNA strands were synthesized by means of automated solid phase synthesis (Scheme III-2). This was accomplished by first coupling BocLys(Fmoc)-OH to the downloaded

resin. Following Boc deprotection, D-BocLys(Fmoc)-OH is then coupled. This alternating-stereochemistry, dual lysine motif makes up the core of the tethered PNA. All the protecting groups from the appended lysine are then removed. The three PNA strands are then assembled in a parallel fashion from each of the three free primary amines, four guanine residues long. After the synthesis of the three PNA strands and cleavage from the resin, the PNA was precipitated from ether, purified using reverse-phase HPLC and characterized by means of electrospray mass spectroscopy to yield **PNA III-9**. Despite the “parallel synthesis” of the three PNA strands from a relatively congested core structure (therefore increasing the likelihood of inter-strand aggregation and lowered yields), the product isolation and purification did not differ from other PNAs synthesized in our laboratory.

Scheme III-2: Solid Phase Synthesis of Tethered PNA Trimer. (**PNA III-9** is $n=4$).



III.4.2 Melting Studies of Tethered Guanine aegPNA

A series of UV melting profiles were planned for the tethered guanine PNAs, using short, guanine rich DNA. When the tethered guanine PNAs were annealed in buffered solution (150 nM NaCl), UV absorbance showed a strong hyperchromicity at 295 nm, despite the absence of complementary DNA (Figure III-15). This binding event was shown to be intermolecular by the T_m dependence on concentration. Although the tethered guanine PNAs forming some type of

PNA quadruplex is worthy of further investigation, UV analysis of possible PNA:DNA complexes was rendered impossible under these conditions.

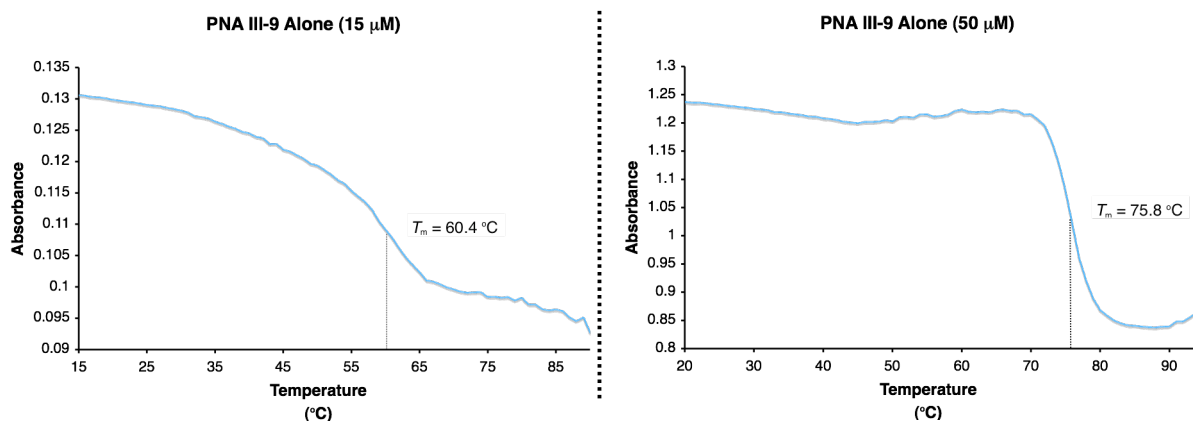


Figure III-15: Annealing Profiles of PNA III-9 at 15 and 50 μM .

III.4.3 Circular Dichroism Studies of Tethered Guanine *aeg*PNA

Like G_4 *aeg*PNA, *PNA III-9* does not exhibit a strong CD spectrum despite the chirality inherent in the lysine core. In the presence of guanine rich DNA (3'-GGG GT-5'), however, a CD spectrum similar to the PNA:DNA antiparallel spectrum was observed (Figure III-16). When a continuous variation experiment was carried out using the maximum at 260 nm as the reference point, a stoichiometry of 1:1 was observed (Figure III-17). Although this does not rule out higher ordered structures (2:2, 3:3, etc.), the simplest explanation is a 1:1 quadruplex made up of one DNA strand and the three tethered PNAs (Figure III-18). Furthermore, when G_4 DNA was annealed in the presence of *PNA III-9* (2:1 PNA:DNA ratio), the CD spectrum revealed no evidence for the presence of the G_4 DNA homodimer and only a PNA:DNA complex (Figure III-19).

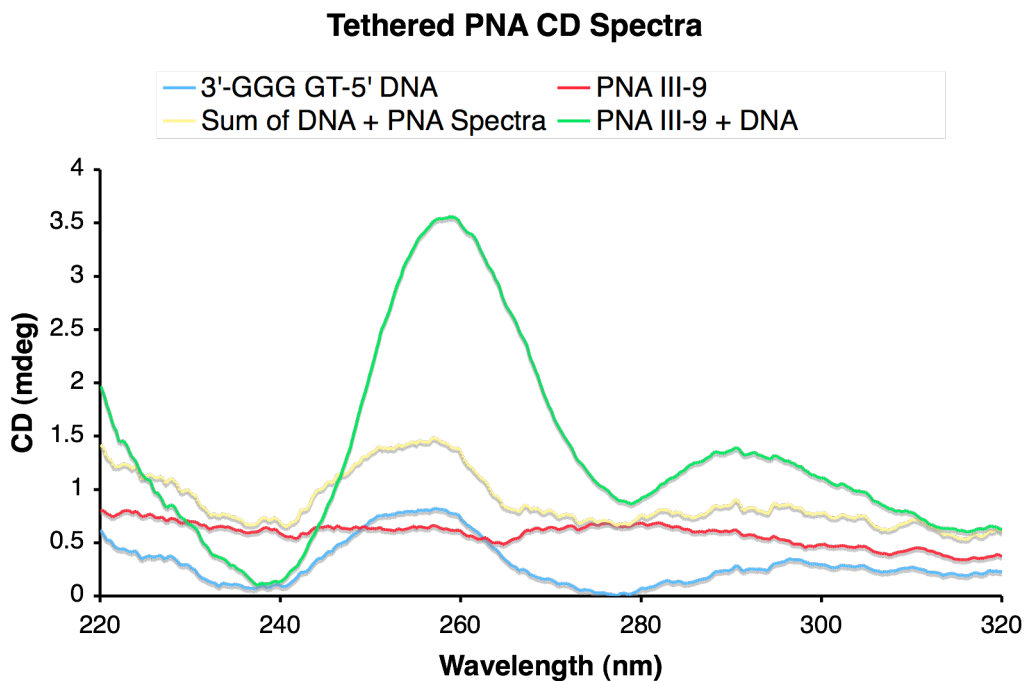


Figure III-16: CD Spectrum of *PNA III-9* with Guanine-Rich ssDNA

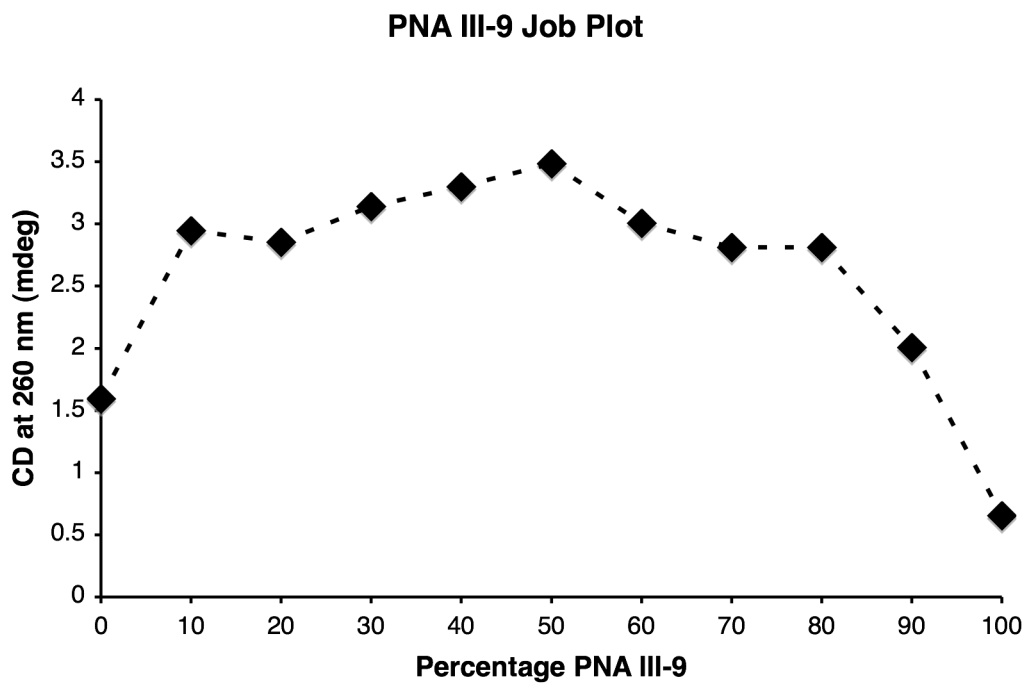


Figure III-17: Job Plot of *PNA III-9* with Guanine-Rich ssDNA

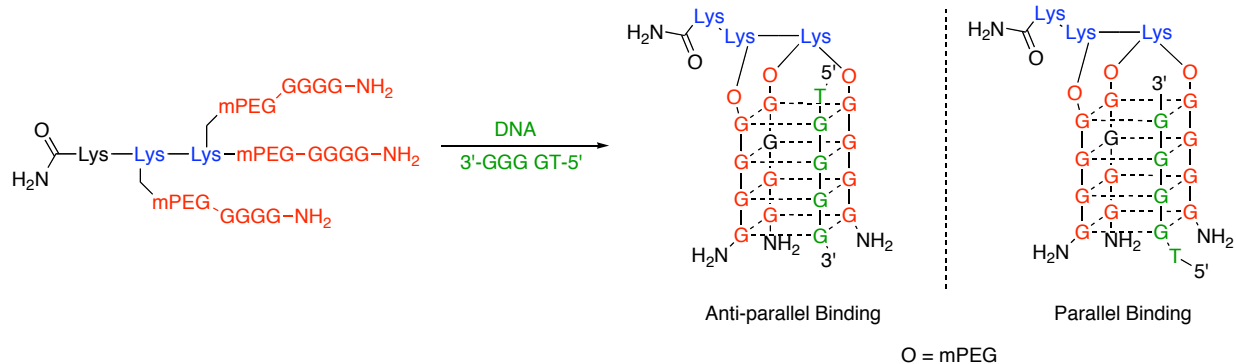


Figure III-18: Possible Modes of *PNA III-9* Binding DNA.

CD Spectra of PNA III-9 + G₄ DNA

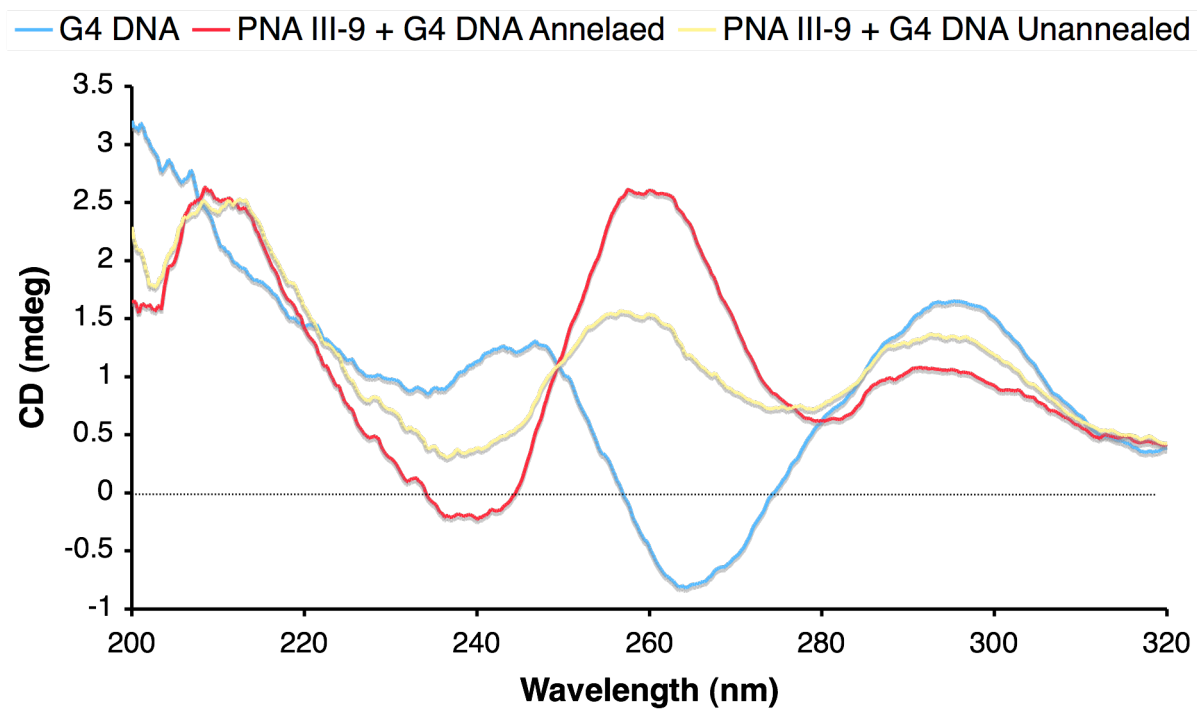


Figure III-19: CD Spectra of *PNA III-9* with G₄ DNA.

III.5 Summary and Conclusions

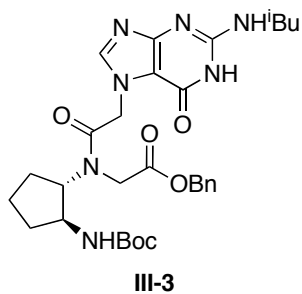
In this chapter, I have described the contribution our laboratory has made towards understanding and controlling complex, non-standard nucleic acid secondary structure. By reducing the binding entropy of the explored systems, through rigidifying and tethering, we have improved the molecular recognition properties of non-Watson Crick hydrogen bonding motifs and taken steps to control the stoichiometry of such systems. In regards to the binding characteristics of bis-triplex and guanine quadruplex forming PNA, this suggests further applications for the already useful (*S,S*)-*trans*-cyclopentane PNA developed in our lab. Furthermore, this is the first time modified PNA has been shown to have an effect on the formation of guanine tetrads. The ability to bind guanine rich DNA through tethered PNA has also not been reported. Armitage and coworkers recently reported a G-rich PNA probe that is specific to a telomere bound in a 2:1 PNA to DNA stoichiometry.³⁰ With the potential to form a general guanine-rich nucleic acid probe, we will continue to explore the binding characteristics of this molecule while further optimizing its already unusual binding characteristics.

III.6 Experimental Data and Procedures

III.6.1 Synthesis of *tcyp*PNA N7 Guanine(ⁱBu) Monomer from Benzyl Ester Backbone

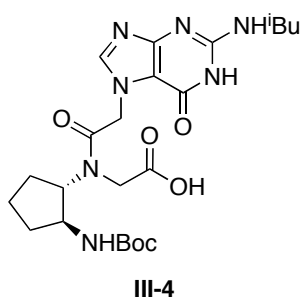
The general methods are the same enumerated in Chapter II.9.1a, page 82. Dr. Witchi originally worked out this synthesis from isobutyryl guanine benzyl ester. Although he was able to synthesize the isobutyryl guanine and N7-guanine acetic acids through this route, neither would couple to the *tcyp*PNA backbone. Dr. Xu's method for reaching isobutyryl guanine and N7-guanine acetic acids went through a *tert*-Butyl ester intermediate. This data documents the protected N7-guanine acetic acid starting from Dr. Hu's procedure. The coupling proceeded to

the products Dr. Witschi had observed, although in slightly lower yields. The ^1H NMR spectra matched Dr. Witschi's previously recorded spectra.



Benzyl *N*-[(2*S*)-*tert*-Butoxycarbonylaminocyclopent-(1,*S*)-yl]-*N*-[[2-*N*-(isobutyryl)guanin-7-yl]acetyl]glycinate (III-3**).** PNA backbone **III-2** (180 mg, 0.51 mmol), *N*²-(Isobutyryl)-7-(carboxymethyl)guanine (210 mg, 0.76 mmol), and HOBt (8 mg, 0.05 mmol) were added to an oven dry 10 mL RBF. Dry DMF (3 mL) was added and the reaction

flask was cooled to 0 °C. EDC (195 mg, 1.02 mmol) was added and the mixture was allowed to slowly warm to rt over 1 h. The reaction was stirred for 16 h. The reaction mixture was diluted with H₂O (3 mL) and extracted with EtOAc (3 x 3 mL). The organic solution was washed with sat. NaCl solution (5 mL), dried over Na₂SO₄, concentrated under reduced pressure, and dried under vacuum. The crude product was purified by column chromatography (solvent system: CH₂Cl₂/MeOH, 95/5) to afford **III-3** (126 mg, 41% yield) as a white solid. ^1H NMR (DMSO-*d*₆, 500 MHz): Major Rotamer: δ 12.09 (s, 1H, amide-NH), 11.56 (br s, 1H, amide-NH), 7.96 (s, 1H, guanine-CH), 7.32 (m, 5H, Ph), 6.93 (br d, *J* = 8.0 Hz, 1H, carbamate-NH), 5.31 (q, 2H, N⁷-CH₂-CO), 5.06 (s, 2H, Ph-CH₂), 4.50-3.80 (m, 4H, BnOOC-CH₂ + BocHN-CH + N-CH), 2.74 (sep, 1H, -CH(CH₃)₂), 2.00-1.40 (m, 6H, ring-CH₂) 1.38 (s, 9H, *t*-butyl-CH₃), 1.12 (d, *J* = 7.0 Hz, 6H, -CH(CH₃)₂); Minor Rotamer: δ 6.70 (br d, *J* = 8.0 Hz, 1H, carbamate-NH), 5.22 (s, 2H, Ph-CH₂), 1.34 (s, 9H, *t*-butyl-CH₃).



N-[(2*S*)-*tert*-Butoxycarbonylamino]cyclopent-(1,*S*)-yl]-*N*-[[2-*N*-(isobutyryl)guanin-9-yl]acetyl]glycine (**III-4**). Benzyl *N*-[(2*S*)-*tert*-Butoxycarbonylamino]cyclopent-(1,*S*)-yl]-*N*-[[2-*N*-(isobutyryl)guanin-7-yl]acetyl]glycinate **III-3** (120 mg, 0.19 mmol) was dissolved in MeOH (20 mL) and added to an oven dry 500 mL Parr flask charged

with 10% Pd/C (40 mg). The reaction vessel was flushed with H₂(g) and placed under a H₂(g) atmosphere (50 psi). The flask was shaken on a Parr apparatus until complete disappearance of the ester starting material (approx. 3 h) as evidenced by TLC. The solution was filtered through celite, concentrated under reduced pressure, and dried under vacuum to yield 78 mg (79%) of **III-4** as a white solid. ¹H NMR (DMSO-*d*₆, 500 MHz): Major Rotamer: δ 12.12 (s, 1H, amide-NH), 11.57 (br s, 1H, amide-NH), 7.98 (s, 1H, guanine-CH), 6.90 (br d, J = 8.0 Hz, 1H, carbamate-NH), 5.41 (s, 2H, Ph-CH₂), 5.30-5.00 (m, 2H, N⁷-CH₂-CO), 4.40-3.70 (m, 4H, BnOOC-CH₂ + BocHN-CH + N-CH), 2.74 (sep, 1H, -CH(CH₃)₂), 2.00-1.40 (m, 6H, ring-CH₂), 1.36 (s, 9H, *t*-butyl-CH₃), 1.11 (d, J = 7.0 Hz, 6H, -CH(CH₃)₂); Minor Rotamer: δ 6.66 (br d, J = 8.0 Hz, 1H, carbamate-NH), 1.33 (s, 9H, *t*-butyl-CH₃); ¹³C NMR (DMSO-*d*₆, 125 MHz): δ 180.0, 170.4, 166.9, 156.5, 155.4, 152.6, 147.1, 145.2, 112.1, 77.9, 61.4, 53.0, 46.9, 43.9, 34.7, 28.1, 26.1, 18.9

III.6.2 Solid-Phase Synthesis *tcyp*PNA and Tethered Oligomers

PNA III-2 and *PNA III-3* were both synthesized via manual solid phase synthesis as described in Chapter II.9.2a, page 82. All other PNA oligomers were synthesized by means of automated synthesis as described in Chapter II.9.2b, with minor modifications to be discussed here.

III.6.2a Solid-Phase Synthesis of *tcyp*PNA Oligomers

Because of the problems that can occasionally beset coupling and deprotections of *tcyp*PNA residues as reported by Dr. Pokorski of our lab, extra precaution was used in TFA treatments and coupling times. The automated peptide synthesizer was thus programmed to increase the coupling time allotted *tcyp*PNA monomers from the original 20 minutes to a full hour. Deprotections of *tcyp*PNA monomers accomplished using the typical treatment of TFA (4 min x 2), followed by DCM washing and an additional TFA deprotection cycle (4 min x 2).

Once coupling the final residue in *PNA III-5* through *PNA III-8* was completed, an additional TFA deprotection cycle was initiated, followed by our standard solid-phase “capping” procedure (acetic anhydride in pyridine and DMF) to acetylate the N terminus.

Upon cleavage from the resin and precipitation from ether, crude oligomer containing the iso butyryl-protected guanines were dissolved in 40% aqueous methylamine solution overnight (5 mL, >12 hours). The methylamine solution was then evaporated off via vacuum centrifugation to afford brown oil. The oil was immediately dissolved in deionized water (5 mL), made acidic with ~50 μ L of TFA (or until residue completely dissolved), and purified via reverse-phase HPLC.

III.6.2b Solid-Phase Synthesis Tethered Oligomers

The lysine residues, as shown in Scheme III-2, were coupled using the standard automated procedures. Once both lysine residues were coupled to the resin, the side chains were decoupled simultaneously under the presence of 20 piperidine/DMF (4 x 5 minutes), followed by vigorous washing (DMF, NMP, and DCM). The single Boc group was then removed using TFA/*m*-cresol. Coupling procedures to the three lysine primary amines were altered in the following manner: although the amount of monomer/linker used was identical to previous

synthesis (0.5 mmol/g of resin), immediately following an hour of coupling time/NMP wash, an additional coupling step was programmed delivering fresh cartridge of monomer/linker (0.5 mmol/g resin) along with fresh HBTU solution. This step was also allowed to couple for a full hour. Cleavage, precipitation and purification were identical to the procedures described before.

III.6.3 Characterization of *tcyp*PNA and Tethered Oligomers

Table III-5: PNA Oligomer Mass Spectrometry Data.

PNA	Sequence ^a	Mass (Calculated) ^b	Mass (Observed) ^c
III-1	H-OO-TCTCTCTC-OOO- G ^{N7} TG ^{N7} TG ^{N7} TG ^{N7} T-NH ₂	5041.1	5043.3
III-2	H-OO-TCTCTCTC-OOO- CTCTCTCT-NH ₂	4881.0	4876.8
III-3	H-OO-TCTCT <u>I</u> CTC-OOO- G ^{N7} TG ^{N7} <u>T</u> G ^{N7} TG ^{N7} T-NH ₂	5121.1	5123.3
III-7	H- <u>GGGG</u> TTTT <u>GGGG</u> -Lys-NH ₂	3741.5	3743.0
III-8	H- <u>GGGG</u> TTTTGGGG-Lys-NH ₂	3741.5	3742.8
III-9	H-(GGGG) ₃ -Lys-Lys-Lys-NH ₂	4333.2	4332.5

^a PNA oligomers not listed did not give clean mass spectra, either via electrospray or MALDI-TOF. However, each sample extensively purified (one main peak crude) and renaturation experiments were consistent with literature. Bases that are in bold/underlined denote the inclusion of a *tcyp*PNA residue. ^b Calculated as the M+1 Peak. ^c Determined using electrospray.

III.6.4 Melting Experiments of *tcyp*PNA and Tethered Oligomers

For *PNA III-1* through *PNA III-4*, solutions were prepared in 5 μ M concentration with the complementary DNA in standard phosphate buffered saline (PBS, 150 mM NaCl). The solutions were heated to 90 °C for five minutes and allowed to cool slowly to room temperature over a period of several hours (as the heating blocks cooled). The solutions were then stored in the refrigerator overnight before running the annealing experiment. Some heating and cooling

UV profiles produced what appeared to be multiple transitions. This is not uncommon in triplex forming oligonucleotides;³¹ we reported the higher temperature (usually larger absorbance) transition. The G₄ PNAs (*PNA III-5* through *PNA III-8*) were run with in the absence of DNA at 10 to 20 μM concentrations in standard PBS. UV samples were heated to 91 °C for 5 minutes, cooled to 20 °C at a rate of 1 degree/minute, heated to 90 °C at a rate of 1 degree/minute, and then cooled once more at the same rate. Neither the melting temperatures, nor the percentage of absorbance changed when any run was reduced to 0.5 degrees/minute. There was usually less than a degree of hysteresis between cooling and heating profiles. The T_m s generated from first and second cooling profiles in each run matched closely as well, although the second cooling profile was usually understandably noisier with slight changes in absorbance due to evaporation.

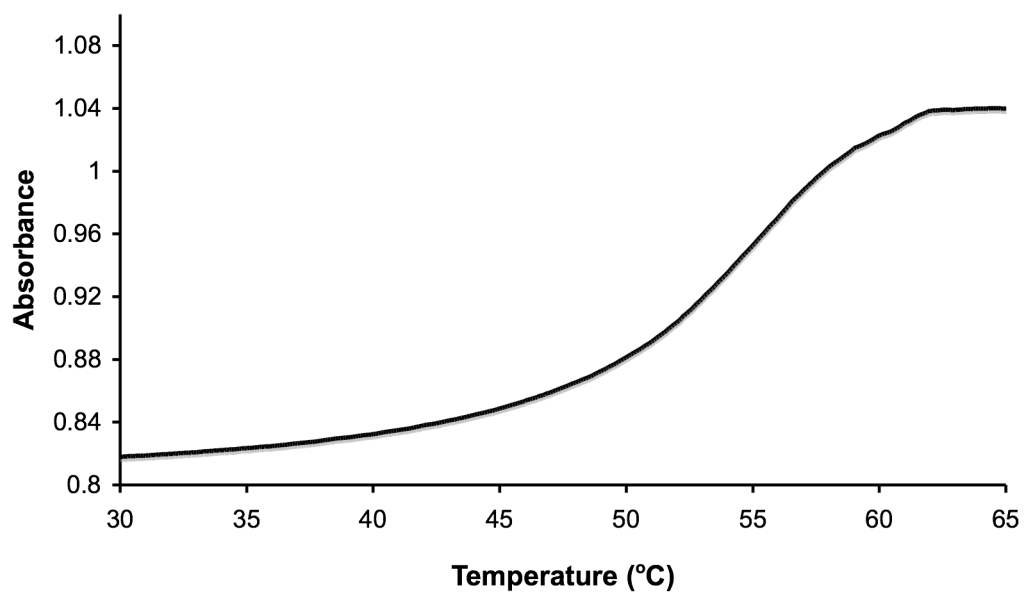
III.6.5 Circular Dichroism Experimental

CD experiments were carried out on a Jastko J-175 spectrophotometer. Each sample was prepared in standard PBS matching the melting experiments, and each sample was annealed by heating to 90 °C for five minutes, followed by cooling over several hours unless explicitly noted.

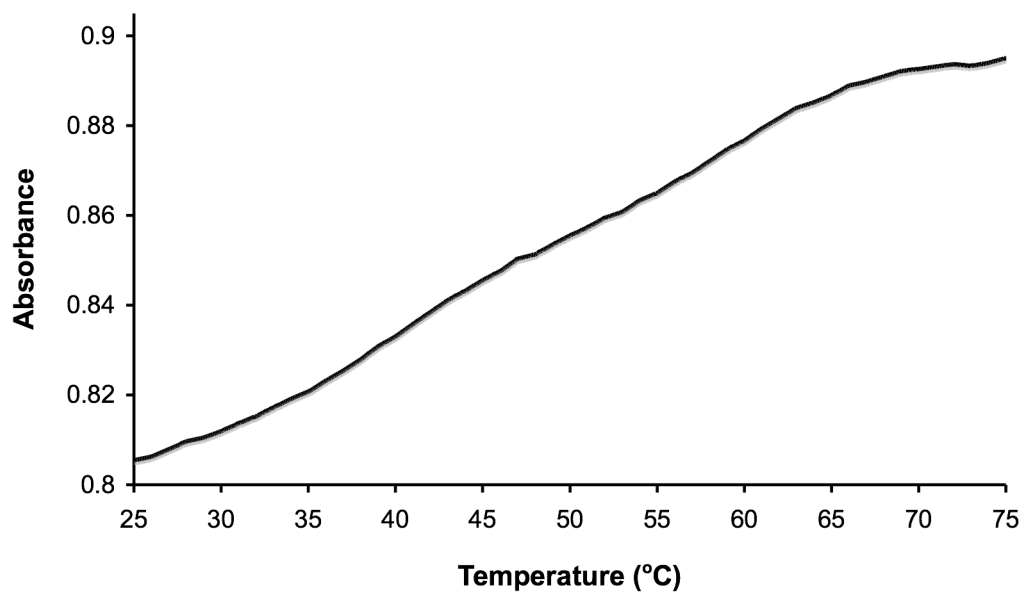
III.6.6 Additional Selected Spectra

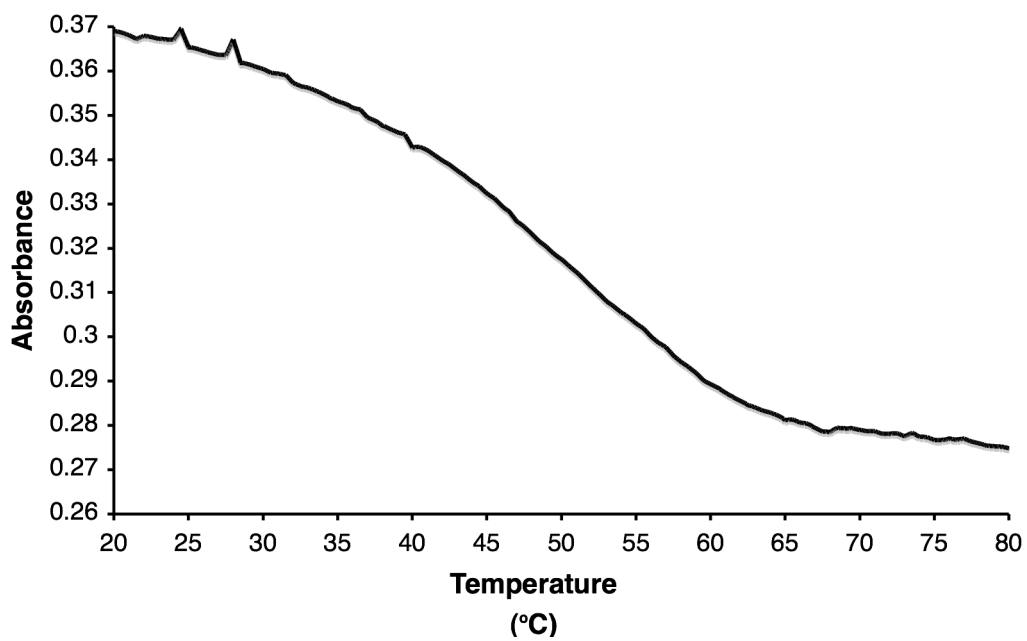
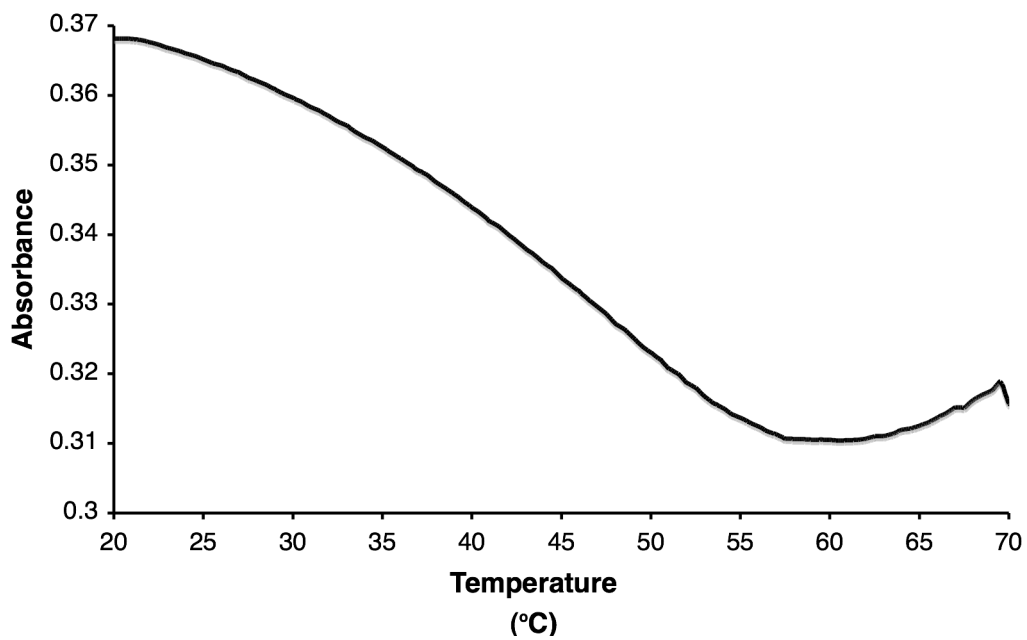
III.6.6a Additional Melting Experiments

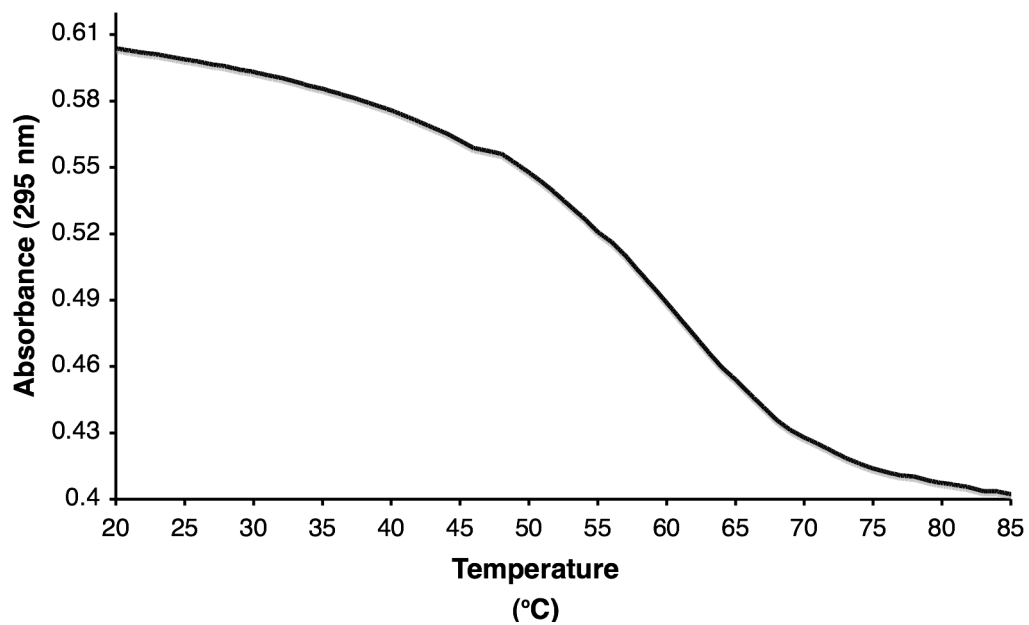
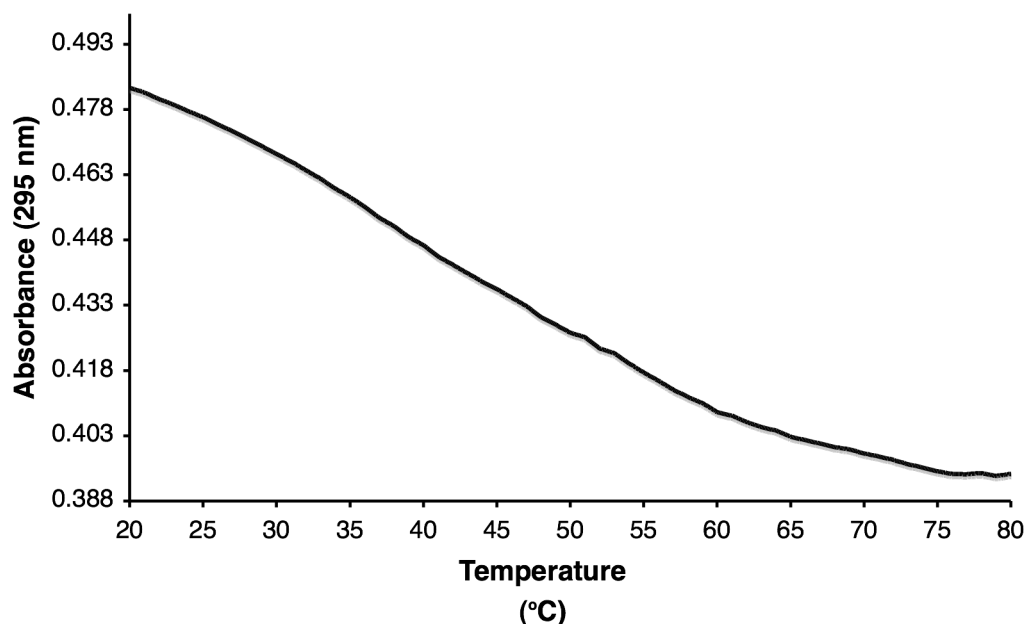
PNA III-2 with Complementary DNA

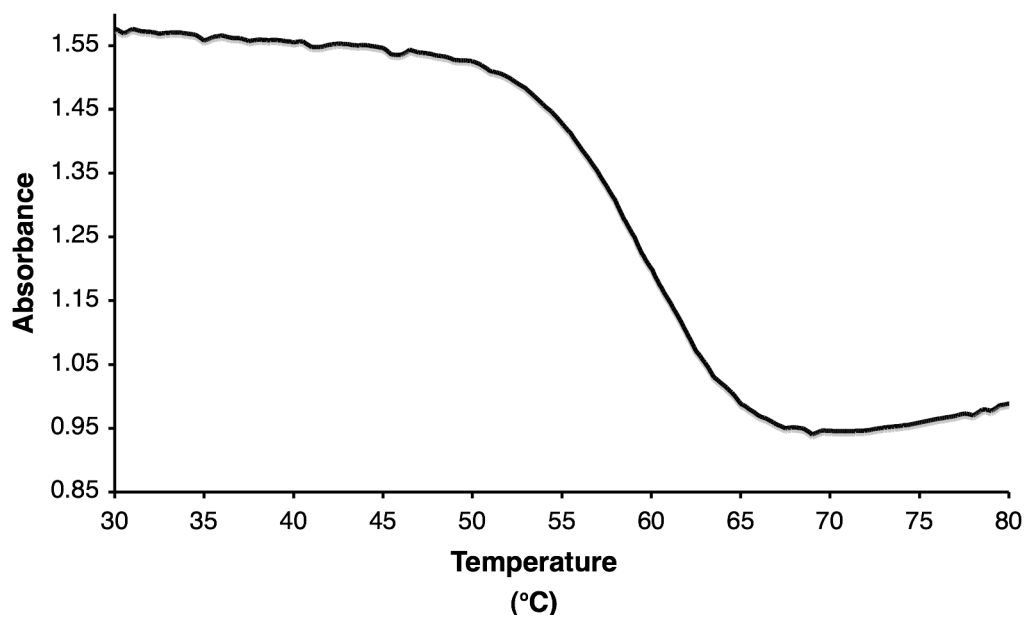
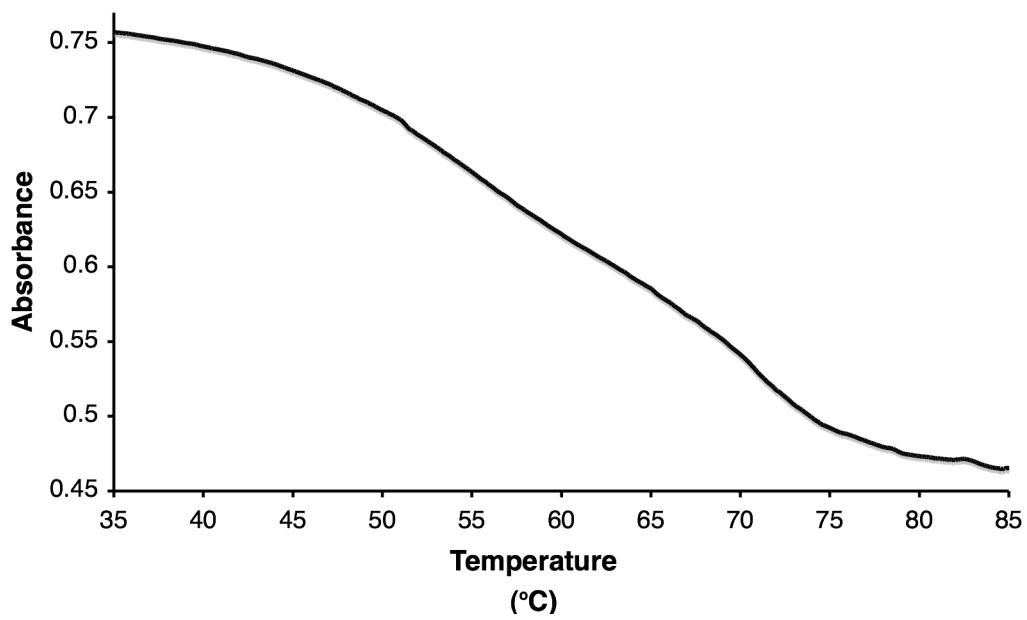


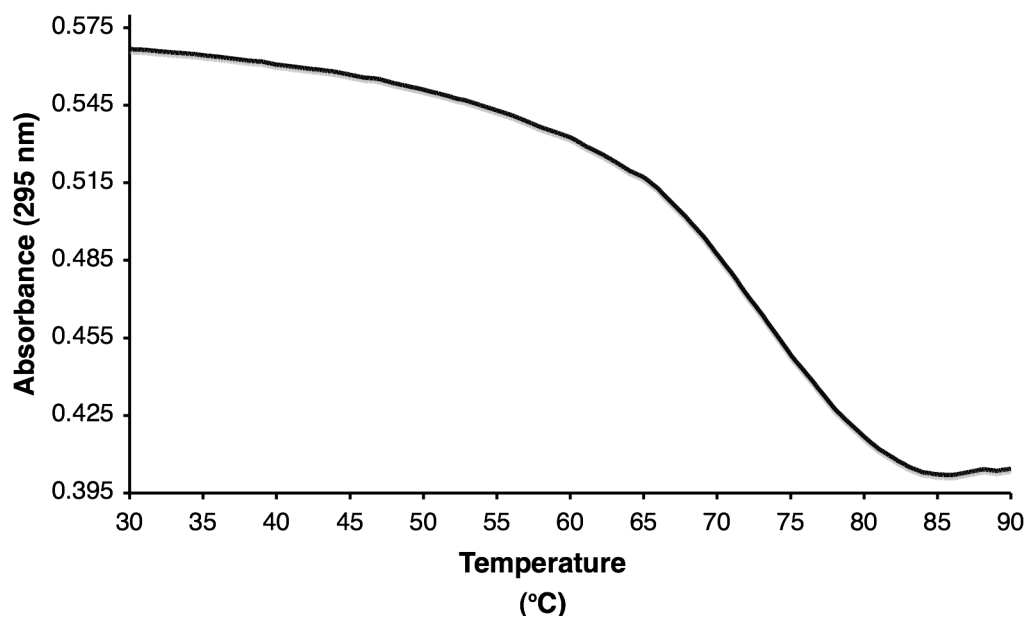
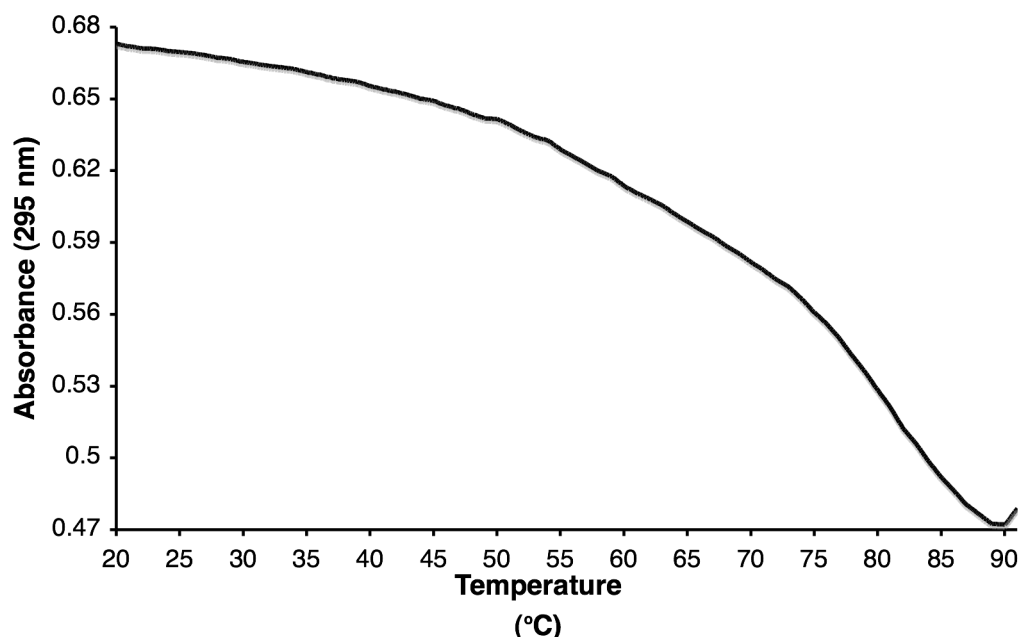
PNA III-3 with Complementary DNA



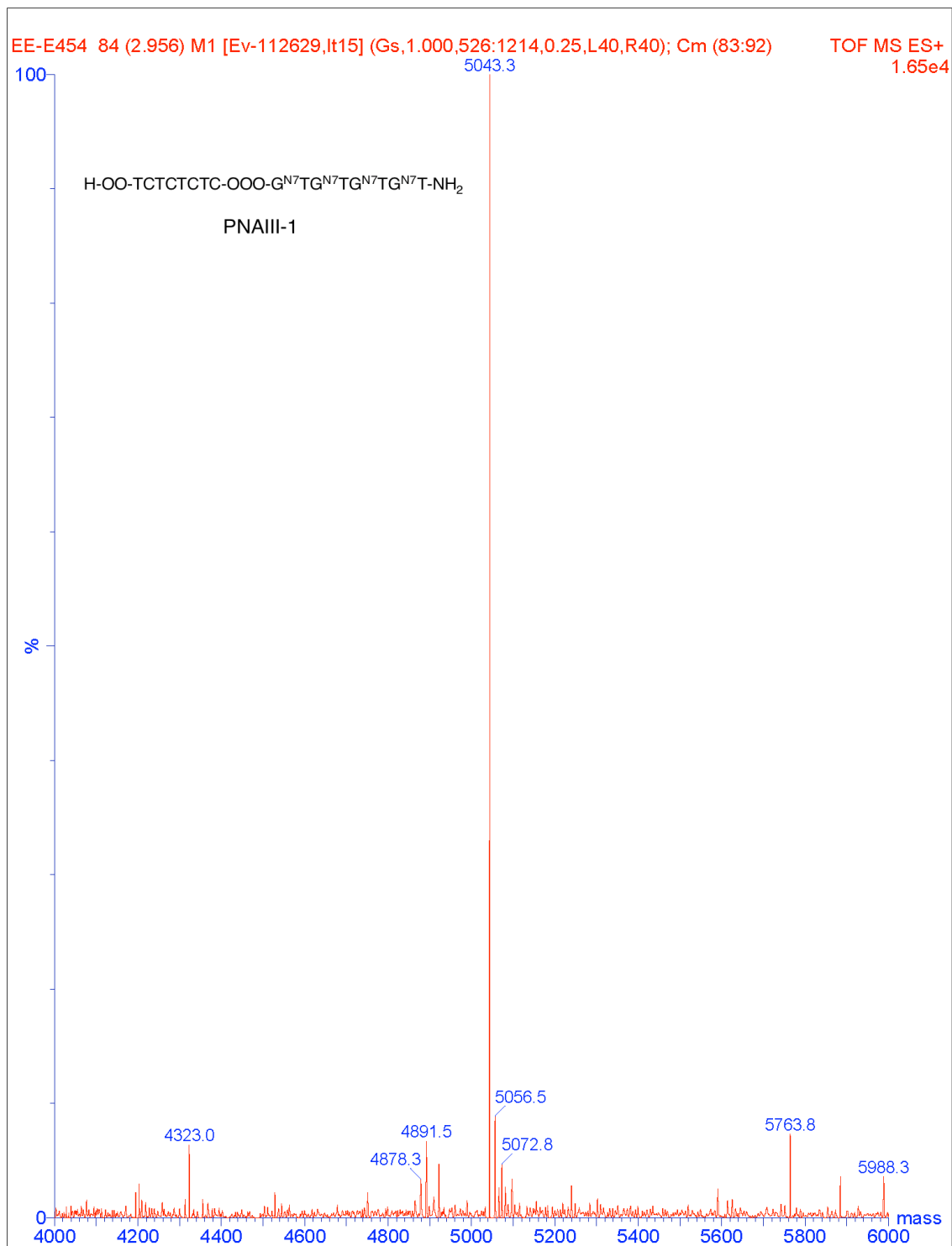
PNA III-5 Alone**PNA III-6 Alone**

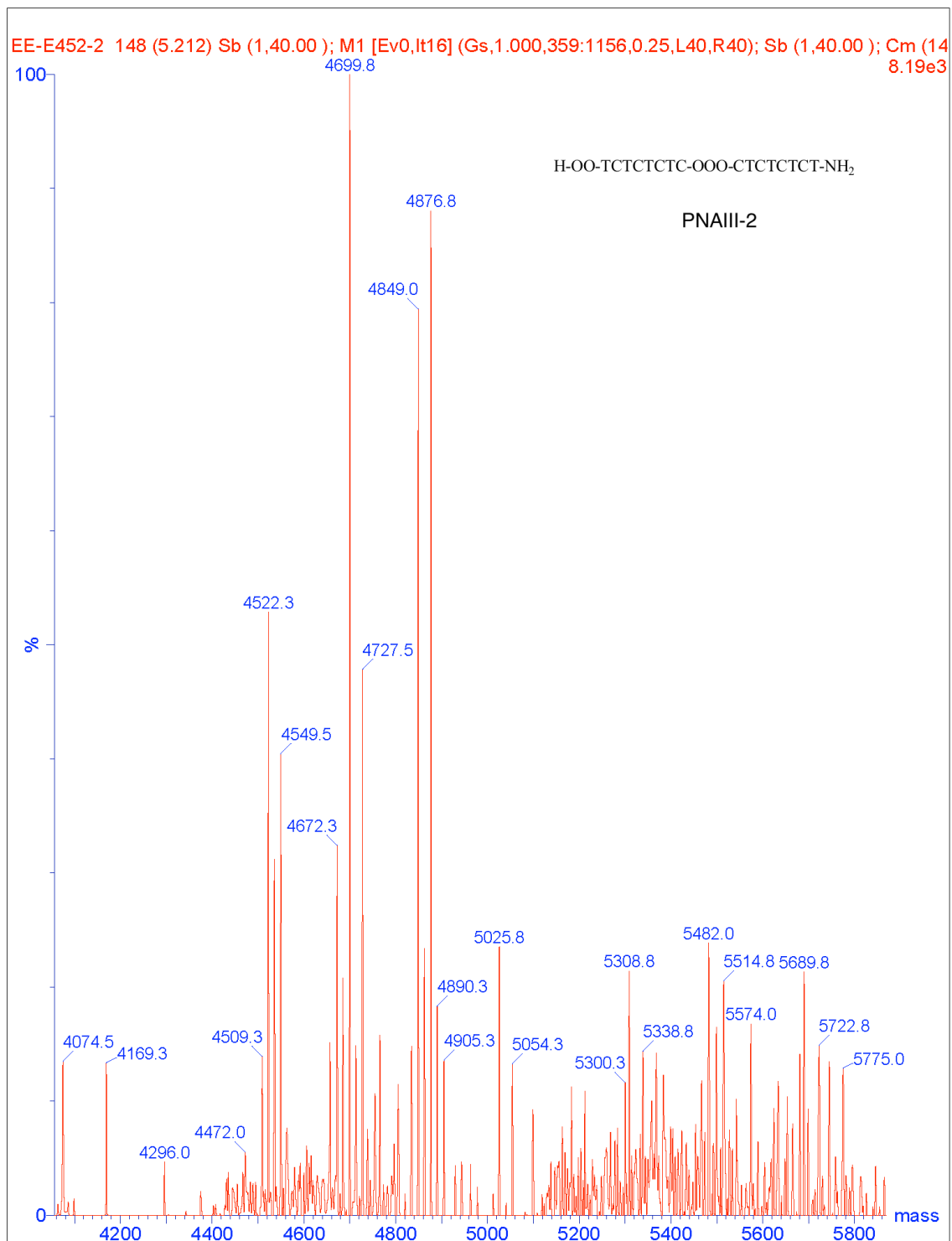
PNA III-7 Alone**PNA III-8 Alone**

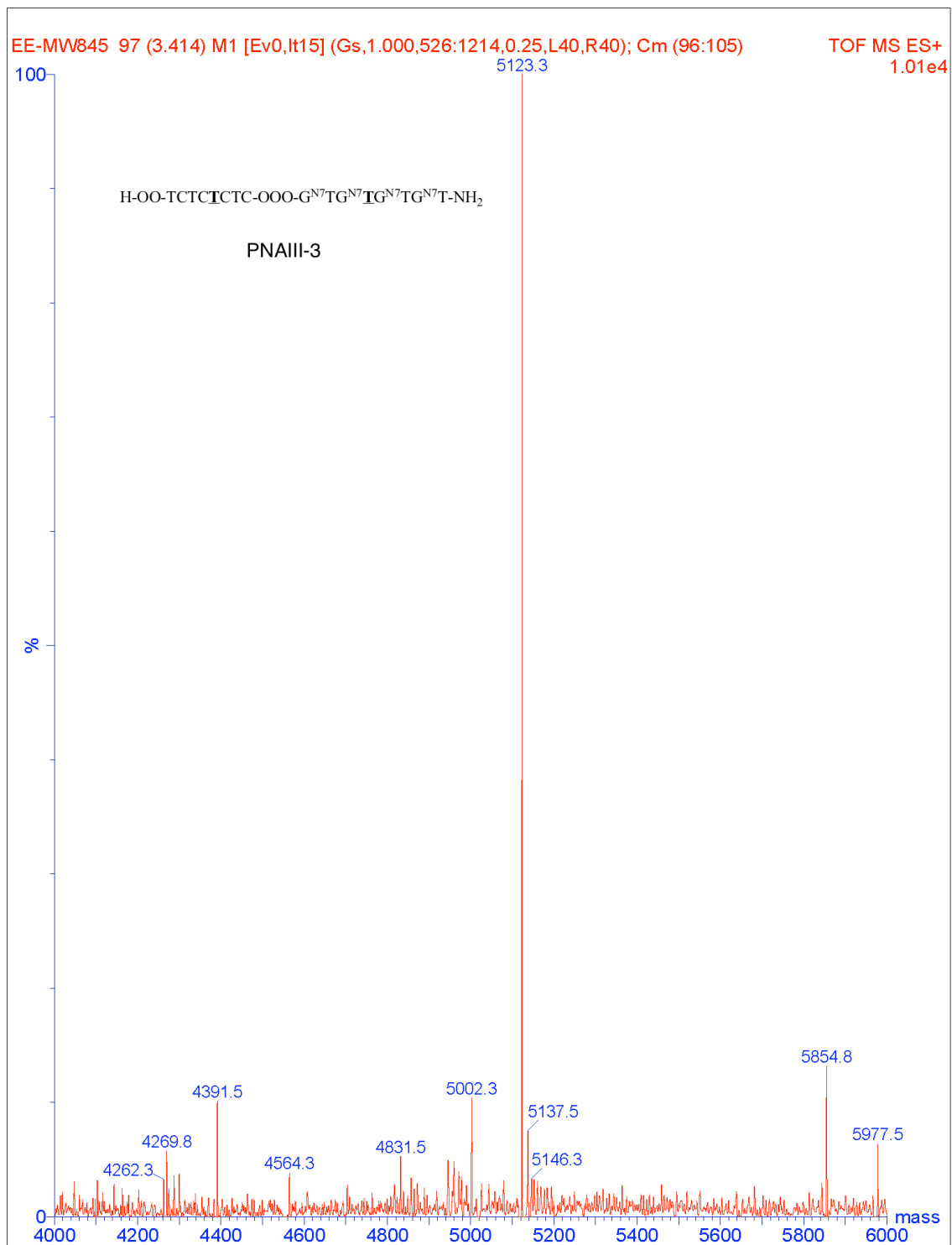
PNA III-5 + G₄-DNA**PNA III-6 + G₄-DNA**

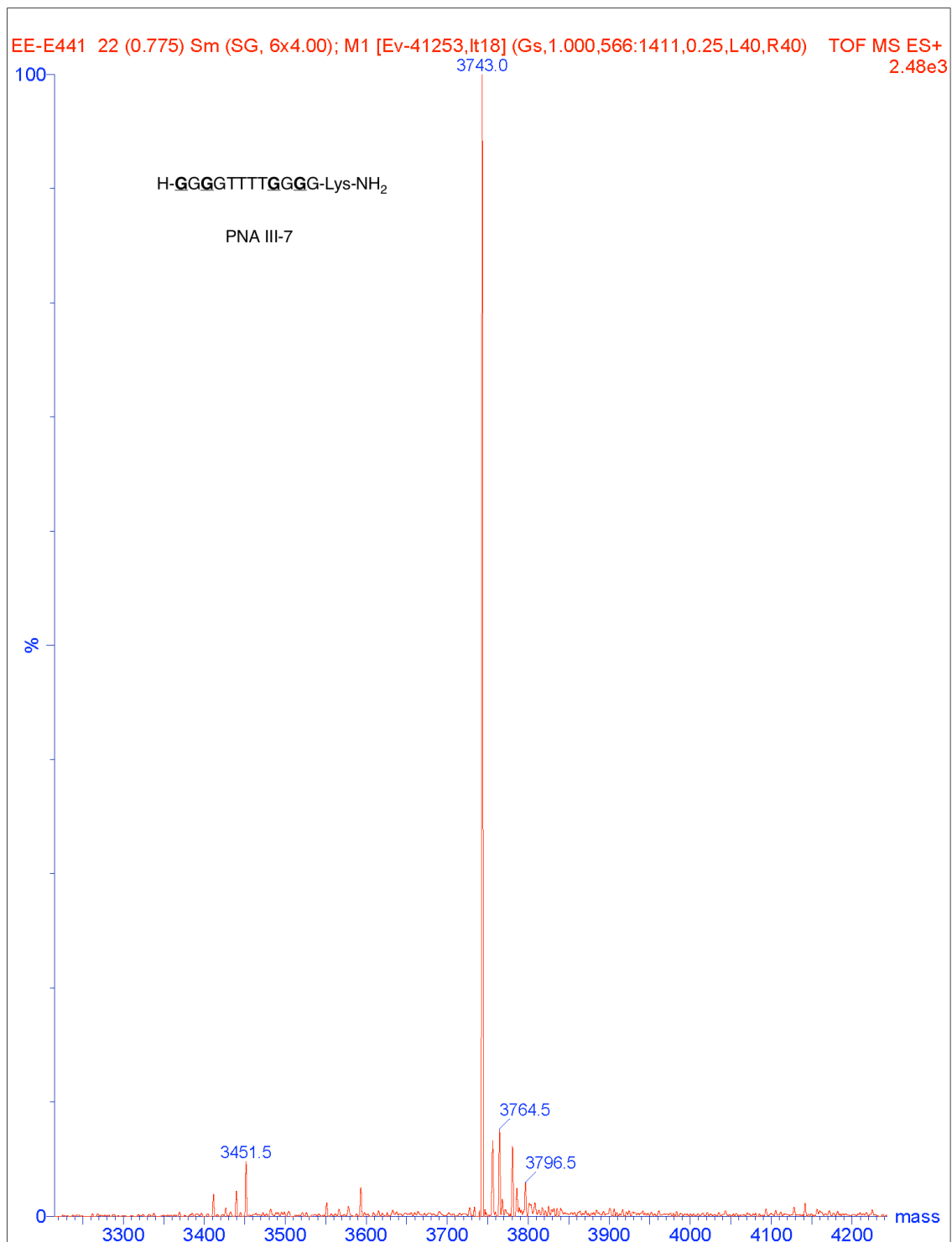
PNA III-7 + G₄-DNA**PNA III-8 + G₄-DNA**

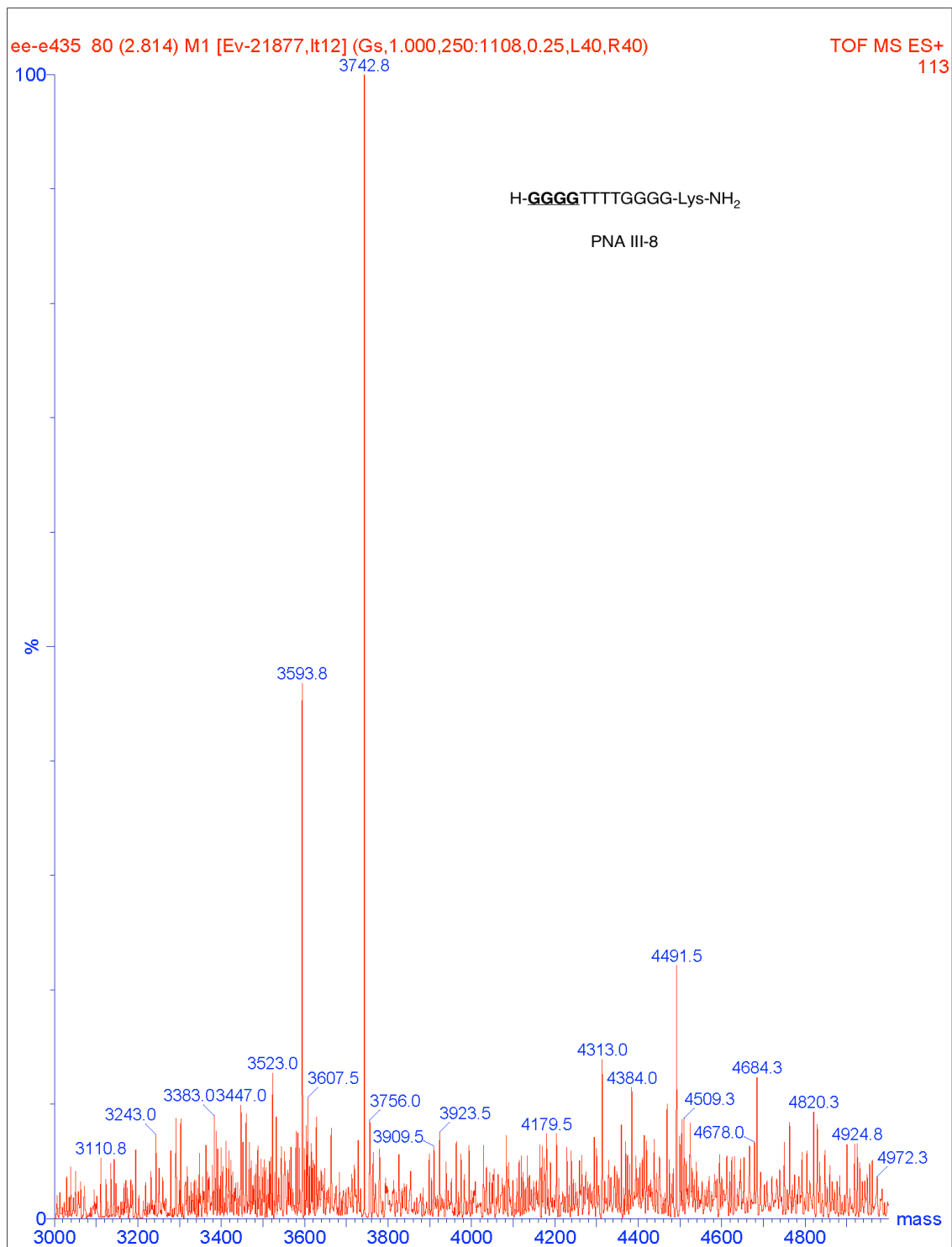
III.6.6b Mass Spectrometry Data

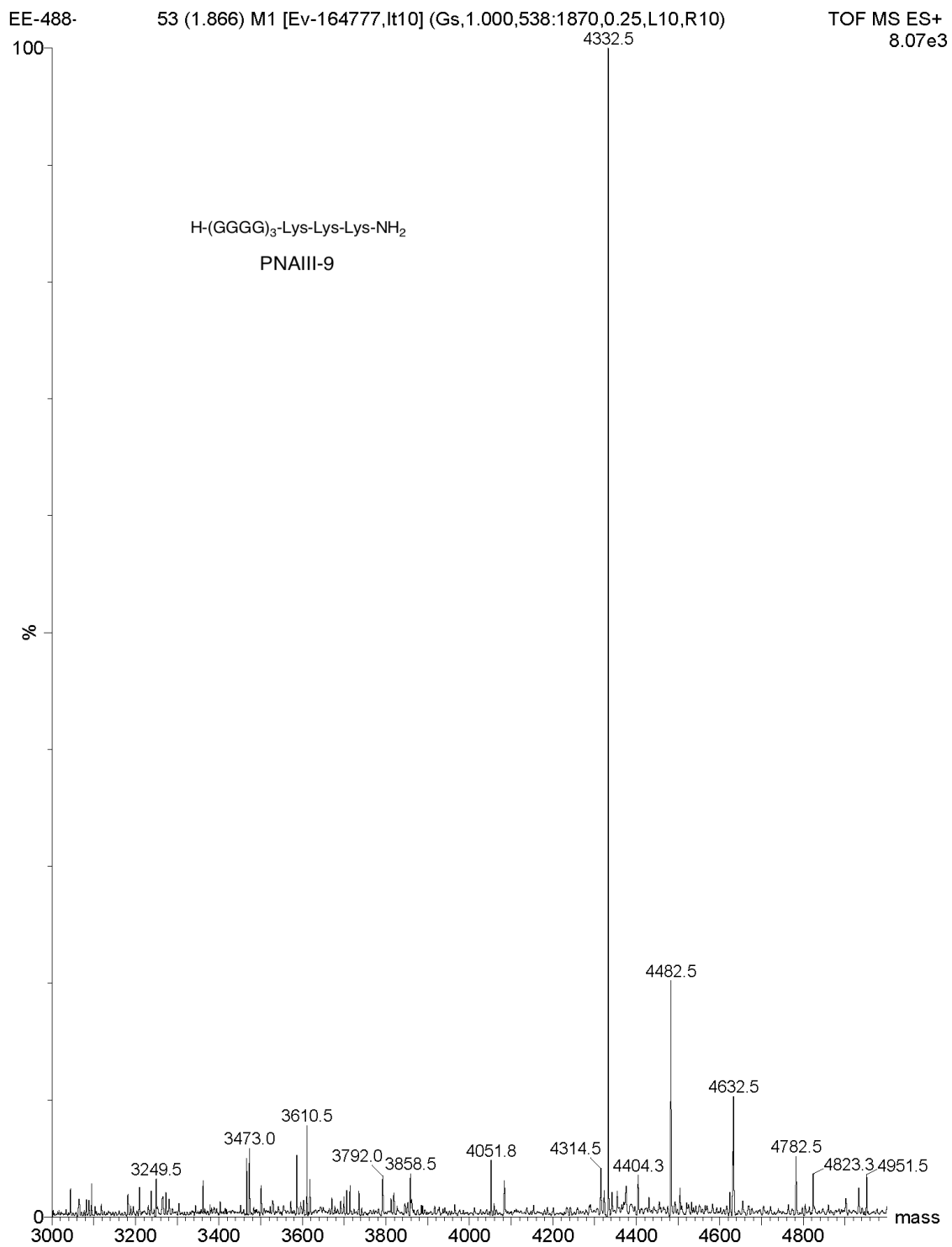












Chapter IV

Conclusions and Future Studies

IV.1 Conclusion

In summation, many of our initial hypotheses have held true to our original designs; even those hypotheses that were errant have been, for the most part, illustrative and useful in directing our research. We have developed a unique peptide nucleic acid residue ($^L\text{K}\gamma\text{-PNA}$) that we envision has a great deal of potential for PNA-based applications. As we have shown in Chapter II, the potential utility of this PNA derivative lies in its versatility, as this modification allows researchers to drastically alter the physical characteristics of PNA while keeping the essential affinity and selectivity intact. In Chapter III, we have described our successful efforts to manipulate nucleic acid architecture using (*S,S*)-*tcyp*PNA in ways that had not been reported until our investigations. Although, we have progress in exploring these research projects, there is much more research possible into both the underlying systems as well as new and innovative applications due to the novelty of the described research.

IV.2 Future Projects and Avenues of Research

IV.2.1 Overview: Basic Studies

As one looks towards future directions for a promising research project, it is important to look back on the basic studies that got curtailed in lieu of more exciting applications and grand schemes. In this regard, because γ -substituted PNA has been neglected until recently, there is a large amount of fundamental research that needs to be carried out. The understanding of the thermodynamics and kinetics of these preorganized systems is still rudimentary compared to *aeg*PNA.^{1,2} The ability to manipulate these binding characteristics is important in many biological applications. This is especially true of anti-gene techniques, where tightly bound chromosomal DNA must be successfully invaded and the resulting structure must be stable enough to resist DNA duplex formation.³

The $^L\text{K}\gamma\text{-PNA}(\text{Cbz})$ monomers could be quickly utilized for interesting applications employing *aeg*PNA or α -substituted PNA. Debane and coworkers recently demonstrated that $^D\text{K}\alpha\text{-PNA}$ showed much improved aqueous solubility as well as reduced aggregation.⁴ It is well documented that charged PNA oligomers are more cell permeable than standard *aeg*PNA oligomers. Furthermore, Ly and coworkers recently showed significant anti-sense activity in mixed-base PNA oligomers, based on the arginine PNA ($^D\text{R}\alpha\text{-PNA}$) residues developed in their lab.⁵ It is especially noteworthy that although the cellular uptake rivals that of typically used poly-arginine peptide conjugates, the cytotoxicity is greatly reduced.

IV.2.2 Useful $^L\text{K}\gamma\text{-PNA}$ Monomer Targets

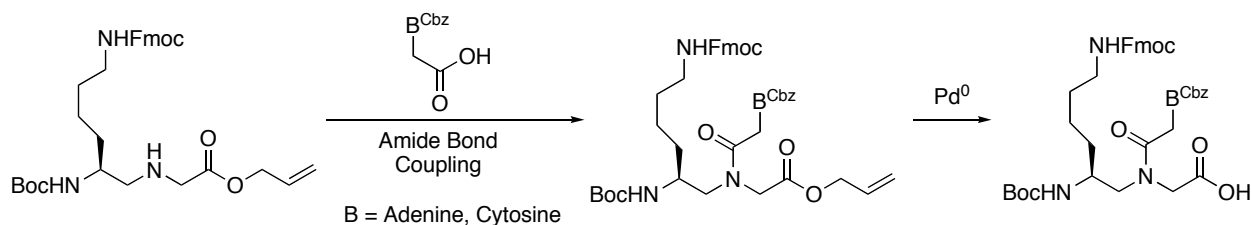
Although we synthesized enough different monomers to produce a wide variety of functionally diverse PNA oligomers, a broader range of nucleobase and solid-phase synthesis options would greatly extend the utility of $^L\text{K}\gamma\text{-PNA}$ in general. Strategies to synthesize adenine, and cytosine $^L\text{K}\gamma\text{-PNA}(\text{Fmoc})$ monomers should be addressed. Furthermore, these syntheses should also be amenable to guanine.

IV.2.2a Extended $^L\text{K}\gamma\text{-PNA}(\text{Fmoc})$ Bases: Adenine, Cytosine

Adenine(Cbz) acetic acid and cytosine(Cbz) acetic acid, commonly used in PNA synthesis, are both inexpensive and relatively easy to synthesize.⁶ These nucleobase acetic acids were fully compatible with the $^L\text{K}\gamma\text{-PNA}(\text{Cbz})$ monomer synthesis. However, when incorporating Fmoc-protected sidechains, problems with the orthogonal protecting groups arise. We earlier described the synthesis of $^L\text{K}\gamma\text{-PNA}(\text{Fmoc})$ cytosine(Cbz) monomers by hydrolysis of a benzyl ester. Although producing enough monomer for our studies, the reaction was slow and inefficient. In all likelihood, a new monomer ester that is orthogonal to Boc, Fmoc, and Cbz protecting groups, such as monomer allyl esters, will need to be developed (Scheme IV-1).⁷

Expanding the possible $^L\text{K}\gamma\text{-PNA}(\text{Fmoc})$ monomers to include adenine and cytosine would greatly improve the utility of our sidechain strategies.

Scheme IV-1: Proposed Synthesis of Adenine and Cytosine $^L\text{K}\gamma\text{-PNA}(\text{Fmoc})$ Monomers.



IV.2.2b Guanine Monomers

Any useful PNA modification should be extended to all four natural nucleobases. Considering our interest in PNA quadruplex formation, guanine is an especially important addition to this research.⁸ Hamilton and coworkers recently used a DNA quadruplex as a scaffold to display protein-binding moieties.⁹ Using PNA as such a scaffold is a task well suited for $^L\text{K}\gamma\text{-PNA}$. Although guanine(Cbz) acetic acid is synthetically accessible, the production is more strenuous compared to adenine and cytosine and is more expensive because of the necessity of starting from 5-chloro 2-aminopurine rather than guanine. In addressing this problem, our group has turned to isobutyryl protection as a useful substitute.¹⁰ Although this strategy might work for $^L\text{K}\gamma\text{-PNA}(\text{Cbz})$ monomers, functionalizing side chains on solid support might present problems. Deprotection of Fmoc-protected sidechains could facilitate inadvertent removal of the ^tBu group or produce an acyl transfer reaction, thus capping the γ -sidechain. Finding a protecting strategy compatible with $^L\text{K}\gamma\text{-PNA}(\text{Fmoc})$ monomers starting from commercially available, but notoriously insoluble guanine is a daunting obstacle.

IV.2.2c Fmoc-PNA Oligomer Synthesis

Although Boc-PNA solid phase synthesis is robust and high yielding, the harsh conditions used to cleave oligomers from the resin limits the variety of functionality that can be conjugated on solid support. This is especially true for many acid-sensitive (and expensive) fluorescent and fluorescence-quenching molecules used in molecular beacons.¹¹ For this reason, ^LK γ -PNA designed for Fmoc-PNA synthesis could find a potentially valuable niche. There are several orthogonal protecting groups that could be deprotected on solid support for these applications. Dose and coworkers recently functionalized a lysine primary amine during Fmoc-PNA solid-phase synthesis after removal of an Alloc protecting group with substoichiometric amounts of palladium.¹² Also, Diaz-Mochon and coworkers recently demonstrated an orthogonal Fmoc/Dde solid phase strategy (Dde groups are selectively removed with NH₂OH•HCl/imidazole) to make PNA-peptide conjugates.¹³ Either one of these strategies could potentially be utilized for Fmoc-protected ^LK γ -PNA monomers (Figure IV-1).

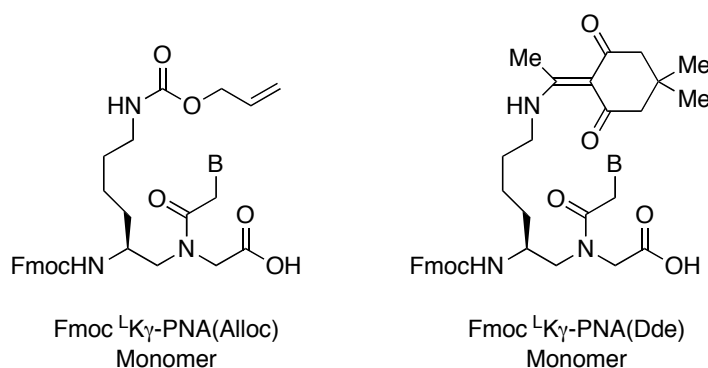


Figure IV-1: Proposed ^LK γ -PNA Monomers for Fmoc Solid-Phase Synthesis.

Debane and coworkers recently synthesized Fmoc ^LK γ -PNA(Boc) monomers based in part on our research.⁴ They found the yields were unusually poor after the second or third incorporation of their ^LK γ -PNA monomers in the same oligomer, however. Even with the

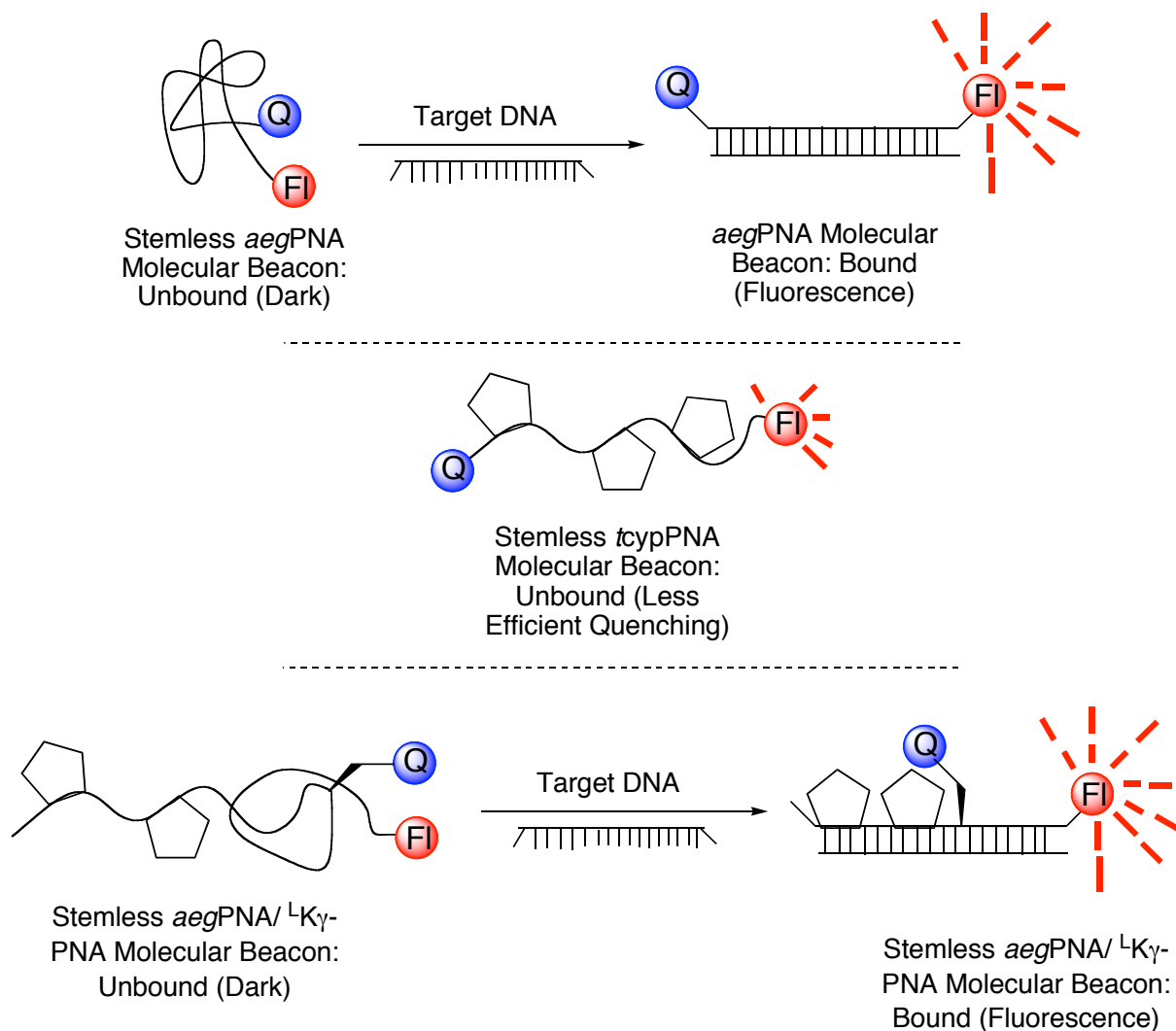


Figure IV-3: The Combination of ^LK γ -PNA and *tcyp*PNA: Molecular Beacons.

quenching. Utilizing the ^LK γ -PNA to display a fluorophore or quencher in an *aeg*PNA portion of the probe could solve this potential problem.

IV.2.4 ^LK γ -PNA As Protein-Binding Molecules

Because ^LK γ -PNA residues can be effectively used in succession, construction of densely functionalized oligomers using PNA as a scaffold can now be investigated. Controlling the

display of complex functionality over a large surface area could have an immense impact in bio-macromolecular manipulation.

Protein-protein interactions are ubiquitous in cellular processes such as cell growth, signal transduction, and cell death.¹⁷ While some protein-protein interactions are disrupted by small molecules, protein surfaces have proven to be difficult drug targets. Many protein-protein interactions depend on large, heterogeneous protein surface areas, using multiple points of contact as their source of binding affinity and specificity. Thus, functional groups important in these binding events are often too widely dispersed on a protein surface for small molecules to bind effectively. Well-conceived aptamers, generated from a randomized library, have proven to be useful molecules that possess the large size and broad functionality required to disrupt large-scale protein-protein interactions.¹⁸ Aptamers, however, suffer from a lack of stability, bioavailability, and complex chemical functionality. It is likely that the use of highly functionalized non-natural oligomers would alleviate these problems.

Aptamers based on functionalized ^LK γ -PNA could be designed to bind to specific targets. Another option for employing such molecules would be the construction of randomized libraries. PNA-encoded libraries are becoming a common means of effectively identifying peptides and small molecules of biological activity. ^LK γ -PNA could be used in a similar fashion, however, taking on dual roles of both code bearer (nucleobase recognition) and protein-hybridization substrate (sidechain display).

Chapter I References

1. Watson, J. D.; Crick, F. H. C., "Molecular structure of nucleic acids; A structure for deoxyribose nucleic acid." *Nature* **1953**, *171*, 737-738.
2. Watson, J. D.; Crick, F. H. C., "Genetical implications of the structure of deoxyribonucleic acid." *Nature* **1953**, *171*, 964-967.
3. Crick, F. H. C., "Central dogma of molecular biology." *Nature* **1970**, *227*, 561-563.
4. Volk, D. E.; Yang, X.; Fennewald, S. M.; King, D. J.; Bassett, S. E.; Venkitachalam, S.; Herzog, N.; Luxon, B. A.; Gorenstein, D. G., "Solution structure and design of dithiophosphate backbone aptamers targeting transcription factor NF-kappaB." *Bioorg. Chem.* **2002**, *30*, 396-419.
5. Access Excellence @ National Health Museum
6. Frank-Kamenetskii, M. D.; Mirkin, S. M., "Triplex DNA structures." *Annu. Rev. Biochem.* **1995**, *64*, 65-95.
7. Chin, J. Y.; Schleifman, E. B.; Glazer, P. M., "Repair and recombination induced by triple helix DNA." *Front. Biosci.* **2007**, *12*, 4288-4297.
8. Chan, P. P.; Glazer, P. M., "Triplex DNA: fundamentals, advances, and potential applications for gene therapy." *J. Mol. Med.* **1997**, *75*, 267-282.
9. Sen, D.; Gilbert, W., "Formation of parallel four-stranded complexes by guanine-rich motifs in DNA and its implications for meiosis." *Nature* **1988**, *334*, 364-366.
10. Arthanari, H.; Bolton, P. H., "Functional and dysfunctional roles of quadruplex DNA in cells." *Chem. Biol.* **2001**, *8*, 221-230.
11. Parkinson, G. N.; Lee, M. P.; Neidle, S., "Crystal structure of parallel quadruplexes from human telomeric DNA." *Nature* **2002**, *417*, 876-880.
12. Opalinska, J. B.; Gewirtz, A. M., "Nucleic-acid therapeutics: basic principles and recent applications." *Nat. Rev. Drug Disc.* **2002**, *1*, 503-514.
13. Fry, D. C.; Vassilev, L. T., "Targeting protein-protein interactions for cancer therapy." *J. Mol. Med.* **2005**, *83*, 955-963.
14. Melton, D. W., "Gene targeting in the mouse." *BioEssays* **1994**, *16*, 633-638.

15. Paterson, B. M.; Roberts, B. E.; Kuff, E. L., "Structural gene identification and mapping by DNA-mRNA hybrid-arrested cell-free translation." *Proc. Natl. Acad. Sci. USA* **1977**, *74*, 4370-4374.
16. Tachikawa, K.; Briggs, S. P., "Targeting the human genome." *Curr. Opin. Biotechnol.* **2006**, *17*, 659-665.
17. Stephenson, M. L.; Zamecnik, P. C., "Inhibition of Rous sarcoma viral RNA translation by a specific oligonucleotide." *Proc. Natl. Acad. Sci. USA* **1978**, *75*, 285-288.
18. Wong, L-J. C.; Boles, R. G., "Mitochondrial DNA analysis in clinical laboratory diagnostics." *Clin. Chim. Acta* **2005**, *354*, 1-20.
19. Monis, P. T.; Giglio, S., "Nucleic acid amplification-based techniques for pathogen detection and identification." *Infect. Genet. Evol.* **2006**, *6*, 2-12.
20. Tan, W.; Kemin, W.; Drake, T. J., "Molecular beacons." *Curr. Opin. Chem. Biol.* **2004**, *8*, 547-553.
21. Elghanian, R.; Storhoff, J. J.; Mucic, R. C.; Letsinger, R. L.; Mirkin, C. A., "Selective colorimetric detection of polynucleotides based on the distance-dependant optical properties of gold nanoparticles." *Science* **1997**, *277*, 1078-1081.
22. Yu, C. J.; Wan, Y.; Yowanto, H.; Li, J.; Tao, C.; James, M. D.; Tan, C. L.; Blackburn, G. F.; Meade, T. J., "Electronic detection of single-base mismatches in DNA with ferrocene-modified probes." *J. Am. Chem. Soc.* **2001**, *123*, 11155-11161.
23. Eckstein, F.; Gish, G., "Phosphorothioates in molecular biology." *Trends Biochem. Sci.* **1989**, *14*, 97-100.
24. Le Bec, C.; Wickstrom, E., "Stereospecific Grignard-activated solid phase synthesis of DNA methylphosphonate dimers." *J. Org. Chem.* **1996**, *61*, 510-513.
25. Browne, K. A.; Dempcy, R. O.; Bruce, T. C., "Binding studies of cationic thymidyl deoxyribonucleic guanidine to RNA homopolynucleotides." *Proc. Natl. Acad. Sci. USA* **1995**, *92*, 7051-7055.
26. Gogoi, K.; Gunjal, A. D.; Phalgune, U. D.; Kumar, K. A., "Synthesis and RNA binding selectivity of oligonucleotides modified with five-atom thioacetamido nucleic acid backbone structures." *Org. Lett.* **1997**, *9*, 2697-2700.
27. Sindelar, L. E.; Jaklevic, J. M., "High-throughput DNA synthesis in a multichannel format." *Nucleic Acids Res.* **1995**, *23*, 982-987.

28. De Bouvere, B.; Kerremans, L.; Hendrix, C.; De Winter, H.; Schepers, G.; Van Aerschot, A.; Herdewijn, P., "Hexitol nucleic acids (HNA): synthesis and properties." *Nucleosides Nucleotides* **1997**, *16*, 973-976.
29. Damha, M. J.; Wilds, C. J.; Noronha, A.; Bruckner, I.; Borkow, G.; Arion, D.; Parniak, M. A., "Hybrids of RNA and arabinonucleic acids (ANA and 2'F-ANA) are substrates of Ribonuclease H." *J. Am. Chem. Soc.* **1998**, *120*, 12976-12977.
30. Trempe, J-F.; Wilds, C. J.; Denisov, A. Yu.; Pon, R. T.; Damha, M. J.; Gehring, K., "NMR solution structure of an oligonucleotide hairpin with a 2'F-ANA/RNA stem: implications for RNase H specificity toward DNA/RNA hybrid duplexes." *J. Am. Chem. Soc.* **2001**, *123*, 4896-4903.
31. McKay, R. A.; Miraglia, L. J.; Cummins, L. L.; Owens, S. R.; Sasmor, H.; Dean, N. M., "Characterization of a potent and specific class of antisense oligonucleotide inhibitor of human protein Kinase C- α Expression." *J. Biol. Chem.* **1999**, *274*, 1715-1722.
32. Zellweger, T.; Miyake, H.; Cooper, S.; Chi, K.; Conklin, B. S.; Monia, B. P.; Gleave, M. E., "Antitumor activity of antisense clusterin oligonucleotides is improved in vitro and in vivo by incorporation of 2'-O-(2-Methoxy)Ethyl chemistry." *J. Pharmacol. Exp. Ther.* **2001**, *298*, 934-940.
33. Obika, S.; Nanbu, D.; Hari, Y.; Morio, K.; In, Y.; Ishida, T.; Imanishi, T., "Synthesis of 2'-O, 4'-C-Methylenuridine and -cytosine. Novel bicyclic nucleosides having a fixed C_{3'}-endo sugar puckering." *Tetrahedron Lett.* **1997**, *50*, 8735-8738.
34. Singh, S. K.; Nielsen, P.; Koshkin, A. A.; Wengel, J., "LNA (locked nucleic acids): synthesis and high-affinity nucleic acid recognition." *Chem. Commun.* **1998**, 455-456.
35. Jepsen, J. S.; Wengel, J., "LNA-Antisense rivals siRNA for gene silencing." *Curr. Opin. Drug Discov. Devel.* **2004**, *7*, 188-194.
36. Swayze, E. E.; Siwkowski, A. M.; Wancewicz, E.V.; Migawa, M. T.; Wyrzykeiwicz, T. K.; Hung, G.; Monia, B. P.; Bennett, C. F., "Antisense oligonucleotides containing locked nucleic acid improve potency but cause significant hepatotoxicity in animals." *Nucleic Acids Res.* **2007**, *35*, 687-700.
37. Nielsen, P. E.; Egholm, M.; Berg, R. H.; Buchardt, O., "Sequence-selective recognition of DNA by strand displacement with a thymine-substituted polyamide." *Science* **1991**, *254*, 1497-1500.
38. Egholm, M.; Buchardt, O.; Christensen, L.; Behrens, C.; Freier, S. M.; Driver, D. A.; Berg, R. H.; Kim, S. K.; Norden, B.; Nielsen, P. E., "PNA hybridizes to complementary oligonucleotides obeying the Watson-Crick hydrogen-bonding rules." *Nature* **1993**, *365*, 566-568.

39. Tomac, S.; Sarkar, M.; Ratilainen, T.; Wittung, P.; Nielsen, P. E.; Norden, B.; Graslund, A., "Ionic effects on the stability and conformation of peptide nucleic acid complexes." *J. Am. Chem. Soc.* **1996**, *118*, 5544-5552.
40. Sen, A.; Nielsen, P. E., "On the stability of peptide nucleic acid duplexes in the presence of organic solvents." *Nucleic Acids Res.* **2007**, *35*, 3367-3374.
41. Demidov, V. V.; Potaman, V. N.; Frank-Kamenetskii, M. D.; Egholm, M.; Buchardt, O.; Sonnichsen, S. H.; Nielsen, P. E., "Stability of peptide nucleic acids in human serum and cellular extracts." *Biochem. Pharmacol.* **1994**, *48*, 1310-1313.
42. Kaihatsu, K.; Janowski, B. A.; Corey, D. R., "Recognition of chromosomal DNA by PNAs." *Chem. Biol.* **2004**, *11*, 749-758.
43. Larsen, H. J.; Bentin, T.; Nielsen, P. E., "Antisense properties of peptide nucleic acid." *Biochim. Biophys. Acta* **1999**, *1489*, 159-166.
44. Demidov, V. V., "PNA and LNA throw light on DNA." *Trends Biotechnol.* **2003**, *21*, 4-7.
45. Brandt, O.; Hoheisel, J. D., "Peptide nucleic acids on microarrays and other biosensors." *Trends Biotechnol.* **2004**, *22*, 617-622.
46. Egholm, M.; Buchardt, O.; Nielsen, P. E.; Berg, R. H., "Peptide nucleic acids (PNA). Oligonucleotide analogues with an achiral peptide backbone." *J. Am. Chem. Soc.* **1992**, *114*, 1895-1897.
47. Betts, L.; Josey, J. A.; Veal, J. M.; Jordan, S. R., "A nucleic acid triple helix formed by a peptide nucleic acid-DNA complex." *Science* **1995**, *270*, 1838-1841.
48. Rasmussen, H.; Kastrop, J. S.; Nielsen, J. N.; Nielsen, J. M.; Nielsen, P. E., "Crystal structure of a peptide nucleic acid (PNA) duplex at 1.7 Å resolution." *Nature Struct. Bio.* **1997**, *4*, 98-101.
49. Egholm, M.; Christensen, L.; Dueholm, K. L.; Buchardt, O.; Coull, J.; Nielsen, P. E. "Efficient pH-independent sequence-specific DNA binding by pseudoisocytosine-containing bis-PNA." *Nucleic Acids Res.* **1995**, *23*, 217-222.
50. Krishnan-Gosh, Y.; Stephens, E.; Balasubramanian, S., "A PNA₄ quadruplex." *J. Am. Chem. Soc.* **2004**, *126*, 5944-5945.
51. Datta, B.; Bier, M. E.; Roy, S.; Armitage, B. A., "Quadruplex formation by a guanine-rich PNA oligomer." *J. Am. Soc. Chem.* **2005**, *127*, 4199-4207.

52. Datta, B.; Schmitt, C.; Armitage, B. A., "Formation of a PNA₂-DNA₂ hybrid quadruplex." *J. Am. Soc. Chem.* **2003**, *125*, 4111-4118.
53. Koppelhus, U.; Awasthi, S. K.; Zachar, V.; Holst, H. U.; Ebbesen, P.; Nielsen, P. E., "Cell-dependent differential cellular uptake of PNA, peptides and PNA-peptide conjugates." *Antisense Nucleic Acid Drug Dev.* **2002**, *12*, 51-63.
54. McMahon, B. M.; Mays, D.; Lipsky, J. A.; Fauq, A.; Richelson, E., "Pharmacokinetics distribution of a peptide nucleic acid after intravenous administration." *Antisense Nucleic Acid Drug Dev.* **2002**, *12*, 65-70.
55. Armitage, B. A., "The impact of nucleic acid secondary structure on PNA hybridization." *Drug Discov. Today* **2003**, *8*, 222-228.
56. Bentin, T.; Nielsen, P. E., "Enhanced peptide nucleic acid binding to supercoiled DNA: possible implications for DNA "breathing" dynamics." *Biochemistry* **1996**, *35*, 8863-8869.
57. Venkatesan, N.; Kim, B. H., "Peptide conjugates of oligonucleotides: synthesis and applications." *Chem. Rev.* **2006**, *106*, 3712-3761.
58. Zhilina, Z. V.; Ziemba, A. J.; Ebbinghaus, S. W., "Peptide nucleic acid conjugates: synthesis, properties and applications." *Curr. Top. Med. Chem.* **2005**, *5*, 1119-1131.
59. Biessen, E. A. L.; Sliedregt-Bol, K.; 'T Hoen, P. A. Chr.; Prince, P.; Van der Bilt, E.; Valentijn, A. R. P. M.; Meeuwenoord, N. J.; Princen, H.; Bijsterbosch, M. K.; Van der Marel, G. A.; Van Boom, J. H.; Van Berkel, T. J. C., "Design of a targeted peptide nucleic acid prodrug to inhibit hepatic human microsomal triglyceride transfer protein expression in Hepatocytes." *Bioconjugate Chem.* **2002**, *13*, 295-302.
60. Turner, J. J.; Ivanova, G. D.; Verbeure, B.; Williams, D.; Arzumanov, A. A.; Abes, S.; Lebleu, B.; Gait, M., "Cell-penetrating peptide conjugates of peptide nucleic acids (PNA) as inhibitors of HIV-1 Tat-dependent *trans*-activation in cells." *Nucleic Acid Res.* **2005**, *33*, 6837-6849.
61. Shiraishi, T.; Bendifallah, N.; Nielsen, P. E., "Cellular delivery of polyheteroaromate-peptide nucleic acid conjugates mediated by cationic lipids." *Bioconjugate Chem.* **2006**, *17*, 189-194.
62. Ljungstrom, T.; Knudsen, H.; Nielsen, P. E., "Cellular uptake of adamantly conjugated peptide nucleic acids." *Bioconjugate Chem.* **1999**, *10*, 965-972.
63. Bentin, T.; Nielsen, P. E., "Superior duplex DNA strand invasion by acridine conjugated peptide nucleic acids." *J. Am. Chem. Soc.* **2003**, *125*, 6378-6379.

64. Ortiz, E.; Estrada, G.; Lizardi, P. M., "PNA molecular beacons for rapid detection of PCR amplicons." *Mol. Cell. Probes* **1998**, *12*, 219-226.
65. Chandler, D. P.; Stults, J. R.; Cebula, S.; Schuck, B. L.; Weaver, D. W.; Anderson, K. K.; Egholm, M.; Brockman, F. J., "Affinity purification of DNA and RNA from environmental samples with peptide nucleic acid clamps." *Appl. Environ. Microbiol.* **2000**, *66*, 3438-3445.
66. Svanik, N.; Westman, G.; Wang, D.; Kubista, M., "Light-up probes: Thiazole orange-conjugated peptide nucleic acid for detection of target nucleic acid in homogeneous solution." *Anal. Biochem.* **2000**, *281*, 26-35.
67. Vilaivan, T.; Lowe, G., "A novel pyrrolidinyl PNA showing high sequence specificity and preferential binding to DNA over RNA." *J. Am. Chem. Soc.* **2002**, *124*, 9326-9327.
68. Govindaraju, T.; Kumar, V. A.; Ganesh, K. N., "(SR/RS)-cyclohexyl PNAs: Conformationally preorganized PNA analogues with unprecedented preference for duplex formation with RNA." *J. Am. Chem. Soc.* **2005**, *127*, 4144-4145.
69. Sforza, S.; Corradini, R.; Ghirardi, S.; Dossena, A.; Marchelli, R., "DNA binding of a D-lysine-based chiral PNA: Direction control and mismatch recognition." *Eur. J. Org. Chem.* **2000**, 2905-2913.
70. Vilaivan, T.; Srisuwannaket, C., "Hybridization of pyrrolidinyl peptide nucleic acids and DNA: Selectivity, base-pairing specificity, and direction of binding." *Org. Lett.* **2006**, *8*, 1897-1900.
71. Kuwahara, M.; Arimitsu, M.; Sisido, M., "Novel peptide nucleic acid that shows high sequence specificity and all-or-none-type hybridization with the complementary DNA." *J. Am. Chem. Soc.* **1999**, *121*, 256-257.
72. Efimov, V. A.; Chakhmakhcheva, O. G.; Wickstrom, E., "Synthesis and application of negatively charged PNA analogues." *Nucleosides Nucleotides Nucleic Acids* **2005**, *24*, 1853-1874.
73. Howarth, N. M.; Wakelin, L. P. G.; Walker, D. M., " α -cycloPNA: 1-aminocyclopentane-1-carboxylic acid-derived peptide nucleic acid." *Nucleosides Nucleotides Nucleic Acids* **2003**, *22*, 1351-1353.
74. Krotz, A. H.; Larsen, S.; Buchardt, O.; Eriksson, M.; Nielsen, P. E., "A 'retro-inverso' PNA: Structural implications for DNA and RNA binding." *Bioorg. Med. Chem.* **1998**, *6*, 1983-1992.
75. Sforza, S.; Galaverna, G.; Dossena, A.; Corradini, R.; Marchelli, R., "Role of chirality and optical purity in nucleic acid recognition by PNA and PNA analogs." *Chirality* **2002**, *14*, 591-598.

76. Roviello, G. N.; Moccia, M.; Saoui, R.; Valente, M.; Bucci, E. M.; Castiglione, M.; Pedone, C.; Perretta, G.; Benedetti, E.; Musumeci, D., "Synthesis, characterization and hybridization studies of new nucleo- γ -peptides based on diaminobutyric acid." *J. Pept. Sci.* **2006**, *12*, 829-835.
77. Hyrup, B.; Egholm, M.; Nielsen, P. E. Wittung, P.; Norden, B.; Buchardt, O., "Structure-activity studies of the binding of modified peptide nucleic acids (PNAs) to DNA." *J. Am. Chem. Soc.* **1994**, *116*, 7964-7970.
78. Dueholm, K. L.; Petersen, K. H.; Jensen, D. K.; Egholm, M.; Nielsen, P. E.; Buchardt, O., "Peptide nucleic acid (PNA) with a chiral backbone based on alanine." *Bioorg. Med. Chem. Lett.* **1994**, *4*, 1077-1080.
79. Puschl, A.; Sforza, S.; Haaima, G.; Dahl, O.; Nielsen, P. E., "Peptide nucleic acids (PNAs) with a functional backbone." *Tetrahedron Lett.* **1998**, *39*, 4707-4710.
80. Haaima, G.; Lohse, A.; Buchardt, O.; Nielsen, P. E., "Peptide nucleic acids (PNAs) containing thymine monomers derived from chiral amino acids: hybridization and solubility properties of D-lysine PNA." *Angew. Chem. Int. Ed.* **1996**, *35*, 1939-1942.
81. Dragulescu-Andrasi, A.; Zhou, P.; He, G.; Ly, D. H., "Cell-permeable GPNA with appropriate backbone stereochemistry and spacing binds sequence-specifically to RNA." *Chem. Commun.* **2005**, 244-246.
82. Zhou, P.; Wang, M.; Du, L.; Fisher, G. W.; Waggoner, A.; Ly, D. H., "Novel binding and efficient cellular uptake of guanidine-based peptide nucleic acids (GPNA)." *J. Am. Chem. Soc.* **2003**, *125*, 6878-6879.
83. Hamzavi, R.; Dolle, F.; Tavitian, B.; Dahl, O.; Nielsen, P. E., "Modulation of the pharmacokinetic properties of PNA: preparation of galactosyl, mannosyl, fucosyl, N-acetylgalactosaminyl, and N-acetylglucosaminyl derivatives of aminoethylglycine peptide nucleic acid monomers and their incorporation into PNA oligomers." *Bioconjugate Chem.* **2003**, *14*, 941-954.
84. Kosynkina, L.; Wang, W.; Liang, T. C., "A convenient synthesis of chiral peptide nucleic acid (PNA) monomers." *Tetrahedron Lett.* **1994**, *35*, 5173-5176.
85. Wu, Y.; Xu, J.-C., "Synthesis of chiral peptide nucleic acids using Fmoc chemistry." *Tetrahedron* **2001**, *57*, 8107-8113.
86. Falkiewicz, B.; Kolodziejczyk, A. S.; Liberek, B.; Wisniewski, K., "Synthesis of achiral and chiral peptide nucleic acid (PNA) monomers using Mitsunobu reaction." *Tetrahedron* **2001**, *57*, 7909-7917.

87. Maison, W.; Schlemminger, I.; Westerhoff, O.; Martens, J., "Multicomponent synthesis of novel amino acid-nucleobase chimeras: a versatile approach to PNA-monomers." *Bioorg. Med. Chem.* **2000**, *8*, 1343-1360.
88. Gopi, H. N.; Englund, E. A.; Appella, D. H., Unpublished.
89. Kool, E. T., "Preorganization of DNA: Design principles for improving nucleic acid recognition by synthetic oligonucleotides." *Chem. Rev.* **1997**, *97*, 1473-1487.
90. Kumar, V. A., "Structural preorganization of peptide nucleic acids: Chiral cationic analogues with five- or six-membered ring structures." *Eur. J. Org. Chem.* **2002**, 2021-2032.
91. Pokorski, J. K.; Myers, M. C.; Appella, D. H., "Cyclopropane PNA: observable triplex melting in a PNA constrained with a 3-membered ring." *Tetrahedron* **2005**, *46*, 915-917.
92. Govindaraju, T.; Kumar, V. A.; Ganesh, K. N., "cis-cyclopentyl PNA (cpPNA) as constrained chiral PNA analogues: stereochemical dependence of DNA/RNA hybridization." *Chem. Commun. (Camb.)* **2004**, *7*, 860-861.
93. Govindaraju, T.; Kumar, V. A.; Ganesh, K. N., "(1S,2R/1R,2S)-cis-cyclopentyl PNAs (cpPNAs) as constrained PNA analogues: synthesis and evaluation of aeg-cpPNA chimera and stereopreferences in hybridization with DNA/RNA." *J. Org. Chem.* **2004**, *69*, 5725-5734.
94. Wittung, P.; Nielsen, P. E.; Norden, B., "Observation of a PNA-PNA-PNA triplex." *J. Am. Chem. Soc.* **1997**, *119*, 3189-3190.
95. Myers, M. C.; Witschi, M. A.; Larionova, N. V.; Franck, J. M.; Haynes, R. D.; Hara, T.; Grajkowski, A.; Appella, D. A. "A cyclopentane conformational restraint for a peptide nucleic acid: design, asymmetric synthesis, and improved binding affinity to DNA and RNA." *Org. Lett.* **2003**, *5*, 2695-2698.
96. Pokorski, J. K.; Witschi, M. A.; Purnell, B. L.; Appella, D. H., "(S,S)-trans-cyclopentane-constrained peptide nucleic acids. A general backbone modification that improves binding affinity and sequence specificity." *J. Am. Chem. Soc.* **2004**, *126*, 15067-15073.
97. Pokorski, J. K.; Nam, J.-M.; Vega, R. A.; Mirkin, C. A.; Appella, D. H., "Cyclopentane-modified PNA improves the sensitivity of nanoparticle-based scanometric DNA detection." *Chem. Commun.* **2005**, 2101-2103.
98. Zhang, N.; Appella, D. H., "Colorimetric detection of anthrax DNA with a peptide nucleic acid sandwich-hybridization assay." *J. Am. Chem. Soc.* **2007**, *129*, 8424-8425.
99. Englund, E. A.; Appella, D. H., "Synthesis of γ -substituted peptide nucleic acids: a new place to attach fluorophores without affecting DNA binding." *Org. Lett.* **2005**, *7*, 3465-3467.

100. Dose, C.; Seitz, O., "Single nucleotide specific detection of DNA by native chemical ligation of fluorescence labeled PNA-probes." *Bioorg. Med. Chem.* **2007**, Article in Press.
101. Leijon, M.; Graslund, A.; Nielsen, P. E.; Buchardt, O.; Norden, B.; Kristensen, S. M.; Eriksson, M., "Structural characterization of PNA-DNA duplexes by NMR. Evidence for DNA in a B-like conformation." *Biochemistry* **1994**, *33*, 9820-9825.
102. Wittung, P.; Eriksson, M.; Lyng, R.; Nielsen, P. E.; Norden, B. "Induced chirality in the PNA-PNA duplexes." *J. Am. Chem. Soc.* **1995**, *117*, 10167-10173.
103. Sforza, S.; Haaima, G.; Marchelli, R.; Nielsen, P. E., Chiral peptide nucleic acids (PNAs): Helix handedness and DNA recognition." *Eur. J. Org. Chem.* **1999**, 197-204.
104. Oleszuk, M.; Rodziewicz-Motowidlo, S.; Falkiewicz, B., "Restricted rotation in chiral peptide nucleic acid (PNA) monomers – influence of substituents by means of ¹H NMR." *Nucleosides Nucleotides Nucleic Acids* **2001**, *20*, 1399-1402.
105. Brown, S. C.; Thomson, S. A.; Veal, J. M.; Davis, D. G., "NMR solution structure of a peptide nucleic acid complexed with RNA." *Science* **1994**, *265*, 777-780.
106. Thesis of Dr. Mark A. Witschi, "Modified Peptide Nucleic Acids (PNA) and Amonafide Derivatives: Synthesis and Applications of *trans*-Cyclopentane and *trans*-Pyrrolidine PNAs and Small Molecules Derived from Amonafide." **December 2006**, Northwestern University.

Chapter II References

1. Dueholm, K. L.; Eghom, M.; Behrens, C.; Christensen, L.; Hansen, H. F.; Vulpius, T.; Petersen, K. H.; Berg, R. H.; Nielsen, P. E.; Buchardt, O., "Synthesis of peptide nucleic acid monomers containing the four natural nucleobases: Thymine, cytosine, adenine, and guanine and their oligomerization." *J. Org. Chem.* **1994**, *59*, 5767-5773.
2. Purchased from Advanced ChemTech, Louisville, KY.
3. Boutin, R. H.; Loundon, G. M., "Conversion of aliphatic amides into amines with [*I,I*-Bis(trifluoroacetoxy)iodo]benzene. 2. Kinetics and mechanism." *J. Org. Chem.* **1984**, *49*, 4277-4284.
4. Radhakrishna, A. S.; Parham, M. E.; Riggs, R. M.; Loundon, G. M., "New method for direct conversion of amides to amines." *J. Org. Chem.* **1979**, *38*, 1746-1747.
5. Waki, M.; Kitajima, Y.; Izumiya, N., "A facile synthesis of N²-protected L-2,3-diaminopropanoic acid." *Synthesis* **1981**, 266-267.
6. Arttamangkul, S.; Murray, T. F.; DeLander, G. E.; Aldrich, J. V., "Synthesis and opioid activity of conformationally constrained Dynorphin A analogues. 1. Conformational constraint in the "message" sequence." *J. Med. Chem.* **1995**, *38*, 2410-2417.
7. Purchased from Aldrich, Milwaukee, WI.
8. Theon, J. C.; Morales-Ramos, A. I.; Lipton, M. A., "Synthesis of the unnatural amino acid AGDHE, a constituent of the cyclic depsipeptides Callipeltins A and D." *Org. Lett.* **2002**, *4*, 4455-4458.
9. Salituro, F. G.; Agarwal, N.; Hofmann, T.; Rich, D. H., "Inhibition of aspartic proteinases by peptides containing lysine and ornithine side-chain analogues of Statine." *J. Med. Chem.* **1987**, *30*, 286-295.
10. Robert, J. L.; Chan, C., "Asymmetric synthesis of differentially protected *meso*-2,6-diaminopimelic acid." *Tetrahedron Lett.* **2002**, *43*, 7679-7682.
11. Deng, J.; Hamada, Y.; Shioiri, T., "A new synthesis of Cyclotheonamide B via guanidination of ornithine." *Tetrahedron Lett.* **1996**, *37*, 2261-2264.
12. Duggan, M. E.; Imagire, J. S., "Copper(I) chloride catalyzed addition of alcohols to alkyl isocyanates A mild and expedient method for alkyl carbamate formation." *Synthesis* **1989**, 131.
13. Nahm, S.; Weinreb, S. M., "N-methoxy-N-methylamides as effective acylating agents." *Tetrahedron Lett.* **1981**, *22*, 3815-3818.

14. Stanfield, C. F.; Parker, J. E.; Kanellis, P., "Preparation of protected amino aldehydes." *J. Org. Chem.* **1981**, *46*, 4797-4798.
15. Rittle, K. E.; Homnick, C. F.; Ponticello, G. S.; Evans, B. E., "A synthesis of statine utilizing an oxidative route to chiral α -amino aldehydes." *J. Org. Chem.* **1982**, *47*, 3016-3018.
16. Thompson, S. A.; Josey, J. A.; Cadilla, R.; Gaul, M. D.; Hassman, F.; Luzzio, M. J.; Pipe, A. J.; Reed, K. L.; Ricca, D. J.; Wiethe, R. W.; Noble, S. A., "Fmoc mediated synthesis of peptide nucleic acids." *Tetrahedron* **1995**, *51*, 6179-6194.
17. Huffman, W. F.; Hall, R. F.; Grant, J. A.; Holden, K. G., "Nuclear analogues of β -lactam antibiotics. Total synthesis of bisnorisopenicillins from antibacterially active monocyclic β -lactam precursors." *J. Med. Chem.* **1978**, *21*, 413-415.
18. Carpino, L. A., "The 9-fluorenylmethyloxycarbonyl family of base-sensitive amino-protecting groups." *Acc. Chem. Res.* **1987**, *20*, 401-407.
19. Koch, T.; Hansen, H. F.; Andersen, P.; Larsen, T.; Batz, H. G.; Otteseon, K. Orum, H., "Improvements in automated PNA synthesis using Boc/Z monomers." *J. Pept. Res.* **1997**, *49*, 80-88.
20. Egholm, M.; Buchardt, O.; Christensen, L.; Behrens, C.; Freier, S. M.; Driver, D. A.; Berg, R. H.; Kim, S. K.; Norden, B.; Nielsen, P. E., "PNA hybridizes to complementary oligonucleotides obeying the Watson-Crick hydrogen-bonding rules." *Nature* **1993**, *365*, 566-568.
21. Yajima, H.; Fujii, N.; Ogawa, H.; Kawatani, H., "Trifluoromethanesulphonic acid, as a deprotecting reagent in peptide chemistry." *J. Chem. Soc., Chem. Commun.* **1974**, 107-108.
22. Eriksson, M.; Christensen, L.; Schmidt, J.; Haaima, G.; Niesen, P. E., "Sequence dependent N-terminal rearrangement and degradation of peptide nucleic acid (PNA) in aqueous solution." *New J. Chem.* **1998**, *22*, 1055-1059.
23. Mergny, J.-L.; Lacroix, L., "Analysis of thermal melting curves." *Oligonucleotides* **2003**, *13*, 515-537.
24. Marky, L. A.; Breslauer, K. J., "Calculating thermodynamic data for transitions of any molecularity from equilibrium melting curves." *Biopolymers* **1987**, *26*, 1601-1620.
25. de Koning, M. C.; van der Marel, G. A.; Overhand, M., "Synthetic developments towards PNA-peptide conjugates." *Curr. Opin. Chem. Biol.* **2003**, *7*, 734-740.
26. Sen, A.; Nielsen, P. E., "Unique properties of purine/pyrimidine asymmetric PNA·DNA duplexes: differential stabilization of PNA·DNA duplexes by purines in the PNA strand." *Biophys. J.* **2006**, *90*, 1329-1337.

27. Pokorski, J. K.; Witschi, M. A.; Purnell, B. L.; Appella, D. H., "(S,S)-*trans*-cyclopentane-constrained peptide nucleic acids. A general backbone modification that improves binding affinity and sequence specificity." *J. Am. Chem. Soc.* **2004**, *126*, 15067-15073.
28. Haaima, G.; Lohse, A.; Buchardt, O.; Nielsen, P. E., "Peptide nucleic acids (PNAs) containing thymine monomers derived from chiral amino acids: hybridization and solubility properties of D-lysine PNA." *Angew. Chem. Int. Ed.* **1996**, *35*, 1939-1942.
29. Sforza, S.; Corradini, R.; Ghirardi, S.; Dossena, A.; Marchelli, R., "DNA binding of a D-lysine-based chiral PNA: direction control and mismatch recognition." *Eur. J. Org. Chem.* **2000**, 2905-2913.
30. Wittung, P.; Nielsen, P. E.; Buchardt, O.; Egholm, M.; Norden, B., "DNA-like double helix formed by peptide nucleic acid." *Nature* **1994**, *368*, 561-563.
31. Sforza, S.; Haaima, G.; Marchelli, R.; Nielsen, P. E., "Chiral peptide nucleic acids (PNAs): Helix handedness and DNA recognition." *Eur. J. Org. Chem.* **1999**, 197-204.
32. Dragulescu-Andrasi, A.; Rapireddy, S.; Frezza, B. M.; Gayathri, C.; Gil, R. R.; Ly, D. H., "A simple γ -backbone modification preorganizes peptide nucleic acid into a helical structure." *J. Am. Chem. Soc.* **2006**, *128*, 10258-10267.
33. Kuhn, H.; Demidov, V. V.; Coull, J. M.; Fiandaca, M. J.; Gildea, B.D.; Frank-Kamenetskii, M. D., "Hybridization of DNA and PNA molecular beacons to single-stranded and double-stranded DNA targets." *J. Am. Chem. Soc.* **2002**, *124*, 1097-1103.
34. Seitz, O., "Solid-phase synthesis of doubly labeled peptide nucleic acids as probes for the real-time detection of hybridization." *Angew. Chem. Int. Ed.* **2000**, *39*, 3249-3252.
35. Apicella, B.; Ciajolo, A.; Tregrossi, A., "Fluorescence spectroscopy of complex aromatic mixtures." *Anal. Chem.* **2004**, *76*, 2138-2143.
36. Telser, J.; Cruickshank, K. A.; Morrison, L. E.; Nextel, T. L., "Synthesis and characterization of DNA oligomers and duplexes containing covalently attached molecular labels: comparison of biotin, fluorescein, and pyrene labels by thermodynamic and optical spectroscopic measurements." *J. Am. Chem. Soc.* **1989**, *111*, 6966-6976.
37. Hwang, G. T.; Seo, Y. J.; Kim, B. H., "A highly discriminating quencher-free molecular beacon for probing DNA." *J. Am. Chem. Soc.* **2004**, *126*, 6528-6529.
38. Svanvik, N.; Nygren, J.; Westman, G.; Kubista, M., "Free-probe fluorescence of light-up probes." *J. Am. Chem. Soc.* **2001**, *123*, 803-809.

39. Lee, L. G.; Chen, C.-H.; Chiu, L. A., "Thiazole orange: a new dye for reticulocyte analysis." *Cytometry* **1986**, *7*, 508-517.
40. Karunakaran, V.; Lustres, J. L. P.; Zhao, L.; Ernsting, N. P.; Seitz, O., "Large dynamic stokes shift of DNA intercalation dye thiazole orange has contribution from a high-frequency mode." *J. Am. Chem. Soc.* **2006**, *128*, 2954-2962.
41. Nygren, J.; Svanik, N. Kubista, M., "The interactions between the fluorescent dye thiazole orange and DNA." *Biopolymers* **1998**, *46*, 39-51.
42. Svanvik, N.; Westman, G.; Wang, D.; Kubita, M, "Light-up probes: thiazole orange-conjugated peptide nucleic acid for detection of target nucleic acid in homogeneous solution." *Anal. Biochem.* **2000**, *281*, 26-35.
43. Kohler, O.; Jarikote, D. V.; Seitz, O., "Forced intercalation probes (FIT probes): thiazole orange as a fluorescent base in peptide nucleic acids for homogeneous single-nucleotide-polymerism detection." *ChemBioChem* **2005**, *6*, 69-77.
44. Hamzavi, R.; Dolle, F.; Tavitian, B.; Dahl, O.; Nielsen, P. E., "Modulation of the pharmacokinetic properties of PNA: preparation of galactosyl, mannosyl, fucosyl, N-acetylgalactosaminyl, and N-acetylglucosaminyl derivatives of aminoethylglycine peptide nucleic acid monomers and their incorporation into PNA oligomers." *Bioconjugate Chem.* **2003**, *14*, 941-954.
45. Tedeschi, T.; Sforza, S.; Corradini, R.; Marchelli, R., "Synthesis of new chiral PNAs bearing a dipeptide-mimic monomer with two lysine-derived stereogenic centres." *Tetrahedron Lett.* **2005**, *46*, 8395-8399.
46. Dose, C.; Seitz, O., "Convergent synthesis of peptide nucleic acids by native chemical ligation." *Org. Lett.* **2005**, *7*, 4365-68.
47. Pangborn, A. B.; Giardello, M. A.; Grubbs, R. H.; Rosen, R. K.; Trimmers, F. J., "Safe and convenient procedure for solvent purification." *Organometallics* **1996**, *15*, 1518-1520.
48. Ongeri, S.; Aiken, D. J.; Husson, H. P., "A short synthesis of trans-cyclopentane-1,2-diamine." *Synth. Commun.* **2000**, *30*, 2593-2597.
49. Kaiser, E.; Colecott, R. L.; Bossinger, C. D.; Cook, P. I., "Color test for detection of free terminal amino groups in the solid-phase synthesis of peptides." *Anal. Biochem.* **1970**, *34*, 595-598.
50. Warshaw, M. M.; Tinoco, I. Jr., "Optical properties of sixteen dinucleoside phosphates." *J. Mol. Biol.* **1966**, *20*, 29-38.

Chapter III References

1. Porcheddu, A.; Giacomelli, G., "Peptide nucleic acids (PNAs), a chemical overview." *Curr. Med. Chem.* **2005**, *12*, 2561-2599.
2. Myers, M. C.; Witschi, M. A.; Larionova, N. V.; Franck, J. M.; Haynes, R. D.; Hara, T.; Grajkowski, A.; Appella, D. H., "A cyclopentane conformational restraint for a peptide nucleic acid: design, asymmetric synthesis, and improved binding affinity to DNA and RNA." *Org. Lett.* **2003**, *5*, 2695-2698.
3. Bentin, T.; Hansen, G. I.; Nielsen, P. E., "Structural diversity of target-specific homopyrimidine peptide nucleic acid-dsDNA complexes." *Nucleic Acids Res.* **2006**, *34*, 5790-5799.
4. Hansen, G. I.; Bentin, T.; Larsen, H. J.; Nielsen, P. E., "Structural isomers of bis-PNA bound to a target in duplex DNA." *J. Mol. Biol.* **2001**, *307*, 67-74.
5. Bastide, L.; Boehmer, P. E.; Villani, G.; Lebleu, B., "Inhibition of a DNA-helicase by peptide nucleic acids." *Nucleic Acids Res.* **1999**, *27*, 551-554.
6. Svahn, M. G.; Lundin, K. E.; Ge, R.; Tornquist, E.; Simonson, E. O.; Oscarsson, S.; Leijon, M.; Branden, L. J.; Smith, C. I. E., "Adding functional entities to plasmids." *J. Gene Med.* **2004**, *6*, S36-S44.
7. Zelphati, O.; Liang, X.; Hobart, P.; Felgner, P. L., "Gene chemistry: functionally and conformationally intact fluorescent plasmid DNA." *Hum. Gene Ther.* **1999**, *10*, 15-24.
8. Gasiorowski, J. Z.; Dean, D. A., "Postmitotic nuclear retention of episomal plasmids is altered by DNA labeling and detection methods." *Mol. Ther.* **2005**, *12*, 460-467.
9. D'Costa, M.; Kumar, V. A.; Ganesh, K. N., "N7-guanine as a C⁺ in hairpin *aeg/aep*PNA-DNA triplex: probing binding selectivity by UV-T_m and kinetics by fluorescence-based strand-invasion assay." *J. Org. Chem.* **2003**, *68*, 4439-4445.
10. Hillery, E.; Munkonge, F. M.; Xenariou, S.; Dean, D. A.; Alton, E. W. F. W., "Nondisruptive, sequence-specific coupling of fluorochromes to plasmid DNA." *Anal. Biochem.* **2006**, *352*, 169-175.
11. Thompson, S. A.; Josey, J. A.; Cadilla, R.; Gaul, M. D.; Hassman, F.; Luzzio, M. J.; Pipe, A. J.; Reed, K. L.; Ricca, D. J.; Wiethe, R. W.; Noble, S. A., "Fmoc mediated synthesis of peptide nucleic acids." *Tetrahedron* **1995**, *51*, 6179-6194.

12. Jenny, T. F.; Schneider, K. C.; Benner, S. A., "N²-isobutyryl-O⁶-[2-(*p*-nitrophenyl)ethyl]guanine: a new building block for the efficient synthesis of carbocyclic guanosine analogs." *Nucleosides Nucleotides* **1992**, *11*, 1257-1261.
13. Liu, Z.; Shin, D.; Lee, K.; Jun, B.; Kim, Y.; Lee, Y., "Synthesis of photolabile *o*-nitroveratryloxycarbonyl (NVOC) protected peptide nucleic acid monomers." *Tetrahedron* **2005**, *61*, 7967-7973.
14. Xu, Q.; Appella, D. H., "Practical synthesis of *trans*-*tert*-butyl-2-aminocyclopentylcarbamate and resolution of enantiomers." *J. Org. Chem.* **2006**, *71*, 8655-8657.
15. Eriksson, M.; Christensen, L.; Schmidt, J.; Haaima, G.; Niesen, P. E., "Sequence dependent N-terminal rearrangement and degradation of peptide nucleic acid (PNA) in aqueous solution." *New J. Chem.* **1998**, *22*, 1055-1059.
16. Egholm, M.; Christensen, L.; Dueholm, K. L.; Buchardt, O.; Coull, J.; Nielsen, P. E. "Efficient pH-independent sequence-specific DNA binding by pseudoisocytosine-containing bis-PNA." *Nucleic Acids Res.* **1995**, *23*, 217-222.
17. Schultz, P.; Hud, N. V.; Smith, F. W.; Feigon, J., "The effect of sodium, potassium and ammonium ions on the conformation of the dimeric quadruplex formed by the *Oxytricha nova* telomere repeat oligonucleotide d(G(4)T(4)G(4))." *Nucleic Acids Res.* **1999**, *27*, 3018-3028.
18. Smith, F. W.; Feigon, J., "Strand orientation in the DNA quadruplex formed from the *Oxytricha* telomere repeat oligonucleotide d(G4T4G4) in solution." *Biochemistry* **1993**, *32*, 8682-8692.
19. Haider, S.; Parkinson, G. N.; Neidle, S., "Crystal structure of the potassium form of an *Oxytricha nova* G-quadruplex." *J. Mol. Biol.* **2002**, *320*, 189-200.
20. Datta, B.; Bier, M. E.; Roy, S.; Armitage, B. A., "Quadruplex formation by a guanine-rich PNA oligomer." *J. Am. Soc. Chem.* **2005**, *127*, 4199-4207.
21. Datta, B.; Schmitt, C.; Armitage, B. A., "Formation of a PNA₂-DNA₂ hybrid quadruplex." *J. Am. Soc. Chem.* **2003**, *125*, 4111-4118.
22. Mergny, J.-L.; Phan, A.-T.; Lacroix, L., "Following G-quartet formation by UV-spectroscopy." *FEBS Lett.* **1998**, *435*, 74-78.
23. Pokorski, J. K.; Witschi, M. A.; Purnell, B. L.; Appella, D. H., "(S,S)-*trans*-cyclopentane-constrained peptide nucleic acids. A general backbone modification that improves binding affinity and sequence specificity." *J. Am. Chem. Soc.* **2004**, *126*, 15067-15073.
24. Hoff, A. J.; Roos, A. L. M., "Hysteresis of denaturation of DNA in the melting range." *Biopolymers* **1972**, *11*, 1289-1294.

25. Dapic, V.; Abdomerovic, V.; Marrington, R.; Peberdy, J.; Rodger, A.; Trent, J. O.; Bates, P. J., "Biophysical and biological properties of quaruplex oligodeoxyribosenucleotides." *Nucleic Acids Res.* **2003**, *31*, 2097-2107.
26. Wittung, P.; Nielsen, P. E.; Buchardt, O.; Egholm, M.; Norden, B., "DNA-like double helix formed by peptide nucleic acid." *Nature* **1994**, *368*, 561-563.
27. Krishnan-Gosh, Y.; Stephens, E.; Balasubramanian, S., "A PNA₄ quadruplex." *J. Am. Chem. Soc.* **2004**, *126*, 5944-5945.
28. Giraldo, R.; Suzuki, M.; Chapman, L.; Rhodes D. "Promotion of parallel DNA quadruplexes by a yeast telomere binding protein: a circular dichroism study." *Proc. Nat. Acad. Sci. U.S.A.* **1994**, *91*, 7658-7662.
29. Kool, E. T., "Preorganization of DNA: Design principles for improving nucleic acid recognition by synthetic oligonucleotides." *Chem. Rev.* **1997**, *97*, 1473-1487.
30. Roy, S.; Tanious, F.A.; Wilson, W. D.; Ly, D. H.; Armitage, B. A., "High-affinity homologous peptide nucleic acid probes for targeting a quadruplex-forming sequence from a MYC promoter element." *Biochemistry*, **2007**, *in press*.
31. Hashem, G. M.; Wen, J.-D.; Do, Q.; Gray, D. M., "Evidence from CD spectra and melting temperatures for stable Hoogsteen- paired oligomer duplexes derived from DNA and hybrid triplexes." *Nucleic Acids Res.* **1999**, *27*, 3371-3379.

Chapter IV References

1. Ratilainen, T., Holmen, A., Tuite, E., Nielsen, P. E., and Norden, B., "Thermodynamics of sequence-specific binding of PNA to DNA." *Biochemistry* **2000**, *39*, 7781–7791.
2. Jensen, K. K.; Orum, H.; Nielsen, P. E.; Norden, B., "Kinetics for hybridization of peptide nucleic acids (PNA) with DNA and RNA studies with the BIAcore technique." *Biochemistry* **1997**, *36*, 5072-5077.
3. Demidov, V. V.; Protozanova, E.; Izvolsky, K. I.; Price, C.; Nielsen, P. E.; Frank-Kamenetskii, M. D., "Kinetics and mechanism of the DNA double helix invasion by pseudocomplementary peptide nucleic acids." *Proc. Natl. Acad. Sci. USA* **2002**, *99*, 5953-5958.
4. Debane, F.; Da Silva, J. A.; Pianowski, Z; Duran, R. J.; Winssinger, N., "Expanding the scope of PNA-encoded libraries: divergent synthesis of libraries targeting cysteine, serine and metalloproteases as well as tyrosine phosphatases." *Tetrahedron* **2007**, *63*, 6577-6586.
5. Dragulescu-Andrasi, A.; Rapireddy, S.; He, G.; Bhattacharya, B.; Hyldig-Nielsen, J. J.; Zon, G.; Ly, D. H., "Cell-permeable peptide nucleic acid designed to bind to the 5'-untranslated region of E-cadherin transcript induces potent and sequence-specific antisense effects." *J. Am. Chem. Soc.* **2006**, *128*, 16104-16112.
6. Thompson, S. A.; Josey, J. A.; Cadilla, R.; Gaul, M. D.; Hassman, F.; Luzzio, M. J.; Pipe, A. J.; Reed, K. L.; Ricca, D. J.; Wiethe, R. W.; Noble, S. A., "Fmoc mediated synthesis of peptide nucleic acids." *Tetrahedron* **1995**, *51*, 6179-6194.
7. Guibe, F., "Allylic protecting groups and their use in a complex environment part II: allylic protecting groups and their removal through catalytic palladium π -allyl methodology." *Tetrahedron* **1998**, *54*, 2967-3042.
8. Englund, E. A.; Xu, G.; Witschi, M. A.; Appella, D. H., "PNA-DNA duplexes, triplexes, and quadruplexes are stabilized with *trans*-cyclopentane units." *J. Am. Chem. Soc.* **2006**, *128*, 16456-16457.
9. Tagore, D. M.; Sprinz, K. I.; Flecher, S.; Jayawickramarajah, J.; Hamilton, A. D., "Protein recognition and denaturation by self-assembling fragments on a DNA quadruplex scaffold." *Angew. Chem. Int. Ed.* **2007**, *46*, 223-225.
10. Jenny, T. F.; Schneider, K. C.; Benner, S. A., "N²-isobutyryl-O⁶-[2-(p-nitrophenyl)ethyl]guanine: a new building block for the efficient synthesis of carbocyclic guanosine analogs." *Nucleosides Nucleotides* **1992**, *11*, 1257-1261.

11. Kruger, R. G.; Dostal, P.; McCafferty, D. G., "An economical and preparative orthogonal solid phase synthesis of fluorescein and rhodamine derivatized peptides: FRET substrates for *Staphylococcus aureus* sortase SrtA transpeptidase reaction." *Chem Commun.* **2002**, 2092-2093.
12. Dose, C.; Seitz, O., "Single nucleotide specific detection of DNA by native chemical ligation of fluorescence labeled PNA-probes." *Bioorg. Med. Chem.* **2007**, Article in Press.
13. Diaz-Mochon, J. J.; Bialy, L.; Bradley, M., "Full orthogonality between Dde and Fmoc: the direct synthesis of PNA-peptide conjugates." *Org. Lett.* **2004**, *6*, 1127-1129.
14. Englund, E. A.; Appella, D. H., " γ -Substituted peptide nucleic acids constructed from L-lysine are a versatile scaffold for multifunctional display." *Angew. Chem. Int. Ed.* **2007**, *46*, 1414-1418.
15. Pokorski, J. K.; Witschi, M. A.; Purnell, B. L.; Appella, D. H., "(S,S)-*trans*-cyclopentane-constrained peptide nucleic acids. A general backbone modification that improves binding affinity and sequence specificity." *J. Am. Chem. Soc.* **2004**, *126*, 15067-15073.
16. Kuhn, H.; Demidov, V. V.; Coull, J. M.; Fiandaca, M. J.; Gildea, B.D.; Frank-Kamenetskii, M. D., "Hybridization of DNA and PNA molecular beacons to single-stranded and double-stranded DNA targets." *J. Am. Chem. Soc.* **2002**, *124*, 1097-1103.
17. Yin, H.; Hamilton, A. D., "Strategies for targeting protein-protein interactions with synthetic agents." *Angew. Chem. Int. Ed. Engl.* **2005**, *44*, 4130-4163.
18. Bunka, D. H. J.; Stockley, P. G., "Aptamers come of age - at last." *Nat. Rev. Microbiol.* **2006**, *4*, 588-596.

Ethan A. Englund

Laboratory of Bioorganic Chemistry
NIDDK, NIH, DHHS
(301) 451-0339

9000 Rockville Pike
Bethesda Md. 20892
e-englund@northwestern.edu

EDUCATION:

PhD., Organic Chemistry, Northwestern University. Fall 2007. Advisor: Dr. Daniel Appella.

Bachelor of Arts, ACS Approved Chemistry Major with Math and Physics Minors, Augustana College. May 2002. Advisor: Dr. Arlen Viste.

RESEARCH EXPERIENCE:

Doctoral Research, Northwestern University/NIH, 9/02-12/4; Predoctoral IRTA, LBC, NIH 1/05 to present

1) The synthesis, characterization, and studies of γ -side chain Peptide Nucleic Acid derived from lysine, and 2) their application towards fluorescent molecular beacons and nucleic acid detection assays. 3) Examination of versatility of $^1K\gamma$ -PNA conjugation and progress towards protein binding oligomers. 4) The study of PNA₂/DNA triplexes and guanine tetrads containing (*S,S*) *trans*-cyclopentane PNA. Dr. Daniel Appella, Department of Chemistry

Undergraduate Research Assistant, Augustana College, 6/01-5/02

The elucidation of computational methods describing host-guest chemical interactions. Dr. Jetty Duffy-Matzner

PUBLICATIONS:

γ -Substituted Peptide Nucleic Acids Constructed from L-Lysine are a Versatile Scaffold for Multifunctional Display

Englund, E. A.; Appella, D. H. *Angew. Chem. Int. Ed.* **2007**, *46*, 1414-1418.

PNA-DNA Duplexes, Triplexes, and Quadruplexes Are Stabilized with *trans*-Cyclopentane Units

Englund, E. A.; Hu, Q.; Witschi, M. A.; Appella, D. H. *J. Am. Chem. Soc.* **2006**, *128*, 16456-16457.

Synthesis of γ -Substituted Peptide Nucleic Acids: A New Place to Attach Fluorophores without Affecting DNA Binding

Englund, E. A.; Appella, D. H. *Org. Lett.* **2005**, 7(16), 3465-3467.

An Efficient Synthesis of a Probe for Protein Function: 2,3-Diaminopropionic Acid with Orthogonal Protecting Groups

Englund, E. A.; Gopi, H. N.; Appella, D. H. *Org. Lett.* **2004**, 6(2), 213-215.

PROFESSIONAL AFFILIATIONS:

American Chemical Society (Student Member)

ACTIVITIES AND AWARDS:

2005-*Present* NIH Predoctoral Fellow
2004 PLU Honorary Chemical Society, Northwestern University
2002 Outstanding Undergraduate Teaching Assistant, Augustana College
2001 Outstanding Qualitative Analysis Student of the Year, Augustana College
2000 Outstanding Organic Student of the Year, Augustana College

ORAL PRESENTATIONS:

"Nucleic acid molecular beacons based on γ substituted PNA" Englund, E. A.; Appella, D. H. American Chemical Society Meeting, Washington DC, August 2005.

POSTER PRESENTATIONS:

"Nucleic Acid Molecular Beacons based on γ -substituted PNA" Englund, E. A.; Appella, D. H. National Organic Symposium. Salt Lake City, UT. June 2005.

"Functionalized PNA as fluorescent probes" Englund, E. A.; Appella, D. H. American Chemical Society Meeting, Philadelphia, August 2004.

"Synthesis and Analysis of Functionalized PNA" Englund, E. A.; Appella, D. H. International Symposium on Supramolecular Chemistry, South Bend, IN, July 2004.